



THE 'BLACK FUNGUS':

**ELUCIDATING CELL WALL CHANGES IN THE *MUCOR CIRCINELLOIDES*
GERMINATING SPORE AND ITS INFLUENCE ON HOST INTERACTION**

by

Harlene Ghuman

A thesis submitted to the University of Birmingham for the degree of

DOCTOR OF PHILOSOPHY

Institute of Microbiology and Infection

School of Biosciences

College of Life and Environmental Sciences

University of Birmingham

April 2022

UNIVERSITY OF
BIRMINGHAM

University of Birmingham Research Archive

e-theses repository

This unpublished thesis/dissertation is copyright of the author and/or third parties. The intellectual property rights of the author or third parties in respect of this work are as defined by The Copyright Designs and Patents Act 1988 or as modified by any successor legislation.

Any use made of information contained in this thesis/dissertation must be in accordance with that legislation and must be properly acknowledged. Further distribution or reproduction in any format is prohibited without the permission of the copyright holder.

ABSTRACT

The filamentous fungal pathogen, *Mucor circinelloides*, is a causative agent of the fatal invasive fungal infection, mucormycosis, recently termed the 'black fungus'. During the COVID-19 pandemic there was a dramatic increase in the incidence of mucormycosis, which has mortality rates approaching 100%. The objective of this research was to enhance our understanding of *M. circinelloides* spore germination, and determine how this influences the interaction between spores and the host immune cells, macrophages and platelets. Firstly, (i) RNA-sequencing was employed to determine differentially expressed genes and processes during *M. circinelloides* spore germination, with an emphasis on those implicated in cell wall biosynthesis, and (ii) transmission electron microscopy was utilised to investigate the ultrastructure of spores during germination, and (iii) fluorescence microscopy and flow cytometry were employed to determine cell wall compositional changes. Elucidation of significantly differentially expressed genes during germination, showed that from resting spore to fully swollen spore, there is an upregulation of genes associated with cell wall biosynthesis pathways including, mannoprotein glycosylation, β -glucan biosynthesis and chitin biosynthesis. Accordingly, investigating the ultrastructure of the *M. circinelloides* spore cell wall during germination, showed extensive cell wall remodelling. Germination is at the crux of mucormycetes pathogenicity, and the first point-of-contact for host immune cells is the fungal cell wall. To investigate whether the developmental stage – where significant compositional cell wall changes occur - of *M. circinelloides* spores influences host-spore interaction, the interplay between spores at different stages of germination with macrophages and platelets was investigated. This research showed that *M. circinelloides* spore developmental stage plays a significant role in its interaction with macrophages and platelets, with spores at the mid-point swelling displaying the greatest phagocytic uptake and inducing the most platelet aggregation. Furthermore, phagocytosis of *M. circinelloides* spores was shown to be dependent upon mannose receptors, and characterisation of the platelet activation pathway showed platelet IgG receptor Fc γ RIIa and surface integrin α IIb β 3 to mediate platelet

activation in response to *M. circinelloides* spores. Collectively, this research provides findings that could be further investigated in the bid to identify novel targets for mucormycosis treatment.

ACKNOWLEDGEMENTS

The journey of this PhD has been one which has been most challenging, yet most rewarding. From having my first child to surviving a global pandemic, there have been many extremely testing times, and I must credit reaching the 'end-point' to not only myself but also the strong support network I have been blessed with.

I would like to express my gratitude to all of those who have supported me over the last few years – this really would not have been possible without you. First and foremost, I would like to thank my supervisors Rebecca Hall and Elizabeth Ballou. Through the times that I have doubted myself and wavered, you have not only encouraged and supported me, but provided me with two astounding examples of female figures in science – a true credit to the community. I also have to thank the members of the HAPI lab, for not only the warmth and support, but also for enduring my million and one questions on just about anything and everything!

To my friends and family - I always say this is not my PhD but ours, for it has really been a team effort on many fronts. Thank you to my mum, for being my rock and pillar of support. You have unfathomable patience and kindness, shown through your willingness to undertake the care of your first grandchild so that I could return to my PhD. I am forever indebted to you. Thank you to my dad, for instilling a strong work ethic and love for academia from a young age. Thank you to my siblings, Paul, Karan and Kiran, for always humbling me and constantly reminding me that I may be book smart but I have no common sense. Thank you to my sister-in-law Helen, for the copious banana bread supplies and always being so encouraging. Thank you to my best friend Aysha. From the very beginning as undergraduates to the very end of our PhDs, you have always been there, listened, supported and reminded me of my strength – we did it!

Last but most definitely not least, thank you to my son Curren, for allowing me to become a mother and experience overwhelming love. For being a bundle of joy after a hard day in the lab or library. Whilst being a single mother has been incredibly difficult you've made it so easy in so many ways. Through periods of darkness, you have given me light.

STATEMENT OF COLLABORATIVE WORK

There is data within this thesis that has been the result of collaboration. Collaborators and their contributions are listed below.

1. Transmission Electron Microscopy of Germinating Spores

Sample preparation was performed by Delma Childers and Gillian Milne (Histology and Microscopy Facility, University of Aberdeen), sectioning, staining and imaging was performed by Ian Brown, University of Kent.

2. RNA-Sequencing

Library preparation and RNA sequencing was conducted by GENEWIZ as a paid service (GENEWIZ UK LTD, Essex, UK).

DECLARATION OF AUTHORSHIP

This is to confirm that Harlene Ghuman was first author and major contributor to the publication '*Mucor circinelloides* induces platelet aggregation through integrin $\alpha\text{IIb}\beta 3$ and Fc Fc γ RIIA.' This was published in *Platelets* in 2019, with Dr Kerstin Voelz as the corresponding author. Text from this publication has been included in the thesis 'The 'black' fungus: elucidating cell wall changes in the *Mucor circinelloides* germinating spore and its influence on host interaction' submitted to the University of Birmingham in May 2021. Parts of this publication have been included in chapters 2.6 and 5.2, as also declared in each chapter.

Signed:



Harlene Ghuman



Dr Kerstin Voelz
(corresponding author)

DECLARATION OF DISRUPTION TO RESEARCH

Planned research was disrupted by the COVID-19 pandemic during the completion of this PhD, in the following ways:

(1) Cell Wall Characterization of *M. circinelloides* Spores During Germination

- High-Performance Liquid Chromatography: to enable characterisation of the cell wall at various stages of *M. circinelloides* spore germination – namely identify known and/or unknown cell wall components – research employing HPLC was planned. However, due to the imposition of restrictions impairing collaborative work, and delays in processing samples upon the return to research, this could not be conducted.
- Immunogold Labelling and TEM - to identify the character of cell wall layers at different stages of germination, immunogold labelling and staining for known fungal cell wall components was going to be performed. Due to disruptions in sample processing as a result of COVID-19 delays, only a preliminary TEM experiment without immunogold labelling could be performed.

(2) Determining Macrophage Receptors Mediating *M. circinelloides* Uptake

- Phagocytosis in Primary Human Macrophages - to confirm the results of the phagocytosis data generated using a murine macrophage cell line, investigation of *M. circinelloides* interaction with primary human macrophages was planned, such as cytokine profiling in human PBMCs upon spore exposure. Due to restrictions imposed by COVID-19 human PBMCs could not be isolated for research and therefore this could not be performed.
- Bone-Marrow Derived Macrophage Knockout Investigations - to identify key receptors involved in macrophage recognition of *M. circinelloides*, BMDM knockouts for specific receptors (i.e. Dectin-2^{-/-}, MR^{-/-}) were to be employed. This would have enabled the determination of the role of specific mannose receptors involved in spore phagocytosis.

To compensate for disruptions to planned research, the following were undertaken:

(1) Cell Wall Characterization of *M. circinelloides* Spores During Germination

- Cell wall staining with fungal cell wall stains and characterising by means of flow cytometry and microscopy was employed to determine the compositions of known cell wall components during *M. circinelloides* germination
- TEM without optimisation and staining was performed to provide a descriptive analysis of ultrastructural changes in *M. circinelloides* spores during germination

(2) Determining Macrophage Receptors Mediating *M. circinelloides* Uptake

- Broad spectrum inhibition of mannose receptor(s) in a murine macrophage cell line was performed to determine the role of mannose receptors in *M. circinelloides* phagocytosis
- Alternative factors of *M. circinelloides*-macrophage interaction were investigated, such as phagosome maturation and spore killing.

TABLE OF CONTENTS

LIST OF FIGURES	XIV
LIST OF TABLES	XVI
LIST OF ABBREVIATIONS	XVII
1. INTRODUCTION	1
1.1 MUCORMYCOSIS – AN EMERGING FATAL FUNGAL INFECTION	1
1.1.1 EPIDEMIOLOGY	2
1.1.2 CAUSATIVE AGENTS	2
1.1.3 INFECTION AND CLINICAL PRESENTATION	3
1.1.3.1 RHINOCEREBRAL MUCORMYCOSIS	3
1.1.3.2 PULMONARY MUCORMYCOSIS	3
1.1.3.3 CUTANEOUS MUCORMYCOSIS	4
1.1.3.4 GASTROINTESTINAL MUCORMYCOSIS	4
1.1.3.5 DISSEMINATED MUCORMYCOSIS	4
1.1.3.6 MISCELLANEOUS MUCORMYCOSIS	5
1.1.4 DIAGNOSIS	6
1.1.5 TREATMENT	7
1.1.6 PRE-DISPOSING RISK FACTORS	8
1.1.6.1 DIABETES MELLITUS	8
1.1.6.2 IRON OVERLOAD	9
1.1.6.3 CORTICOSTEROID THERAPY	9
1.1.6.4 HEMATOLOGICAL MALIGNANCY	10
1.1.6.5 ORGAN TRANSPLANTATION	10
1.2 SPORE-TO-HYPHAE: GERMINATION AND PATHOGENESIS	10
1.2.1 CUES FOR GERMINATION	11
1.2.2 PHENOTYPIC CHANGES DURING GERMINATION	12
1.2.3 TRANSCRIPTOMICS OF GERMINATION	13
1.2.4 CHARACTERISATION OF GERMINATION IN <i>ASPERGILLUS</i>	13
1.2.4.1 PHENOTYPIC CHANGES DURING <i>ASPERGILLUS</i> GERMINATION	14
1.2.4.2 TRANSCRIPTIONAL PROFILING OF <i>ASPERGILLUS</i> GERMINATION	15
1.3 THE <i>MUCOR</i> CELL WALL	15
1.3.1 MELANIN	16
1.3.2 CHITIN AND CHITOSAN	17

1.3.3 GLUCAN	17
1.3.4 MANNAN	18
1.3.5 MUCORONIC ACID AND MUCORAN	18
1.4 CELL WALL BIOSYNTHESIS PATHWAYS	19
1.4.1 GLYCOSYLATION	20
1.4.1.1 ASSEMBLY OF THE LIPID-LINKED OLIGOSACCHARIDE	20
1.4.1.2 MODIFICATION OF THE GLYCAN CORE: <i>N</i> -LINKED GLYCOSYLATION	21
1.4.1.3 MODIFICATION OF THE GLYCAN CORE: <i>O</i> -LINKED GLYCOSYLATION	22
1.4.2 β -GLUCAN BIOSYNTHESIS	23
1.4.3 CHITIN SYNTHESIS	23
1.4.4 GPI PROTEIN BIOSYNTHESIS	24
1.5 MACROPHAGES IN INNATE IMMUNITY TO MUCORALES	25
1.5.1 PRRs IMPLICATED IN FUNGAL RECOGNITION	25
1.5.2 MACROPHAGE CLEARANCE OF PATHOGENS	26
1.5.2.1 INTERNALISATION	27
1.5.2.2 PHAGOSOME MATURATION	27
1.5.3 THE MACROPHAGE-MUCORALES INTERACTION	29
1.6 PLATELETS IN MUCORMYCOSIS	30
1.6.1 PLATELET FUNCTION	30
1.6.1.1 α -GRANULES	30
1.6.1.2 DENSE GRANULES	31
1.6.1.3 LYSOSOMAL GRANULES	32
1.6.1.4 SECONDARY MEDIATORS	32
1.6.2 PLATELETS AND IMMUNITY	33
1.6.3 PLATELET-BACTERIA INTERACTION	34
1.6.4 PLATELET-FUNGAL INTERACTION	36
1.6.5 PLATELET-MUCORALES INTERACTION	37
1.7 RESEARCH AIMS	38
2 MATERIALS AND METHODS	39
2.1 FUNGAL STRAIN AND GROWTH CONDITIONS	39
2.2 SPORE GERMINATION CHARACTERISATION	39
2.2.1 24-WELL PLATE CULTURE	39
2.2.2 FLASK CULTURE OPTIMISATION	39

2.3 RNA-SEQUENCING OF GERMINATING SPORES	40
2.3.1 SPORE PREPARATION	40
2.3.2 RNA EXTRACTION	40
2.3.3 LIBRARY PREPARATION AND RNA-SEQUENCING	41
2.3.4 BIOINFORMATIC ANALYSIS	42
2.3.5 ENRICHMENT ANALYSIS	44
2.4 CELL WALL CHARACTERISATION OF GERMINATING SPORES	44
2.4.1 SPORE PREPARATION FOR FLOW CYTOMETRY	44
2.4.2 CELL WALL STAINING AND IMAGING	44
2.4.3 TRANSMISSION ELECTRON MICROSCOPY	45
2.5 MACROPHAGE-<i>M. CIRCINELLOIDES</i> STUDIES	45
2.5.1 MACROPHAGE CULTURE AND CONDITIONS	45
2.5.1.1 STORAGE	46
2.5.1.2 THAWING	46
2.5.1.3 PASSAGING	46
2.5.2 PHAGOCYTOSIS ASSAY	47
2.5.2.1 SPORE PREPARATION FOR PHAGOCYTOSIS ASSAY	47
2.5.2.2 PHAGOCYTOSIS ASSAY	47
2.5.3 SPORE VIABILITY POST-PHAGOCYTOSIS	48
2.5.4 PHAGOSOME MATURATION	48
2.5.5 MANNAN INHIBITION	49
2.6 PLATELET – <i>M. CIRCINELLOIDES</i> INVESTIGATION	49
2.6.1 SPORE PREPARATION FOR AGGREGATION ASSAYS	49
2.6.2 BLOOD PREPARATION	49
2.6.3 PLATELET AGGREGOMETRY IN PRP	50
2.6.4 PLATELET AGGREGOMETRY IN WHOLE BLOOD	50
2.6.5 PLATELET STAINING AND MICROSCOPY	50
2.6.6 INHIBITOR TREATMENTS	51
2.6.7 PLATELET RECEPTOR LABELLING	51
2.7 STATISTICAL ANALYSIS	52
3 TRANSCRIPTIONAL PROFILING OF <i>MUCOR CIRCINELLOIDES</i> AT KEY SPORE DEVELOPMENTAL STAGES	53
3.1 INTRODUCTION	53
3.2 RESULTS	54

3.2.1 <i>M. CIRCINELLOIDES</i> SPORES SWELL SIGNIFICANTLY DURING GERMINATION	54
3.2.2 SPORE CONCENTRATION AFFECTS <i>M. CIRCINELLOIDES</i> SPORE SWELLING	56
3.2.3 <i>M. CIRCINELLOIDES</i> SPORE GERMINATION IS SUPPORTED BY SIGNIFICANT TRANSCRIPTIONAL CHANGES	57
3.2.4 A LARGE NUMBER OF <i>M. CIRCINELLOIDES</i> GENES PRODUCTS ARE UNCHARACTERISED	61
3.2.5 FUNCTIONAL ENRICHMENT ANALYSIS	62
3.2.5.1 TRANSCRIPTIONAL PROFILING CONFIRMS THAT SPORES BECOME METABOLICALLY ACTIVE EARLY IN GERMINATION	63
3.2.5.2 TRANSCRIPTIONAL PROFILING SHOWS SPORES DOWNREGULATE AUTOPHAGY AND STRESS RESPONSE IN EARLY GERMINATION	65
3.2.5.3 TRANSCRIPTIONAL PROFILING OF LATE GERMINATION SHOWS RESPONSE TO OXIDATIVE STRESS AND AUTOPHAGY IS UPREGULATED	67
3.2.5.4 TRANSCRIPTIONAL PROFILING OF LATE GERMINATION SHOWS CELL WALL BIOSYNTHESIS IS UPREGULATED	67
3.2.5.5 TRANSCRIPTIONAL PROFILING SHOWS PROTEIN TRANSLATION IS DOWNREGULATED DURING LATE GERMINATION	68
3.2.5.6 TRANSCRIPTIONAL PROFILING SHOWS <i>M. CIRCINELLOIDES</i> SPORES UPREGULATE GENES IMPLICATED IN CELL WALL BIOGENESIS DURING GERMINATION	70
3.2.5.7 TRANSCRIPTIONAL PROFILING SHOWS AUTOPHAGY AND PEROXISOME ORGANISATION IS DOWNREGULATED DURING <i>M. CIRCINELLOIDES</i> GERMINATION	70
3.2.6 CELL WALL-FOCUSSED ANALYSIS	73
3.2.6.1 CELL WALL BIOSYNTHESIS IS DIFFERENTIALLY EXPRESSED DURING <i>M.</i> <i>CIRCINELLOIDES</i> GERMINATION	73
3.2.6.1.1 ANALYSIS OF CELLULAR COMPONENT GO TERMS	73
3.2.6.1.2 ANALYSIS OF MOLECULAR FUNCTION GO TERMS	76
3.2.6.1.3 ANALYSIS OF BIOLOGICAL PROCESS GO TERMS	79
3.2.6.2 GENES ASSOCIATED WITH CHITIN SYNTHESIS ARE DIFFERENTIALLY EXPRESSED DURING <i>M. CIRCINELLOIDES</i> GERMINATION	82
3.2.6.3 GENES IMPLICATED IN β -GLUCAN SYNTHESIS ARE DIFFERENTIALLY EXPRESSED DURING <i>M. CIRCINELLOIDES</i> GERMINATION	84

3.2.6.4 GENES INVOLVED IN GLYCOSYLATION ARE UPREGULATED DURING <i>M. CIRCINELLOIDES</i> GERMINATION	86
3.2.6.5 CELL WALL BIOSYNTHESIS PATHWAYS ARE DIFFERENTIALLY EXPRESSED DURING <i>M. CIRCINELLOIDES</i> GERMINATION	92
3.2.7 <i>M. CIRCINELLOIDES</i> NRRL3631 CELL WALL CONTENT DISPLAYS DYNAMIC CHANGES DURING GERMINATION	99
3.2.7.1 MANNAN CONTENT INCREASES DURING GERMINATION	99
3.2.7.2 GERMINATION RESULTS IN INCREASE CHITIN SYNTHESIS	101
3.2.7.3 CELL WALL β -GLUCAN INCREASES IN LATE GERMINATION	104
3.2.8 <i>M. CIRCINELLOIDES</i> ULTRASTRUCTURAL CHANGES DURING GERMINATION	106
3.3 DISCUSSION	108
4 <i>M. CIRCINELLOIDES</i> SPORE DEVELOPMENT INFLUENCES ITS INTERACTION WITH MACROPHAGES	118
4.1 INTRODUCTION	118
4.2 RESULTS	119
4.2.1 MOI OPTIMISATION	119
4.2.2 <i>M. CIRCINELLOIDES</i> SPORE DEVELOPMENTAL STAGE INFLUENCES PHAGOCYTIC UPTAKE	121
4.2.3 <i>M. CIRCINELLOIDES</i> SPORE GERMINATION STAGE INFLUENCES ITS VIABILITY POST-PHAGOCYTOSIS	123
4.2.4 <i>M. CIRCINELLOIDES</i> SPORES DO NOT INDUCE PHAGOSOME MATURATION	125
4.2.5 <i>M. CIRCINELLOIDES</i> PHAGOCYTOSIS IS MEDIATED BY MACROPHAGE MANNOSE RECEPTORS	127
4.3 DISCUSSION	129
5 <i>M. CIRCINELLOIDES</i> INDUCES PLATELET AGGREGATION THROUGH INTEGRIN αIIBβ3 AND IgG RECEPTOR FcγRIIA	133
5.1 INTRODUCTION	133
5.2 RESULTS	134
5.2.1 <i>M. CIRCINELLOIDES</i> INDUCES PLATELET AGGREGATION IN WHOLE HUMAN BLOOD AND PRP	134
5.2.2 <i>M. CIRCINELLOIDES</i> SPORES FORM LARGE COMPLEX AGGREGATES WITH PLATELETS	137
5.2.3 PLATELET AGGREGATION IN RESPONSE TO <i>M. CIRCINELLOIDES</i> IS SUPPORTED BY INTEGRIN α IIB β 3, IgG RECEPTOR Fc γ RIIA, AND DOWNSTREAM SRC	

AND SYK TYROSINE KINASES	138
5.2.4. SECONDARY MEDIATORS TxA ₂ AND ADP SUPPORT <i>M. CIRCINELLOIDES</i> - INDUCED PLATELET AGGREGATION	140
5.2.5 <i>M. CIRCINELLOIDES</i> SPORES ACTIVATE PLATELETS	142
5.2.6 PLATELET SURFACE α IIb β 3 EXPRESSION INCREASES FOLLOWING <i>M. CIRCINELLOIDES</i> EXPOSURE	143
5.3 DISCUSSION	144
6.0 DISCUSSION	148
6.1 ENHANCING OUR UNDERSTANDING OF <i>M. CIRCINELLOIDES</i> GERMINATION	148
6.2 CELL WALL REMODELLING IN <i>M. CIRCINELLOIDES</i> DURING SPORE DEVELOPMENT	151
6.3 ENHANCING OUR UNDERSTANDING OF THE INTERACTION BETWEEN <i>M. CIRCINELLOIDES</i> AND MACROPHAGES	155
6.4 ELUCIDATING THE PLATELET ACTIVATION PATHWAY IN RESPONSE TO <i>M. CIRCINELLOIDES</i>	158
6.5 LIMITATIONS	
6.6 FUTURE PERSPECTIVES	160
REFERENCES	164
APPENDIX I: PUBLICATIONS	185
APPENDIX II: RNA-SEQUENCING SUPPLEMENTARY DATA	195
I. SEQUENCE QUALITY	195
II. TRANSCRIPTIONAL PROFILING OF <i>M. CIRCINELLOIDES</i> GERMINATION	195

LIST OF FIGURES

FIGURE 1.1	CLINICAL CATEGORIES OF MUCORMYCOSIS	5
FIGURE 1.2	MUCORALES SPORE GERMINATION	11
FIGURE 1.3	SCHEMATIC OF THE <i>MUCOR</i> SPORE AND HYPHAL CELL WALL	19
FIGURE 1.4	LIPID-LINKED OLIGOSACCHARIDE BIOSYNTHESIS PATHWAY	20
FIGURE 1.5	O-GLYCAN BIOSYNTHESIS PATHWAY	22
FIGURE 1.6	PHAGOSOME MATURATION	28
FIGURE 1.7	PLATELET GRANULE RELEASE	33
FIGURE 1.8	BACTERIAL-PLATELET ACTIVATION IS DEPENDENT UPON α IIb β 3 AND Fc γ RIIA.	36
FIGURE 2.1	RNA-SEQUENCING DATA ANALYSIS WORKFLOW	43
FIGURE 3.1	<i>M. CIRCINELLOIDES</i> SPORE SIZE DURING GERMINATION	55
FIGURE 3.2	<i>M. CIRCINELLOIDES</i> SPORE CONCENTRATION AFFECTS GERMINATION	56
FIGURE 3.3	PC AND MA PLOTS FROM RNA-SEQUENCING OF <i>M. CIRCINELLOIDES</i> GERMINATION	59
FIGURE 3.4	COMPARISON OF SIGNIFICANT DEGS DURING <i>M. CIRCINELLOIDES</i> GERMINATION	60
FIGURE 3.5	BIOLOGICAL PROCESS GENE ONTOLOGY (GO) TERMS ASSIGNED TO DEGS BETWEEN 0 HR AND 3 HR <i>M. CIRCINELLOIDES</i> GERMINATION.	66
FIGURE 3.6	BIOLOGICAL PROCESS GENE ONTOLOGY (GO) TERMS ASSIGNED TO DEGS BETWEEN 3 HR AND 6 HR <i>M. CIRCINELLOIDES</i> GERMINATION	69
FIGURE 3.7	BIOLOGICAL PROCESS GO TERMS ASSIGNED TO DEGS BETWEEN 0 HR AND 6 HR <i>M. CIRCINELLOIDES</i> GERMINATION	72
FIGURE 3.8	CELLULAR COMPONENT GO TERMS ASSIGNED TO DEGS BETWEEN 3 HR AND 6 HR SPORE GERMINATION.	75
FIGURE 3.9	MOLECULAR FUNCTION GO TERMS ASSIGNED TO DEGS BETWEEN 0 HR AND 3 HR <i>M. CIRCINELLOIDES</i> GERMINATION.	77
FIGURE 3.10	MOLECULAR FUNCTION GO TERMS ASSIGNED TO DEGS BETWEEN 3 HR AND 6 HR SPORE GERMINATION.	78
FIGURE 3.11	BIOLOGICAL PROCESS GO TERMS ASSIGNED TO DEGS BETWEEN 0 HR AND 3 HR SPORE GERMINATION.	80
FIGURE 3.12	BIOLOGICAL PROCESS GO TERMS ASSIGNED TO DEGS BETWEEN 3 HR AND 6 HR SPORE GERMINATION.	81
FIGURE 3.13	CELLULAR COMPONENT GO TERMS ASSIGNED TO DEGS BETWEEN 0 HR AND 6 HR SPORE GERMINATION.	96

FIGURE 3.14	MOLECULAR FUNCTION GO TERMS ASSIGNED TO DEGS BETWEEN 0 HR AND 6 HR SPORE GERMINATION	97
FIGURE 3.15	BIOLOGICAL PROCESS GO TERMS ASSIGNED TO DEGS BETWEEN 0 HR AND 6 HR SPORE GERMINATION	98
FIGURE 3.16	<i>M. CIRCINELLOIDES</i> SPORE MANNAN CONTENT INCREASES DURING SPORE SWELLING.	100
FIGURE 3.17	<i>M. CIRCINELLOIDES</i> TOTAL CHITIN CONTENT INCREASES DURING GERMINATION	102
FIGURE 3.18	<i>M. CIRCINELLOIDES</i> SURFACE EXPOSED CHITIN CONTENT INCREASES DURING GERMINATION	103
FIGURE 3.19	<i>M. CIRCINELLOIDES</i> β -GLUCAN CONTENT INCREASES DURING GERMINATION	105
FIGURE 3.20	<i>M. CIRCINELLOIDES</i> SPORE WALL DISPLAYS ULTRASTRUCTURAL CHANGES DURING GERMINATION	107
FIGURE 4.1	MOI OPTIMISATION	120
FIGURE 4.2	PHAGOCYTOSIS OF <i>M. CIRCINELLOIDES</i> SPORES IS DEPENDENT UPON SPORE DEVELOPMENT.	122
FIGURE 4.3	<i>M. CIRCINELLOIDES</i> SPORE VIABILITY POST-PHAGOCYTOSIS	124
FIGURE 4.4	<i>M. CIRCINELLOIDES</i> SPORES DO NOT INDUCE PHAGOSOME MATURATION IN MACROPHAGES.	126
FIGURE 4.5	INHIBITION OF MANNOSE RECEPTORS SIGNIFICANTLY INHIBITS <i>M. CIRCINELLOIDES</i> SPORE PHAGOCYTOSIS.	128
FIGURE 5.1	<i>M. CIRCINELLOIDES</i> INDUCES PLATELET AGGREGATION IN PRP AND WHOLE BLOOD	136
FIGURE 5.2	<i>M. CIRCINELLOIDES</i> SPORES FROM LARGE, COMPLEX AGGREGATES WITH HUMAN PLATELETS.	137
FIGURE 5.3	PLATELET AGGREGATION INDUCED BY <i>M. CIRCINELLOIDES</i> IS FACILITATED BY α IIB β 3, Fc γ RIIA AND DOWNSTREAM SRC AND SYK TYROSINE KINASES.	139
FIGURE 5.4	<i>M. CIRCINELLOIDES</i> INDUCED PLATELET AGGREGATION IS SUPPORTED BY SECONDARY MEDIATORS TxA ₂ AND ADP	141
FIGURE 5.5	<i>M. CIRCINELLOIDES</i> ACTIVATES PLATELETS UNDER AGGREGATING CONDITIONS	142
FIGURE 5.6	<i>M. CIRCINELLOIDES</i> INDUCES INCREASED SURFACE α IIB β 3 EXPRESSION BUT SURFACE Fc γ RIIA EXPRESSION REMAINS STABLE	144

LIST OF TABLES

TABLE 1.1	PRRs AND PAMPs IN FUNGAL INNATE IMMUNE RECOGNITION	26
TABLE 3.1	DIFFERENTIALLY EXPRESSED GENES DURING <i>M. CIRCINELLOIDES</i> GERMINATION.	58
TABLE 3.2	PRODUCT CHARACTERISATION OF SIGNIFICANT DEGS DURING <i>M. CIRCINELLOIDES</i> SPORE SWELLING.	62
TABLE 3.3.	COMPARISON OF GO TERMS ASSIGNED TO SIGNIFICANT DEGS DURING <i>M. CIRCINELLOIDES</i> SPORE GERMINATION.	63
TABLE 3.4	GENES ASSOCIATED WITH CHITIN SYNTHESIS ARE DIFFERENTIALLY EXPRESSED DURING <i>M. CIRCINELLOIDES</i> GERMINATION.	83
TABLE 3.5	GENES ASSOCIATED WITH β -GLUCAN SYNTHESIS ARE DIFFERENTIALLY EXPRESSED DURING <i>M. CIRCINELLOIDES</i> GERMINATION.	85
TABLE 3.6	GENES ASSOCIATED WITH GLYCOSYLATION ARE DIFFERENTIALLY EXPRESSED DURING <i>M. CIRCINELLOIDES</i> GERMINATION.	89
TABLE 3.7	SIGNIFICANT UPREGULATED GENES BETWEEN 0 HR AND 6 HR <i>M. CIRCINELLOIDES</i> GERMINATION.	95

LIST OF ABBREVIATIONS

%P	Percentage phagocytosis
%PM	Percentage phagosome maturation
ADP	Adenosine diphosphate
AI	Association index
ALG	Asparagine-linked glycosylation
ANOVA	Analysis of variance
ATP	Adenosine triphosphate
cDMEM	Complete Dulbecco's Modified Eagle Media
CFW	Calcofluor white
CLRs	C-type lectin receptors
ConA	Concanavalin A
CTAP-3	Connective tissue activating peptide 3
DEGs	Differentially expressed genes
DHN	1,8-dihydroxynaphthalene
diSPIM	Dual inverted Selective Plane Illumination Microscope
Dol-PP	Dolichol pyrophosphate
DOPA	3,4-dihydroxyphenylalanine
DPM	Dolichol phosphate mannose
EEA1	Early endosomal antigen 1
ER	Endoplasmic reticulum
FE	Fold-enrichment
FITC	Fluorescein isothiocyanate
FP-A	Fibrinopeptide A
FP-B	Fibrinopeptide B
GlcNAc	<i>N</i> -acetylglucosamine
GO	Gene ontology
GPI	Glycosylphosphatidylinositol
GSL	Glucan synthase-like
IgG	Immunoglobulin G
L-AMB	Liposomal amphotericin B

LAMP	Lysosome-associated membrane proteins
NLRs	NOD-like receptors
NOXs	NADPH oxidases
OST	Oligosaccharyltransferase
PAMPs	Pathogen-associated molecular patterns
PBS	Phosphate buffered saline
PC	Principle component
PF-4	Platelet factor 4
PFA	Paraformaldehyde
PI	Phosphatidylinositol
PI	Phagocytic index
PMA	Phorbol-12-myristate-13-acetate
PRRs	Pattern recognition receptors
ROS	Reactive oxygen species
SAB	Sabouraud dextrose
sfDMEM	Serum-free DMEM
TLRs	Toll-like receptors
TRAP	Thrombin receptor-activating peptide
TRITC	Tetramethylrhodamine conjugate
TxA₂	Thromboxane
TxA₂	Thromboxane
Tβ-4	Thymosin β-4
WGA	Wheat germ agglutinin

1 INTRODUCTION

1.1 MUCORMYCOSIS – AN EMERGING FATAL FUNGAL INFECTION

Mucormycosis - recently coined the 'black fungus' - is an opportunistic invasive fungal infection caused by filamentous fungi of the Mucorales order. Although considered a rare fungal infection, mucormycosis is a fatal invasive fungal infection, affecting primarily immunocompromised individuals and causing an estimated 500 cases per annum in the US (Rees *et al.*, 1998). Incidence of infection has risen over the past decade, and recently during the COVID-19 pandemic there has been a stark increase in reported cases of secondary mucormycosis infections, attributed to the increased use of corticosteroids in COVID-19 patients (Sen *et al.*, 2021). Corticosteroid treatment is a known risk factor for mucormycosis, amongst others, including diabetes mellitus ketoacidosis, solid organ transplantation and chemotherapy (Reid *et al.*, 2020; Skiada, Pavleas and Drogari-Apiranthitou, 2020, Sen *et al.*, 2021).

Diagnosis of mucormycosis is challenging and infection causes a range of clinical presentations. There is a heavy reliance on clinicians suspecting mucormycosis and confirming through means such as tissue biopsy and culture (Skiada, Pavleas and Drogari-Apiranthitou, 2020). Early intervention of invasive fungal infections improves treatment efficacy, and late diagnosis can prove fatal. Estimated mortality rates vary depending upon clinical category of infection, ranging from 50-70% for pulmonary mucormycosis, to >90% for disseminated mucormycosis (Spellberg, Edwards and Ibrahim, 2005, Roden *et al.*, 2005). Treatment for mucormycosis consists of antifungal therapy and often surgical debridement (Skiada *et al.*, 2018). Liposomal amphotericin B (L-AMB) and Isoavuconazole are the front-line drugs used against mucormycosis infections, however, their efficacy is poor estimated at approximately 50% for L-AMB, and global availability is poor due to their high cost (Lanternier *et al.*, 2015, Marty *et al.*, 2016, Hassan and Voigt, 2019).

1.1.1 EPIDEMIOLOGY

The reported cases of mucormycosis have been increasing worldwide over the past decade, especially in those with diabetes mellitus, and those who have undergone corticosteroid treatment for pre-existing conditions and/or infections (Petrikkos *et al.*, 2012, Chakrabarti *et al.*, 2006, Prakash and Chakrabarti, 2019, Skiada, Pavleas and Drogari-Apiranthitou 2020, Sen *et al.*, 2021). Reported mucormycosis cases in developed countries are generally lower than in developing countries, in particular in India where elevated incidence has been contributed to a larger population with diabetes mellitus and the preferential use of corticosteroids (Petrikkos *et al.*, 2012, Chakrabarti *et al.*, 2006, Prakash and Chakrabarti, 2019). A recent global review of reported cases of mucormycosis calculated incidence rates per million population to be 0.05-0.19 per million in India, although many cases are likely not reported due to poor diagnosis so published estimates are likely under-representative of the true incidence and prevalence of invasive mucormycosis (Petrikkos *et al.*, 2012, Cornely *et al.*, 2019).

1.1.2 CAUSATIVE AGENTS

There are 261 species in the Mucorales order, 38 of which have been reported as causative agents of mucormycosis (Walther, Wagner and Kurzai, 2019). The most common causative agents of mucormycosis are *Rhizopus* spp, *Mucor* spp and *Lichtheimia* spp., with their prevalence varying between countries (Skiada *et al.*, 2018, Reid *et al.*, 2020). In France, the most common causative agents are *Rhizopus* spp. (32%) followed by *Lichtheimia* spp. (29%), whilst in India *Rhizopus* spp. (61.5%) are predominantly causing mucormycosis, and the second most causative agent is *Apophysomyces* spp. (27%) (Lanternier *et al.*, 2012, Chakrabarti *et al.*, 2006). There are also several new emerging species, including *Mucor irregularis* and *Rhizopus homothallicus* (Prakash and Chakrabarti, 2019, Lu *et al.*, 2013).

1.1.3 INFECTION AND CLINICAL PRESENTATION

The hallmark of mucormycosis is angioinvasion, which results in thrombosis and tissue necrosis (Spellberg, Edwards and Ibrahim, 2005). The fungus adheres to and damages endothelial cells, enabling angioinvasion and haematological dissemination to other regions of the body (Liu *et al.*, 2010). The most common route of mucormycosis transmission occurs through the inhalation of sporangiospores; however, less frequently transmission can occur through the ingestion of spores, intravenous transmission, and contamination of skin trauma such as burns wounds (Camara-Lemarroy *et al.*, 2014, Hassan and Voigt, 2019). Mucormycosis can result in an array of clinical presentations with varying degrees of morbidity and mortality, dependent on clinical category of infection and underlying conditions (Hassan and Voigt, 2019, Hong *et al.*, 2013). Mucormycosis can be divided into six clinical categories: (1) rhinocerebral, (2) pulmonary, (3) cutaneous, (4) gastrointestinal, (5) disseminated and (6) miscellaneous (Figure 1.1).

1.1.3.1 RHINOCEREBRAL MUCORMYCOSIS

When Mucorales spores are inhaled into the oral and nasal mucosa, infection can occur in the nasal tissues, spreading to the paranasal sinuses and orbit, resulting in rhinocerebral mucormycosis (Camara-Lemarroy *et al.*, 2014). Sinus infections account for the majority of mucormycosis infections, with an estimated 39% of all global mucormycosis cases reported as sinus infections (Roden *et al.*, 2005). Rhinocerebral mucormycosis is seen more frequently in those with diabetes, and carries an estimated mortality rate of >45% (Hassan and Voigt, 2019). Symptoms include fever, swelling and congestion of sinuses, black lesions of the mouth and face, nose and eye discharge, and headache (Hassan and Voigt, 2019, Mohammadi *et al.*, 2014).

1.1.3.2 PULMONARY MUCORMYCOSIS

Pulmonary mucormycosis infections are the second-most common type of mucormycosis infections, accounting for approximately 24% of all globally reported cases and carrying an estimated mortality

rate of 76% (Roden *et al.*, 2005). Those undergoing chemotherapy or hematopoietic stem cell transplants have the highest association with pulmonary mucormycosis (Spellberg, Edwards and Ibrahim, 2005). The inhalation of Mucorales spores into the bronchioles and alveoli can result in the establishment of pulmonary disease, with symptoms including, chest pain, fever, cough and difficulty breathing (Bigby *et al.*, 1986, Wang *et al.*, 2016, Hassan and Voigt, 2019).

1.1.3.3 CUTANEOUS MUCORMYCOSIS

Cutaneous mucormycosis is the third-most common infection type with 19% of all mucormycosis cases attributed to cutaneous infections, and it occurs when lesions of the skin become infected with spores (Roden *et al.*, 2005, Hassan and Voigt, 2019). Immunocompetent individuals are at most risk to cutaneous infection of all the clinical mucormycosis infection categories, with 50% of mucormycosis infections in individuals with no underlying conditions being cutaneous (Roden *et al.*, 2005). Clinical presentation of cutaneous mucormycosis includes, skin ulcerations and blisters, redness and localised inflammation (Hassan and Voigt, 2019).

1.1.3.4 GASTROINTESTINAL MUCORMYCOSIS

Gastrointestinal mucormycosis is rare but most common in premature neonates, individuals with diarrhoea and malnutrition, and patients receiving peritoneal dialysis (Roden *et al.*, 2005, Hassan and Voigt, 2019). Infection is believed to result from the ingestion of Mucorales spores - most commonly from contaminated or spoiled food sources - and mortality is estimated at 85% (Hassan and Voigt, 2019, Roden *et al.*, 2005). Symptoms of gastrointestinal mucormycosis include nausea, vomiting, gastrointestinal bleeding, and abdominal pain (Hassan and Voigt, 2019).

1.1.3.5 DISSEMINATED MUCORMYCOSIS

Disseminated mucormycosis can occur as a result of any primary site of infection but is most commonly seen in those with pulmonary mucormycosis (Spellberg, Edwards Jr and Ibrahim, 2005).

Dissemination of infection is associated with astonishingly high mortality rates approaching 100% in some reports (Spellberg, Edwards Jr and Ibrahim, 2005, Roden *et al.*, 2005). Symptoms of disseminated mucormycosis vary depending upon infected organs, sites of angioinvasion and areas of tissue necrosis (Petrikkos *et al.*, 2012).

1.1.3.6 MISCELLANEOUS MUCORMYCOSIS

Miscellaneous forms of mucormycosis are rare and the least common, accounting for around 10% of all infections (Roden *et al.*, 2005, Petrikkos *et al.*, 2012). Infections belonging to this category of mucormycosis include mucormycotic endocarditis, peritonitis, osteomyelitis and pyelonephritis (Petrikkos *et al.*, 2012). Symptoms vary depending upon location of infection, for example, flank pain is a symptom of mucormycotic pyelonephritis, and joint pain and swelling is a symptom of mucormycotic osteomyelitis (Petrikkos *et al.*, 2012, Harrasser *et al.*, 2014).

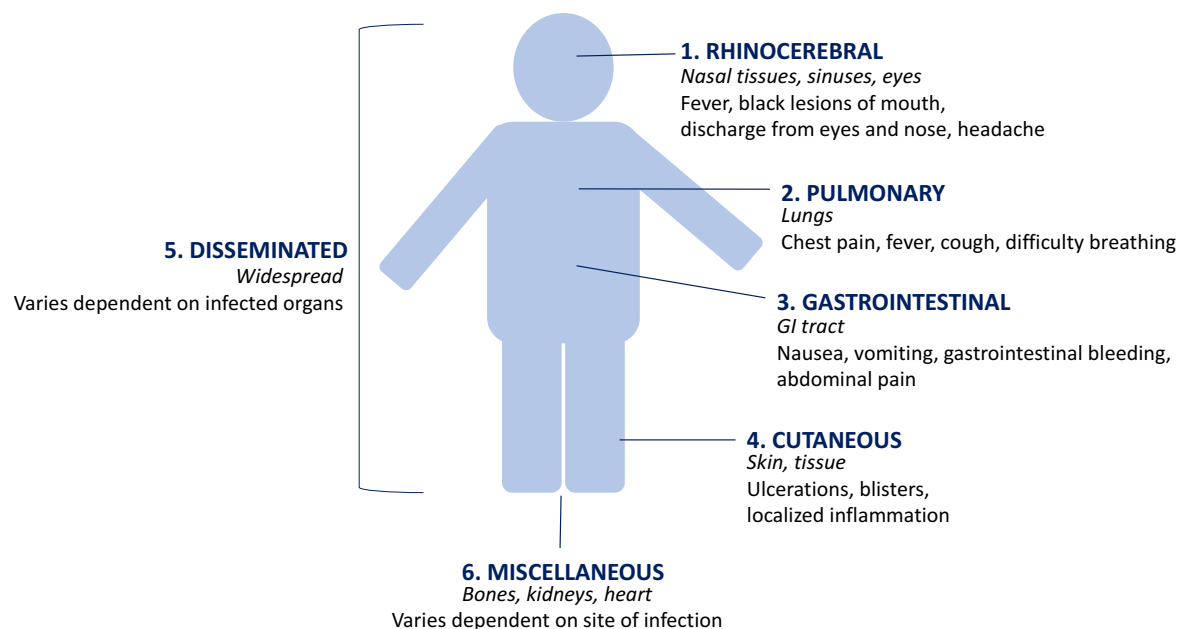


FIGURE 1.1 CLINICAL CATEGORIES OF MUCORMYCOSIS Mucormycosis is categorised based on location of infection into 6 categories: (1) rhinocerebral, (2) pulmonary, (3) gastrointestinal, (4) cutaneous, (5) disseminated and (6) miscellaneous. Symptoms vary dependent upon the infection type and organs affected.

1.1.4 DIAGNOSIS

The early diagnosis of mucormycosis is paramount in treatment, yet is challenging as there are no serological tests for mucormycosis commercially available or routinely in use (Chamilos, Lewis and Kontoyiannis, 2008, Richardson and Page, 2018). Delay in diagnosis correlates with poor prognosis and enhanced mortality (Chamilos, Lewis and Kontoyiannis, 2008). Current clinical diagnosis relies heavily upon a high index of suspicion, direct microscopy and histology, fungal culture, and recently the use of molecular tools such as polymerase chain reaction (PCR) assays (Skiada *et al.*, 2018). The recognition of the patient's susceptibility and risk factors for mucormycosis are key and can play a pivotal role in diagnosis (Skiada *et al.*, 2018, Cortez *et al.*, 2013).

Standard laboratory diagnosis of mucormycosis is achieved through direct microscopy by wet mount, culture and histopathology. Treatment of tissue samples with potassium hydroxide and subsequent staining with optical brighteners such as Calcofluor White, allow for rapid identification of filamentous fungi and characteristic Mucorales hyphae, that are coenocytic and exhibit varied degrees of branching (Skiada *et al.*, 2018). Although useful, direct microscopy is limited in that it cannot identify the genus of the fungus in question. Histopathology can again be used to determine the presence of Mucorales hyphae and whether angioinvasion and/or tissue necrosis is present. Tissue often displays extensive inflammation, with neutrophil and/or granuloma presence in those with progressive mucormycosis (Lass-Flörl, 2009, Skiada *et al.*, 2018). The culture of mucormycetes from biopsy material is difficult where tissue necrosis is prevalent or aggressive processing such as grinding (required to process hardened tissue) has occurred causing irreparable damage to hyphae (Lass-Flörl, 2009, Skiada *et al.*, 2018). If tissue samples are prepared with minimal manipulation; clinical Mucoralean species can be cultured on Saboraud dextrose agar at 37°C in 24 – 48 hr however efficacy of culture is low with a reported estimate of 50% positive cultures in mucormycosis cases (Lass-Flörl, 2009, Walsh *et al.*, 2012, Skiada *et al.*, 2018, Roden *et al.*, 2005).

Molecular methods offer a more sensitive means of diagnosis and may be required to confirm mucormycosis following a negative microbiological culture (Hammond *et al.*, 2011, Walsh *et al.*, 2012).

Internal transcribed spacer (ITS) sequencing and MALDI-TOF are recommended molecular methods for mucormycosis diagnosis (Cornely *et al.*, 2019). The development of aforementioned molecular methods enabling rapid and effective identification of Mucorales is promising in improving diagnostics.

1.1.5 TREATMENT

Current treatment for mucormycosis employs a multi-modal approach, including early and optimal dosage antifungal therapy, surgical debridement of infected tissues, and treatment of pre-disposing and underlying conditions (Skiada *et al.*, 2018). An extensive review of published evidence of mucormycosis management recommended the frontline antifungal, LAmB, should be employed to combat mucormycosis, and is recommended for use in a monotherapy approach (Cornely *et al.*, 2019). Furthermore, no strong evidence was shown to support the idea of combinational antifungal therapy being beneficial. Toxicity is associated with treatment using amphotericin B formulations, thus isavuconazole and posaconazole are recommended as salvage therapy options (Cornely *et al.*, 2019).

Surgical debridement is also recommended for mucormycosis treatment (Skiada *et al.*, 2013, Cornely *et al.*, 2019). Due to delayed diagnosis, disease progression and tissue damage is frequently too far gone to treat with antifungals alone (Skiada *et al.*, 2013). The combination of surgery and antifungal therapy enhances the chance of survival compared to antifungal treatment alone (Cornely *et al.*, 2019). However, surgical intervention is not always possible, for example, patients with haematological malignancies and/or thrombocytopenia are at high risk to secondary infections (Roden *et al.*, 2005, Skiada *et al.*, 2013).

Pre-disposing factors for mucormycosis include diabetes mellitus with ketoacidosis, hematologic malignancy, cancer, iron overload or deferoxamine treatment, and immunosuppressive therapy (Hong *et al.*, 2013). The control, or where possible, correction of underlying conditions is important in the treatment of mucormycosis (Skiada *et al.*, 2013, Cornely *et al.*, 2019). For example, by ceasing or reducing the use of corticosteroids, correcting normal acid-base levels in those with

diabetes with ketoacidosis, and avoiding iron overload, can enhance treatment of mucormycosis (Skiada *et al.*, 2013, Spellberg and Ibrahim, 2010). In particular, iron chelators such as deferasirox, have been shown to be favourable in mucormycosis treatment (Ibrahim *et al.*, 2007).

1.1.6 PRE-DISPOSING RISK FACTORS

There are several risk factors associated with mucormycosis, including, uncontrolled diabetes mellitus, iron overload, corticosteroid use, organ transplantation, and haematological malignancies (Ibrahim *et al.*, 2012). Diabetes mellitus is considered the main pre-disposing risk factor for mucormycosis, however the dominance of certain risk factor(s) varies dependent upon geographical location (Skiada, Pavleas and Drograri-Apiranthitou, 2020). Diabetes mellitus is the main risk factor for mucormycosis in Mexico and India, whilst haematological malignancy appears to be the major risk factor in France and Italy (Corzo-León *et al.*, 2018, Chakrabarti *et al.*, 2006, Patel *et al.*, 2020, Skiada, Pavleas and Drograri-Apiranthitou, 2020, Prakash and Chakrabarti, 2019). Pre-disposing risk factors can also be correlated with mucormycosis infection types, for example, diabetes mellitus is associated with rhinocerebral mucormycosis, and neutropenia with pulmonary mucormycosis (Skiada, Pavleas and Drograri-Apiranthitou, 2020).

1.1.6.1 DIABETES MELLITUS

Globally the prevalence of diabetes has increased over the past few decades, and when considering that it is the predominant risk factor associated with mucormycosis, it is unsurprising diabetes-associated mucormycosis incidences have also risen (Roden *et al.*, 2005, Jeong *et al.*, 2019, Skiada, Pavleas and Drograri-Apiranthitou, 2020). A systematic review reported diabetes mellitus was the most common underlying condition, with 20% of those individuals documenting ketoacidosis (Jeong *et al.*, 2019). Furthermore, diabetes mellitus was more frequently documented as an underlying condition in Asia than other regions of the world (Jeong *et al.*, 2019). An observational study on risk factors of mucormycosis in India reported 73.5 % of cases were associated with diabetes

mellitus, whilst a similar study of mucormycosis in France reported just 23% of cases were associated with diabetes mellitus (Patel *et al.*, 2020, Lanternier *et al.*, 2012).

1.1.6.2 IRON OVERLOAD

Elevated serum iron is a risk factor for mucormycosis, in particular in dialysis recipients receiving deferoxamine - an iron chelator (Ibrahim, Spellberg and Edwards, 2009, Maertens *et al.*, 1999). Individuals undergoing deferoxamine therapy are particularly susceptible to invasive *Rhizopus* infections (Ibrahim, Spellberg and Edwards, 2009). The drug aggravates infection, and associated mortality rates for such individuals are bleak, approaching 90% (Boelaert *et al.*, 1994). In a 10-year review of bone marrow transplant recipients, 1.9% of patients had reported mucormycosis, all of which had iron overload, yet none of which had been receiving chelation therapy (Maertens *et al.*, 1999). Whilst deferoxamine therapy is linked to enhanced risk of invasive mucormycosis, iron overload irrespective of chelator usage, can also render an individual more prone to disease and should be considered when assessing an individual's risk to invasive mucormycosis (Maertens *et al.*, 1999).

1.1.6.3 CORTICOSTEROID THERAPY

Corticosteroid and other immunosuppressive therapies are a risk factor for mucormycosis. They are used in a range of contexts, including transplantation, autoimmune diseases and recently in the treatment of COVID-19 (Youssef, Novosad and Winthrop, 2016, Ahmadikia *et al.*, 2021, Aranjani *et al.*, 2021). A review of mucormycosis cases in Europe between 2005 and 2007, reported that over 40% of mucormycosis patients had prior corticosteroid therapy (Skiada *et al.*, 2011). A retrospective study across India of COVID-19 associated mucormycosis cases showed over 75% of COVID-19 patients had undergone corticosteroid therapy (Patel *et al.*, 2020).

1.1.6.4 HEMATOLOGICAL MALIGNANCY

Haematological malignancy is the most common underlying condition in mucormycosis in Europe (Skiada, Pavleas and Drogari-Apiranthitou, 2020). Common malignancies associated with mucormycosis include acute myeloid leukaemia, acute lymphoblastic leukaemia and non-Hodgkin's lymphoma. A retrospective study of 37 patients with haematological malignancy and mucormycosis, showed that 89% of patients had neutropenia (Pagano *et al.*, 1997). Additionally, prolonged amphotericin B treatment was shown to be a key pre-disposing risk factor for mucormycosis in these patients (Pagano *et al.*, 1997).

1.1.6.5 ORGAN TRANSPLANTATION

Solid organ transplantation has been shown to be a risk factor of mucormycosis and has been reported in cases of renal, liver, heart and lung transplant patients (Almyroudis *et al.*, 2006). A review of solid organ transplant patients with mucormycosis reported the incidence of renal transplant-associated mucormycosis to be 0.4 - 0.5/1000 patients, 4 – 16 /1000 liver organ transplant-associated mucormycosis, 8/1000 heart transplant-associated mucormycosis and 13.7 – 14/1000 lung transplant-associated mucormycosis (Almyroudis *et al.*, 2006). Associated risk factors of mucormycosis in solid organ transplantation patients are diabetes mellitus, kidney failure and neutropenia (Skiada, Pavleas and Drogari-Apiranthitou, 2020, Almyroudis *et al.*, 2006).

1.2 SPORE-TO-HYPHAE: GERMINATION AND PATHOGENESIS

The germination of fungal spores is important for pathogenicity, and encompasses the process of exiting a state of dormancy to actively grow and filament. Maintenance of dormancy allows fungal spores to withstand harsh environmental conditions - such as extreme temperatures and UV exposure - until under favourable germination conditions. The underlying processes of mucormycete spore germination are complex and poorly understood. Germination cues vary between fungal species but include nutrient exposure, pH change and light (Sephton-Clark *et al.*, 2018). The germination of

Mucorales spores can be broadly described as occurring in two stages; (1) the swelling of ellipsoidal resting spores into spherical swollen spores by isotropic growth due to the uptake of water, and (2) the formation of germ tubes (hyphae) by apical growth once maximal swelling has been reached (Medwid and Grant, 1984, Cano and Ruiz-Herrera, 1988) (Figure 1.2). Disruption of the *cnbR* gene encoding the calcineurin B subunit results in *M. circinelloides* mutants locked in the yeast phase (Lee *et al.*, 2013). In a wax moth model, larvae infected with wild-type *M. circinelloides* display 100% mortality 2 days post-infection, however when infected with *cnbR* mutant *M. circinelloides* the mortality rate is 60-70% (Lee *et al.*, 2013). These data indicate germination plays a significant role in Mucorales virulence, particularly the spore-to-hyphae transition.

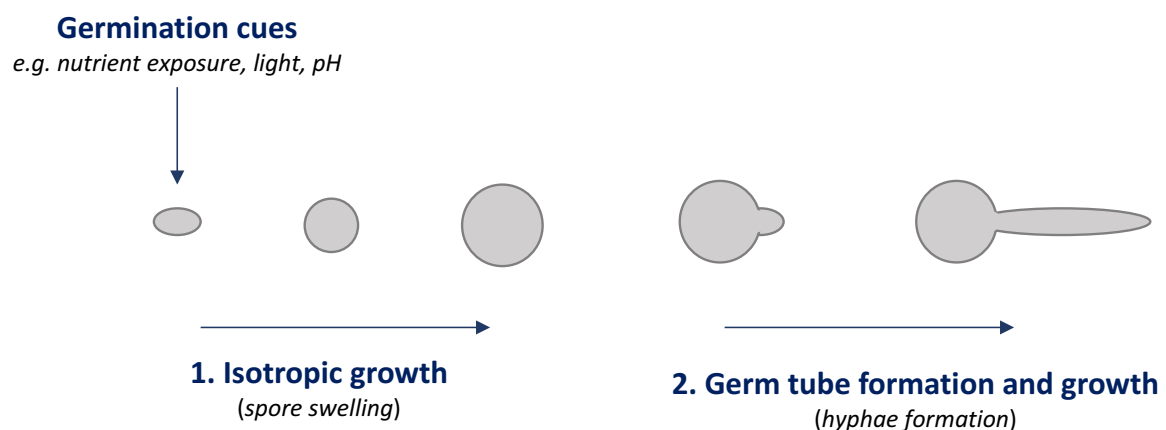


FIGURE 1.2 MUCORALES SPORE GERMINATION. Upon initiation of germination under favourable cues, Mucorales spores undergo: (1) isotropic growth, whereby spores swell, followed by (2) germ tube formation and growth, whereby spores form hyphae.

1.2.1 CUES FOR GERMINATION

Fungal spores are dormant until germination is triggered - a process that can be initiated by a variety of cues. There is little literature addressing the exact cues required for Mucorales spore germination, however exogenous nutrient and iron availability have been shown to be crucial (Medwid and Grant, 1984, Kousser *et al.*, 2019). *Rhizopus* spores appear to lack internal reserves of

nutrients required for germination (Medwid and Grant, 1984). Medwid and Grant (1984), showed that the swelling of *Rhizopus oligosporus* spores is dependent upon the presence of a suitable exogenous carbon source such as D-glucose, whilst germ tube extension requires both a suitable carbohydrate and nitrogen source, such as ammonium sulfate (Medwid and Grant, 1984). In addition to a suitable carbon and nitrogen source Medwid and Grant (1984), identified amino acids such as L-proline and L-alanine promote germination, although the mechanism(s) responsible were not determined (Medwid and Grant, 1984). Additionally, exogenous iron is shown to be crucial to Mucorales spore germination in low iron environments, such as serum (Kousser *et al.*, 2019, Carroll *et al.*, 2017). *Rhizopus*, *Mucor* and other Mucorales spp. secrete a siderophore called rhizoferrin, which chelates iron from the environment. Iron starvation inhibits germination, corroborated in a study showing that *Rhizopus delamar* co-culture with *Pseudomonas aeruginosa* results in the inhibition of *R. delamar* germination by the sequestration of iron by *P. aeruginosa* (Kousser *et al.*, 2019).

1.2.2 PHENOTYPIC CHANGES DURING GERMINATION

The germination of Mucorales spores encompasses spores exiting dormancy to undergo swelling, and then germ tube formation and filamentation (Sephton-Clark *et al.*, 2018). Resting spore size varies between strain and species, for example, *Mucor circinelloides* NRRL3631 resting spores are approximately 5 µm in diameter, whilst *Mucor circinelloides* R7B resting spores are approximately 12 µm in diameter (Li *et al.*, 2011). *Mucor* strains with larger resting spore size, such as *M. circinelloides* CBS277.49, produce germ tubes considerably faster (3-4 hr) than those with smaller resting spores, such as *M. circinelloides* NRRL3631 (6hr), and may even skip isotropic growth prior to germ tube emergence (Li *et al.*, 2011; López-Fernández *et al.*, 2018). The length and width of hypha vary between species and strain and are between 6-16 µm in width for example, *R. delamar* hyphae are approximately 5 µm in width and 135 µm in length (Ribes, Vanover-Sams and Baker, 2000, Sephton-Clark *et al.*, 2018).

1.2.3 TRANSCRIPTOMICS OF GERMINATION

Mucormycete spores exit a state of dormancy, where metabolic activity is low, and enter a stage of high metabolic activity upon germination (Thanh, Rombouts and Nout, 2005). Initially, in the germination process, spores take up water from their surrounding environment. Cano and Ruiz-Herrera (1988) showed the RNA and protein content of germinating *Mucor rouxii* spores increase by 10-fold and that there are three distinct steps in spore germination for which specific mRNAs and proteins are likely required; (i) acquisition of a spherical shape, (ii) reaching maximal spherical volume, and (iii) after germ tube emergence (Cano and Ruiz-Herrera, 1988). DNA biosynthesis occurs in the latter stages of spore germination, preceding germ tube elongation, with inhibition of DNA replication resulting in spores being incapable of forming germ tubes (Cano and Ruiz-Herrera, 1988).

Transcriptional changes during spore germination have been studied in *Rhizopus delamar* (Sephton-Clark *et al.*, 2018). Sephton-Clark *et al.* (2018), show dormant spores have a unique transcriptional profile compared to germinating spores. Resting spores are enriched for transcripts involved in respiration and stress response. Upon germination initiation and during isotropic growth, transcripts with roles in cell wall synthesis and protein synthesis are enriched (Sephton-Clark *et al.*, 2018). At 2 hr germination, more transcripts are downregulated than upregulated, suggested to be a result of the transcripts required for the initial stages of germination being degraded (Sephton-Clark *et al.*, 2018). During hyphal growth, transcriptional profiling showed transcripts with roles in oxidoreductase activity and stress response are enriched.

1.2.4 CHARACTERISATION OF GERMINATION IN *ASPERGILLUS*

The underpinnings of germination in filamentous fungi is best understood in *Aspergillus*, of the fungal order Eurotiales. *Aspergillus* undergoes a similar germination process whereby spores exit dormancy, undergo isotropic growth, and finally polarised growth where hyphae are formed (Baltussen *et al.*, 2020). Like *Mucor*, fungal spores of *Aspergillus* can withstand harsh conditions such as oxidative stress, thermal stress and pH stress. The ability of *Mucor* spores to withstand harsh

pressures has not been explained however in *Aspergillus* several conidial cell components lending the dormant spore protection to stress have been described (Baltussen *et al.*, 2020). Factors contained within the *Aspergillus* conidia provide protection from environmental stresses. Heat shock proteins provide thermotolerance and protection against pH stress, trehalose and mannitol offer protection against oxidative stress and dehydrins against osmotic stress. The conidia also display cell wall layers that enable the dormant spore to withstand harsh environmental conditions, for example, the presence of a hydrophobic rodlet layer comprised of RodA protein in *Aspergillus fumigatus* provides protection against desiccation and detection from human innate immune cells (Cagas *et al.*, 2011, Valsecchi *et al.*, 2017, Valsecchi *et al.*, 2020). Furthermore, an inner layer of the pigment melanin beneath the hydrophobin layer lends the dormant spores protection against environmental stresses such as UV exposure, and prevent phagocytosis and killing by macrophages (Geib *et al.*, 2016; Ferling *et al.*, 2020).

1.2.4.1 PHENOTYPIC CHANGES DURING ASPERGILLUS GERMINATION

The kinetics of conidia spore germination varies between species. Under optimal conditions, *A. fumigatus* conidia exit dormancy and the process of germination begins, although no morphological changes are seen in the first 90 minutes (Lamarre *et al.*, 2008). After 2 hr culture in YPD medium (1% yeast extract, 2% peptone and 2% dextrose) conidia swelling is noted, and hypha formation begins at around 4 hr. As previously described, Mucorales spores require the presence of exogenous materials, particularly carbon and nitrogen, for germination. This is in contrast to what is seen in Eurotiales. For example, *Aspergillus nidulans* conidia only require an exogenous carbon source, such as glucose, to begin germination (Oshero and May, 2000). Iron is an essential nutrient, and required for spore germination. *Aspergillus* contain internal and external siderophores for the acquisition of iron, and the presence of internal siderophores alone can be sufficient to undergo germination (Schrettl *et al.*, 2007). The cell wall of germinating conidia undergoes significant compositional change. Briefly,

conidia lose their outer RodA and melanin layers, unmasking the cell wall which is composed of polysaccharides including β -glucan and chitin (Cagas *et al.*, 2011, Valsecchi *et al.*, 2020)

1.2.4.2 TRANSCRIPTIONAL PROFILING OF *ASPERGILLUS* GERMINATION

Inhibition of DNA and RNA synthesis does not impair germination in *A. nidulans*, however inhibition of protein synthesis prevents germination, suggesting germination is dependent on translation but not transcription (Osherov and May, 2000). Pre-packaged mRNA transcripts are stored within dormant *Aspergillus* conidia, accounting for 27% of gene transcripts in dormant *A. fumigatus* (Lamarre *et al.*, 2008). Transcriptional changes are seen rapidly after germination begins (Lamarre *et al.*, 2008, van Leeuwen *et al.*, 2013). In *A. fumigatus* 25% of genes are differentially expressed within the first 30 minutes of germination, these include genes implicated in protein synthesis and amino acid metabolism (upregulated), cellular transport (upregulated), and cell wall remodelling (downregulated) (Lamarre *et al.*, 2008). Collectively, this suggests *Aspergillus* conidia contain stored mRNA transcripts enabling immediate protein synthesis and rapid germination. van Leeuwen *et al.* (2013) analysed the transcriptome of *Aspergillus niger* conidia during germination (van Leeuwen *et al.*, 2013). Here, dormant conidia were shown to be enriched in transcripts involved in stress protection, such as, trehalose, heat shock protein and catalase synthesis (van Leeuwen *et al.*, 2013). During the first 2 hr of germination, transcripts involved in protein synthesis are enriched, whilst in the latter stages of germination, transcripts involved in cell cycle and DNA processing are enriched (van Leeuwen *et al.*, 2013).

1.3 THE *MUCOR* CELL WALL

The fungal cell wall plays a crucial role in host-pathogen interaction, offering a variety of PAMPs to host immune cells, yet little is known about the composition of the *Mucor* cell wall and cell wall remodelling during spore germination. Generally, the fungal cell wall consists primarily of cross-linked chitin and chitosan, glucans, melanin and glycoproteins (Free, 2013). Components of the fungal

cell wall, such as β -glucan, are not found in mammals, thus making them an ideal target for novel therapeutics. An extensive literature review of research concerning the Mucorales cell wall highlighted findings from the 1960s and few novel findings since (Bartnicki-Garcia and Reyes, 1964, Bartnicki-Garcia and Reyes, 1968). Study of *Mucor rouxii* spore and hyphal cell wall components, showed that melanin, chitin and chitosan, glucan and mannan are found in the cell wall and their abundances change during germination from spore to hyphae (Figure 1.3).

1.3.1 MELANIN

Melanins are natural, dark pigments associated with various biological functions. Fungal melanisation is believed to offer a protective function against harsh environmental conditions and enhance fungal virulence. Despite being associated with various pathogenic properties, little is known about the structure of melanin itself, beyond that they are polymerized from phenolic and/or indolic compounds (Nosanchuk, Stark and Casadevall, 2015). Fungi can produce melanin through one of two pathways, (i) from 3,4-dihydroxyphenylalanine (DOPA), or (ii) from a 1,8-dihydroxynaphthalene (DHN) intermediate (Eisenman and Casadevall, 2012). Melanisation in *Cryptococcus* has been shown to occur through the DOPA pathway, mediated by laccase, which oxidises one of various precursors including, L- and D- DOPA into dopaquinone (Eisenman and Casadevall, 2012, Eisenman *et al.*, 2007). Melanin in *A. fumigatus* is synthesised via the DHN-pathway, mediated by a polyketide synthase encoded by *pksP*, that is essential in melanin biosynthesis (Stappers *et al.*, 2018; Heinekamp *et al.*, 2013). Melanisation in *Cryptococcus* plays a role in its pathogenicity, with over-expression of *LAC1* resulting in higher virulence *in vitro* and *in vivo* (Ngamskulrungraj *et al.*, 2011). Furthermore, disruption of the DHN-melanin pathway in *A. fumigatus* results in reduced mortality when compared to wild-type (Tsai *et al.*, 1998).

Melanin has been shown in the cell wall of *M. rouxii* spores (Bartnicki-Garcia and Reyes, 1964). Andrianaki *et al.* (2018) demonstrated the role of melanin in *Rhizopus* pathogenicity (Andrianaki *et al.*, 2018). *Rhizopus* conidia do not germinate following phagocytosis by alveolar macrophages and arrest phagosome maturation (Andrianaki *et al.*, 2018). Removal of melanin from conidia restores

phagosome maturation (Andrianaki *et al.*, 2018). Chemical comparison with DHN-melanin of *A. fumigatus* shows *Rhizopus* cell wall melanin is not synthesized via the same pathway, but appears to be synthesized by a copper-dependent tyrosine/laccase pathway (Andrianaki *et al.*, 2018).

1.3.2 CHITIN AND CHITOSAN

Chitin is a natural mucobiopolymer comprised of *N*-acetylglucosamine (GlcNAc) monomers, and has a structure similar to cellulose (Abo Elsoud and El Kady, 2019). The content of chitin varies in the fungal cell wall, between species and morphotypes. The polymer is synthesised by chitin synthases, which catalyse the transfer of GlcNAc to the polymer from UDP-GlcNAc (Abo Elsoud and El Kady, 2019, Garcia-Rubio *et al.*, 2020). Chitosan is formed by the deacetylation of chitin, and is formed of 1,4-linked 2-acetamido-2-deoxy-D-glucopyranose and 2-amino-2-deoxy-G-glucopyranose residues (Gachhi and Hungund, 1930).

Chitin and chitosan are found in the cell wall of many fungi, including Mucorales. Characterization of the cell wall of *Rhizopus oryzae* shows chitin and chitosan content increases over germination (Gachhi and Hungund, 1930). Campos-Takaki and Dietrich (2009), isolated the cell wall from the mycelium of several Mucoralean fungi, including *Mucor mucedo*, to investigate the content of polysaccharides, lipids and proteins (Campos-Takaki and Dietrich, 2009). Approximately 37-44% of the Mucoralean hyphal cell wall is composed of chitosan and chitin (Campos-Takaki and Dietrich, 2009).

1.3.3 GLUCAN

Glucan is a key structural polysaccharide in the fungal cell wall, and in most instances, is composed of linear β -1,3- and β -1,6- glucan branches (Garcia-Rubio *et al.*, 2020; Ruiz-Herrera and Ortiz-Castellanos, 2019; Kapteyn, Van Den Ende and Klis, 1999). β -glucans are synthesized by β -glucanases, and alongside chitin, form the backbone of the fungal cell wall maintaining cell rigidity and structure (Shematek and Cabib, 1980, Arroyo *et al.*, 2016). Bartnicki-Garcia and Reyes (1964) identified

glucan as the most abundant cell wall component in *Mucor* spores, accounting for 42.6% of the cell wall (Bartnicki-Garcia and Reyes, 1964). Chamilos *et al.* (2010) showed β -glucan abundance increases in *Rhizopus* from spore to hyphae (Chamilos *et al.*, 2010). *R. oryzae* has a *FKS* gene, encoding an integral membrane protein of the glucan synthesis complex (Ibrahim *et al.*, 2005). Ibrahim *et al.* (2005), investigated the effect of caspofungin – a β -1,3-glucan synthase inhibitor – on *R. oryzae* pathogenicity *in vivo*. Caspofungin treatment of diabetic mice infected with *R. oryzae* increased survival at low doses, indicating β -1,3-glucan plays a key role in *Rhizopus* virulence (Ibrahim *et al.*, 2005).

1.3.4 MANNAN

Mannans are found in the cell walls of yeast and filamentous fungi, and can be divided into three categories: (i) *N*-linked, (ii) *O*-linked and (iii) long mannan chains. In *Candida albicans*, *N*-linked mannans are composed of an α 1,6-mannose backbone with α 1,2-oligomannose sidechains, whilst *O*-linked mannans are composed of linear oligosaccharides, with one to seven α 1,2-linked mannose residues (Mora-Montes *et al.*, 2007). In *A. fumigatus*, mannans are found in the cell wall as long linear chains of α 1,6-, and α 1,2- linked mannose units (Henry *et al.*, 2016). The presence of mannan in the *M. rouxii* spore and hyphal cell wall has been previously reported (Bartnicki-Garcia and Reyes, 1964). Mannan content was shown to decrease during the transition from spore (4.8%) to hyphae (1.6%) (Bartnicki-Garcia and Reyes, 1964).

1.3.5 MUCORONIC ACID AND MUCORAN

Bartnicki-Garcia and Reyes (1968) investigated the presence of polymers containing glucuronic acid in the cell wall of *M. rouxii* spores and hyphae (Bartnicki-Garcia and Reyes, 1968). Mucoronic acid contains D-glucuronic acid in high abundance, contrarily, mucoran contains D-glucuronic acid in small quantities. The abundance of glucuronic acid in the *M. rouxii* cell wall is shown

to vary dependent upon developmental age. Hyphal cell wall content was approximated at 11.8% and spore cell wall content at 1.9% (Bartnicki-Garcia and Reyes, 1968).

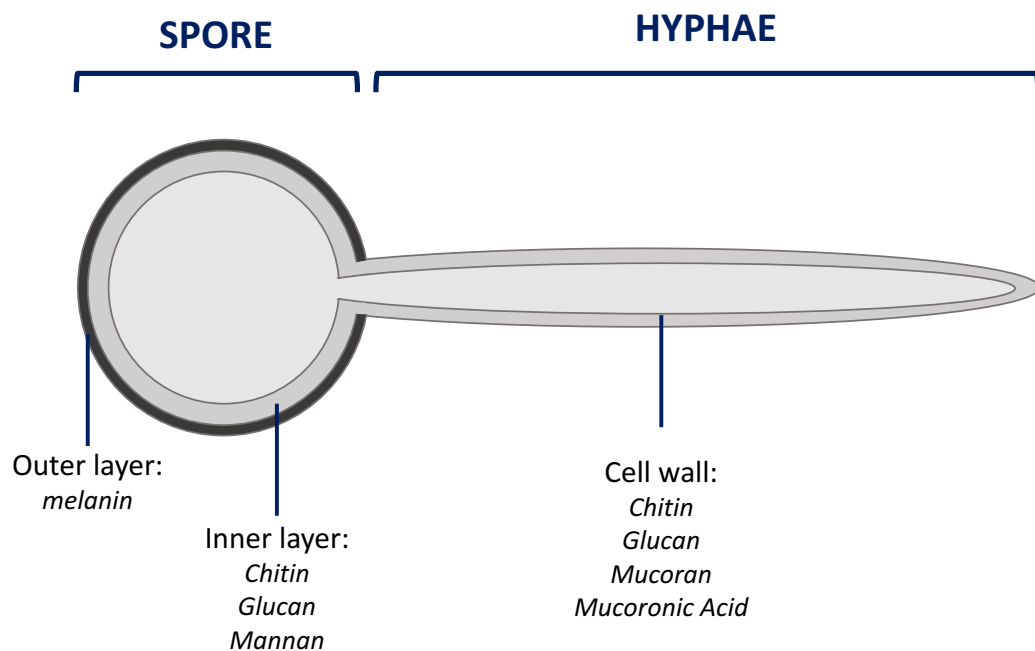


FIGURE 1.3 SCHEMATIC OF THE *MUCOR* SPORE AND HYPHAL CELL WALL. The cell wall of the *Mucor* spore is composed of an outer layer of melanin and an inner layer of polysaccharides including chitin, glucan and mannan. During germination, the melanin layer is shed, unmasking the inner layer of the cell wall, composed of chitin, glucan, mucoran and mucoronic acid. *Figure adapted from Lecointe et al. (2019).*

1.4 CELL WALL BIOSYNTHESIS PATHWAYS

Fungal virulence is in part owed to the cell wall making it an ideal target for novel antifungal strategies. In fungi such as *Saccharomyces cerevisiae* and *C. albicans*, cell wall architecture and biosynthesis pathways are well characterised. The genetic and molecular underpinnings of cell wall biosynthesis have not been explored in *Mucor*. Therefore, here the cell wall biosynthesis pathways for key fungal cell wall components, including mannan, glucan and chitin, in fungal pathogen *C. albicans* and/or *S. cerevisiae* are described.

1.4.1 GLYCOSYLATION

1.4.1.1 ASSEMBLY OF THE LIPID-LINKED OLIGOSACCHARIDE

Glycosylation is a post-translational modification that has been well studied in *S. cerevisiae* and *C. albicans* (Herscovics, 1999, Mora-Montes *et al.*, 2007). Glycosylation begins in the endoplasmic reticulum (ER) with the assembly of the dolichol pyrophosphate (Dol-PP)-linked oligosaccharide $\text{Glc}_3\text{Man}_9\text{GlcNAc}_2$, mediated by enzymes of the Asparagine-Linked Glycosylation (ALG) family (Figure 1.4). Here, the process begins in the cytosol through the activity of an enzyme complex, Alg7/Alg13/Alg14, which adds two GlcNAc from UDP-GlcNAc, to form Dol-PP-GlcNAc₂. Next, mannosyltransferases Alg1, Alg2 and Alg11 sequentially add five mannose residues to form Dol-PP-Man₅GlcNAc₂. The pre-cursor is then flipped into the lumen by Rft1, and mannosyltransferases Alg3, Alg9 and Alg12 add four mannose residues to form Dol-PP-Man₉GlcNAc₂. Finally, Alg6, Alg8 and Alg10 add three glucose to form the complete Dol-PP-GlcNAc₂Man₉Glc₃ precursor (Mora-Montes *et al.*, 2007).

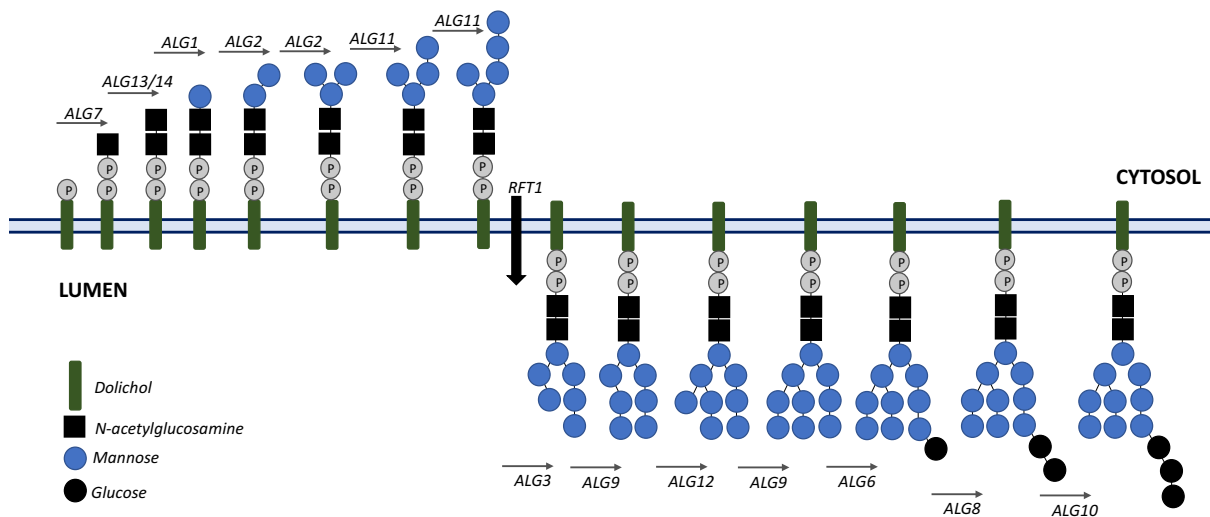


FIGURE 1.4 LIPID-LINKED OLIGOSACCHARIDE BIOSYNTHESIS PATHWAY. The lipid-linked oligosaccharide is synthesised in the ER, through the activity of transferases encoded by genes of the ALG family. *Figure adapted from Aebi, 2013.*

1.4.1.2 MODIFICATION OF THE GLYCAN CORE: N-LINKED GLYCOSYLATION

Following the assembly of the lipid-linked oligosaccharide by Alg enzymes, the oligosaccharide from Dol-PP- Glc₃Man₉GlcNAc₂ is transferred to an asparagine residue on nascent protein by the oligosaccharyltransferase (OST) complex. The yeast OST complex is comprised of eight subunits, grouped into sub-complexes, subcomplex 1 (Ost1 and Ost5), subcomplex 2 (Stt3, Ost4, Ost3/6) and subcomplex 3 (Wbp1, Swp1 and Ost2) (Shrimal and Gilmore, 2019). In *S. cerevisiae*, the terminal α 1,2-linked glucose is first removed by α -glucosidase I (*CWH41*), then two α 1,3-linked glucose residues are cleaved by α -glucosidase II (*ROT2*), and finally α -mannosidase (*MNS1*) removes one of the mannose residues, leaving Man₈GlcNAc₂ isomer B (Herscovics, 1999). Disruption of *CWH41*, *ROT2* and *MNS1* homologs in *C. albicans* display defective *N*-glycan outer-chain elongation, reduced cell wall phosphomannan and decreased cell wall integrity (Mora-Montes *et al.*, 2007).

In *Candida*, elongation of *N*-linked glycans by mannosyltransferases occurs in the Golgi following glycosylation in the ER. α 1,6-mannosyltransferase, Och1, adds an α 1,6-mannose to the *N*-linked glycan outer chain backbone, which is extended by enzyme complexes, mannan polymerase I (Mnn9 and Van1) and mannan polymerase II (Mnn9, Anp1, Mnn10, Mnn11 and Hoc1) (Gómez-Gaviria *et al.*, 2021). Branching of the α 1,6-mannose backbone is achieved via mannosyltransferases Mnt3, Mnt4, Mnt5, Mnn2 and Mnn5, which add α 1,2-oligomannans. In *C. albicans*, side chains are comprised of α 1,2- and α 1,3-linked mannose residues (Bates *et al.*, 2006). Capping of branches occurs via the addition of terminal α 1,3-mannose by α 1,3-mannosyltransferases Mnn1, Mnn12, Mnn13, Mnn14 and Mnn15. *N*-linked glycans can also be modified by phosphomannans, acting as molecular scaffolds to synthesize α 1,2-mannoligosaccharides, by mannosyltransferases Mnt3 and Mnt5 (Mora-Montes *et al.*, 2007).

In *S. cerevisiae* mannose residues are added by α 1,6-, α 1,2- and α 1,3-mannosyltransferases to form mature high mannose oligosaccharide cores of up to 13 mannoses, and large mannans containing outer chains attached to the core structure (Herscovics, 1999). In the Golgi, Och1 initiates outer-chain branching of *N*-glycans by the addition of a single α 1,6-linked mannose residue to the

Man₈GlcNAc₂ core. The α1,6-mannose backbone of the *N*-mannan outer chain is extended by the enzyme complexes mannan polymerase I and II, and branched side chains are attached by a range of Golgi mannosyltransferases (Mora-Montes *et al.*, 2007).

1.4.1.3 MODIFICATION OF THE GLYCAN CORE: O-LINKED GLYCOSYLATION

O-linked glycosylation begins in the ER, where α1,2-linked mannose residues are added to serine or threonine residues in the ER lumen. The process is catalysed by protein mannosyltransferases of the PMT family. In *S. cerevisiae*, seven PMT enzymes have been identified (Pmt1-7), whereas in *C. albicans* five PMT enzymes have been identified (Pmt1-2, and Pmt4-6) (Goto, 2007). Following mannosylation by PMTs, glycoproteins are transported to the Golgi where mannose residues are added by α1,2-mannosyltransferases (Figure 1.5). In *S. cerevisiae*, Kre2p/Mnt1p, Ktr1p and Ktr3p mediate the addition of the second and third mannose residues (Goto, 2007). In *C. albicans*, Mnt1 adds the second mannose and Mnt2 adds the third mannose. The *O*-linked glycans are then extended by the action of α1,3-mannosyltransferases. In *S. cerevisiae*, elongation is performed through the activity of Mnn1, Mnt2 and Mnt3, whilst in *C. albicans* elongation is achieved through Mnn5 (Goto, 2007).

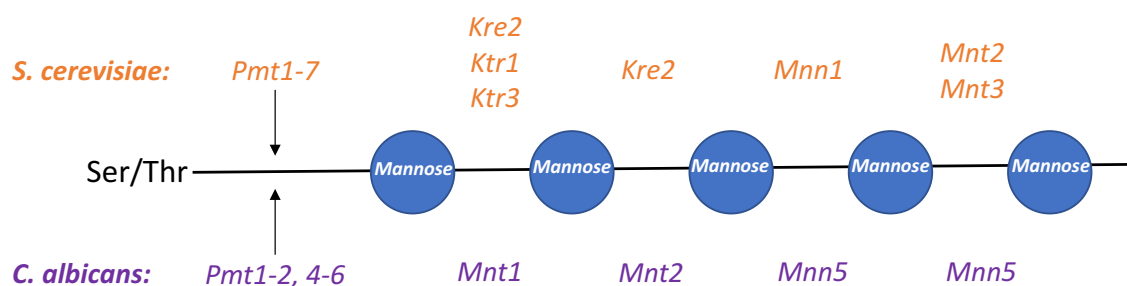


FIGURE 1.5 O-GLYCAN BIOSYNTHESIS PATHWAY. The first mannose residue is added by mannosyltransferases of the PMT family (*S. cerevisiae*: Pmt1-7; *C. albicans*: Pmt1-2, 4-6). Subsequent mannose residues are added through the activity of Mnt1, Mnt2 and Mnn5 in *C. albicans*, and Kre2, Ktr1, Ktr3, Mnn1, Mnt2 and Mnt3 in *S. cerevisiae*. Figure adapted from Goto, 2007.

1.4.2 β -GLUCAN BIOSYNTHESIS

Glucan is the most abundant cell wall polysaccharide of the fungal cell wall, and can be composed of β -1,3-, β -1,6-, β -1,4-, α -1,3- or α -1,4- linked glucose units. β -1,3-glucan is the most predominant form and its synthesis is well characterised in *S. cerevisiae* and *C. albicans*.

The synthesis of β -1,3-glucan is performed by β -1,3-glucan synthases, plasma membrane glucosyltransferases, that use UDP-glucose as a substrate to add glucose residues to the linear polymer (Frost *et al.*, 1994). In *S. cerevisiae*, genes *GSC1* (*FKS1*) and *GSC2* (*FKS2*) have been shown to encode the catalytic subunits of β -1,3-glucan synthase (Inoue *et al.*, 1995). Additionally, gene *RHO1p* encodes the GTP-binding protein Rho1p - the regulatory subunit of β -1,3-glucan synthase (Roh *et al.*, 2002). In *C. albicans*, *S. cerevisiae* *GSC1*/*FKS1* homolog, *GSC1*, and related glucan synthase-like (GSL) genes, *GSL1* and *GSL2*, were identified by Mio *et al.*, (1997).

The biosynthesis of β -1,6-glucan is not well characterised, however has been shown to be partially modulated by genes of the *KRE* family. In *S. cerevisiae*, *KRE1*, *KRE5* and *KRE6* are implicated in β -1,6-glucan biosynthesis (Boone *et al.*, 1990). Homologs of *S. cerevisiae* *KRE1*, *KRE5* and *KRE6* have been identified in *C. albicans* (Herrero *et al.*, 2004).

1.4.3 CHITIN BIOSYNTHESIS

The chitin content of yeast is approximated at 1-2%, whilst for filamentous fungi is approximated at up to 20% (Garcia-Rubio *et al.*, 2020). Chitin is a β -1,4-linked homopolymer of GlcNAc, synthesized through the activity of chitin synthases encoded for by several *CHS* genes (Munro and Gow, 2001, Lenardon, Munro and Gow, 2010). In *S. cerevisiae*, Chs1 is associated with deposition of chitin at the birth scar on daughter cells. Chs2 mediates chitin synthesis in primary septa and Chs3 deposits chitin at the bud scar of mother cells and on the lateral wall. Chs4-7 have been shown to regulate the activity of Chs3 (Munro and Gow, 2001, Lenardon, Munro and Gow, 2010).

In *C. albicans*, four chitin synthases have been identified, Chs1, Chs2, Chs3 and Chs8. Chs1 is an essential chitin synthase, necessary for the formation of the primary septum and maintaining the

integrity of the lateral cell wall (Munro and Gow, 2001). Chs2 plays a role in hyphal chitin deposition, Chs3 synthesises short chitin fibrils at the bud site during septum formation, and Chs8 synthesises long chitin fibrils. Chs3 has been shown to be responsible for the synthesis of approximately 90% of chitin in the *C. albicans* cell wall (Bulawa *et al.*, 1995, Mora-Montes *et al.*, 2011).

1.4.4 GPI PROTEIN BIOSYNTHESIS

GlycosylPhosphatidylinositol (GPI) proteins are found in the fungal cell wall, and act as anchors for cell wall proteins. The GPI anchor is added post-translationally to the protein C-terminal in the ER, and can be cleaved from the membrane and translocated to the cell wall. Here, they are covalently linked to cell wall glucans (Hamada *et al.*, 1999, Pittet and Conzelmann, 2007). Biosynthesis of GPI lipids begins with GlcNAc being added to phosphatidylinositol (PI), a process mediated by a multi-subunit enzyme complex comprised of Gpi3, Gpi1, Gpi2, Gpi15, Gpi19 and Eri1 (Pittet and Conzelmann, 2007). Following this, through the activity of Gpi12, GlcNH₂ is removed from PI-GlcNAc to give GlcN-PI. Next, inositol acylation of GlcN-PI occurs through the activity of Gwt1 in the ER. Following inositol acylation, mannose residues are added through the activity of several Gpi proteins. The first mannose residue is added to GlcN-acyl-PI from Dol-P-Man by Gpi14, the second by Gpi18, the third by Gpi10, and the fourth by Smp3 (Pittet and Conzelmann, 2007). Phosphorylethanolamine is added to the first mannose by Mcd4, to the second by Gpi7, and to the third by Gpi13, and to the second again by Gpi7. The GPI lipid is then transferred to the GPI protein in the ER, a process facilitated by a transamidase complex, which is composed of Gpi8, Gaa1, Gpi17, Gpi16 and Gab1. Subsequently, deacylation of inositol is performed by Bst1, and the GPI anchor is modified through the activity of Gup1 and Cwh43, the exact functions of which are yet to be characterised. The GPI anchors are finally, transported to the plasma membrane and can be incorporated into the cell wall. It is suggested that valine, isoleucine or leucine residues at the GPI attachment sites 4/5, and tyrosine or asparagine residues at attachment site 2 serve as signals for cell wall localisation in yeast (Hamada *et al.*, 1999).

1.5 MACROPHAGES IN INNATE IMMUNITY TO MUCORALES

The innate immune response is 'non-specific' and acts to cease pathogenic spread and prime the adaptive immune response by employing proteins and phagocytic cells to recognize and destroy pathogens. Physical barriers such as the skin and other epithelial surfaces, complement proteins, and immune effector cells such as macrophages and neutrophils, all play a role in innate immunity.

The recognition of pathogens by innate cells is at the crux of pathogenic clearance. This process is achieved through the recognition of conserved pathogen-associated molecular patterns (PAMPs) by innate cell surface receptors termed pattern recognition receptors (PRRs). Upon successful recognition, downstream signalling triggers innate cell activation and processes geared to pathogen destruction, such as phagosome maturation are initiated. Macrophages are a key innate immune effector, and the first innate cell encountered by pathogens. In zebrafish larvae infected with *M. circinelloides*, macrophage depletion with metronidazole resulted in significantly increased mortality to infection in comparison to that of immunocompetent larvae (Voelz, Gratacap and Wheeler, 2015). Understanding the macrophage-*Mucor* interaction is key to understanding the pathogenesis of this filamentous fungus, and could prove fruitful in the design of novel antifungal therapies.

1.5.1 PRRs IMPLICATED IN FUNGAL RECOGNITION

Innate immune responses are mediated through the interaction of PRRs and PAMPs. PRRs expressed on the surface of innate cells can be subdivided into classes, including Toll-like receptors (TLRs), C-type lectin receptors (CLRs), and NOD-like receptors (NLRs). Innate cells contain distinct but overlapping repertoires of PRRs, enabling targeted recognition of fungi, dependent upon the presence of their respective PAMPs (Table 1).

TABLE 1.6 PRRs AND PAMPs IN FUNGAL INNATE IMMUNE RECOGNITION. Several PRRs and PAMPs have been identified in the innate immune response to fungi. These include TLRs, CLRs and NLRs, and their respective fungal PAMPs, including β -1,3-glucan, chitin and mannose. *Adapted from Patin, Thompson and Orr, 2019*

Class	PRR	Innate Cell(s)	PAMPs/ Pathogen(s)	References
TLR	TLR2	Macrophage, DC, neutrophil	Phospholipomannan <i>C. albicans</i>	Jouault <i>et al.</i> , 2003, Ferwerda <i>et al.</i> , 2008, Chai <i>et al.</i> , 2009
	TLR4	Macrophage, DC, neutrophil	Mannan <i>C. albicans</i> , <i>A. fumigatus</i>	Tada <i>et al.</i> , 2002, Chai <i>et al.</i> , 2009
	TLR6	Macrophage	Phospholipomannan <i>C. albicans</i>	Netea <i>et al.</i> , 2008, Jouault <i>et al.</i> , 2003
	TLR9	Macrophage, DC	Unmethylated CpG motif-containing DNA <i>A. fumigatus</i> , <i>C. neoformans</i>	Ramirez-Ortiz <i>et al.</i> , 2008, Nakamura <i>et al.</i> , 2008
CLR	DECTIN-1	Macrophage, DC, neutrophil	β -1,3-glucan <i>C. albicans</i> , <i>A. fumigatus</i>	Thompson <i>et al.</i> , 2019, Gersuk <i>et al.</i> , 2006
	DECTIN-2	Macrophage, DC, neutrophil	α -mannan <i>C. albicans</i> , <i>A. fumigatus</i>	Saijo <i>et al.</i> , 2010, Loures <i>et al.</i> , 2015
	DECTIN-3	Macrophage	α -mannan <i>C. albicans</i>	Zhu <i>et al.</i> , 2013
	DC-SIGN	Macrophage, DC	Mannose <i>C. albicans</i> , <i>A. fumigatus</i>	Cambi <i>et al.</i> , 2008, Serrano-Gómez <i>et al.</i> , 2004
	MANNOSE RECEPTOR	Macrophage	Mannose <i>C. albicans</i> , <i>C. neoformans</i>	van de Veerdonk <i>et al.</i> , 2009, Dan <i>et al.</i> , 2008
	GALECTIN-3	Macrophage	β -1,2-mannosidase <i>C. albicans</i>	Esteban <i>et al.</i> , 2011
NLR	NOD-2	Macrophage, DC	Chitin <i>A. fumigatus</i> , <i>C. albicans</i>	Wagener <i>et al.</i> , 2014,

1.5.2 MACROPHAGE CLEARANCE OF PATHOGENS

Pathogenic clearance by macrophages is mediated primarily by intracellular killing. Following recognition of the pathogen –either directly by PRR-PAMP interaction or indirectly by opsonisation – macrophages internalise the microorganism in a process termed phagocytosis. Following recognition, clearance of pathogens is achieved by phagocytic killing, a process which can be subdivided into the following steps: (i) internalisation and (ii) phagosome maturation (Figure 1.6).

Phagocytic killing can be evaded by pathogens, through a range of strategies. For example, phagocytosed *C. albicans* trigger pyroptosis and produce hyphae, inducing programmed cell death and mechanical damage to the macrophage (Uwamahoro *et al.*, 2014). Dormant spores of *Rhizopus* spp. are able to persist and survive within the macrophage, a result of melanin-induced phagosome maturation arrest (Andrianaki *et al.*, 2018).

1.5.2.1 INTERNALISATION

Ligand-receptor binding triggers downstream signalling resulting in remodelling of the macrophage actin cytoskeleton directly underneath the phagocytic cup, where the pathogen is bound (Castellano, Chavrier and Caron, 2001). The exact mechanistic underpinnings of internalisation are yet to be reported, however several studies have elucidated key factors facilitating the process. In the widely-accepted zipper model of internalisation proposed by Griffin *et al.* (1975), it is suggested that sequential receptor-ligand interaction results in the re-arrangement of the macrophage membrane around the pathogen (Griffin *et al.*, 1975). Cytoskeletal rearrangement mediated by Fcγ-receptors and complement receptors is shown to be facilitated by Rho GTPases Rac1 and Cdc42, and the Arp2/3 complex (Caron and Hall, 1998, May *et al.*, 2000).

1.5.2.2 PHAGOSOME MATURATION

Upon internalisation, phagocytosed particles are contained within vesicles termed phagosomes, which undergo a process known as phagosome maturation. Phagosome maturation is achieved through the sequential delivery and removal of cargo by fusion and fission events, respectively. The process encompasses maturation of the phagosome in the following order: (i) early phagosome, (ii) late phagosome and (iii) phagolysosome. Briefly, in early phagosome maturation endosomes expressing surface protein Rab5, phosphatidylinositol 3-kinase, early endosomal antigen 1 (EEA1), fuse with the phagosome (Lee *et al.*, 2020, Lee *et al.*, 2018, Vieira *et al.*, 2003) (Figure 1.6). Rab4 and Rab11 facilitate the recycling of cargo to the plasma membrane or trans-Golgi network. In

the second stage of maturation, the early phagosome fuses with late endosomes expressing Rab7, so that the phagosome transitions from a Rab5-positive early phagosome to a Rab7-positive late phagosome (Lee *et al.*, 2020, Lee *et al.*, 2018, Vieira *et al.*, 2003). Finally, the late phagosome fuses with a lysosome through lysosome-associated membrane proteins (LAMP) -1 and -2. Lysosomes contain hydrolytic enzymes, such as proteases and DNAses, antimicrobial peptides, and NADPH oxidases (NOXs) that generate reactive oxygen species (ROS), ultimately creating an acidic and degradative environment for the phagolysosome-contained pathogen (Lee *et al.*, 2020, Lee *et al.*, 2018, Vieira *et al.*, 2003).

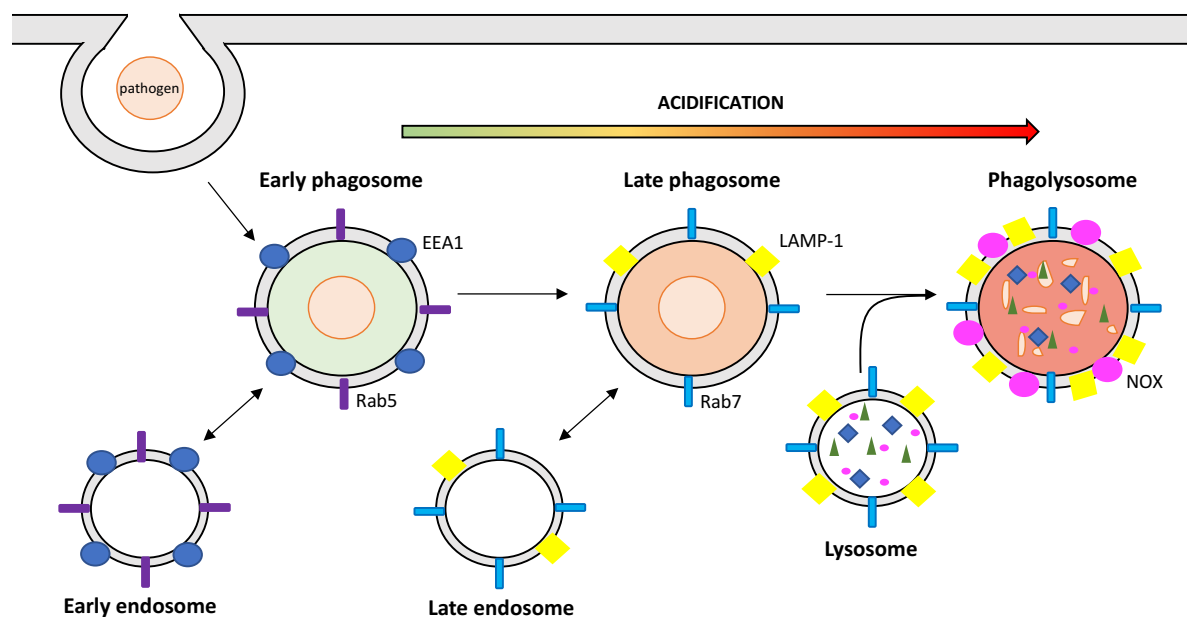


FIGURE 1.6 PHAGOSOME MATURATION Phagosome maturation is a key phagocytic process enabling the damage and degradation of pathogenic organisms. The process encompasses the transition of the phagosome from early phagosome, to late phagosome and finally phagolysosome. Through a series of fusion and fission events, the phagosome gradually becomes more acidic, owing in part to ROS generation by NOXs. Early phagosomes are characterised by Rab5 and late phagosomes by Rab7. Phagolysosomes contain a plethora of antimicrobial peptides, ROS and hydrolytic enzymes. *Figure adapted from Lee et al., 2020.*

1.5.3 THE MACROPHAGE-MUCORALES INTERACTION

The ability of Mucorales to evade phagocytosis is paramount to their dissemination within the host and their pathogenic success (Ibrahim and Voelz, 2017). Macrophages form part of the primary cellular line of defence against foreign organisms. In the classical sense, macrophages recognise pathogen-associated molecular patterns via pattern recognition receptors, enabling subsequent pathogen engulfment, degradation and antigen presentation.

Investigation of the interaction between *Lichtheimia corymbifera* and murine alveolar macrophages showed increased phagocytosis of a virulent strain compared to an attenuated strain (Kraibooj *et al.*, 2014). Whilst, resting spores and swollen spores of virulent *L. corymbifera* spores were more readily phagocytosed than their attenuated counterparts, resting spores and swollen spores of the virulent strain were phagocytosed to a similar degree. However, with the attenuated strain swollen spores were phagocytosed considerably more than resting spores (Kraibooj *et al.*, 2014). It has been suggested that the higher degree of phagocytosis of virulent spores may enable the macrophages being employed as a vector for dissemination, however this is yet to be proven (Kraibooj *et al.*, 2014, Ghuman and Voelz, 2017, Hassan and Voigt, 2019).

The influence of immunosuppression on macrophage-Mucorales interaction has been reported by Waldorf, Levitz and Diamond (1984). Bronchoalveolar macrophages of diabetic and cortisone-treated mice display a significantly reduced capacity to kill *R. oryzae* spores when compared to conidia of *A. fumigatus* (Waldorf, Levitz and Diamond, 1984). The ability of Mucorales spores to withstand phagocytosis under normal conditions is also evident, with *R. oryzae* spore killing by macrophages of normal mice being on par with those exposed to diabetic and cortisone-treated mice. A recent study showed phagocytes are recruited to the site of *M. circinelloides* infection in a zebrafish model (Inglesfield *et al.*, 2018). Dexamethasone treatment reduces the numbers of macrophages and neutrophils at the site of infection, and furthermore, the survival of *M. circinelloides* infected zebrafish in comparison to healthy controls is significantly reduced (Inglesfield *et al.*, 2018). Despite containment of *M. circinelloides* spores in phagocytic granulomas, spores withstand killing and

reactive oxygen burst is absent, enabling establishment of latent infection under immune suppression (Inglesfield *et al.*, 2018).

1.6 PLATELETS IN MUCORMYCOSIS

Platelets are anucleate blood cells that are traditionally associated with playing the role of maintaining haemostasis and thrombosis, and sealing damaged vasculature (Nurden, 2018). Recently, the role of platelets has been extended to include partaking in the resolution of inflammation, aiding immunity, and regulating angiogenesis (Nurden, 2018). Whilst the fundamentals of platelet function in thrombosis and haemostasis are well understood, the field of platelet immunology is relatively novel.

1.6.1 PLATELET FUNCTION

Platelet function is heavily mediated by secreted molecules, which are contained in membrane-bound granules in resting platelets (Ambrosio and Di Pietro, 2017). Platelet granule release is a regulated process, occurring upon platelet activation (Sharda and Flaumenhaft, 2018). Platelets contain three distinct types of secretory granules: (i) α -granules, (ii) dense granules and (iii) lysosomal granules (Figure 1.7). Upon platelet activation, intracellular granules release their contents, which play a crucial role in aiding the primary platelet functions of haemostasis and thrombosis, as well as secondary platelet functions such as inflammation, malignancy and angiogenesis (Golebiewska and Poole, 2015).

1.6.1.1 α -GRANULES

α -granules are the most abundant of the granules, with approximately 50-80 α -granules per platelet, (Blair and Flaumenhaft, 2009, Chen, Yuan and Li, 2018). The total α -granule membrane surface area is approximately $14 \mu\text{M}^2$, enabling the platelet surface membrane to increase up to 4-fold upon activation (Blair and Flaumenhaft, 2009). Multivesicular bodies and α -granules are formed

from budding vesicles in the megakaryocyte trans-Golgi network (Lo *et al.*, 2018). α -granules are transported into proplatelets along microtubule bundles, where they continue to develop to form mature platelets (Lo *et al.*, 2018). α -granule proteins are primarily synthesised in the megakaryocyte ER and transported to the Golgi body where they are sorted to α -granules (Blair and Flaumenhaft, 2009). α -granule cargo is not heterogeneous, for example, some stain for von Willebrand factor, whilst others stain for fibrinogen (Italiano *et al.*, 2008).

α -granules are primarily associated with coagulation, and contain large polypeptides that mediate primary and secondary haemostasis. α -granules secrete von Willebrand factor and fibrinogen, adhesive proteins mediating platelet-platelet and platelet-endothelial interactions (Blair and Flaumenhaft, 2009). In addition to adhesive proteins, adhesive receptors are also found in α -granules (Blair and Flaumenhaft, 2009). Amongst other surface receptors, integrin α IIb β 3 and collagen receptor GPVI can be found in α -granules (Wood, Wolff and Keller, 1986, Nurden *et al.*, 2004). α -granule contained α IIb β 3 and GPVI account for 2/3 and 1/3 of total receptor content in platelets respectively, and are released upon platelet activation (Blair and Flaumenhaft, 2009). Coagulation factors such as factor V, are also found in α -granules (Hayward *et al.*, 1995). Upon platelet activation, coagulation factors are released and partake in secondary haemostasis.

1.6.1.2 DENSE GRANULES

Dense granules are second most abundant to α -granules, with 3-8 δ -granules per platelet (Chen, Yuan and Li, 2017, Sharda and Flaumenhaft, 2018, Ambrosio and Di Pietro, 2017). Dense granules play a key role in haemostasis and contain high concentrations of small molecules such as adenosine diphosphate (ADP), adenosine triphosphate (ATP) and serotonin (Heijnen and Van der Sluijs, 2015, Ambrosio and Di Pietro, 2017). The release of ADP stimulates the platelet P2Y₁₂ receptor to act as a positive feedback mechanism for platelet aggregation and recruitment to site of injury (Dorsam and Kunapuli, 2004, Heijnen and Van der Sluijs, 2015).

Little is known with regards to δ -granule biogenesis however recently some similar and distinct mechanisms between δ -granule and α -granule biogenesis have been discerned. δ -granules are platelet-specific lysosome-related organelles, shown to form from the endosomal system not the trans-Golgi body as is shown with α -granules, and require distinct trafficking machinery (Ambrosio, Boyle and Di Pietro, 2012). Contents are transported into δ -granules by specific membrane pumps, such as ADP and ATP transport by vesicular nucleotide transporter VNUT (Hiasa *et al.*, 2014).

1.6.1.3 LYSOSOMAL GRANULES

Lysosomal granules contain proteolytic enzymes that aid the remodelling and resorption of clot formation (Rendu and Brohard-Bohn, 2001, Meng *et al.*, 2015). There are 1-3 lysosomes found per platelet (Sharda and Flaumenhaft, 2018, Rendu and Brohard-Bohn, 2001). The lysosomal membrane contains lysosomal integral membrane protein LIMP (CD63), a tetraspanin, and LAMP-1 and LAMP-2 (Nishibori *et al.*, 1993, Silverstein and Febbraio, 1992). These glycosylated membrane proteins sit on the luminal side of the lysosomal membrane and create a protective barrier to the hydrolytic enzymes within the granule (Rendu and Brohard-Bohn, 2001). Upon platelet activation and lysosome release, CD63 is expressed on the platelet surface (Kannan *et al.*, 1995).

1.6.1.4 SECONDARY MEDIATORS

Secondary mediators, such as thromboxane (TxA_2) and ADP are released upon platelet activation and act to recruit further platelets aiding thrombus formation (Figure 1.7). Secondary mediators act via G protein-coupled receptors, and downstream signalling pathways that results in increased formation and release of secondary mediators, acting as a positive feedback loop (Jantzen *et al.*, 1999, Paul, Jin and Kunapuli, 1999). Platelet activation by ADP occurs through, P2Y_1 and P2Y_{12} , whilst activation by TxA_2 occurs through the TxA_2 receptor (Jantzen *et al.*, 1999, Paul, Jin and Kunapuli, 1999).

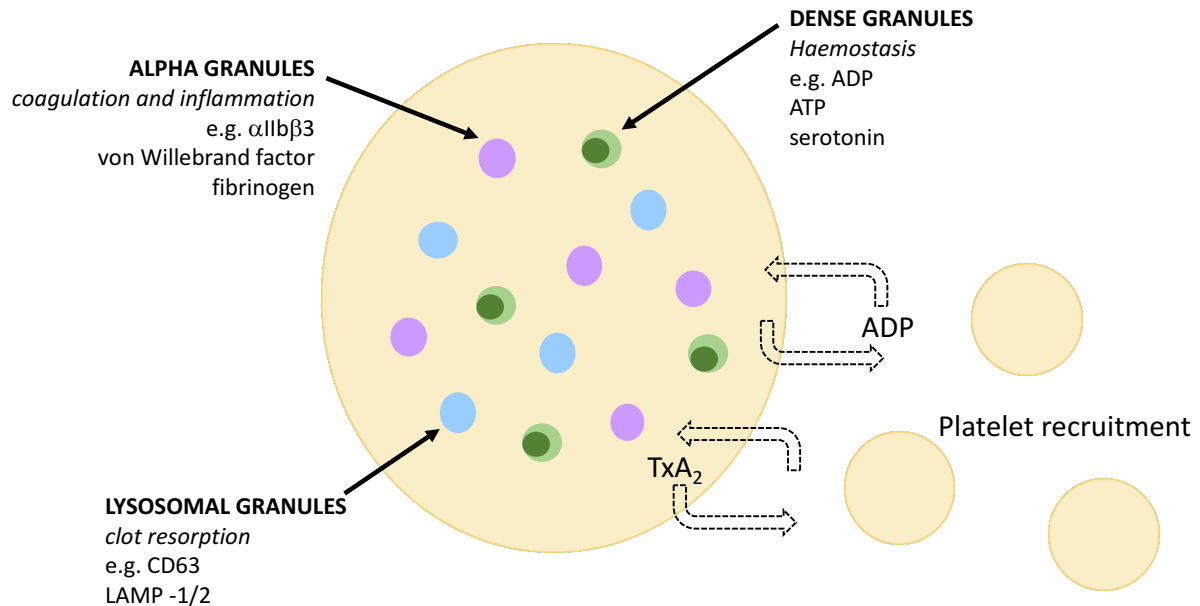


Figure 1.7 PLATELET GRANULE RELEASE. Upon activation, platelets release an array of factors from contained granules. Such granules are distinct in their cargo and affiliated functions. Alpha granules mediate coagulation and inflammation and contain factors such as fibrinogen. Dense granules play a role in haemostasis and contain factors such as ADP. Lysosomal granules aid clot resorption and carry plasma membrane-associated LAMP-1 and LAMP-2. In addition to granular release, secondary mediators such as ADP and TxA₂ are released. Secondary mediators partake in a positive feedback loop, whereby they recruit further platelets to the thrombus and generate their own release and activation.

1.6.2 PLATELETS AND IMMUNITY

Recently, platelets have been recognised as immune effectors (Tang, Yeaman and Selsted, 2002). There are similarities between platelets and phagocytes that suggests the role of platelets may be extended beyond the classical view of maintaining haemostasis and sealing damaged vasculature, to also include aiding pathogenic defence. For example, platelets and phagocytes both express P-selectin (Tchernychev, Furie and Furie, 2003). Furthermore, platelets generate ROS in response to micro-organisms and are chemotactic to complement proteins at sites of infection (Yeaman *et al.*, 1997, Zander and Klinger, 2009). The phagocytic ability of platelets and ability to release antimicrobial peptides has been shown with HIV and *Staphylococcus aureus* (Youssefian *et al.*, 2002, Seyoum, Enawgaw, and Mulugeta, 2018, Yeaman, 1997). Antimicrobial peptides include: platelet factor 4 (PF-4), RANTES, connective tissue activating peptide 3 (CTAP-3), platelet basic protein, thymosin β -4 (T β -4),

4), fibrinopeptide B (FP-B), and fibrinopeptide A (FP-A) (Tang, Yeaman and Selsted, 2002). The antimicrobial activity of platelet antimicrobial peptides has been investigated against *Escherichia coli*, *S. aureus*, *C. albicans* and *Cryptococcus neoformans* (Tang, Yeaman and Selsted, 2002). Platelet antimicrobial peptides show varying degrees of efficacy depending on the micro-organism and conditions (Tang, Yeaman and Selsted, 2002). For example, PF-4 and RANTES have broad spectrum antimicrobial efficacy, whereas FP-A, FP-B, platelet basic protein and CTAP-3 are ineffective against *C. albicans*, and T β -4 is ineffective against *C. albicans* and *C. neoformans* (Tang, Yeaman and Selsted, 2002).

1.6.3 PLATELET-BACTERIA INTERACTION

Infection has been associated with the development and progression of cardiovascular disease, endocarditis and sepsis (Arman *et al.*, 2014). The study of platelet-bacterial interplay has elucidated three modes of interaction: (1) direct binding of bacterial surface protein(s) to platelet surface receptor(s), (2) indirect binding of bacterial surface protein(s) to platelet receptor(s) via a bridging protein such as fibrinogen, and (3) binding of secreted bacterial protein(s) to platelet receptor(s) (Hamzeh-Cognasse *et al.*, 2015).

Direct bacteria-platelet binding has been shown in several species, such as *Streptococcus sanguinis* and *Staphylococcus aureus* (Kerrigan *et al.*, 2002, Miajlovic *et al.*, 2010). *S. sanguinis* is a Gram-positive bacterium that is associated with infective endocarditis, and that can cause heart failure and even death. A study investigating the mechanism of *S. sanguinis*-platelet interaction showed glycoprotein Ib inhibition resulted in abrogation of platelet activation and aggregation to *S. sanguinis* (Kerrigan *et al.*, 2002). GPIb is a receptor of plasma protein von Willebrand factor, however vWf was not essential for platelet activation by *S. sanguinis*, suggesting the bacterial-platelet interaction is direct. Further research identified a serine-rich glycoprotein known as serine rich protein A (SrpA) a key adhesin in the platelet-*S. sanguinis* interaction (Plummer *et al.*, 2005).

Indirect bacteria-platelet binding is mediated by plasma proteins such as fibrinogen (Arman *et al.*, 2014). *Staphylococcus aureus* expresses cell wall proteins clumping factor A and B, which bind to fibrinogen and immunoglobulin G (IgG), which interact with $\alpha\text{IIb}\beta 3$ and Fc γ RIIA, respectively (Arman *et al.*, 2014). Indirect platelet activation by bacteria can also be mediated by bacterial secreted toxins (Arman *et al.*, 2014). *Porphyromonas gingivalis* is a Gram-negative bacterium responsible for periodontal disease, and is the most abundant species found in the coronary and femoral arteries of patients with atherosclerotic cardiovascular disease (Mougeot *et al.*, 2017, Loubakos *et al.*, 2001). *P. gingivalis* secretes proteases known as gingipains, which activate platelets through protease-activated receptors, PAR-1 and PAR-4 (Loubakos *et al.*, 2001).

Platelet-bacteria interaction is mediated via a range of bacterial surface proteins and platelet receptors. Arman *et al.* show platelet surface integrin $\alpha\text{IIb}\beta 3$ and IgG receptor Fc γ RIIA are essential in platelet activation by a range of Gram-positive bacterial species (Arman *et al.*, 2014). Investigation of platelet activation by *Streptococcus sanguinis*, *Staphylococcus aureus*, *Streptococcus gordonii*, *Streptococcus oralis* and *Streptococcus pneumoniae* shows that the interaction with platelet immune receptor Fc γ RIIA and integrin $\alpha\text{IIb}\beta 3$ is essential in subsequent platelet activation and aggregation (Arman *et al.*, 2014). Inhibiting either $\alpha\text{IIb}\beta 3$ or Fc γ RIIA, led to significantly impaired platelet aggregation as recorded via light-transmission aggregometry, and a failure to activate platelets as measured by dense granule secretion (ATP release) and PF-4 secretion (Arman *et al.*, 2014). Similarly, it has been shown that Gram-negative bacteria *Escherichia coli* activates platelets through the same pathway, through $\alpha\text{IIb}\beta 3$ and Fc γ RIIA (Watson *et al.*, 2016). Downstream activation of the Src and Syk tyrosine kinases and the release of secondary mediators ADP and TxA₂ are also essential for platelet aggregation (Arman *et al.*, 2014, Watson *et al.*, 2016).

Research suggests a common pathway to bacterial-induced platelet aggregation, whereby interaction of platelet surface integrin $\alpha\text{IIb}\beta 3$ and IgG activates receptor Fc γ RIIA, which in turn activates downstream activation of the Src and Syk tyrosine kinases (Figure 1.8). Aggregation is supported by, and dependent upon the secondary mediators ADP and TxA₂.

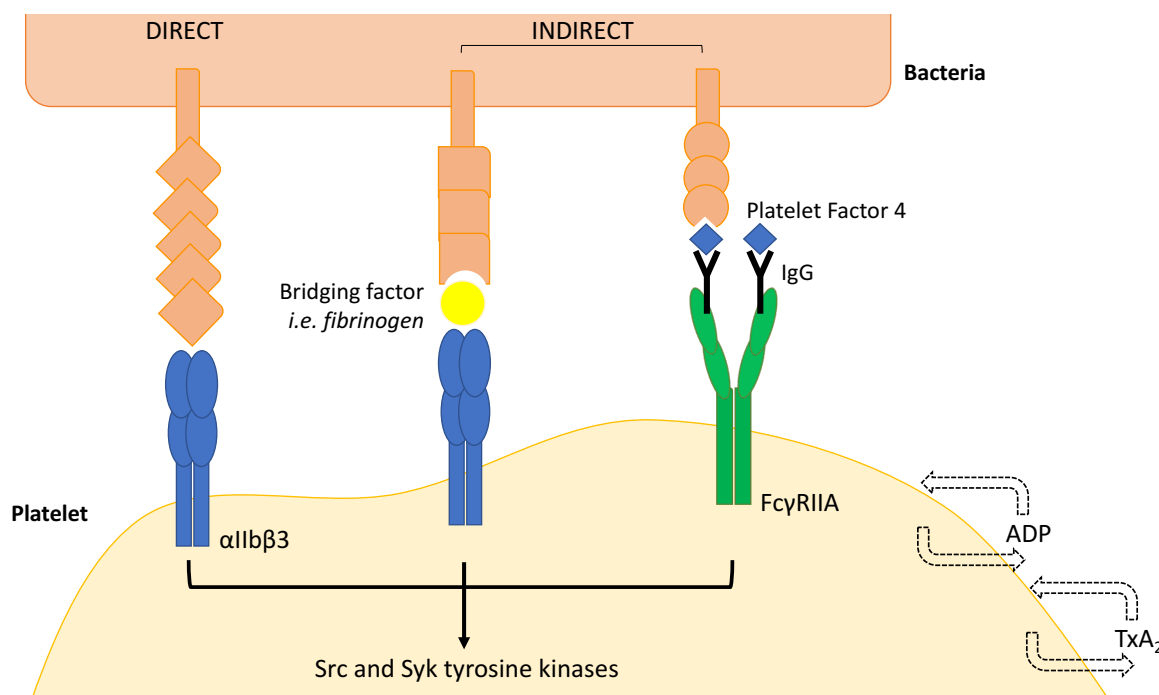


FIGURE 1.8 BACTERIAL PLATELET ACTIVATION IS DEPENDENT UPON α IIb β 3 AND Fc γ RIIA. A common pathway of platelet activation by bacteria has been proposed. Engagement of surface integrin α IIb β 3 and IgG receptor Fc γ RIIA results in the activation of the Src and Syk tyrosine kinases and subsequent platelet activation. Aggregation is supported through the activity of secondary mediators ADP and TxA₂.

1.6.4 PLATELET-FUNGAL INTERACTION

The interaction of platelets with fungi has been explored in several species, including *Aspergillus* and *Candida*. The key role of platelets in aspergillosis has recently been reported in a murine model (Tischler *et al.*, 2020). Thrombocytopenic mice are more susceptible to *A. fumigatus* infection and mortality is reached quicker than in healthy counterparts, indicating platelets play a key role in host immunity to *Aspergillus* (Tischler *et al.*, 2020). Platelets are also shown to be activated in response to *A. fumigatus* conidia and hyphae, displayed by the expression of platelet activation marker, CD62P (Rødland *et al.*, 2010). There is a marginal increase in platelet CD62P surface expression between resting conidia and swollen conidia, however a significant increase in expression

is displayed with platelets that are co-incubated with *A. fumigatus* hyphae (Rødland *et al.*, 2010). Furthermore, platelet release of lysosomal granules displayed by the platelet surface marker, CD63, is minimal in response to resting and swollen conidia, but considerably greater when platelets are exposed to hyphae (Rødland *et al.*, 2010). Together, this suggests platelets play a role in *Aspergillus* immunity, and germination and influences the interaction of *Aspergillus* with platelets.

C. albicans are not able to activate platelets, shown by platelet CD62P surface expression maintaining basal levels when exposed to *C. albicans* (Shultz *et al.*, 2020). Not only do platelets not aggregate when exposed to *C. albicans*, aggregation to agonist ADP is markedly dampened in the presence of *C. albicans*, suggesting an inhibitory effect of the fungus on platelet aggregation (Schultz *et al.*, 2020). Interestingly, *Candida albicans* viability is significantly reduced when incubated with releasate from platelets that have been pre-treated with the agonist, thrombin (Schultz *et al.*, 2020). This suggests platelets have indirect fungicidal properties against *Candida*.

1.6.5 PLATELET-MUCORALES INTERACTION

Thrombosis is a hallmark of mucormycosis, and thrombocytopenia is a pre-disposing risk factor. This suggests platelets may play a key role in the progression of this invasive fungal infection, however little is known regarding the platelet-Mucorales interaction. Platelets are shown to adhere to and inhibit the germination of *Rhizopus* and *Mucor* spores, potentially aiding the dampening of disease progression (Perkhofer *et al.*, 2009). Additionally, platelet activation following exposure to *Rhizopus* and *Mucor* spores and hyphae has also been shown, and platelets display antifungal properties noted through the damage of hyphae (Perkhofer *et al.*, 2009). The molecular underpinnings of platelet activation in response to Mucorales have not been described, however could prove fruitful in the design of novel therapeutic strategies.

1.7 RESEARCH AIMS

The ability of Mucorales spores to germinate and produce hyphae is integral to their pathogenic success, yet little is known about the germination process of this invasive fungal pathogen. During the process of germination, mucormycetes spores undergo a period of swelling, increasing considerably in size and displaying changes in cell wall composition. There are no current reports determining key changes occurring during *M. circinelloides* spore germination, nor the influence of developmental stage on host-interaction. This research was performed to enhance our understanding of *M. circinelloides* germination and its influence on host interaction.

The aims of this research were as follows:

- (1) To elucidate transcriptional changes during *M. circinelloides* germination (Chapter 3.0)
- (2) To characterise changes in the *M. circinelloides* cell wall during germination (Chapter 3.0)
- (3) To investigate *M. circinelloides*-macrophage interaction (Chapter 4.0)
- (4) To determine the platelet activation pathway in response to *M. circinelloides*. (Chapter 5.0)

2 MATERIALS AND METHODS

Materials and methods from 2.6 have been published in:

Ghuman H, Shepherd-Roberts A, Watson S, Zuidschewoude M, Watson SP, Voelz K. *Mucor circinelloides* induces platelet aggregation through integrin $\alpha\text{IIb}\beta 3$ and Fc γ RIIA. Platelets. 2019;30(2):256-263. doi: 10.1080/09537104.2017.1420152. Epub 2018 Jan 3. PMID: 29297721.

2.1 FUNGAL STRAIN AND GROWTH CONDITIONS

The *Mucor circinelloides* strain used was *Mucor circinelloides* f. sp. *lusitanicus* strain NRRL3631, a clinical isolate from the Queen Elizabeth Hospital (Birmingham, UK). For routine maintenance, the strain was grown on Sabouraud dextrose (SAB) agar (Merck-Millipore, Billerica, MA, USA) at room temperature for 7-14 days.

2.2 SPORE GERMINATION CHARACTERISATION

2.2.1 24-WELL PLATE CULTURE

M. circinelloides spores were collected in phosphate buffered saline (PBS) and centrifuged at $1811 \times g$ for three minutes. The spore pellet was then washed twice with PBS and re-suspended in SAB broth (Sigma-Aldrich, St. Louis, MO, USA) at 1×10^4 spores/mL. Spores in suspension were seeded in 24-well plates (1 mL per well; final concentration 1×10^4 spores/mL). Spores were imaged every 20 minutes over 12 hr and imaging was temperature-controlled at 37°C. Brightfield images were taken using 20x magnification on Nikon Eclipse Ti Live microscope (Nikon, Tokyo, Japan) with a QICAM Fast 1934 Digital Camera (QICAM, Surrey, BC, Columbia). Images were analysed using Fiji software. Spore size was calculated as $((\text{length}/2) \times (\text{width}/2)) \times \pi$.

2.2.2 FLASK CULTURE OPTIMISATION

M. circinelloides spores were collected in PBS and centrifuged at $1811 \times g$ for three minutes. The spores were washed twice with PBS and then re-suspended in SAB broth (Sigma-Aldrich, St. Louis, MO,

USA) at 1×10^4 spores/mL and 1×10^5 spores/mL. 50 mL spores in suspension was cultured in 250 mL flasks at 37°C with shaking at 45 rpm. Spores were collected at 6 hr germination and imaged using 20x magnification on Nikon Eclipse Ti Live microscope (Nikon, Tokyo, Japan) with a QICAM Fast 1934 Digital Camera (QICAM, Surrey, BC, Columbia). Images were analysed using Fiji software. Spore sizes of flask cultures were compared with those cultured in 24-well plates as per 2.2.1. At 6 hr germination spores of flask cultures at 1×10^4 spores/mL did not reach maximal swelling as determined in 2.2.1. Spores of flask cultures at 1×10^5 spores/mL did reach maximal swelling as determined in 2.2.1 and were therefore used for at this concentration in subsequent investigations, unless stated otherwise.

2.3 RNA-SEQUENCING OF GERMINATING SPORES

2.3.1 SPORE PREPARATION

Spores were collected and cultured in SAB broth at 1×10^5 spores/mL, as stated in 2.2.2 with the following amendment: culture times 0, 3 and 6 hr. Subsequently, spores were centrifuged at $1811 \times g$ for three minutes and spore pellet washed in PBS twice. The spore pellet was re-suspended in PBS and snap frozen in liquid nitrogen. Samples were stored at -80°C until RNA extraction.

2.3.2 RNA EXTRACTION

Spore samples were retrieved from -80°C and lysed by maceration, followed by bead beating. For maceration, liquid nitrogen was added to the sample and it was ground using pestle and mortar. TRIzol™ (Thermo Fisher Scientific, Waltham, MA, USA) was then added to the sample and it was ground again, followed by liquid nitrogen and a final round of grinding. The sample was then allowed to defrost, dispensed into an Eppendorf tube and placed in liquid nitrogen. For bead beating, RLT1 buffer (QIAGEN, Hilden, Germany) and 2-mercaptoethanol (Thermo Fisher Scientific, Waltham, MA, USA) was added to the sample, which was then transferred to a screw-capped tube containing glass

beads. Samples were bead beat for 5 cycles (2 x 20s @ 6500) with 5 minutes on ice between each cycle.

RNA extraction was performed using the QIAGEN RNeasy Plus Mini Kit (QIAGEN, Hilden, Germany) and all reagents stated in the remainder of this section are from QIAGEN unless stated otherwise. Samples were transferred into a QIA shredder column and centrifuged at 13,000 rpm for 2 min. Flow-through was then transferred into a gDNA eliminator column and centrifuged at 10,000 rpm for 1 min. 70% ethanol was added to supernatant and transferred into a RNeasy column and centrifuged at 10,000 rpm for 30 sec. Flow-through was discarded, RW1 buffer was added and centrifuged at 10,000 rpm for 30 sec. Next, RDD buffer:RNase free DNase, mix (7:1) was added to the centre of the spin column and incubated at room temperature for 20 min. RW1 buffer was added and centrifuged at 10,000 rpm for 30 sec. Flow-through was discarded and RPE buffer added, and centrifuged at 10,000 rpm for 30 sec. Flow-through was discarded and RPE buffer was added, and centrifuged at 10,000 rpm for 2 min. Flow-through was discarded and column was transferred to a collection tube and centrifuged at 13,000 rpm for 1 min. Column was transferred to 1 mL Eppendorf, RNase free water added, and incubated at room temperature for 1 min. Sample was centrifuged at 10,000 rpm for 1 min. Finally, RNase free water was added and incubated at room temperature for 1 min, and the sample was centrifuged at 10,000 rpm for 1 min. RNA concentration was confirmed using NanoDrop™ and samples were stored at -80°C.

2.3.3 LIBRARY PREPARATION AND RNA-SEQUENCING

Library preparation and RNA-sequencing was performed by GENEWIZ (GENEWIZ, Essex, UK) as a paid service. Library preparation encompassed target (non-ribosomal) RNA enrichment, fragmentation, reverse transcription (cDNA synthesis) and sequencing adapter ligation and amplification. Sequencing was performed using Illumina® NovaSeq™ (2 x 150 bp configuration). Briefly, this involves loading sequencing libraries onto flow cells, library hybridization to flow cell which are amplified to generate clustered clones, and sequencing cycles to allow sequential identification of

nucleotides within each cluster, building a digital image. Sequencing data was delivered as FASTQ files and corroborating quality reports.

2.3.4 BIOINFORMATIC ANALYSIS

FASTQ files from GENEWIZ were further analysed using VEuPathDB Galaxy Data Analysis Service, a free online platform, and workflow for 'RNA-Seq DESeq2: paired-end unstranded (V.4)' available at: <https://veupathdb.org/veupathdb/app/galaxy-orientation> . Briefly, FASTQ files were uploaded to Galaxy and a quality control step performed by the 'FASTQC' operation (Figure 2.1). Next, 'FASTQ Groomer' converted FASTQ files into Sanger-conforming fastq files for downstream application. The sequences were then trimmed by 'Trimmomatic', by the 'sliding window' operation, where trims are made when the average quality within a window is below a threshold (number of bases to average across:4, average quality required: 20). Next, sequences were aligned with a built-in reference genome (*Mucor lusitanicus* CBS277.49; FungiDB-51_Mlusitanicus CBS277-49_genome) by 'HISAT2'. BAM files were then converted to BigWig (coverage track) files by the 'BAM to BigWig' operation. Penultimately, aligned reads that overlap genomic features were counted by 'HTSEQ-COUNT' (genome annotation used: *M. lusitanicus* CBS277.49; FungiDB-51_Mlusitanicus CBS277-49_genome; minimum alignment quality:10). Finally, differentially expressed genes were determined using the 'DESeq2' operation (filter out absolute normalised reads with counts lower than 10.0). Principle Component (PC) plots were generated to investigate similarities within conditions between biological repeats. and between conditions themselves. Sequencing reads and gene hit count tables are available at the Gene Expression Omnibus (GEO) database (<https://www.ncbi.nlm.nih.gov/geo/>).

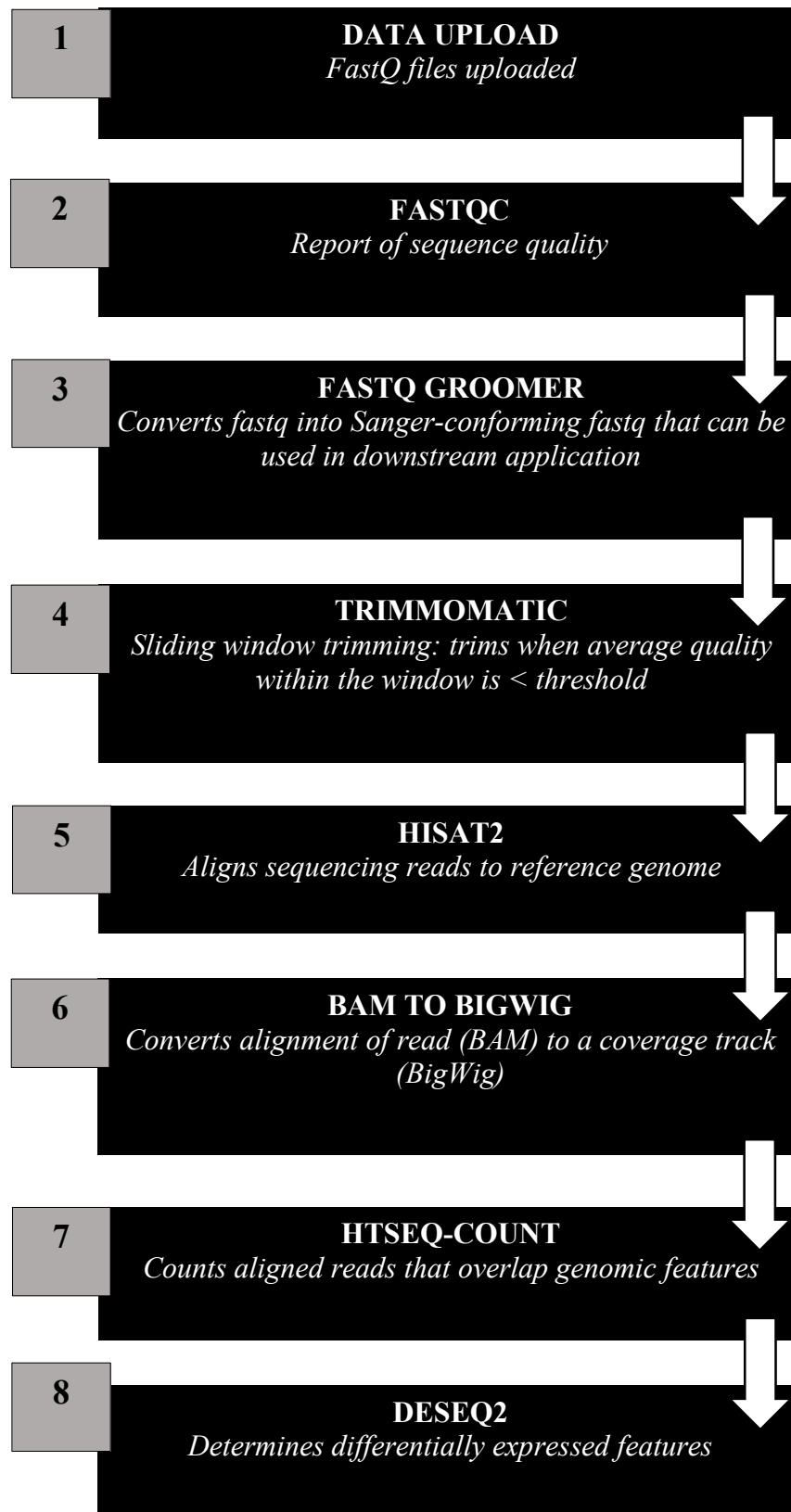


FIGURE 2.1 RNA-SEQ DATA ANALYSIS WORKFLOW. FASTQ files were analysed using the VeuPathDB Galaxy pipeline (<https://veupathdb.org/veupathdb/app/galaxy-orientation>).

2.3.5 ENRICHMENT ANALYSIS

Functional enrichment analysis was performed using the FungiDB pipeline (<https://fungidb.org/fungidb/app>). First, genes were determined to be differentially expressed if P_{adj} is ≤ 0.05 and the Log2fold change is ≥ 1 (upregulated) or ≤ -1 (downregulated). Genes meeting the aforementioned criteria were then input into the FungiDB pipeline and *Mucor lusitanicus* CBS277.49 used as the reference genome (*M. circinelloides* NRRL3631 genome unavailable). Gene Ontology (GO) enrichment was explored by across all three categories 'biological process', 'molecular function' and 'cellular component'. Statistical significance of GO terms assigned to the input genes is calculated by the FungiDB pipeline by the Fisher's exact test with the Benjamini and Hochberg method for false discovery rate (FDR) correction ($FDR \leq 0.05$). Enrichment of GO terms is calculated as: (number of input genes assigned to GO term/number of database genes assigned to the GO term). To infer greater detail, orthologs of notable genes were drawn from well-annotated genome of *Candida albicans* SC5314.

2.4 CELL WALL CHARACTERISATION OF GERMINATING SPORES

2.4.1 SPORE PREPARATION FOR FLOW CYTOMETRY

Spores were cultured as per 2.3.1 up to the point of snap freezing. Instead, the spore pellet was washed twice with PBS and re-suspended in 100 μ L 4% paraformaldehyde (PFA) (VWR International, Radnor, PA, USA) for 15 min. Spores were centrifuged at 1811 x g for five minutes and washed twice in PBS and kept at 4°C prior to staining.

2.4.2 CELL WALL STAINING AND IMAGING

Spores were centrifuged at 1811 x g for five min. Spore pellet was re-suspended in 2% Bovine Serum Albumin (Sigma-Aldrich, St. Louis, MO, USA) for 30 minutes at 4°C. Spores were centrifuged at 1811 x g and pellet washed with PBS three times. Spores were stained with Concanavalin A (ConA), Tetramethylrhodamine Conjugate (TRITC) (50 μ g ml^{-1} , Thermo Fisher Scientific, Waltham, MA, USA),

Wheat Germ Agglutinin (WGA) TRITC ($25 \mu\text{g ml}^{-1}$, Thermo Fisher Scientific, Waltham, MA, USA), Calcofluor White (CFW) ($0.1 \mu\text{g ml}^{-1}$, Sigma-Aldrich, St. Louis, MO, USA), or Fc-Dectin-1 ($3 \mu\text{g ml}^{-1}$) and secondary Goat F(ab')₂ Anti-Human IgG (γ) Alexa Fluor™ 488 (1:200, Thermo Fisher Scientific, Waltham, MA, USA). Flow cytometry analysis was conducted using an Attune NxT Flow Cytometer and BL1 and YL1 fluorescence channels (Thermo Fisher Scientific, Waltham, MA, USA). Samples were run for 10000 events, and cell count vs fluorescence recorded. Samples were also imaged using 20x magnification on Nikon Eclipse Ti Live microscope (Nikon, Tokyo, Japan) with a QICAM Fast 1934 Digital Camera (QICAM, Surrey, BC, USA). WGA-TRITC and Fc-Dectin-1-Alexa Fluor™ 488 in microscopy was too low to quantify, so only flow cytometry was used for these samples. CFW fluorescence range between 0 hr and 6 hr conditions fell outside the parameters of the flow cytometer, so only fluorescence microscopy was used for these samples. Images were analysed using Fiji software. Flow cytometry data was analysed used FLOWJO software.

2.4.3 TRANSMISSION ELECTRON MICROSCOPY

M. circinelloides spores were prepared as stated in 2.2.2 and frozen under high pressure using a Leica EM PACT 2 (Leica Microsystems, Milton Keynes, UK), and embedded in resin. 70 nm sections were cut and mounted on 400 mesh copper grids stained with 4.5% uranyl acetate in 1% acetic acid for 45 min, and Reynolds lead citrate for 7 min. Samples were imaged using a Jeol 1230 transmission electron microscope (JEOL Ltd., Tokyo, Japan) at 80 kV accelerating voltage, fitted with a Gatan 791 multiscan camera (Gatan, Inc., Pleasanton, CA, USA).

2.5 MACROPHAGE-*M. CIRCINELLOIDES* STUDIES

2.5.1 MACROPHAGE CULTURE AND CONDITIONS

The murine BALB/c monocyte macrophage cell line, J774A.1 (ATCC, Manassas, VA, USA), was used. Macrophages were cultured in complete Dulbecco's Modified Eagle Media (cDMEM) (Sigma-Aldrich, St. Louis, MO, USA) (cDMEM; 10% Fetal Bovine Serum (FBS), 1% Penicillin-Streptomycin and

1% L-Glutamine) at 37°C, 5% CO₂ in T75 culture flasks. Macrophages were used between passage 5 and 15. Macrophages were routinely stored in liquid nitrogen, thawed for use and passaged as described in 2.5.1.1-2.5.1.3.

2.5.1.1 STORAGE

At passage 2 and upon confluency, cDMEM was replaced with fresh media and macrophages transferred into 50 mL Falcon tubes. Suspension was centrifuged at 1000 x *g* for 7 minutes at 21°C. Supernatant was discarded and the cell pellet was resuspended in freezing media (50% FBS, 40% serum-free DMEM, 10% DMSO). 1 mL of cells in freezing media were aliquoted into cryovials and stored in -80°C for 24 hr. Finally, samples were transferred and stored in liquid nitrogen.

2.5.1.2 THAWING

Macrophages were retrieved from liquid nitrogen and thawed in a 37°C water bath. The sample was then transferred into a 15 mL Falcon tube containing 10 mL cDMEM and centrifuged at 1000 x *g* for 7 minutes at 21°C. Supernatant was discarded and the pellet resuspended in 15 mL cDMEM. Suspension was finally transferred into a T75 culture flask and incubated at 37°C, 5% CO₂ for 24 hr prior to subsequent passage.

2.5.1.3 PASSAGING

Macrophages were required to reach approximately 80% confluence prior to passage. Upon confluency, cDMEM was replaced with fresh media and cells were scraped and aliquoted into new T75 flasks for culture at 37°C, 5% CO₂, at dilutions ranging from 1/2 to 1/10 depending on desired time to reach confluency.

2.5.2 PHAGOCYTOSIS ASSAY

2.5.2.1. SPORE PREPARATION FOR PHAGOCYTOSIS ASSAY

Spores were collected in PBS and centrifuged at 1811 x *g* for three min. The spore pellet was washed twice with PBS and then re-suspended in SAB broth (Sigma-Aldrich, St. Louis, MO, USA) to 1 x 10⁵ spores/mL. Spores were cultured at 37°C with 45 rpm shaking for 0, 3 and 6 hr. Following this, spores were pelleted at 1811 x *g* for three minutes and the pellet was washed twice with PBS. Finally, the pellet was resuspended in serum-free DMEM (sfDMEM) (1% Penicillin-Streptomycin and 1% L-Glutamine) at the concentration required in the phagocytosis assay.

2.5.2.2 PHAGOCYTOSIS ASSAY

Macrophages were seeded in cDMEM and incubated at 37°C, 5% CO₂ overnight to allow for 1 x 10⁵ cells/well the following day and *M. circinelloides* spores were prepared as per 2.5.2. Macrophages were washed with PBS twice and then serum-starved by incubating in serum-free DMEM (sfDMEM) and 150 ng/mL phorbol-12-myristate-13-acetate (PMA) for 1 hr to activate macrophages. sfDMEM + PMA was then replaced with fresh sfDMEM and spores were added at the following concentrations for (a) MOI determination: (i) 1 x 10⁵ spores/well, (ii) 2.5 x 10⁵ spores/well, and (iii) 5 x 10⁵ spores/well or (b) all other experiments: 5 x 10⁵ spores/well. Spores and macrophages were incubated for 2 hr at 37°C, 5% CO₂. Following incubation, macrophages were washed with PBS twice and cells were fixed in 4% PFA, at room temperature for 10 min. Following fixation, cells were washed with PBS twice. To identify spores that have been phagocytosed, samples were stained with 50 µg/mL ConA-TRITC (Thermo Fisher Scientific, Waltham, MA, USA) for 30 min. Samples were then washed with PBS thrice and imaged using 20x magnification on Nikon Eclipse Ti Live microscope (Nikon, Tokyo, Japan) with a QICAM Fast 1934 Digital Camera (QICAM, Surrey, BC, Columbia). Images were analysed using Fiji software.

Spores displaying no fluorescence were counted as phagocytosed, whereas those displaying fluorescence were counted as adhered/unphagocytosed. Phagocytic index (PI) was calculated as (total

number of phagocytosed yeast)/(total number of macrophages) x 100, association index (AI) was calculated as (total number of associated and phagocytosed yeast)/(total number of macrophages) x 100, and percentage phagocytosis (%P) was calculated as (number of phagocytosed yeast/number of phagocytosed and associated yeast) x 100.

2.5.3 SPORE VIABILITY POST-PHAGOCYTOSIS

Spores and phagocytosis assays were conducted as per 2.5.2-2.5.3. Spores were incubated with macrophages over 0, 2 and 18 hr at 37°C, 5% CO₂. Following phagocytosis, cells were washed in PBS thrice to remove unphagocytosed spores/hyphae, and macrophages lysed with 1 mL ddH₂O. Suspension was then aspirated, spores pelleted and washed a further two times in PBS, and a spore count taken. 100 spores were plated on SAB agar plates at room temperature for 12 hr and colony counts taken.

2.5.4 PHAGOSOME MATURATION

Macrophages were stained with LysoTracker™ Red (50 nM, ThermoFisher Scientific, Waltham, MA, USA) - a dye for labelling acidic organelles such as maturing phagosomes – 1 hr prior to co-incubation with spores. Spores were prepared as per 2.5.2 with the following amendment: for heat-killed spores, 0, 3 and 6 hr spores were incubated at 65°C for 2 hr, prior to phagocytosis assays. Phagocytosis and phagosome maturation was imaged by live fluorescence microscopy at 20x magnification on a Zeiss Axio Observer microscope (Zeiss, Oberkochen, Germany). Images were taken every 5 minutes for 2 hr and analysed using Fiji software. Percentage phagosome maturation (%PM) of 100 phagosomes per condition calculated as (number of lysotracker-red positive phagosomes/total number of phagosomes) x100.

2.5.5 MANNAN INHIBITON

Macrophages were pre-treated with exogenous mannan (from *Saccharomyces cerevisiae*; Sigma-Aldrich, St. Louis, MO, USA) for 30 minutes prior to the addition of *M. circinelloides* spores. Mannan was added at the following concentrations: 0, 10, 50, 100, 250 and 500 µg/mL. Spores were prepared as per 2.5.2 but only for spores at the mid-point (3 hr). Phagocytosis assays were conducted and analysed as per 2.5.3.

2.6 PLATELET – *M. CIRCINELLOIDES* INVESTIGATION

2.6.1 SPORE PREPARATION FOR AGGREGATION ASSAYS

Spores were collected in PBS and centrifuged at 1811 x *g* for three min. The spore pellet was washed twice with PBS and then re-suspended in Saboraud broth (Sigma-Aldrich, St. Louis, MO, USA). Spores were cultured at 37°C with shaking at 45 rpm, over 0, 3, 6, and 48 h. Following incubation, spore suspensions were centrifuged at 1811 x *g* for three min. The spore pellet was washed twice, and re-suspended in PBS at concentrations to allow for 1:10, 1:20, 1:100, and 1:500 spore:platelet ratios. Spore suspensions were kept on ice until used for aggregometry.

2.6.2 BLOOD PREPARATION

Blood samples were collected from healthy human donors into 4% (w/v) citrate (Sigma-Aldrich, St. Louis, MO, USA). The study design was approved by the University of Birmingham's research ethics committee (ERN_11-0175). Blood was centrifuged at 200 x *g* for 20 minutes and platelet-rich plasma (PRP) collected. For light-transmission aggregometry, a PRP platelet count was taken using Coulter® Z2 Particle Counter (Beckman Coulter, Pasadena, CA, US) in triplicate and averaged. For multiple-electrode aggregometry, a whole blood platelet count was taken using Sysmex XN-1000 Hematology Analyzer (Sysmex, Hyogo, Japan).

2.6.3 PLATELET AGGREGOMETRY IN PRP

PRP was incubated at 37°C for 1 minute and then stirred for 1 min. Spores were added to PRP at 1:10, 1:20, 1:100, and 1:500 spore:platelet concentration, and platelet aggregation recorded over 30 minutes using light-transmission aggregometer PAP-8E (Bio/Data Corporation, Horsham, PA, USA). As a positive control, 100 μ M Thrombin Receptor-Activating Peptide (TRAP) (Severn Biotech, Kidderminster, UK) was added to PRP, and PBS added as a negative control.

2.6.4 PLATELET AGGREGOMETRY IN WHOLE BLOOD

Whole blood was added to sodium chloride and incubated for 3 minutes at 37°C. Spores at 3 hr germination was added to PRP at a 1:10 spore:platelet ratio, and platelet aggregation recorded over 30 minutes using multiple electrode aggregometer, Multiplate® Analyzer (Roche, Basel, Switzerland) . 100 μ M TRAP was added to PRP as a positive control and PBS as a negative control.

2.6.5 PLATELET STAINING AND MICROSCOPY

Platelets were stained with CellMask Deep Red Plasma Membrane Stain for 30 min prior to co-incubation with spores (1:2000, Thermo Fisher Scientific, Waltham, MA, USA), and spores with Concanavalin A, Alexa fluor™ 488 conjugate (300 μ g ml⁻¹, Thermo Fisher Scientific, Waltham, MA, USA). Aggregates were immobilized on poly-L-lysine (Sigma-Aldrich, St. Louis, MO, USA) coated 25 x 50 mm glass coverslips, fixed using 4% PFA, washed and placed in the imaging chamber filled with PBS. Orthogonal views of the aggregates were acquired on a Marianas LightSheet (Intelligent Imaging Innovations, Denver, CO, USA), a dual inverted Selective Plane Illumination Microscope (diSPIM). Volumes of 200 image planes were captured using both arms sequentially in slice scan mode, with a step size of 0.5 μ m, for both 488 nm and 640 nm excitation wavelengths, on ORCA-Flash4.0 V3 sCMOS cameras (Hamamatsu). Image analysis was performed using Fiji software.

2.6.6 INHIBITOR TREATMENTS

Platelets were treated with the following inhibitors for 1 minute at room temperature for inhibition studies: 9 μ M eptifibatide (GlaxoSmithKline, Coventry, UK) to inhibit α IIb β 3, 10 μ M mAbIV.3 to inhibit Fc γ RIIA (hybridoma from American Tissue Culture Corporation (Manassas, Virginia), 4 μ M dasatinib (D-3307, LC Laboratories, Woburn, MA, USA) and 10 μ M PRT-060318 (AdipoGen Life Sciences, Liestal, Switzerland) to inhibit Src and Syk tyrosine kinases respectively, and 30 μ M Indomethacin (I7378, Sigma-Aldrich, St. Louis, MO, USA) and 2 U Apyrase (A6535, Sigma-Aldrich, St. Louis, MO, USA) to inhibit secondary mediators TxA₂ and ADP with respectively. Platelet aggregation was assessed by light-transmission in a PAP-8E aggregometer over 30 min.

2.6.7 PLATELET RECEPTOR LABELLING

For platelet receptor labelling the platelets were labelled with the following for 30 minutes prior to flow cytometry: conjugated anti-human CD32 (#60012; mouse; StemCell Technologies, Vancouver, Canada) and anti-mouse 2° Alexa Fluor™ 488 conjugate (A10680; goat; Invitrogen, Carlsbad, CA, USA) to label Fc γ RIIA, anti-Human CD41a-APC (BD559777; mouse; BD Biosciences, San Jose, CA, USA) to label α IIb β 3, and CD62P-Fluorescein isothiocyanate (FITC) (BC A07790; mouse; Beckman Coulter, Brea, CA, USA) to label CD62P. Platelet aggregation was assessed by light-transmission in a PAP-8E aggregometer over 30 min. Flow cytometry analysis was conducted using BD Accuri™ C6 Plus (BD Biosciences, Oxford, UK). Samples were run for 10000 events, and cell count vs fluorescence recorded.

2.7 STATISTICAL ANALYSIS

Statistical analysis was conducted using GraphPad Prism 9.02. Data are presented as mean \pm SEM, unless stated otherwise. Data was analysed using one of the following statistical analyses as stated in figure legends: Mann–Whitney *U*-test, one-way analysis of variance (ANOVA) with post-hoc Dunnett's, Kruskal–Wallis, Tukey's, or Šídák's multiple comparison test. $p < 0.05$ was deemed to be statistically significant. Technical repeats were conducted at $n = 3$, and biological repeats at $n = 5$ unless otherwise stated.

3 TRANSCRIPTIONAL PROFILING OF *MUCOR CIRCINELLOIDES* DURING SPORE DEVELOPMENT

3.1 INTRODUCTION

To enhance our understanding of the dynamic changes of the *Mucor circinelloides* cell wall during spore swelling, RNA-sequencing was employed. RNA-sequencing is a form of next generation sequencing that allows for transcriptional profiling of cell(s) at a particular developmental stage or under a particular physiological condition (Wang *et al.*, 2009). The transcriptome refers to the RNA transcripts expressed by a cell or population (Wang *et al.*, 2009; Manzoni *et al.*, 2018). Comparison of the transcriptomes of *M. circinelloides* at different stages of germination, highlights differences in gene expression that are quantifiable and thus can be analysed to enhance our understanding of transcriptional changes during spore germination.

RNA-sequencing requires the isolation of RNA foremost. Following RNA extraction, library preparation is conducted which involves the enrichment of mRNA performed by rRNA depletion or poly(A) selection, fragmentation, reverse transcription (cDNA synthesis), sequencing adapter ligation and amplification by PCR (Hrdlickova, Toloue and Tian, 2016). Libraries are sequenced using NGS platforms, such as Illumina® whereby the sequencing library is loaded onto a flow cell – a glass slide with complementary oligonucleotides to the adapter sequence (Slatko, Gardner and Ausubel, 2018). Library hybridization to the flow cell ensues, creating clustered clones, which finally undergo sequencing cycles to allow sequential identification of nucleotides within each cluster to provide a digital image readout. Once libraries have been sequenced, data analysis can be performed. Data analysis varies but generally follows the workflow: (1) evaluate raw data for sequence quality, (2) remove adapter sequences and low-quality reads (trimming), (3) map reads to reference genome, (4) generate hit counts for genes for expression quantification, (5) compare hit counts to determine differential expression, and (6) analyse by means such as gene ontology (functional enrichment) (Yalamanchili, Wan and Liu, 2017).

Transcriptional profiling of *M. circinelloides* NRRL3631 spores at different stages of germination has not previously been reported, and the genome of *M. circinelloides* NRRL3631 has yet to be published. Here, we utilise RNA-sequencing to measure the expression of genes at different stages of *M. circinelloides* NRRL3631 spore swelling (0, 3 and 6 hr) to identify differential gene expression, with a focus on cell wall biosynthesis.

3.2 RESULTS

3.2.1 *M. CIRCINELLOIDES* SPORES SWELL SIGNIFICANTLY DURING GERMINATION

To characterise *M. circinelloides* spore size during germination, spores were cultured from resting state to maximal-swelling state. The maximal swelling state was defined as spores reaching maximal capacity up to the point of germ-tube formation. Spores reached fully swollen stage before germ tube emergence at 6 hr germination ($97.17 \mu\text{m} \pm 21.04 \mu\text{m}$) (Figure 3.1). As *Mucor* spores reached maximal swelling at 6 hr germination, spores at the mid-point of time to reach maximal swelling (3 hr) were characterised for size and carried forward in subsequent experiments. Spores at 3 hr germination were significantly larger than resting (0 hr) spores (3hr: $29.32 \mu\text{m} \pm 8.85 \mu\text{m}$; 0hr: $14.83 \mu\text{m} \pm 4.38 \mu\text{m}$; $p \leq 0.0001$), and significantly smaller than fully swelling spores (3 hr: $29.32 \mu\text{m} \pm 8.85 \mu\text{m}$; 6 hr: $97.17 \mu\text{m} \pm 21.04 \mu\text{m}$; $p < 0.0001$) (Figure 3.1).

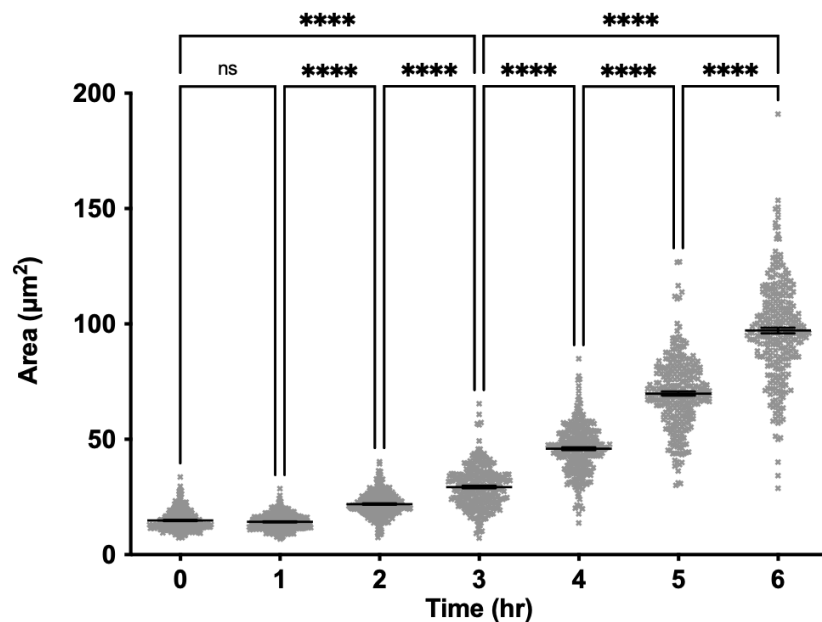
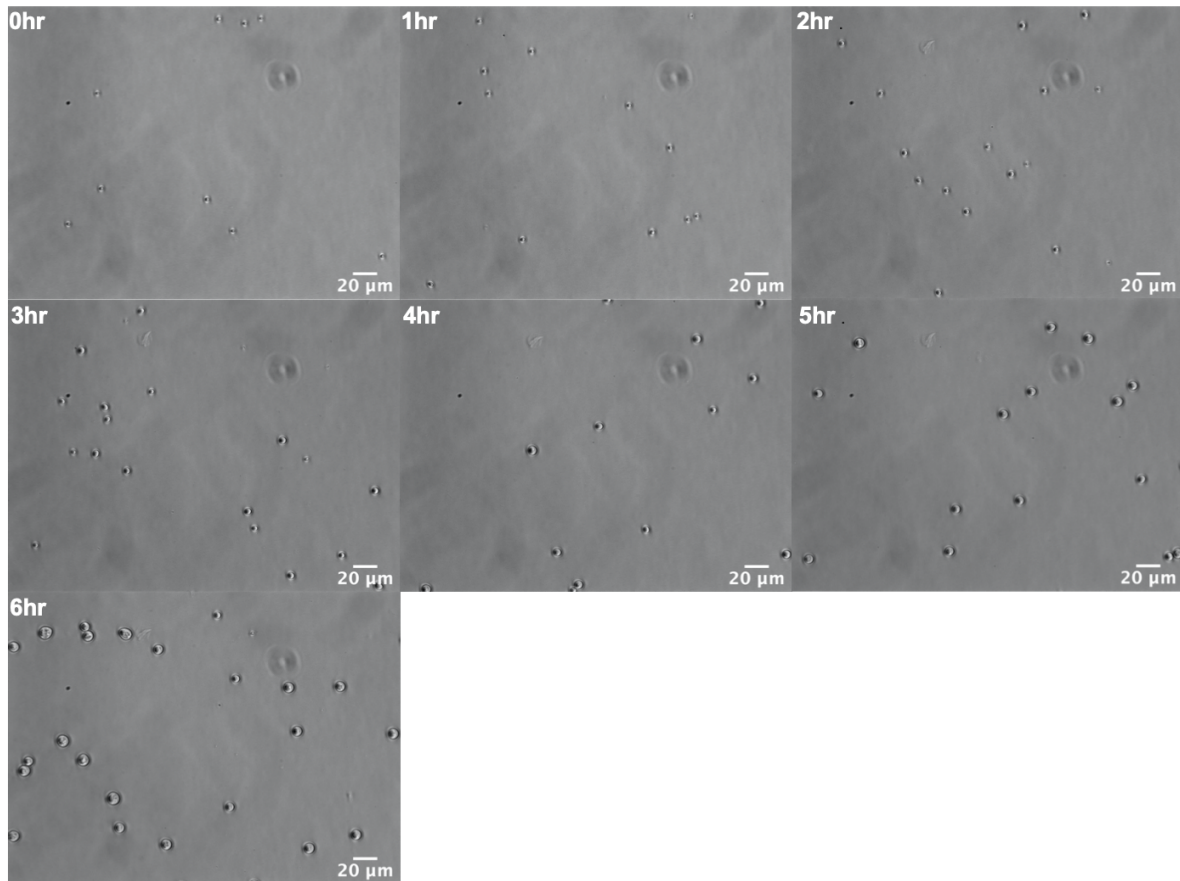


FIGURE 3.1. *M. CIRCINELLOIDES* SPORE SIZE DURING GERMINATION. Spores were cultured in SAB broth at 37°C, over 12 hr. Spores were imaged every 20 minutes using 20x objective. Images were analysed using Fiji software. Data shown are mean \pm SEM of three independent experimental repeats; **** p <0.0001, One-way ANOVA, Kruskal-Wallis Test.

3.2.2 SPORE CONCENTRATION AFFECTS *M. CIRCINELLOIDES* SPORE SWELLING

M. circinelloides spore swelling was initially characterised using time-lapse imaging in static 24-well plates. Spores were cultured at 1×10^4 spores/mL in a total volume of 1 mL to allow for individual spores to be analysed. For large-scale investigations, cultures would be needed at greater volumes. To ensure *M. circinelloides* spores are reaching maximal swelling size in large culture volumes, spores were cultured in flasks at 1×10^4 spore/mL and 1×10^5 spores/mL in a total volume of 50 mL. Analysis of spore size at 6 hr germination, between plate cultures and flask cultures showed spores were significantly smaller when cultured in flasks at 1×10^4 spore/mL than when cultured in plates at the same concentration (1×10^4 flask: $83.64 \mu\text{m} \pm 15.49 \mu\text{m}$; 1×10^4 plate: $94.92 \mu\text{m} \pm 10.07 \mu\text{m}$; $p < 0.0001$) (Figure 3.2). Upon increasing the concentration to 1×10^5 spores/mL the spore size was not significantly different at 6 hr culture compared to plate cultures (1×10^5 flask: $92.13 \mu\text{m} \pm 18.56 \mu\text{m}$; 1×10^4 plate: $94.92 \mu\text{m} \pm 10.07 \mu\text{m}$; ns) (Figure 3.2). For all further investigations, spores were cultured in flasks at 1×10^5 spores/mL to ensure spores reach maximal swelling at 6 hr germination.

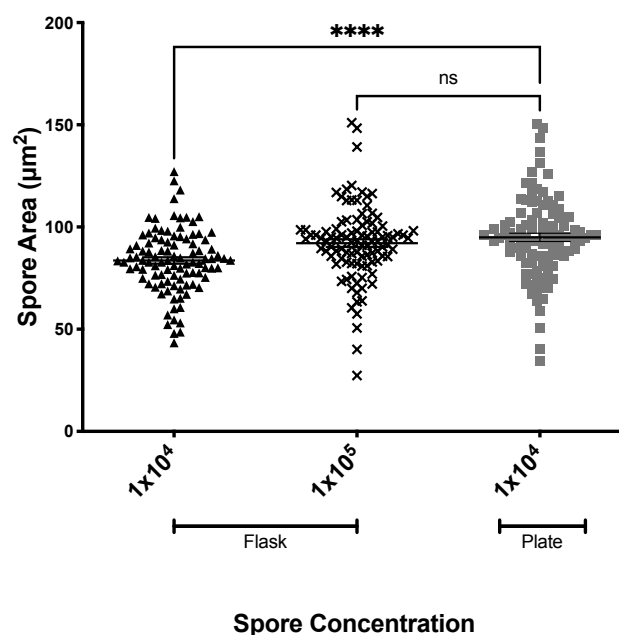


FIGURE 3.2 *M. CIRCINELLOIDES* SPORE CONCENTRATION AFFECTS GERMINATION. Spores were cultured in SAB broth at 37°C, in either a 250 mL flask or 24-well plate. Images were analysed using Fiji software. Data shown are mean \pm SEM; **** $p < 0.0001$, One-way ANOVA, Kruskal-Wallis Test.

3.2.3 *M. CIRCINELLOIDES* SPORE GERMINATION IS SUPPORTED BY SIGNIFICANT TRANSCRIPTIONAL CHANGES

To identify how the germination process is regulated at the transcriptional level, the global transcriptome of *M. circinelloides* was determined through RNA-sequencing in, resting (0 hr) spores, spores that had initiated germination (3 hrs) and spores that were fully swollen (6 hrs). Sequencing reads were aligned to the *Mucor lusitanicus* CBS277.49 genome. To identify genes whose expression was differentially regulated throughout the germination process, the transcriptional profiles were compared using DESeq2, as follows: (1) 3 hr vs. 0 hr, (2) 6 hr vs 3 hr, and (3) 6 hr vs. 0 hr spores.

Differentially expressed genes (DEGs) between the early (0 hr vs. 3 hr), late (3 hr vs. 6 hr) and complete (0 hr vs. 6 hr) stages of germination prior to germ tube emergence were initially identified. Subsequently, genes were considered to be significant DEGs if they had a $P_{adj} \leq 0.05$, and $\text{Log}_2\text{fold change} \geq 1$ (upregulated genes) or (ii) $\text{Log}_2\text{fold change} \leq -1$ (downregulated genes). Under the aforementioned criteria, 7292 genes were identified as being significant DEGs between 0 hr and 3 hr, 7421 between 0 hr and 6 hr, and 1719 genes between 3 hr and 6 hr (Table 3.1). Of the significant DEGs between 0 hr and 3 hr, 4018 genes were significantly upregulated and 3274 were significantly downregulated. Between 3 hr and 6 hr, 1544 genes were significantly upregulated and 175 genes were significantly downregulated, and between 0 hr and 6 hr, 4248 genes were significantly upregulated and 3173 genes were significantly downregulated. (Table 3.1).

From this initial analysis, it would appear that the majority of differential gene expression occurs in the early stages of germination, with the total number of significant DEGs between 0 hr and 3 hr (7292 genes) being over four-fold the total seen between 3 hr and 6 hr (1719 genes). Notably, between 0 hr and 3 hr, the proportion of upregulated and downregulated genes was fairly even; 55.1% (4018 genes) upregulated and 44.9% (3274 genes) downregulated. This is in contrast to in the latter stages of germination between 3 hr and 6 hr, where there was a larger proportion of upregulated genes compared to downregulated genes in the total DEG set (89.8% (1544) genes upregulated and 10.2% (175) downregulated).

TABLE 3.1. DIFFERENTIALLY EXPRESSED GENES DURING *M. CIRCINELLOIDES* GERMINATION. Transcriptional profiles of early (0 hr vs 3 hr), late (3 hr vs 6 hr) and complete (0 hr vs 6 hr) germination, were analysed for significant DEGs. Genes were determined to be significantly differentially expressed if $P_{adj} \leq 0.05$, and (i) $\text{Log}_2\text{fold change} \geq 1$ (upregulated genes) or (ii) $\text{Log}_2\text{fold change} \leq -1$ (downregulated genes).

		Condition		
		0 hr vs. 3 hr	3 hr vs. 6 hr	0 hr vs. 6 hr
Number of Significant DEGs	Upregulated	4018	1544	4248
	Downregulated	3274	175	3173
	<i>Total</i>	<i>7292</i>	<i>1719</i>	<i>7421</i>

Principle component analysis showed little variation between biological repeats within each condition (Figure 3.3). Each condition displayed distinct clusters indicative of their distinct transcriptional profiles. Distribution of gene expression in the three conditions was shown by MA plots (Figure 3.3). MA plots showed a relatively even distribution of upregulated genes in the 0hr vs 3 hr and 0hr vs 6 hr conditions, however distribution was uneven in the 3hr vs 6 hr condition with greater distribution of upregulated genes than downregulated genes (Figure 3.3).

When considering the transcriptional profile of the 0 hr vs 6 hr condition, a large proportion of upregulated genes (80%; 3674 genes) and downregulated genes (82.9%; 2923 genes) were shared between the 0 hr vs 3 hr profile and the 0 hr vs 6 hr profile. To compare the transcriptional profiles of *M. circinelloides* spores, significant DEGs were compared between all three conditions using Venn diagrams (Figure 3.4). Of the upregulated genes, only 8.3% (425 genes) were shared between the 0 hr vs 3 hr profile and 3 hr vs 6 hr profile, and fewer downregulated genes were found in common (1.3%; 44 genes) (Figure 3.4). The low percentage of shared DEGs between the early stages of germination (0 hr vs 3 hr) and late stages of germination (3 hr vs 6 hr) suggests that they have two distinct transcriptional profiles. A smaller proportion of upregulated genes (15.1%; 760) and downregulated genes (2.2%; 72 genes) were shared between the 3 hr vs 6 hr profile and the 0 hr vs 6 hr profile (Figure 3.4).

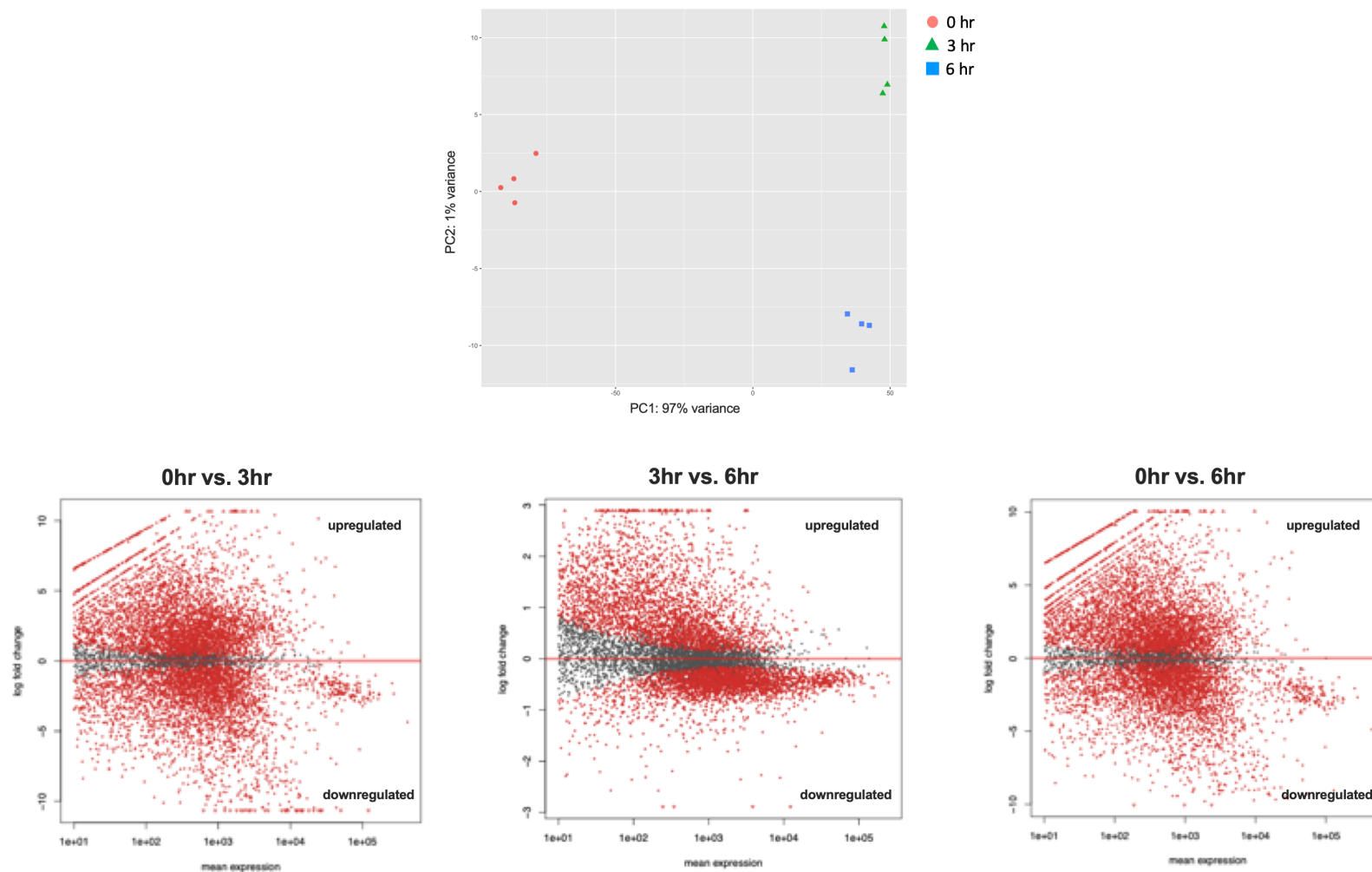
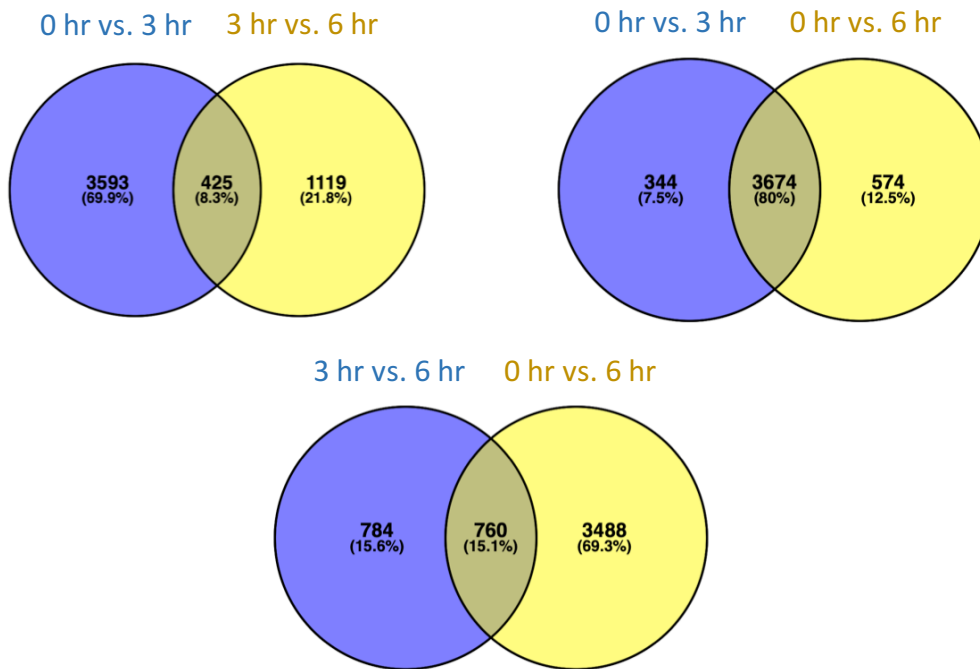


FIGURE 3.3. PC AND MA PLOTS FROM RNA-SEQUENCING OF *M. CIRCINELLOIDES* GERMINATION. Top: PCA plots shows little variation between biological repeats within each condition, and distinct clustering between conditions. Bottom: MA plots show there is an even distribution of upregulated and downregulated genes during early and complete *M. circinelloides* spore germination. During late germination, there is a greater distribution of upregulated genes than downregulated genes.

UPREGULATED:



DOWNREGULATED:

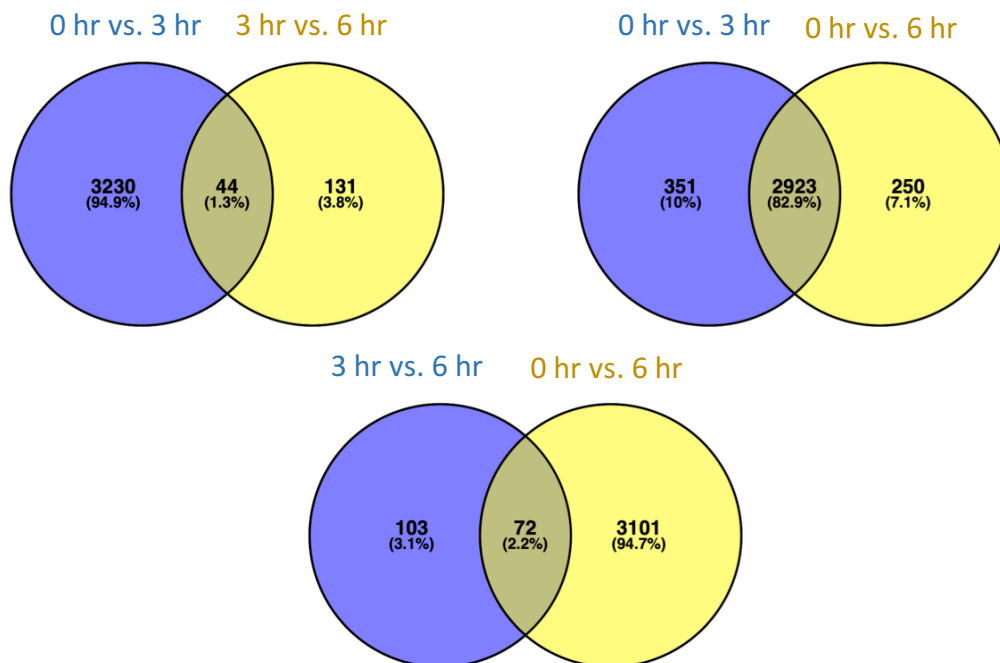


FIGURE 3.4. COMPARISON OF SIGNIFICANT DEGS DURING *M. CIRCINELLOIDES* GERMINATION. Significant DEGs ($P_{\text{adj}} \leq 0.05$) were compared between early (0 hr vs 3 hr), late (3 hr vs 6 hr) and complete (0 hr vs 6 hr) germination. Venn diagrams generated with Venny 2.1 (<https://bioinfogp.cnb.csic.es/tools/venny/>)

3.2.4 A LARGE NUMBER OF *M. CIRCINELLOIDES* GENES PRODUCTS ARE UNCHARACTERISED

Analysis of DEGs highlighted 4018 significantly upregulated genes when comparing 0 hr spores with 3 hr spores, 28.99% of these (1165 genes) had unspecified products, and 2.19% (88 genes) uncharacterised proteins (Table 3.2). Similarly, of the 3274 significantly downregulated genes, 33.90% (1110 genes) had unspecified products, and 2.26% (74 genes) had uncharacterised proteins. A similar pattern was seen when comparing significant DEGs between 3 hr and 6 hr spores, with 37.63% (581/1544 genes) of upregulated gene products being unspecified and 1.88% (29/1544 genes) being uncharacterised, and 43.43% (76/175 genes) of downregulated gene products being unspecified and 1.71% (3/175 genes) being uncharacterised (Table 3.2). Analysis of DEGs between 0 hr and 6 hr spores highlighted 30.63% (1301/4248 genes) of upregulated gene products as unspecified and 1.91% (81/4248 genes) as uncharacterised, and 34.26% (1087/3173 genes) of downregulated gene products as unspecified and 2.46% (78/3173 genes) as uncharacterised (Table 3.2).

The high proportion of unspecified and uncharacterised products reflects the poor annotation of the *Mucor* genome, although they were still able to be assigned to GO terms and orthologous genes could be run against them using the FungiDB pipeline. Further analysis of DEGs by means of functional enrichment analysis and orthologs(s) analysis was employed to gain greater insight into potential gene function.

TABLE 3.2 PRODUCT CHARACTERISATION OF SIGNIFICANT DEGS DURING *M. CIRCINELLOIDES* SPORE SWELLING. Comparison of product characterisation of significant DEGs, during early (0 hr vs. 3 hr), late (3 hr vs. 6 hr) and complete (0 hr vs 6 hr) *M. circinelloides* germination. Genes categorised as ‘characterised’, ‘unspecified product’ and ‘uncharacterised protein’ using FungiDB analysis pipeline.

		Condition		
		0 hr vs. 3 hr	3 hr vs. 6 hr	0 hr vs. 6 hr
UPREGULATED GENE PRODUCTS (NUMBER/%)	Unspecified	1165 (28.99%)	581 (37.63%)	1301 (30.63%)
	Uncharacterised	88 (2.19%)	29 (1.88%)	81 (1.91%)
	Characterised	2765 (68.82%)	934 (60.49%)	2866 (67.46%)
	<i>Total</i>	<i>4018</i>	<i>1544</i>	<i>4248</i>
DOWNREGULATED GENE PRODUCTS (NUMBER/%)	Unspecified	1110 (33.90%)	76 (43.43%)	1087 (34.26%)
	Uncharacterised	74 (2.26%)	3 (1.71%)	78 (2.46%)
	Characterised	2090 (63.84%)	96 (54.86%)	2008 (63.28%)
	<i>Total</i>	<i>3274</i>	<i>175</i>	<i>3173</i>

3.2.5 FUNCTIONAL ENRICHMENT ANALYSIS

To identify the processes that are differentially regulated between the different stages of germination, functional enrichment analysis was performed. Functional enrichment analysis of significant DEGs was performed using the FungiDB online analysis platform. Briefly, significant DEGs ($P_{adj} \leq 0.05$; $\text{Log}_2\text{fold} \geq 1$) were entered into the search gene ID(s) pipeline, and as the *M. circinelloides* NRRL3631 genome is unavailable, the closest species with an annotated available genome, *Mucor lusitanicus* CBS 277.49, was used as a reference. Once gene ID(s) had been processed through the pipeline, basic information on genes such as product descriptions could be obtained. To gather more insight into gene function, GO term analysis was run on the pipeline, whereby *M. circinelloides* significant DEGs within a condition, i.e. 3 hr vs. 6 hr, are analysed under (G)ene (O)ntology categories

‘biological process’, ‘molecular function’, and ‘cellular component’. Finally, genes of interest were noted specifically for cell wall association and probed further. As the *Mucor* genome is poorly annotated, orthologs from the fungal pathogen *Candida albicans* (SC5314) which has a well-annotated genome, were analysed.

To identify key process that are differentially regulated during germination, GO analysis was performed. Here genes are assigned to GO terms that describe the molecular function of the gene product, the biological process that the product enacts in, and the cellular component where it is found (Balakrishnan *et al.*, 2013). *Mucor* genes that are significantly upregulated and downregulated between 0hr and 3hr, 3hr and 6hr, and 0hr and 6hr conditions were assigned to GO terms across all three categories: biological processes, molecular function and cellular components. The number of GO terms associated within each analysis is summarised in Table 3.3.

TABLE 3.3. COMPARISON OF GO TERMS ASSIGNED TO SIGNIFICANT DEGS DURING *M. CIRCINELLOIDES* SPORE GERMINATION. Comparison of number of GO terms across all three categories (1) biological process, (2) molecular function and (3) cellular component, assigned to significantly upregulated or downregulated genes across the three conditions (1) 0 hr vs. 3 hr, (2) 0 hr vs. 6 hr and (3) 3 hr vs. 6 hr.

Condition	GO Term Category		
	Biological Process	Molecular Function	Cellular Component
0 hr vs 3 hr	273 upregulated 117 downregulated	113 upregulated 61 downregulated	126 upregulated 22 downregulated
3 hr vs 6 hr	90 upregulated 19 downregulated	92 upregulated 17 downregulated	13 upregulated 7 downregulated
0 hr vs 6 hr	214 upregulated 92 downregulated	115 upregulated 46 downregulated	106 upregulated 23 downregulated

3.2.5.1 TRANSCRIPTIONAL PROFILING CONFIRMS SPORES BECOME METABOLICALLY ACTIVE EARLY IN GERMINATION

Analysis of GO terms associated with significant upregulated genes between 0 hr and 3 hr, highlighted a large number of genes are significantly upregulated that were involved in metabolic

processes (1157/4018 upregulated genes). Over 30% (84/261) of biological process GO terms assigned to upregulated genes between 0 hr and 3 hr spore germination were of metabolic processes, and include 'tRNA metabolic process', 'glycolipid metabolic process' and 'glycoprotein metabolic process' (See Table S2. Appendix II.II for full list of upregulated biological process GO terms referring to metabolic processes). The upregulation of metabolic processes reflects the resting spore (0 hr) exiting dormancy and becoming metabolically active in the early stages of germination (by 3 hr).

Furthermore, when considering the fold-enrichment (FE) (the percent of genes within a GO term divided by the percent of genes with this term in the background) of biological process GO terms, processes facilitating protein synthesis are heavily enriched, including 'cytoplasmic translation' (2.64 FE), 'protein folding' (1.89 FE), and 'protein N-linked glycosylation' (2.20 FE) (Figure 3.5) (See Table S3, Appendix II.II for full list of upregulated biological process GO terms). The upregulation of these processes suggests that once germination ensues, there is a heavy focus on protein synthesis. Genes associated with cytoplasmic translation had the greatest FE. Numerous *Mucor* genes encoding translation initiation factor subunits were noted, including *QYA_160001* encoding translation initiation factor 3 subunit e (eIF-3e) and *QYA_160001* encoding translation initiation factor 3 subunit b (eIF-3b).

Alongside translation, protein folding was heavily enriched in the early stages of *Mucor* germination. There are 40 upregulated genes in the early stages of germination in the 'protein folding' GO term, including *QYA_185166* encoding a molecular chaperone (HSP90 family), *QYA_108714* encoding β -tubulin folding cofactor A, and *QYA_183435* encoding chaperonin complex component, TCP-1 alpha subunit (CCT1). The upregulation of protein folding in the early stages of germination suggests protein synthesis is initiated in early *Mucor* spore germination.

3.2.5.2 TRANSCRIPTIONAL PROFILING SHOWS SPORES DOWNREGULATE AUTOPHAGY AND STRESS RESPONSE IN EARLY GERMINATION

Analysis of GO terms associated with significant downregulated genes between 0 hr and 3 hr, highlighted a large number of genes that are involved in metabolic processes (861/3274 downregulated genes). Just under 30% (35/118) of GO terms assigned to downregulated genes between 0 hr and 3 hr spore germination were of metabolic processes, and included processes such as, organonitrogen compound metabolic process and cellular macromolecule metabolic process (See Table S4 Appendix II.II for full list of downregulated biological process GO terms referring to metabolic processes).

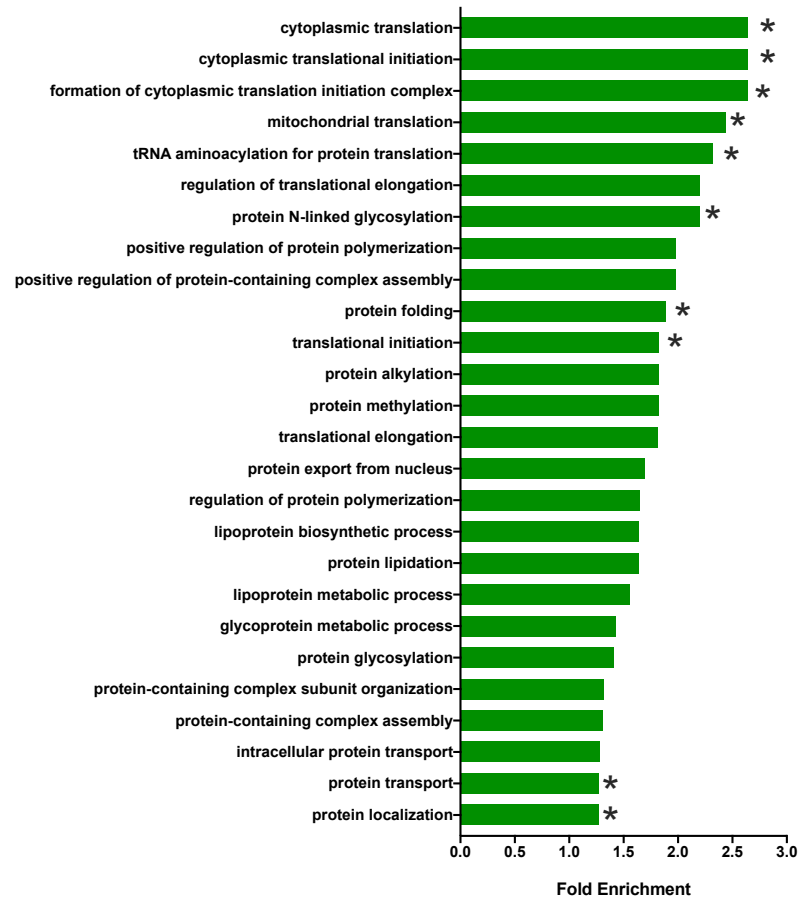
When considering the FE of downregulated biological processes between 0 hr and 3 hr, processes such as autophagy (2.58 FE), process using autophagic mechanism (2.58 FE), peroxisomal membrane transport (2.92 FE) and protein import into peroxisome matrix (2.80 FE) were all enriched (Figure 3.5) (See Table S5 Appendix II.II for full list of downregulated biological process GO terms). The downregulation of such processes, in addition to the downregulation of response to oxidative stress (1.75 FE) and response to stress (1.24 FE), may be indicative of spores downregulating processes responding to conditions of stress when under optimal growth conditions.

There were 14 downregulated genes associated with biological process GO term 'autophagy' in the 0 hr vs 3 hr profile, including *QYA_155143* which encodes a protein required for autophagy during starvation. Additionally, there were 11 downregulated genes associated with the biological process GO term 'peroxisome organisation' and 6 with 'peroxisomal transport'. Genes included *QYA_109975* encoding peroxisomal biogenesis protein (peroxin 16) and *QYA_158038* encoding peroxisomal assembly protein PEX3 were significantly downregulated.

The GO terms 'response to stress' and 'response to oxidative stress' were also seen in biological process GO term analysis in the 0 hr vs 3 hr downregulated DEG set. There were 56 genes assigned to 'response to stress' and 10 genes assigned to 'response to oxidative stress'. Several genes encoding catalases, such as *QYA_115786*, were seen in these terms.

GO CATEGORY: BIOLOGICAL PROCESS
0 hr vs. 3 hr

UPREGULATED



DOWNREGULATED

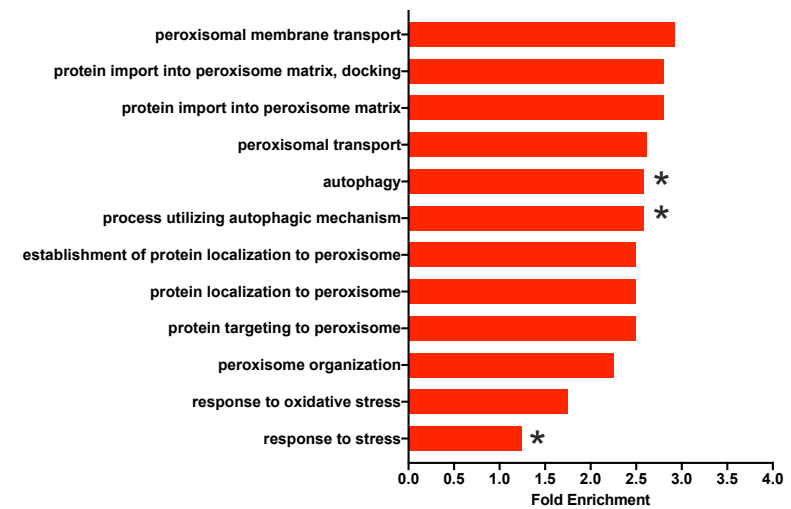


FIGURE 3.5. BIOLOGICAL PROCESS GENE ONTOLOGY (GO) TERMS ASSIGNED TO DEGS BETWEEN 0 HR AND 3 HR *M. CIRCINELLOIDES* GERMINATION. GO terms referring to metabolic processes and protein synthesis are heavily abundant in the upregulated gene set, whilst those referring to peroxisome biogenesis and autophagy are seen in the downregulated set. Fisher's exact test with the Benjamini and Hochberg method for false discovery rate (FDR) correction (*FDR \leq 0.05)

3.2.5.3 TRANSCRIPTIONAL PROFILING OF LATE GERMINATION SHOWS RESPONSE TO OXIDATIVE STRESS AND AUTOPHAGY IS UPREGULATED

In the early stages of *Mucor* spore germination (0hr vs 3 hr) dormant spores become metabolically active and there is an upregulation of protein translation, glycosylation and transport, and a downregulation of response to stress and autophagy (Figure 3.6). Analysis of GO terms associated with significantly upregulated genes between 3 hr and 6 hr spores shows biological processes, such as response to oxidative stress and autophagy were upregulated in late germination (Figure 3.6) (See Table S6 Appendix II.II for full list of upregulated biological process GO terms).

Fungi must be able to withstand a variety of stresses, both in the host and also in the environment. The ability to respond to stress is at the crux of fungal survival and pathogenicity. In the late stages of germination (3hr vs. 6hr), several genes encoding catalases were significantly upregulated, including *QYA_110016*, *QYA_113167* and *QYA_186396*, and a gene encoding a peroxidase/oxygenase, *QYA_133651* was also upregulated. Additionally, there were 6 genes associated with the biological process GO term 'autophagy', including *QYA_91441* encoding a cysteine protease required for autophagy (Apg4p/Aut2p) and *QYA_155732* encoding a microtubule-associated anchor protein involved in autophagy and membrane trafficking.

3.2.5.4 TRANSCRIPTIONAL PROFILING OF LATE GERMINATION SHOWS CELL WALL BIOSYNTHESIS IS UPREGULATED

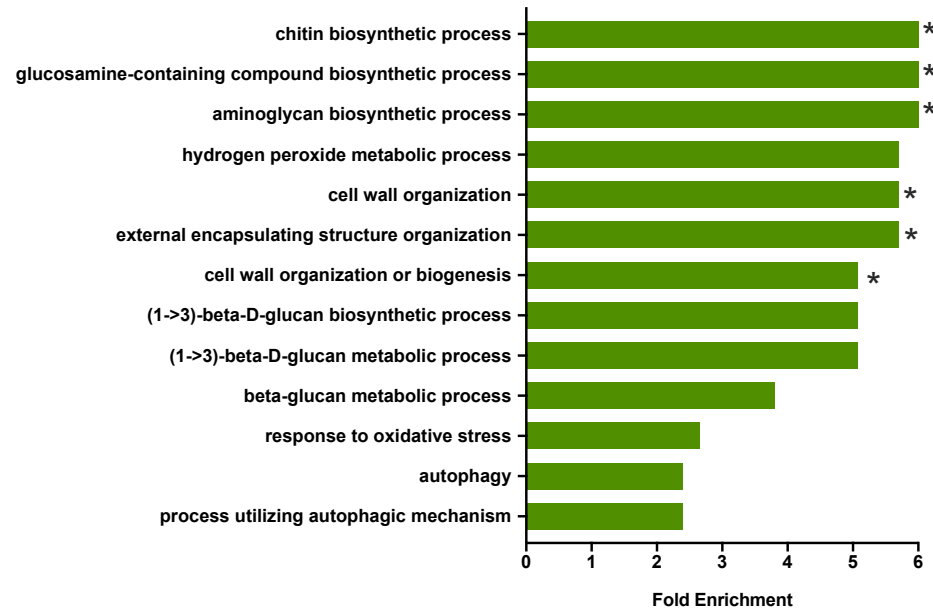
In the late stages of germination, spores undergo morphological change, as they swell significantly in size up to the point of germ tube formation. Analysis of the GO terms assigned to significant upregulated genes between 3 hr and 6 hr spores, highlighted biological processes, such as cell wall organization, chitin biosynthesis and 1-3- β glucan biosynthesis (Figure 3.6). The upregulation of these processes suggests that during late germination there is an upregulation in processes contributing to cell wall biosynthesis and organization.

3.2.5.5 TRANSCRIPTIONAL PROFILING SHOWS PROTEIN TRANSLATION IS DOWNREGULATED DURING LATE GERMINATION

In the early stages of *Mucor* spore germination dormant spores become metabolically active and there is an upregulation of protein translation, glycosylation and transport. Analysis of biological process GO terms, assigned to significant downregulated genes between 3 hr and 6 hr spores, showed processes such as positive regulation of translational elongation, positive regulation of translation termination and transport were downregulated in the late stages of germination (Figure 3.6) (See Table S7 Appendix II.II for full list of downregulated biological process GO terms). In early germination, between 0 hr and 3 hr, genes associated with cytoplasmic translation were upregulated the most, including genes encoding translation initiation factors. In the late stages of germination between 3 hr and 6 hr, translational processes were downregulated, although only 1 gene is assigned to these processes, *QYA_116320* encoding translation initiation factor 5A (eIF-A) (Figure 3.6).

GO CATEGORY: BIOLOGICAL PROCESS
3 hr vs. 6 hr

UPREGULATED



DOWNREGULATED

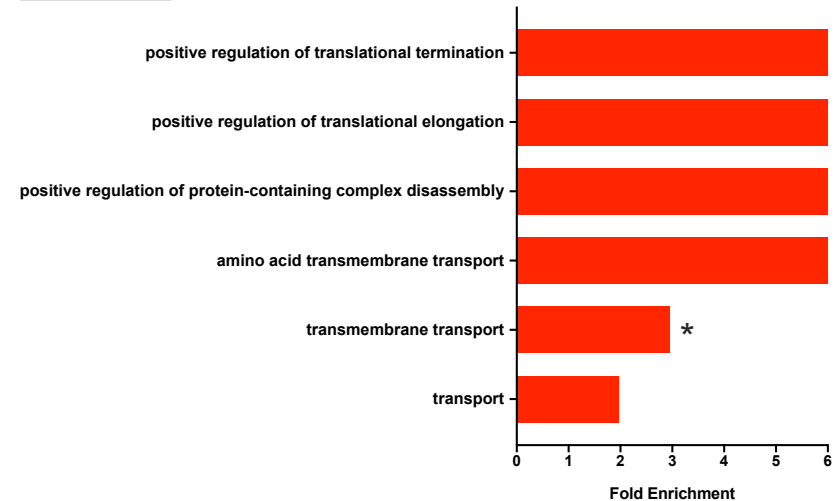


FIGURE 3.6. BIOLOGICAL PROCESS GENE ONTOLOGY (GO) TERMS ASSIGNED TO DEGS BETWEEN 3 HR AND 6 HR *M. CIRCINELLOIDES* GERMINATION. GO terms with associations to cell wall biosynthesis pathways are seen in the upregulated gene set, whilst those affiliated with protein translation and transport are seen in the downregulated gene set. Fisher's exact test with the Benjamini and Hochberg method for false discovery rate (FDR) correction (*FDR≤0.05)

3.2.5.6 TRANSCRIPTIONAL PROFILING SHOWS *M. CIRCINELLOIDES* SPORES UPREGULATE GENES IMPLICATED IN CELL WALL BIOGENESIS DURING GERMINATION

Analysis of GO terms assigned to significant upregulated genes during complete germination, from resting state (0hr) to maximal swelling state (6hr), showed biological processes such as protein translation, glycosylation and folding were upregulated, alongside cell wall organization/biogenesis (Figure 3.7) (See Table S8 Appendix II.II for full list of upregulated biological process GO terms). Transcriptional profiling of spores in 0 hr vs 6 hr profile, showed that a large bulk of upregulated genes and corresponding processes were affiliated with the biosynthesis of cell wall proteins, such as β -glucan, chitin and *O*- and *N*- linked glycans.

3.2.5.7 TRANSCRIPTIONAL PROFILING SHOWS AUTOPHAGY AND PEROXISOME ORGANISATION IS DOWNREGULATED DURING *M. CIRCINELLOIDES* GERMINATION

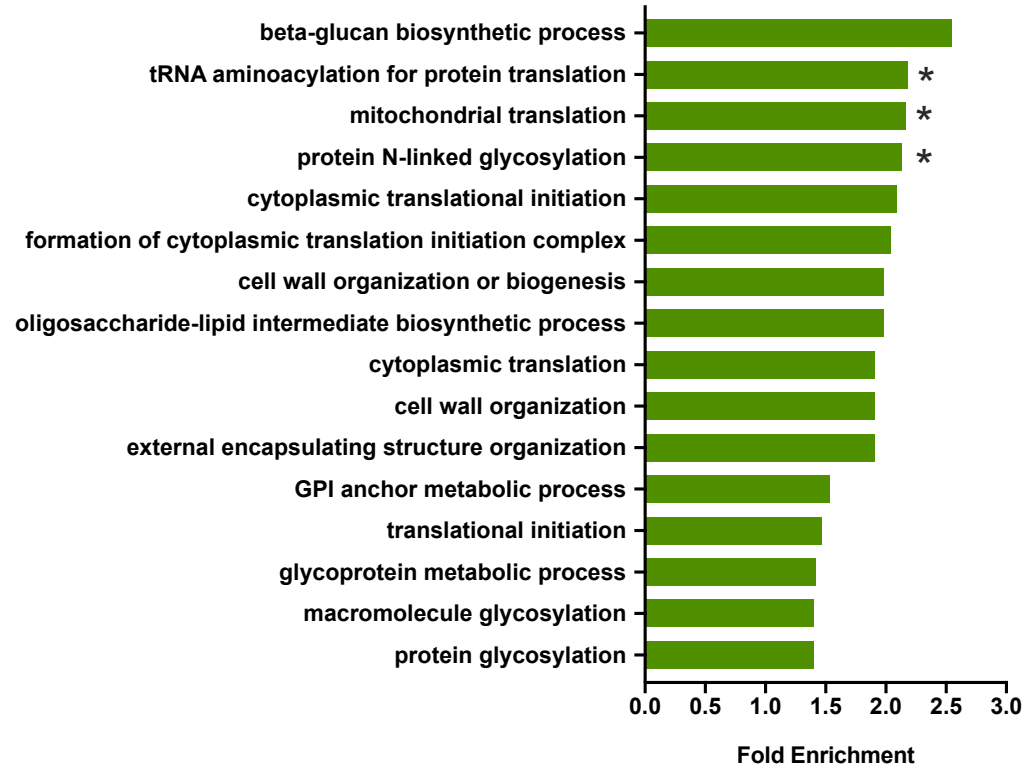
Transcriptional profiling of *Mucor* spores, between resting (0hr) and maximal swelling (6hr), showed that there is a downregulation of processes such as, autophagy and DNA repair (Figure 3.7) (See Table S9 Appendix II.II for full list of downregulated biological processes). Autophagy embodies the degradation of damaged or excess proteins and organelles that accumulate during cellular metabolism, playing a key role in maintaining cellular homeostasis and promoting cell survival (Hewitt and Korolchuk, 2017). There were 13 genes associated with the biological process GO term 'autophagy', including QYA_155143, encoding a protein involved in autophagocytosis during starvation.

Peroxisomes are ubiquitous cell organelles consisting of a single membrane-enclosed protein matrix, containing a range of enzymes (Hynes *et al.*, 2008; van der Klei and Veenhuis, 2013). They contain enzymes mediating fatty acid β -oxidation and the detoxification of ROS (Peraza-Reyes and Berteaux-Lecellier, 2013). Analysis of biological process GO terms assigned to significant downregulated genes between 0 hr and 6 hr *M. circinelloides* spore germination highlighted several terms associated with peroxisomal processes. There were 11 genes assigned to the GO term

‘peroxisome organization’, including *QYA_158038* encoding peroxisomal assembly protein PEX3, and *QYA_156615* encoding peroxisomal biogenesis protein (peroxin).

GO CATEGORY: BIOLOGICAL PROCESS
0 hr vs. 6 hr

UPREGULATED



DOWNREGULATED

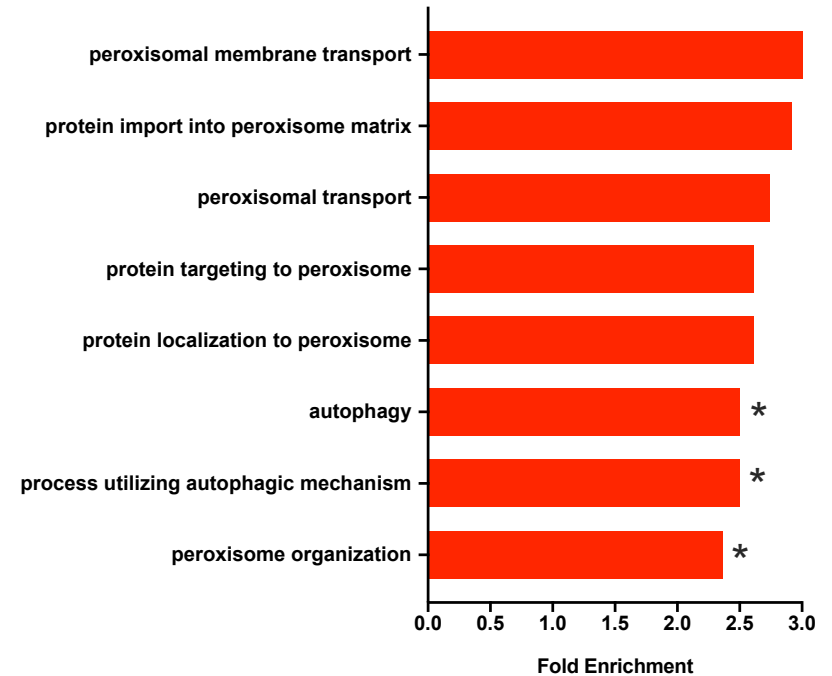


FIGURE 3.7. BIOLOGICAL PROCESS GO TERMS ASSIGNED TO DEGS BETWEEN 0 HR AND 6 HR *M. CIRCINELLOIDES* GERMINATION. GO terms implicated in cell wall biosynthesis pathways and translation are seen in the upregulated gene set, whilst those associated with peroxisome biogenesis and autophagy are seen in the downregulated gene set. Fisher's exact test with the Benjamini and Hochberg method for false discovery rate (FDR) correction * $FDR \leq 0.0$

3.2.6 CELL WALL-FOCUSED ANALYSIS

3.2.6.1 CELL WALL BIOSYNTHESIS IS DIFFERENTIALLY EXPRESSED DURING *M. CIRCINELLOIDES* GERMINATION

Germination of *Mucor* spores is key to their pathogenicity. During spore germination, *Mucor* spores undergo morphological changes, and there is significant swelling from resting spores to swollen spores up to the point of germ tube formation. It has been shown that dormant spores lose an outer melanin layer upon germination, exposing an inner layer of chitins, mannans and glucans (Bartnicki-Garcia and Reyes, 1964, Bartnicki-Garcia and Reyes, 1968). The fungal cell wall offers a variety of PAMPs to host immune cells (Arroyo *et al.*, 2016). Components of the fungal cell wall such as β -glucan are not found in mammals, making them an ideal target for novel therapeutics. Research into the cell wall composition of *Mucor* spores has not been revisited since the early discoveries of the 1960s. To enhance our understanding of the cell wall architecture of *Mucor* spores at different stages in germination (0 hr, 3 hr and 6 hr), GO term analysis of significant DEGs - focussing on cell wall biosynthesis – was conducted across the three GO categories (i) biological process, (ii) molecular function and (iii) cellular component. Genes were analysed within GO terms, and as detailed annotation is limited in the *Mucor* genome, orthologs were analysed in *C. albicans* SC5314.

3.2.6.1.1 ANALYSIS OF CELLULAR COMPONENT GO TERMS

GO analysis of terms within the ‘cellular component’ category indicate where gene products are active. Between 0 hr and 3 hr, there were a total of 126 cellular component GO terms assigned to upregulated genes and 22 to downregulated genes (See Tables S10 and S11 Appendix II.II, for full list of cellular component go terms assigned to upregulated and downregulated genes, respectively). Analysis of upregulated genes highlighted one cellular component GO term associated with the cell wall, ‘obsolete cell part’ containing 286 genes. 4/286 genes were highlighted as being implicated in cell wall biosynthesis/organisation.

Between 3 hr and 6 hr, there were a total of 13 cellular component GO terms assigned to upregulated genes and 7 to downregulated genes (See Tables S14 and S15 Appendix II.II, for full list of cellular component GO terms assigned to upregulated and downregulated genes, respectively). Upregulated cellular component GO terms included cell periphery, plasma membrane and integral component of the membrane, whilst downregulated terms included intrinsic component of membrane and membrane. Analysis of GO terms highlighted three cellular component terms of interest assigned to the upregulated gene subset and three terms to the downregulated gene subset with cell wall association (Figure 3.8). Upregulated cellular component GO terms 'cell periphery' contained 24 genes and 'integral component of membrane' contained 303 genes. Of these genes, 12 were noted as of interest regarding cell wall association. Analysis of downregulated genes in late (3 hr vs 6 hr) germination, highlighted the cellular component GO terms 'cell wall', 'cell periphery' and 'external encapsulating structure' (Figure 3.8). There were 2 genes in the 'cell wall' term, 6 in 'cell periphery', and 2 in 'external encapsulating structure' of which 2 with cell wall association were noted.

GO CATEGORY: CELLULAR COMPONENT
CELL WALL ASSOCIATED TERMS
3 hr vs. 6 hr

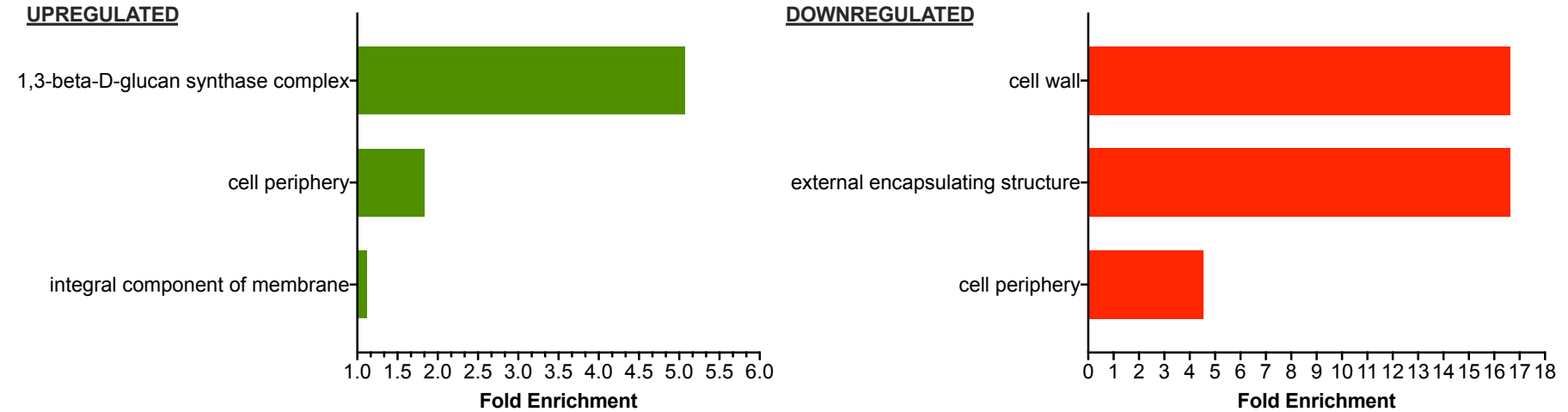


FIGURE 3.8. CELLULAR COMPONENT GO TERMS ASSIGNED TO DEGS BETWEEN 3 HR AND 6 HR SPORE GERMINATION. Analysis highlighted three upregulated cellular component GO terms of interest with regard to cell wall association, and three downregulated cellular component GO terms of interest.

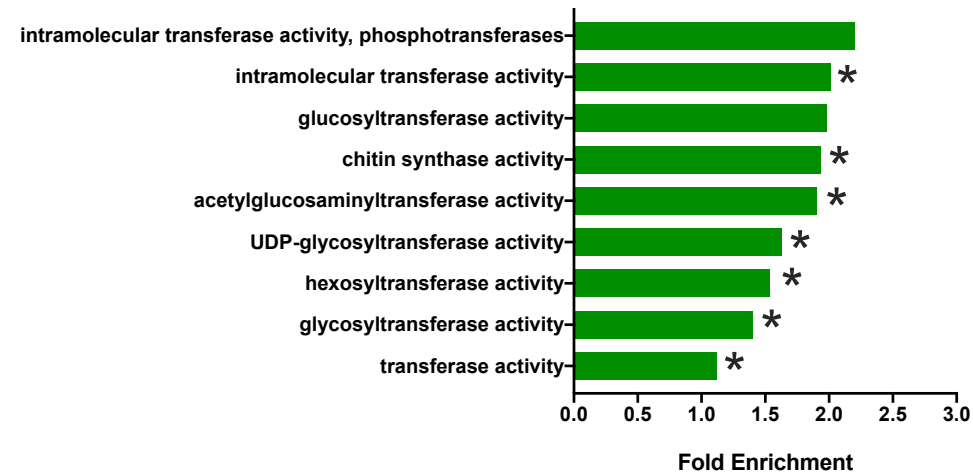
3.2.6.1.2 ANALYSIS OF MOLECULAR FUNCTION GO TERMS

Analysis of GO terms within the 'molecular function' category, elucidates the molecular function of gene products. Between 0 hr and 3 hr, there were a total of 113 molecular function GO terms assigned to significant upregulated genes and 61 to downregulated genes (See Tables S12 and S13 Appendix II.II for full list of molecular function GO terms assigned to upregulated and downregulated genes, respectively). Upregulated molecular function GO terms included, translation regulator activity, ligase activity and transferase activity, and downregulated terms include galactosidase activity, lipase activity and protein kinase activity. Analysis of GO terms assigned to upregulated and downregulated DEGs in the 0 hr vs 3 hr profile, highlighted several molecular function GO terms with cell wall synthesis association, including, glucosyltransferase activity (9 genes; upregulated), and alpha-mannosidase activity (6 genes; downregulated) (Figure 3.9).

Between 3 hr and 6 hr, there were a total of 92 molecular function GO terms assigned to significantly upregulated genes and 17 to downregulated genes (See Tables S16 and S17 Appendix II.II for full list of molecular function GO terms assigned to upregulated and downregulated genes, respectively). Upregulated molecular function GO terms included, catalase activity, amino acid binding and lipase activity, and downregulated terms include transporter activity, hydrolase activity and oxidoreductase activity. Analysis highlighted several molecular function GO terms of interest with cell wall synthesis association (Figure 3.10). These include terms assigned to upregulated genes, mannosidase activity and 1,3- β -D-glucan synthase activity, and terms assigned to downregulated genes include hydrolase activity and chitosanase activity.

GO CATEGORY: MOLECULAR FUNCTION
0 hr vs. 3 hr

UPREGULATED



DOWNREGULATED

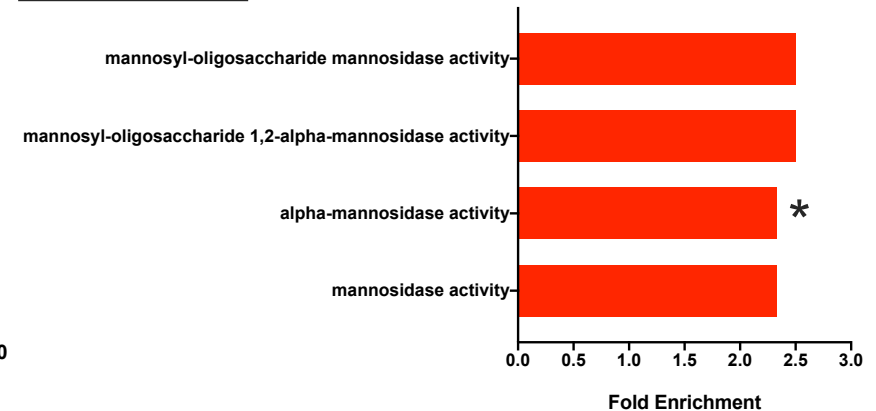
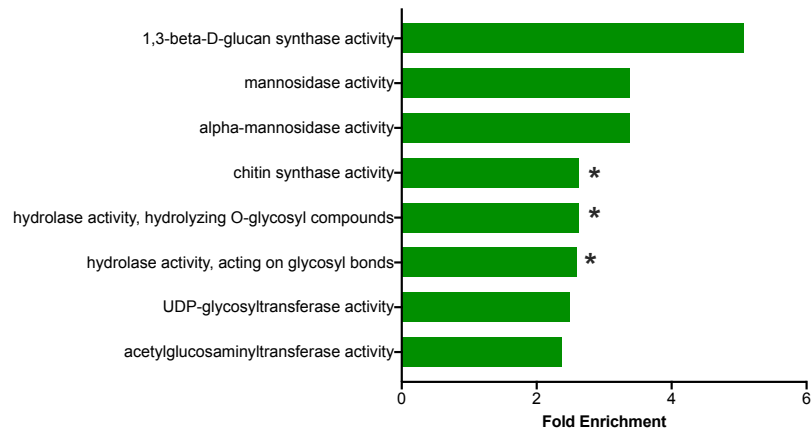


FIGURE 3.9. MOLECULAR FUNCTION GO TERMS ASSIGNED TO DEGS BETWEEN 0 HR AND 3 HR *M. CIRCINELLOIDES* GERMINATION. Analysis highlighted molecular function GO terms of interest with regard to cell wall association, GO terms with transferase activity are seen in the upregulated gene subset, whilst those with mannosidase activity are seen in the downregulated subset. Fisher's exact test with the Benjamini and Hochberg method for false discovery rate (FDR) correction * $FDR \leq 0.05$

GO CATEGORY: MOLECULAR FUNCTION
3 hr vs. 6 hr
CELL WALL ASSOCIATED

UPREGULATED



DOWNREGULATED

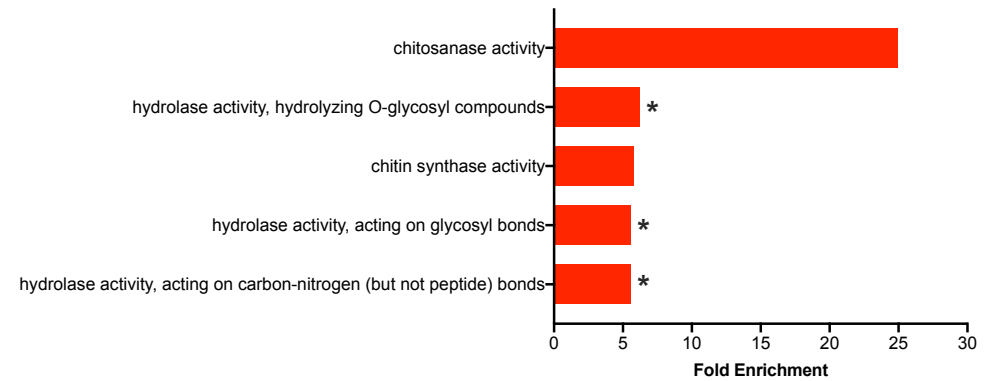


FIGURE 3.10. MOLECULAR FUNCTION GO TERMS ASSIGNED TO DEGS BETWEEN 3 HR AND 6 HR SPORE GERMINATION. Analysis highlighted several upregulated and downregulated molecular function GO terms of interest with regard to cell wall association. Fisher's exact test with the Benjamini and Hochberg method for false discovery rate (FDR) correction * $FDR \leq 0.05$

3.2.6.1.3 ANALYSIS OF BIOLOGICAL PROCESS GO TERMS

Analysis of GO terms within the 'biological process' category, elucidates the biological processes of which gene products partake in. Between 0 hr and 3 hr, there were a total of 273 biological process GO terms assigned to significantly upregulated genes and 117 to downregulated genes. Upregulated biological process GO terms included, cytoplasmic translation, mitochondrial gene expression and response to temperature stimulus, and downregulated terms included autophagy, fatty acid oxidation and response to oxidative stress. Analysis of biological process GO terms assigned to upregulated genes highlighted several terms of interest with cell wall synthesis association (Figure 3.11). Terms included, protein glycosylation (33 genes) and oligosaccharide-lipid intermediate biosynthetic process (7 genes). Analysis of downregulated biological process GO terms did not return any process of interest regarding cell wall.

Between 3 hr and 6 hr, there were a total of 90 biological process GO terms assigned to significantly upregulated genes and 19 to downregulated genes. Upregulated biological process GO terms included calcium-mediated signalling, response to oxidative stress and microtubule-based movement, and downregulated terms included transmembrane transport and establishment of localization. Analysis of upregulated and downregulated terms highlighted several upregulated biological processes of interest with cell wall synthesis association (Figure 3.12). These included 'cell wall organization', '(1->3)- β -D-glucan biosynthetic process' and 'chitin biosynthetic process'. Analysis of downregulated biological process GO terms did not return any terms of interest regarding cell wall.

GO CATEGORY: BIOLOGICAL PROCESS
CELL WALL ASSOCIATED TERMS
0 hr vs. 3 hr

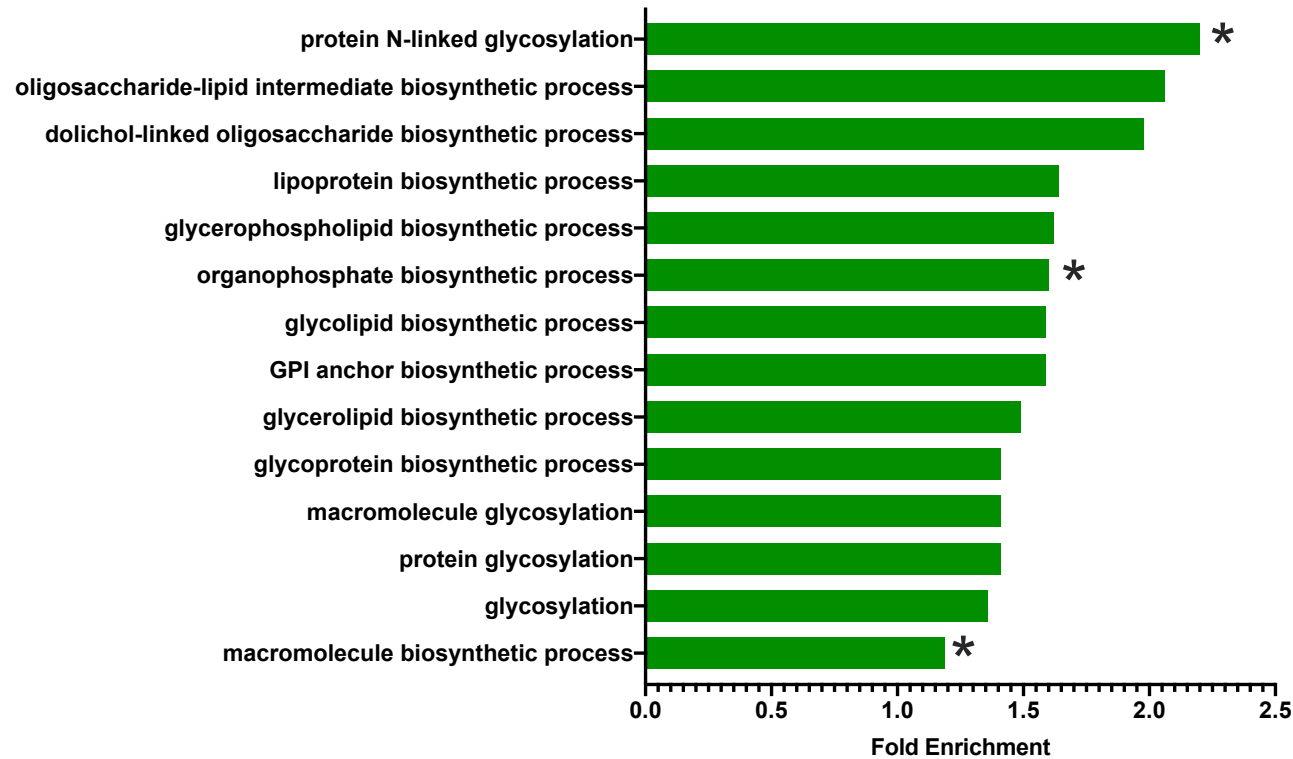


FIGURE 3.11. BIOLOGICAL PROCESS GO TERMS ASSIGNED TO DEGS BETWEEN 0 HR AND 3 HR SPORE GERMINATION. GO terms with associations to cell wall biosynthesis are seen in the upregulated gene subset. No biological process GO terms of interest were noted in the downregulated gene subset. Fisher's exact test with the Benjamini and Hochberg method for false discovery rate (FDR) correction * $FDR \leq 0.005$

GO CATEGORY: BIOLOGICAL PROCESS
3 hr vs. 6 hr
CELL WALL ASSOCIATED

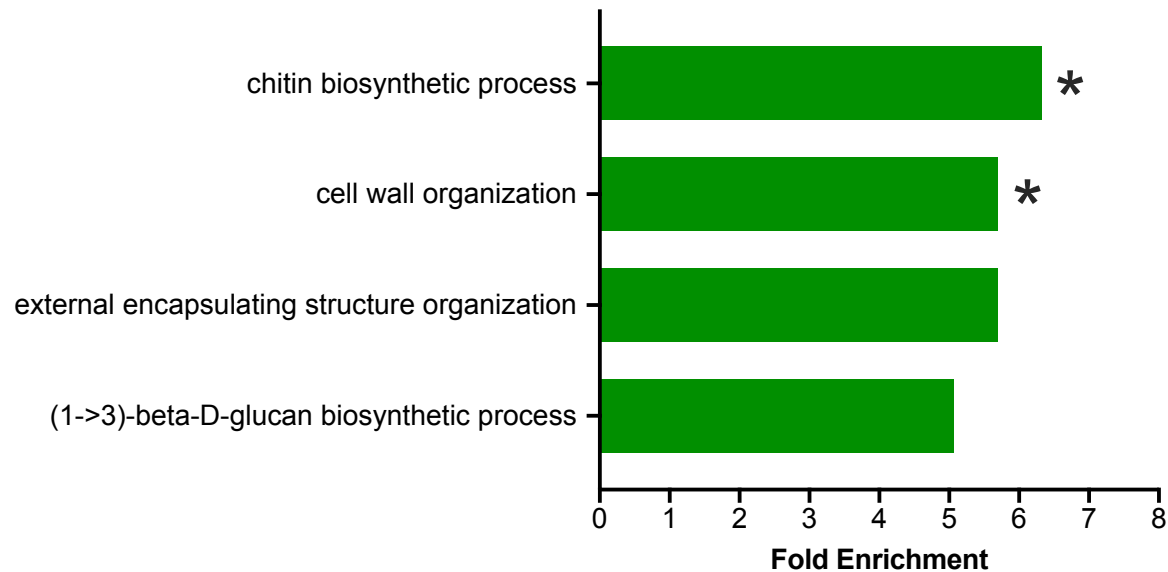


FIGURE 3.12. BIOLOGICAL PROCESS GO TERMS ASSIGNED TO DEGS BETWEEN 3 HR AND 6 HR SPORE GERMINATION. Analysis highlighted several upregulated biological processes of interest with regards to cell wall association, whilst no biological process GO terms of interest were seen in the downregulated gene set. Fisher's exact test with the Benjamini and Hochberg method for false discovery rate (FDR) correction * $FDR \leq 0.05$

3.2.6.2 GENES ASSOCIATED WITH CHITIN SYNTHESIS ARE DIFFERENTIALLY EXPRESSED DURING *M. CIRCINELLOIDES* GERMINATION

In early *M. circinelloides* germination, genes encoding chitin synthases were upregulated (Table 3.4). The chitin biosynthesis pathway has not been reported in *M. circinelloides*. The *C. albicans* orthologs of these genes are *CHS1*, *CHS2*, *CHS3*, *CHS7* and *CHS8* (Table 3.4). In *Candida*, *CHS1* is necessary for the formation of the primary septum, *CHS2* is implicated in hyphal chitin deposition, *CHS3* synthesises short chitin fibrils deposited in the hyphal cell wall, *CH7* regulates chitin synthase III (*CHS3*), and *CHS8* mediates chitin deposition in hyphae (Munro and Gow, 2001, Sanz *et al.*, 2005, Lenardon, Munro and Gow, 2010). From this analysis, it suggests cell wall chitin synthesis is upregulated during the early stages of *Mucor* germination, between 0 hr and 3 hr. During late *M. circinelloides* germination between 3 hr and 6 hr, chitin synthases orthologous to *C. albicans* *CHS1*, *CHS2*, *CHS3* and *CHS8* were also upregulated, suggesting a continuation in the upregulation of chitin synthesis, as is seen in early germination (Table 3.4).

Analysis of downregulated genes between 3 hr and 6 hr *M. circinelloides* germination, highlighted a gene orthologous to *CHS1*, *CHS2* and *CHS8*, suggesting the downregulation of chitin synthesis during late *M. circinelloides* germination, between 3 hr and 6 hr (Table 3.4). Chitin synthases play a variety of roles regarding type of chitin deposition and location, therefore it is important to consider that whilst orthologous genes can offer some insight into the potential roles of genes in *M. circinelloides* the exact nature of the chitin synthase in *M. circinelloides* may differ.

TABLE 3.4. GENES ASSOCIATED WITH CHITIN SYNTHESIS ARE DIFFERENTIALLY EXPRESSED DURING *M. CIRCINELLOIDES* GERMINATION. Genes were screened during the analysis of GO terms. Genes with implications in cell wall chitin biosynthesis and organization are reported. Significant upregulated genes were determined as $P_{adj} \geq 0.05$ and $\text{Log}_2\text{Fold} \geq 1$.

Profile	<i>M. circinelloides</i> Gene(s)	Product Description(s)	Ortholog(s)	Ortholog Product Description(s)
0 hr – 3 hr UPREGULATED	QYA_151786	Chitin synthase/hyaluronan synthase	CHS1	Chitin synthase
	QYA_188342	(glycosyltransferases)	CHS2	CHS1: essential, for primary septum synthesis in yeast and hyphae, 1 of several chitin synthases. CHS2: nonessential, required for wild-type chitin deposition in hyphae. CHS8: Chitin synthase required for synthesis of long-chitin fibrils, nonessential, induced during cell wall regeneration
	QYA_85917		CHS8	
	QYA_114562	Unspecified product/chitin synthases/hyaluronan synthase	CHS3	Major chitin synthase of yeast and hyphae, synthesizes short-chitin fibrils
	QYA_138564	(glycosyltransferases)		
	QYA_146431			
	QYA_154997			
	QYA_168848			
	QYA_72427			
	QYA_154683	Unspecified product	CHS7	Protein required for wild-type chitin synthase III activity
	QYA_77324			
3 hr – 6 hr UPREGULATED	QYA_114551	Chitin synthase/hyaluronan synthase	CHS1	Chitin synthase
	QYA_151786	(glycosyltransferases)	CHS2	CHS1: essential, for primary septum synthesis in yeast and hyphae, 1 of several chitin synthases. CHS2: nonessential, required for wild-type chitin deposition in hyphae. CHS8: Chitin synthase required for synthesis of long-chitin fibrils, nonessential, induced during cell wall regeneration
	QYA_188342		CHS8	
	QYA_71463			
	QYA_85917			
	QYA_138564	Unspecified product/chitin synthases/hyaluronan synthase	CHS3	Major chitin synthase of yeast and hyphae, synthesizes short-chitin fibrils
	QYA_146431	(glycosyltransferases)		
3 hr – 6 hr DOWNREGULATED	QYA_40808	Chitin synthase/hyaluronan synthase	CHS1	Chitin synthase
		(glycosyltransferases)	CHS2	CHS1: essential, for primary septum synthesis in yeast and hyphae, 1 of several chitin synthases. CHS2: nonessential, required for wild-type chitin deposition in hyphae. CHS8: Chitin synthase required for synthesis of long-chitin fibrils, nonessential, induced during cell wall regeneration
			CHS8	

3.2.6.3 GENES IMPLICATED IN β -GLUCAN SYNTHESIS ARE DIFFERENTIALLY EXPRESSED DURING *M. CIRCINELLOIDES* GERMINATION

Analysis of significantly upregulated genes during early *M. circinelloides* germination (0hr to 3 hr) highlighted genes orthologous to *C. albicans* *GSC1*, *GSL1* and *GSL2*, and *KRE5* (Table 3.5). The biosynthesis pathway of cell wall β -1,3-glucan is facilitated by the activity of β -1,3-glucan synthases encoded by *GSC1*, *GLS1* and *GLS2* (Douglas, 2001). The biosynthesis of β -1,6-glucan is not well characterised, however *KRE5* has been implicated (Herrero *et al.*, 2004). This analysis, suggests that during early *M. circinelloides* germination β -1,3-glucan and β -1,6-glucan biosynthesis is upregulated. Analysis of significantly upregulated genes in early *M. circinelloides* germination also highlighted a gene orthologous to *C. albicans* *PHR1*, *PHR2* and *PHR3* that encodes glycosidases implicated in β -1,3- and β -1,6- glucan crosslinking. (Table 3.5). In *Candida*, cross-linking of β -1,3- and β -1,6- glucan is shown to be mediated by *PHR1* and *PHR2* (Fonzi, 1999, Douglas, 2001). Analysis here, suggests that β -1,3- and β -1,6- glucan crosslinking is upregulated in the early stages of *M. circinelloides* germination.

Between 3 hr and 6 hr, significantly upregulated genes orthologous to *GSL1*, *GSL2* and *GSC1* are also noted, suggesting a continuation of β -glucan synthesis upregulation in late *M. circinelloides* germination. Additionally, a gene orthologous to *C. albicans* *BGL2*, a 1,3- β -glucosyltransferase that transfers a β -1,3-glucan chain to another to form a β -1,6-linkage in *C. albicans* was upregulated in late germination (Table 3.5). Here, analysis suggests cell wall β -1,3-glucan crosslinking and β -1,6-glucan formation may be downregulated during late *M. circinelloides* germination, between 3 hr and 6 hr.

A gene orthologous to *C. albicans* *UTR2* was also downregulated in late *M. circinelloides* germination (Table 3.5). *UTR2* encodes a putative GPI anchored cell wall glycosidase that binds chitin and is been proposed to play a role in the formation of β -1,3-glucan and chitin linkages in *C. albicans* (Pardini *et al.*, 2006). Here analysis suggests there is a downregulation of β -1,3-glucan crosslinking during the late stages of *M. circinelloides* germination, between 3 hr and 6 hr.

TABLE 3.5. GENES ASSOCIATED WITH β -GLUCAN SYNTHESIS ARE DIFFERENTIALLY EXPRESSED DURING *M. CIRCINELLOIDES* GERMINATION. Genes were screened during the analysis of GO terms. Genes with implications in cell wall β -glucan biosynthesis and organization are reported. Significant upregulated genes were determined as $P_{adj} \geq 0.05$ and $\text{Log}_2\text{Fold} \geq 1$.

Profile	<i>M. circinelloides</i> Gene(s)	Product Description(s)	Ortholog(s)	Ortholog Product Description(s)
0 hr – 3 hr UPREGULATED	<i>QYA_135619</i> , <i>QYA_153484</i>	1,3- β -glucan synthase/callose synthase catalytic subunit	<i>GSL1</i> <i>GSL2</i> <i>GSC1</i>	<i>GSL1</i> : essential β -1,3-glucan synthase subunit. <i>GSL2</i> : Protein similar to β -1,3-glucan synthase. <i>GSC1</i> : Essential β -1,3-glucan synthase subunit
	<i>QYA_189922</i>	UDP-glucose glycoprotein glucosyltransferase	<i>KRE5</i>	UDP-glucose:glycoprotein glucosyltransferase, 1,6- β -D- glucan biosynthesis
	<i>QYA_129129</i>	Unspecified Product	<i>PHR1</i> <i>PHR2</i> <i>PHR3</i>	<i>PHR1</i> : cell surface glycosidase, may act on cell-wall β -1,3- glucan prior to β -1,6-glucan linkage. <i>PHR2</i> : glycosidase, low pH, high iron or fluconazole induced. <i>PHR3</i> : putative β -1,3- glucanosyltransferase with similarity to the <i>A. fumigatus</i> GEL family
3 hr – 6 hr UPREGULATED	<i>QYA_152798</i> <i>QYA_153484</i>	1,3- β -glucan synthase/callose synthase catalytic subunit	<i>GSL1</i> / <i>GSC1</i> , <i>GSL2</i>	<i>GSL1/GSC1</i> : essential β -1,3-glucan synthase subunit. <i>GSL2</i> : protein similar to β -1,3-glucan synthase
3 hr – 6 hr DOWNREGULATED	<i>QYA_121348</i>	Unspecified Product	<i>BGL2</i>	Cell wall 1,3- β -glucosyltransferase
	<i>QYA_82616</i>	Unspecified Product	<i>UTR2</i>	Putative GPI anchored cell wall glycosidase, chitin-binding, glycosyl hydrolase domains, induced during cell wall regeneration

3.2.6.4 GENES INVOLVED IN GLYCOSYLATION ARE UPREGULATED DURING *M. CIRCINELLOIDES* GERMINATION

Analysis of significant DEGs in early (0 hr – 3 hr) and late (3 hr – 6 hr) *M. circinelloides* germination, highlighted numerous genes implicated in glycosylation (Table 3.6).

Analysis of upregulated genes between 0 hr and 3 hr *M. circinelloides* spore germination highlighted genes implicated in the assembly of the lipid-linked oligosaccharide during protein glycosylation (Table 3.6). Gene products included mannosyltransferases, glycosyltransferases and glucosyltransferases of the Alg family. Orthologs in *C. albicans* belonged to the ALG family and included *ALG1* involved in *N*-linked protein glycosylation, *ALG8* involved in cell wall mannan biosynthesis and *ALG14* involved in lipid-linked oligosaccharide biosynthesis. Here, analysis suggests there is an upregulation in transferase activity mediating the assembly of the lipid-linked oligosaccharide and protein glycosylation, in the early stages of *M. circinelloides* spore germination, between 0 hr and 3 hr.

Genes encoding mannosyltransferases orthologous to *C. albicans* *MNN*, *MNT* and *PMT* genes were also highlighted in the analysis of upregulated genes in early and late *M. circinelloides* germination, indicating the upregulation of *N*-linked and *O*-linked glycosylation. Capping of branches during *N*-linked glycosylation in *C. albicans* occurs via the addition of terminal α 1,3-mannose by α 1,3-mannosyltransferases Mnn1, Mnn12, Mnn13, Mnn14 and Mnn15, and branching of the α 1,6-mannose backbone is achieved via mannosyltransferases Mnt3, Mnt4, Mnt5, Mnn2 and Mnn5, which add α 1,2-oligomannans. Here, analysis suggests transferases implicated in *N*-linked glycosylation are upregulated during early *M. circinelloides* germination, between 0 hr and 3 hr. During *O*-linked glycosylation, α 1,2-linked mannose residues are added to serine or threonine residues in the ER lumen, catalysed by protein mannosyltransferases of the *PMT* gene family (*PMT1*, *PMT2*, *PMT4*, *PMT5* and *PMT6*). Subsequently, glycoproteins are transported to the Golgi where mannose residues are added by Golgi α 1,2-mannosyltransferases Mnt1 and Mnt2. Mnt1 adds the second mannose and Mnt2

adds the third mannose to O-linked glycans. Analysis here suggests transferases involved in *N*- and *O*-linked glycosylation are upregulated in the early and late stages of *M. circinelloides* germination.

Between 0 hr and 3 hr germination, analysis of significantly upregulated genes highlighted a gene with a nuclear division RFT1 protein product, and another encoding an oligosaccharyltransferase (Table 3.6). Ortholog analysis showed the *C. albicans* orthologs of these to be *RFT1* and *OST1*, respectively. In *C. albicans*, *RFT1* partakes in *N*-linked glycosylation, by flipping the precursor into the lumen during the assembly of the lipid-linked oligosaccharide (Mora-Montes *et al.*, 2007). *OST1* is also implicated in *N*-linked glycosylation, and forms part of the OST complex which transfers the Glc₃Man₉GlcNAc₂ from the glycan precursor to an asparagine residue on nascent protein in the ER (Shrimal and Gilmore, 2019).

Significantly upregulated genes between 0 hr and 3 hr included genes involved in GPI anchor biosynthesis (Table 3.6). Ortholog analysis showed the orthologs of these to be *GPI1*, *GPI2*, *GPI7*, *GPI14* and *GPI18*. GPI proteins have not been reported in the *Mucor* cell wall but are found in the cell wall of fungi such as *Candida* and *Saccharomyces*, where they act as anchors for cell wall proteins. The GPI biosynthesis pathway has been partially characterised in *Candida*. Gpi1 and Gpi2p form parts of the multi-subunit enzyme complex that mediates the addition of GlcNAc to PI, Gpi14 and Gpi18 mediate the addition of mannose residues, and Gpi7 catalyses the addition of phosphorylethanolamine. Analysis here suggests that during early *M. circinelloides* germination between 0 hr and 3 hr, transferase activity implicated in cell wall GPI anchor biosynthesis is upregulated.

Analysis of upregulated genes between 3 hr and 6 hr germination highlighted one gene encoding an alpha-mannosidase orthologous to *C. albicans* *MNS1* and another encoding an alpha-1,2-mannosidase orthologous to *AMS1*. *MNS1* and *AMS1* have been implicated in *N*-linked glycosylation. In *C. albicans* *MNS1* encodes an alpha-1,2-mannosidase in *C. albicans* that is homologous to *S. cerevisiae* *MNS1*, that has been shown to process the Man₉GlcNAc₂ oligosaccharide to Man₈GlcNAc₂ isomer B during *N*-glycosylation (Moras-Metnes *et al.*, 2007). The role of *AMS1* has not been defined in *C. albicans*, however in *S. cerevisiae* *AMS1* has been shown to catalyse the processing of free

cytosolic *N*-glycans. Additionally, genes with mannosyltransferase activity implicated in glycosylation were noted, including genes orthologous to genes of the *PMT* family and the *MNT* family (not reported). Here, analysis supports the notion that there is a continuation of the upregulation of mannosyltransferase and mannosidase activity partaking in *N*- and *O*- linked glycosylation in late germination, between 3hr and 6hr.

TABLE 3.6. GENES ASSOCIATED WITH GLYCOSYLATION ARE DIFFERENTIALLY EXPRESSED DURING *M. CIRCINELLOIDES* GERMINATION. Genes with implications in the synthesis and /or organisation of the cell wall were analysed. Here genes that play a role in cell wall glycosylation are reported. Significant upregulated genes were determined as $P_{adj} \geq 0.05$ and $\text{Log}_2\text{Fold} \geq 1$.

Profile	<i>M. circinelloides</i> Gene(s)	Product Description(s)	Ortholog(s)	Ortholog Product Description
0 hr – 3 hr UPREGULATED	QYA_129928	B-1,4-mannosyltransferase	ALG1	Mannosyltransferase involved in N-linked protein glycosylation
	QYA_154315	Glycosyltransferase	ALG2	Putative mannosyltransferase involved in cell wall mannan biosynthesis
	QYA_114182	Glucosyltransferase – Alg6p	ALG6	Putative glucosyltransferase involved in cell wall mannan biosynthesis
	QYA_187164	Glucosyltransferase – Alg8p	ALG8	Putative glucosyltransferase involved in cell wall mannan biosynthesis
	QYA_109009	Mannosyltransferase	ALG9	Putative mannosyltransferase similar to <i>S. cerevisiae</i> Alg9p
	QYA_49883	Predicted glycosyltransferase	ALG13	Ortholog(s) have a role in dolichol-linked oligosaccharide biosynthetic process
	QYA_39631	Predicted glycosyltransferase	ALG14	Required for the 2nd step of dolichyl-linked oligosaccharide synthesis
	QYA_156380 QYA_161614	Unspecified product	MNN1 MNN12-14 MNN15 MNT4	MNN1: putative alpha-1,3-mannosyltransferase, of the mannosyltransferase complex. MNN12-14: predicted alpha-1,3-mannosyltransferase activity with a role in protein glycosylation. MNN15: putative alpha-1,3-mannosyltransferase, predicted role in protein O-linked glycosylation. MNT4: predicted alpha-1,3-mannosyltransferase with a role in protein glycosylation.
	QYA_151673 QYA_152471	Glycolipid 2-alpha-mannosyltransferase (alpha-1,2-mannosyltransferase)	MNT1 MNT2 MNT3	MNT1: alpha-1,2-mannosyl transferase, predicted type II Golgi membrane protein, adds 2nd mannose during cell wall mannoprotein biosynthesis. MNT2: alpha-1,2-mannosyl transferase, adds 3rd mannose in cell-wall mannoprotein biosynthesis. MNT3: mannosyltransferase

<i>QYA_146788</i>	Dolichyl-phosphate-mannose:protein O-mannosyl transferase	<i>PMT1-2</i>	Protein mannosyltransferase
<i>QYA_151650</i>		<i>PMT5-6</i>	
<i>QYA_160449</i>	Dolichyl-phosphate-mannose:protein O-mannosyl transferase	<i>PMT4</i>	Protein mannosyltransferase, required for WT cell wall composition
<i>QYA_138695</i>	Nuclear division RFT1 protein	<i>RFT1</i>	<i>S. cerevisiae</i> ortholog Rft1p has role in glycolipid translocation and protein N-linked glycosylation
<i>QYA_11299</i>	Oligosaccharyltransferase, alpha subunit (ribophorin I)	<i>OST1</i>	Alpha subunit of the oligosaccharyltransferase complex of the ER lumen, catalyses asparagine-linked glycosylation of newly synthesized proteins
<i>QYA_134917</i>	N-acetylglucosaminyltransferase complex, subunit PIG-Q/GPI1, required for phosphatidylinositol biosynthesis	<i>GPI1</i>	Putative protein of GPI synthesis
<i>QYA_160852</i>	N-acetylglucosaminyltransferase complex, subunit PIG-C/GPI2, required for phosphatidylinositol biosynthesis	<i>GPI2</i>	Subunit of the GPI-N-acetylglucosaminyl transferase that catalyses the first step in GPI anchor biosynthesis
<i>QYA_127486</i>	Glycosylphosphatidylinositol anchor synthesis protein	<i>GPI7</i>	Protein involved in attachment of GPI-linked proteins to cell wall
<i>QYA_37192</i>	Mannosyltransferase	<i>GPI14</i>	Catalytic subunit of glycosylphosphatidylinositol-alpha 1,4 mannosyltransferase I, involved in GPI anchor biosynthesis

	<i>QYA_155971</i>	Predicted Dolichyl-phosphate-mannose-protein mannosyltransferase	<i>GPI18</i>	Mannosyltransferase activity and role in GPI anchor biosynthesis
3 hr – 6 hr UPREGULATED	<i>QYA_161253</i>	Predicted membrane protein	<i>MNN1</i> <i>MNN12-14</i> <i>MNN15</i> <i>MNT4</i>	<i>MNN1</i> : putative alpha-1,3-mannosyltransferase, of the mannosyltransferase complex. <i>MNN12-14</i> : predicted alpha-1,3-mannosyltransferase activity with a role in protein glycosylation. <i>MNN15</i> : putative alpha-1,3-mannosyltransferase, predicted role in protein O-linked glycosylation. <i>MNT4</i> : predicted alpha-1,3-mannosyltransferase with a role in protein glycosylation.
	<i>QYA_141532</i>	Glycolipid 2-alpha-mannosyltransferase (alpha-1,2-mannosyltransferase)	<i>MNT1</i> <i>MNT2</i> <i>MNT3</i>	<i>MNT1</i> : alpha-1,2-mannosyl transferase, predicted type II Golgi membrane protein, adds 2nd mannose during cell wall mannoprotein biosynthesis. <i>MNT2</i> : alpha-1,2-mannosyl transferase, adds 3rd mannose in cell-wall mannoprotein biosynthesis. <i>MNT3</i> : mannosyltransferase
	<i>QYA_13406</i>	Oligosaccharyltransferase, alpha subunit (ribophorin I	<i>OST1</i>	Alpha subunit of the oligosaccharyltransferase complex of the ER lumen
	<i>QYA_127793</i>	Dolichyl-phosphate-mannose:protein O-mannosyl transferase	<i>PMT1-2</i> <i>PMT5-6</i>	Protein mannosyltransferase
	<i>QYA_112156</i>	Dolichyl-phosphate-mannose:protein O-mannosyl transferase	<i>PMT4</i>	Protein mannosyltransferase, required for WT cell wall composition
	<i>QYA_149517</i>	Alpha-mannosidase	<i>MNS1</i>	Alpha-1,2-mannosidase, processes Man ₉ GlcNAc ₂ to Man ₈ GlcNAc ₂ isomer B
	<i>QYA_142223</i>	Mannosyl-oligosaccharide alpha-1,2-mannosidase and related glycosyl hydrolases	<i>AMS1</i>	Putative alpha-mannosidase, transcript regulated by Nrg1, induced during cell wall regeneration

3.2.6.5 CELL WALL BIOSYNTHESIS PATHWAYS ARE DIFFERENTIALLY EXPRESSED DURING *M. CIRCINELLOIDES* GERMINATION

Analysis of GO terms assigned to DEGs during *M. circinelloides* germination from resting spore to maximal-swollen spore (between 0 hr and 6 hr) supported the results of the analysis of GO terms assigned to DEGs during both early (between 0 hr and 3 hr) and late (between 3 hr and 6 hr) germination. Expectedly, analysis of GO terms highlighted many of the same genes that are seen in the analysis of early and late germination independently, and therefore only those which have not been mentioned previously are noted here.

Between 0 hr and 6 hr *M. circinelloides* spore germination, there were 106 upregulated cellular component GO terms (See Table S18 Appendix II.II for full list of cellular component GO terms assigned to upregulated genes). When considering those with cell wall associations, several GO terms were highlighted, including 'oligosaccharyltransferase complex', 'obsolete cell part' and 'cell periphery' (Figure 3.13). Analysis of downregulated cellular component GO terms showed 23 terms are downregulated during germination between 0 hr and 6 hr, none of which were noted as of interest in regards to cell wall biosynthesis (See Table S19 Appendix II.II for full list of cellular component GO terms assigned to downregulated genes). Analysis of upregulated cellular component GO terms between 0 hr and 6 hr *M. circinelloides* germination highlighted just one gene not seen in previous analyses (Table 3.7). The product description for this gene was an adaptor protein NCK/Dock that contains SH2 and SH3 domains. The *C. albicans* ortholog of this gene was *SSU81*, encoding a predicted adaptor protein, Sho1p, involved in activation of MAP kinase-dependent signalling pathway, which links response to oxidative stress to morphogenesis and cell wall biosynthesis. Sho1p has been implicated in cell wall mannan biosynthesis (Li *et al.*, 2010). (Table 3.7).

During *M. circinelloides* germination between 0 hr and 6 hr, there were 115 upregulated and 46 downregulated molecular function GO terms (See Tables S20 and S21 Appendix II.II for full list of molecular function GO terms assigned to upregulated and downregulated genes, respectively). Again, numerous GO terms of interest were highlighted when considering implication in cell wall

biosynthesis, including 'chitin synthase activity' and 'glycosyltransferase activity' (Figure 3.14). Analysis of upregulated molecular function GO terms supported the findings of early and late germination analysis, whilst also yielding additional genes of interest (Table 3.7). This included genes encoding an OST STT3 subunit, orthologous to *C. albicans*, *STT3*. In *N*-linked glycosylation in *C. albicans*, following the assembly of the lipid-anchored oligosaccharide, Glc₃Man₉GlcNAc₂ from the precursor is transferred to nascent protein by the OST complex. The yeast OST complex is comprised of eight subunits, grouped into sub-complexes, subcomplex 1 (Ost1 and Ost5), subcomplex 2 (Stt3, Ost4, Ost3/6) and subcomplex 3 (Wbp1, Swp1 and Ost2) (Shrimal and Gilmore, 2019). Additionally, genes with products described as Dolichyl-phosphate-mannose:protein O-mannosyl transferases, are seen here, suggesting they play a role in *O*-linked glycosylation (Table 3.7). The *C. albicans* orthologs of these is *PMT6*. In *C. albicans* during *O*-glycosylation, alpha-1,2-linked mannose residues are added to serine or threonine residues, a process is catalysed by protein mannosyltransferases of the *PMT* family (*PMT1*, *PMT2*, *PMT4*, *PMT5* and *PMT6*). Analysis of molecular function GO terms assigned to downregulated genes in the 0 hr vs 6 hr profile, highlighted the term 'mannosidase activity' to be downregulated between 0 hr and 6 hr *M. circinelloides* germination, as is seen in the analysis of early germination between 0 hr and 3 hr. No additional genes of interest are noted to those that encode alpha mannosidases orthologous to *C. albicans* *AMS1* and *MNS1*, respectively.

During *M. circinelloides* germination from 0 hr to 6 hr, there are 214 biological process GO terms assigned to upregulated genes and 92 terms to downregulated genes. Of the upregulated terms, several cell wall-associated terms were highlighted, including 'β-glucan biosynthetic process', 'cell wall organization' and 'protein *N*-linked glycosylation'. When considering downregulated biological process GO terms with cell wall associations, numerous terms are noted including 'macromolecule biosynthetic process' and 'translation' (Figure 3.15). Analysis of the biological process GO term 'β-glucan biosynthetic process' highlighted several significantly upregulated genes seen in the analysis of early and late germination, including genes encoding β-glucan transferases orthologous to *C. albicans* *GSL1*, *GSL2* and *GSC1*. Furthermore, analysis yielded a gene with an unspecified product, but

that was orthologous to *C. albicans*, *BIG1* (Table 3.7). The exact role of the *BIG1* product, Big1p, in β -1,6-glucan synthesis has not been reported, however it has been implicated in cell wall β -1,6-glucan biosynthesis in the *C. albicans* (Umeyama *et al.*, 2006).

Analysis of the upregulated biological process GO term 'glycolipid biosynthesis' highlighted numerous genes associated with GPI anchor biosynthesis that have been previously noted, including genes orthologous to *GPI1* and *GPI2*. Additionally, analysis also highlighted a gene with an uncharacterised membrane protein product (Table 3.7). The ortholog of this gene was *GWT1*, the product of which is an inositol acyltransferase. During GPI biosynthesis, Gwt1 catalyses the inositol acylation of GlcN-PI prior to the addition of mannose residues (Pittet and Conzelmann, 2007).

Analysis also highlighted two upregulated genes encoding a dolichol phosphate-mannose regulatory protein (DPM2) and a dolichol-phosphate mannosyltransferase, subunit 3, respectively (Table 3.7). Orthologs of these genes in *C. albicans* are *DPM2* and *DPM3*, respectively. Dolichol phosphate mannose (DPM) synthase plays a key role in *N*- and *O*- linked glycosylation, and GPI anchor biosynthesis. In *C. albicans*, DPM synthase is comprised of three subunits, Dpm1, Dpm2, and Dpm3 (Juchimiuk, Kruszewska and Palamarczyk, 2015). Additionally, analysis highlighted one gene encoding an OST β subunit, the ortholog of which is *C. albicans* *WBP1* (Table 3.7). The OST complex is comprised of eight subunits, grouped into sub-complexes, subcomplex 1 (Ost1 and Ost5), subcomplex 2 (Stt3, Ost4, Ost3/6) and subcomplex 3 (Wbp1, Swp1 and Ost2) (Shrimal and Gilmore, 2019).

Analysis of biological process GO terms assigned to downregulated genes during *M. circinelloides* germination, between 0 and 6 hr, highlighted genes encoding chitin synthases noted previously.

TABLE 3.7 SIGNIFICANT UPREGULATED GENES BETWEEN 0 HR AND 6 HR *M. CIRCINELLOIDES* GERMINATION. Genes of interest were screened for during the analysis of molecular function, biological process and cellular component GO terms. Genes with implications in the synthesis and /or organisation of the cell wall were analysed. Significant upregulated genes were determined as $P_{adj} \geq 0.05$ and $\text{Log}_2\text{Fold} \geq 1$.

<i>M. circinelloides</i> Gene(s)	Product Description(s)	Ortholog(s)	Ortholog Product Description
QYA_112730	Adaptor protein NCK/Dock, contains SH2 and SH3 domains	SSU81	Predicted adaptor protein involved in activation of MAPK-dependent signalling pathways, links response to oxidative stress to morphogenesis and cell wall biosynthesis
QYA_187400	Oligosaccharyltransferase, STT3 subunit	STT3	Putative oligosaccharyltransferase complex component
QYA_146788 QYA_151650	Dolichyl-phosphate-mannose:protein O-mannosyl transferase	PMT6	Protein mannosyltransferase, required for hyphal growth
QYA_155422	Unspecified product	BIG1	Endoplasmic reticulum protein, required for β -1,6-glucan biosynthesis
QYA_161029	Uncharacterised membrane protein	GWT1	Inositol acyltransferase with role in early steps of GPI anchor biosynthetic process
QYA_110286	Dolichol phosphate-mannose regulatory protein (DPM2)	DPM2	Dolichol-phosphate mannose synthase subunit
QYA_141643	Dolichol-phosphate mannosyltransferase, subunit 3	DPM3	Dolichol-phosphate mannose synthase subunit
QYA_42653	Oligosaccharyltransferase, β subunit	WBP1	Putative oligosaccharyltransferase subunit

GO CATEGORY: CELLULAR COMPONENT
0 hr vs. 6 hr
CELL WALL ASSOCIATED TERMS

UPREGULATED

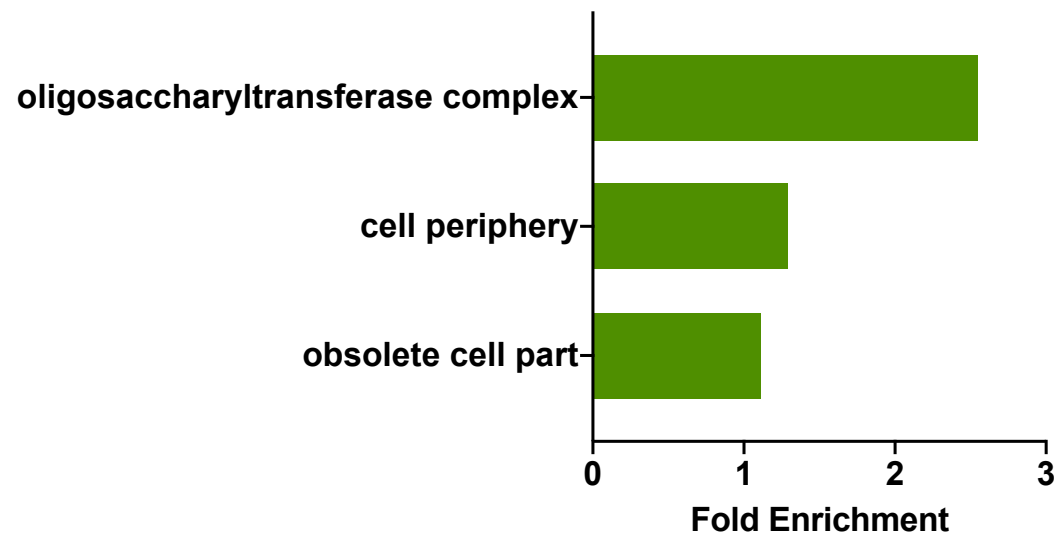
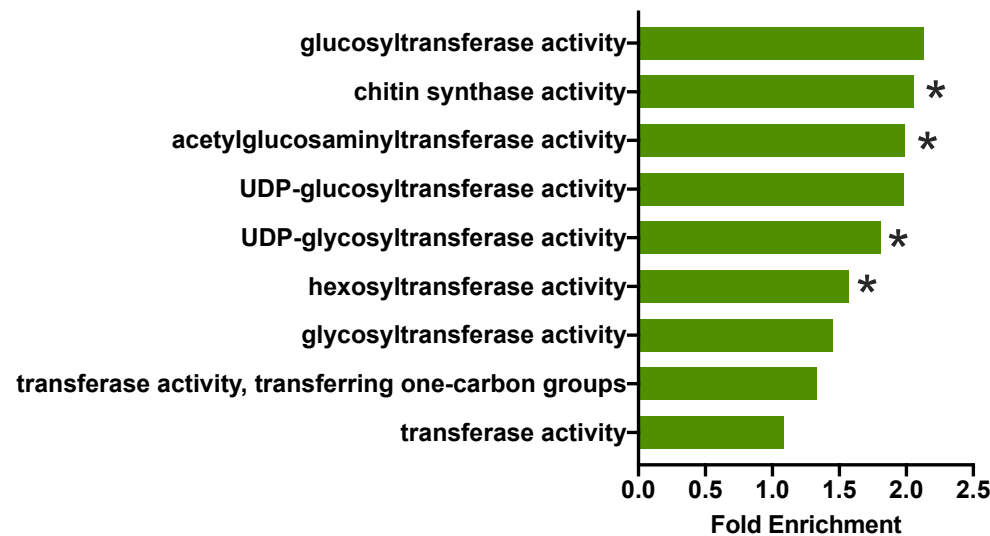


FIGURE 3.13. CELLULAR COMPONENT GO TERMS ASSIGNED TO DEGS BETWEEN 0 HR AND 6 HR SPORE GERMINATION. Analysis highlighted several upregulated cellular component GO terms of interest with regard to cell wall association. Fisher's exact test with the Benjamini and Hochberg method for false discovery rate (FDR) correction * $FDR \leq 0.0$.

GO CATEGORY: MOLECULAR FUNCTION
0 hr vs. 6 hr
CELL WALL ASSOCIATED TERMS

UPREGULATED



DOWNREGULATED

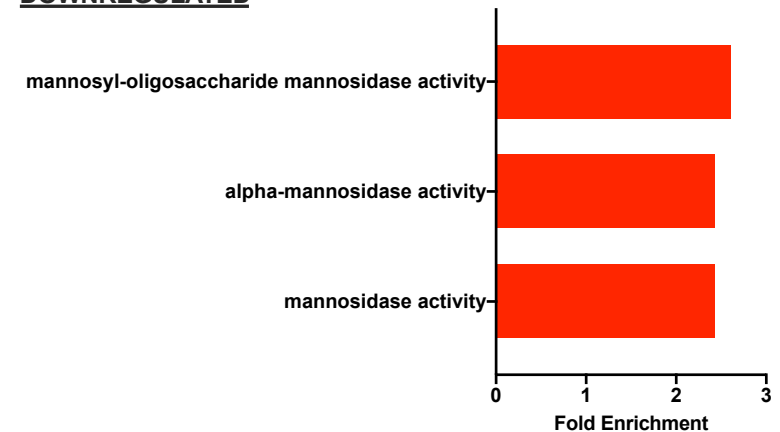


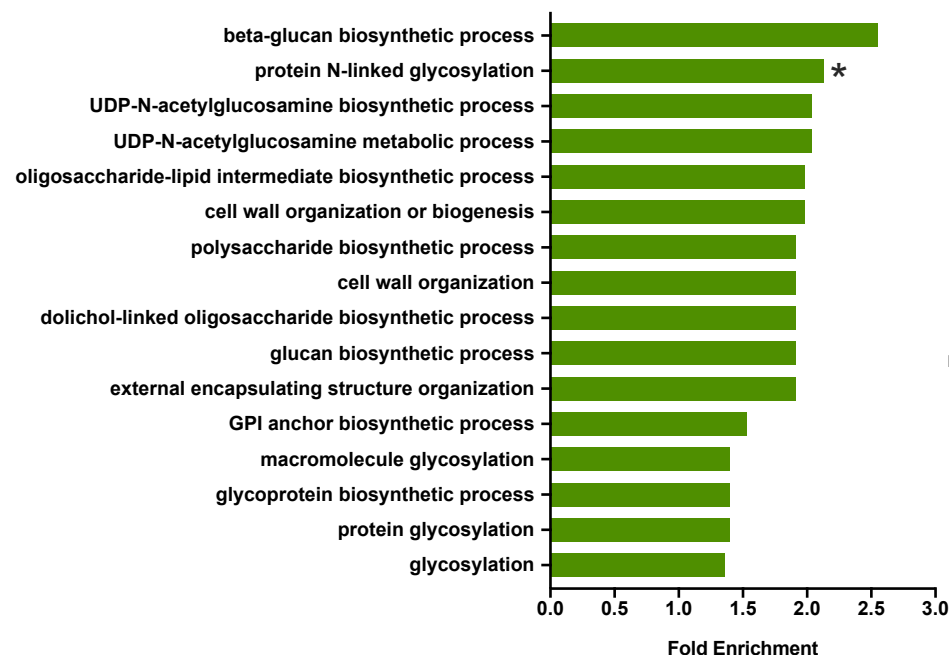
FIGURE 3.14. MOLECULAR FUNCTION GO TERMS ASSIGNED TO DEGS BETWEEN 0 HR AND 6 HR SPORE GERMINATION. Analysis highlighted several upregulated and downregulated molecular function GO terms of interest with regard to cell wall association. Fisher's exact test with the Benjamini and Hochberg method for false discovery rate (FDR) correction * $FDR \leq 0$.

GO CATEGORY: BIOLOGICAL PROCESS

0 hr vs. 6 hr

CELL WALL ASSOCIATED TERMS

UPREGULATED



DOWNREGULATED

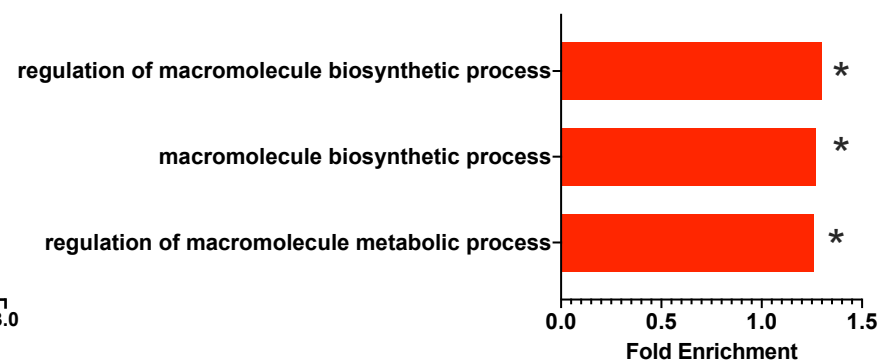


FIGURE 3.15. BIOLOGICAL PROCESS GO TERMS ASSIGNED TO DEGS BETWEEN 0 HR AND 6 HR SPORE GERMINATION. Analysis highlighted several upregulated and downregulated biological process GO terms of interest with regard to cell wall association. Fisher's exact test with the Benjamini and Hochberg method for false discovery rate (FDR) correction * $FDR \leq 0.05$.

3.2.7 *M. CIRCINELLOIDES* NRRL3631 CELL WALL CONTENT DISPLAYS DYNAMIC CHANGES DURING GERMINATION

RNA-sequencing analysis highlighted that genes predicted to be involved in the synthesis of key cell wall polysaccharides were upregulated during the germination process. The cell surface is the first point of contact between the invading pathogen and the innate immune system. Therefore, changes in the cell surface during germination may impact the host-pathogen interaction. To investigate whether differential regulation of cell wall biosynthesis genes correlates with changes in the fungal cell wall composition, the cell wall of *M. circinelloides* spores at 0, 3 and 6 hr germination was analysed using a series of dyes, lectins and Fc-receptors to probe for key cell wall polysaccharides. These included, ConA-TRITC, which detects mannan, Fc-Dectin-1-Alexa Fluor™488, which detects surface exposed β -glucan, WGA-TRITC, which detects surface exposed chitin, and Calcofluor White (CFW), which detects total chitin levels.

3.2.7.1 MANNAN CONTENT INCREASES DURING GERMINATION

Con-A is a lectin that binds to mannose residues of glycoproteins, and can serve as a read out of total mannan levels in the fungal cell wall (Tkacz, Cybulska and Lampen, 1971). Staining of *M. circinelloides* spores at 0 hr (resting), 3 hr (mid-point) and 6 hr (fully swollen) with Con-A confirmed that as the spores undergo germination, more Con-A binds to the spores, indicating that the process of germination results in increased mannan deposition (MFI 0 hr: 21359.0 ± 1139.7 ; 3 hr: 210176.6 ± 88630.9 ; 6 hr: 338791.0 ± 28941.5) (Figure 3.16). Fluorescence microscopy of ConA stained spores corroborated this, with the fluorescence intensity increasing as the spore germination stages progressed from 0, to 3, to 6 hr (Figure 3.16). Staining of fully swollen spores showed patchy staining with a ring-like region of higher intensity at the periphery, suggesting the mannan distribution on the cell wall of fully swollen spores is not uniform (Figure 3.16). These data agree with the RNA-sequencing data (Table 3.6, Figure 3,15), where a number of mannan biosynthetic genes were identified as being significantly upregulated during germination.

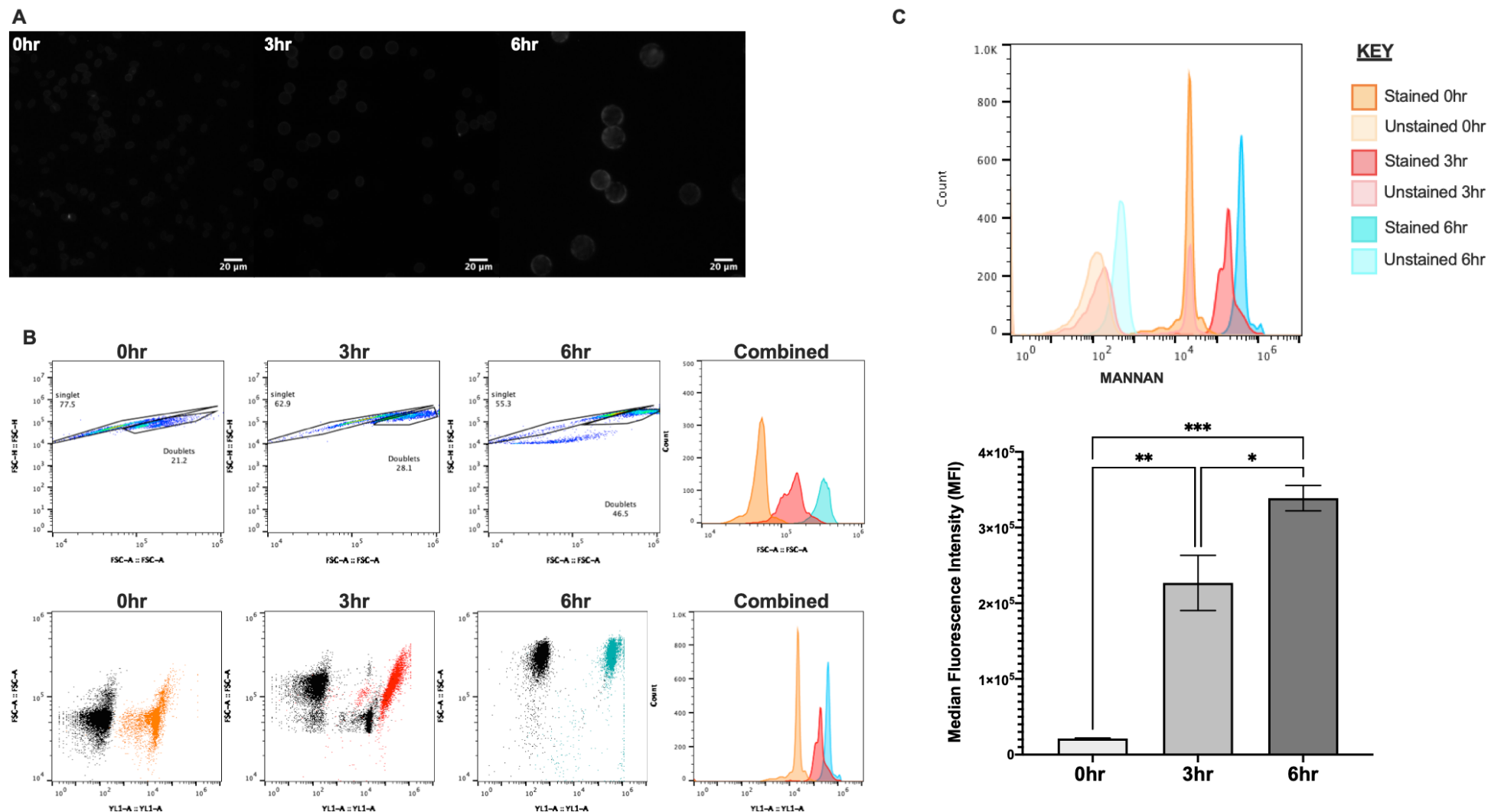


Figure 3.16 *M. circinelloides* spore mannan content increases during spore swelling. *M. circinelloides* spores at 0 hr, 3 hr and 6 hr germination were stained with ConA-TRITC and mannan content investigated by flow cytometry and fluorescence microscopy. (A) Fluorescence microscopy of spores stained with ConA-TRITC shows an increase in fluorescence as spore germination progresses. Spores at 6 hr displayed patchy staining with regions of greater intensity at the spore periphery. (B) Gating strategy for flow cytometry analysis of cell wall staining. Top panel: spores gated for singlets and plotted for size by forward-scatter against count. Bottom panel: singlets of unstained and stained spores plotted for fluorescence by forward scatter against fluorescence. (C) Pooled data shows *M. circinelloides* spore mannan content increases over germination. Data shown are mean \pm SEM of three independent experimental repeats; *** p <0.001, ** p <0.01, * p <0.05. One-way ANOVA, Tukeys multiple comparisons.

3.2.7.2 GERMINATION RESULTS IN INCREASE CHITIN SYNTHESIS.

CFW is a small, membrane permeable, dye that binds to N-acetylglucosamine and is frequently used to quantify total chitin levels in fungal cell walls (Afshar, Larijani and Rouhanizadeh, 2018). Staining of *M. circinelloides* spores at 0 hr (resting), 3 hr (mid-point) and 6 hr (fully swollen) with CFW confirmed that resting spores hardly took up the dye indicating low total chitin content. However, spores that had been germinating for 6 hrs readily took up the dye (Figure 3.17), suggesting that as germination progresses more chitin is synthesised. Fluorescence microscopy of 0, 3 and 6 hr spores was utilised to visualise CFW binding to the *M. circinelloides* spore. Resting spores took up very little CFW and displayed low fluorescence, however upon germination, 3 hr spores displayed slight increase in CFW staining albeit to varying degrees with visible differences in the fluorescence intensity between 3 hr spores themselves (Figure 3.17). Fully swollen spores displayed a significant increase in CFW binding with spores visibly displaying higher fluorescence by microscopy (Figure 3.17). To differentiate between total chitin levels and surface exposed chitin spores were stained with WGA-TRITC. WGA is a large, membrane impermeable, lectin that binds to exposed chitin and is frequently used to quantify the amount of surface exposed chitin (Esher *et al.*, 2018). Similar to the CFW staining WGA staining was minimal in resting spores and increased upon the induction of germination, with fully swollen spores displaying the greatest amount of surface exposed chitin (MFI 0 hr: 38.7 ± 9.6 ; 3 hr: 116.0 ± 43.5 ; 6 hr: 19488 ± 644.9) (Figure 3.18). This cell wall staining agrees with the RNA-seq data (Table 3.4, Figure 3.14) where genes involved in chitin biosynthesis were identified as being significantly upregulated.

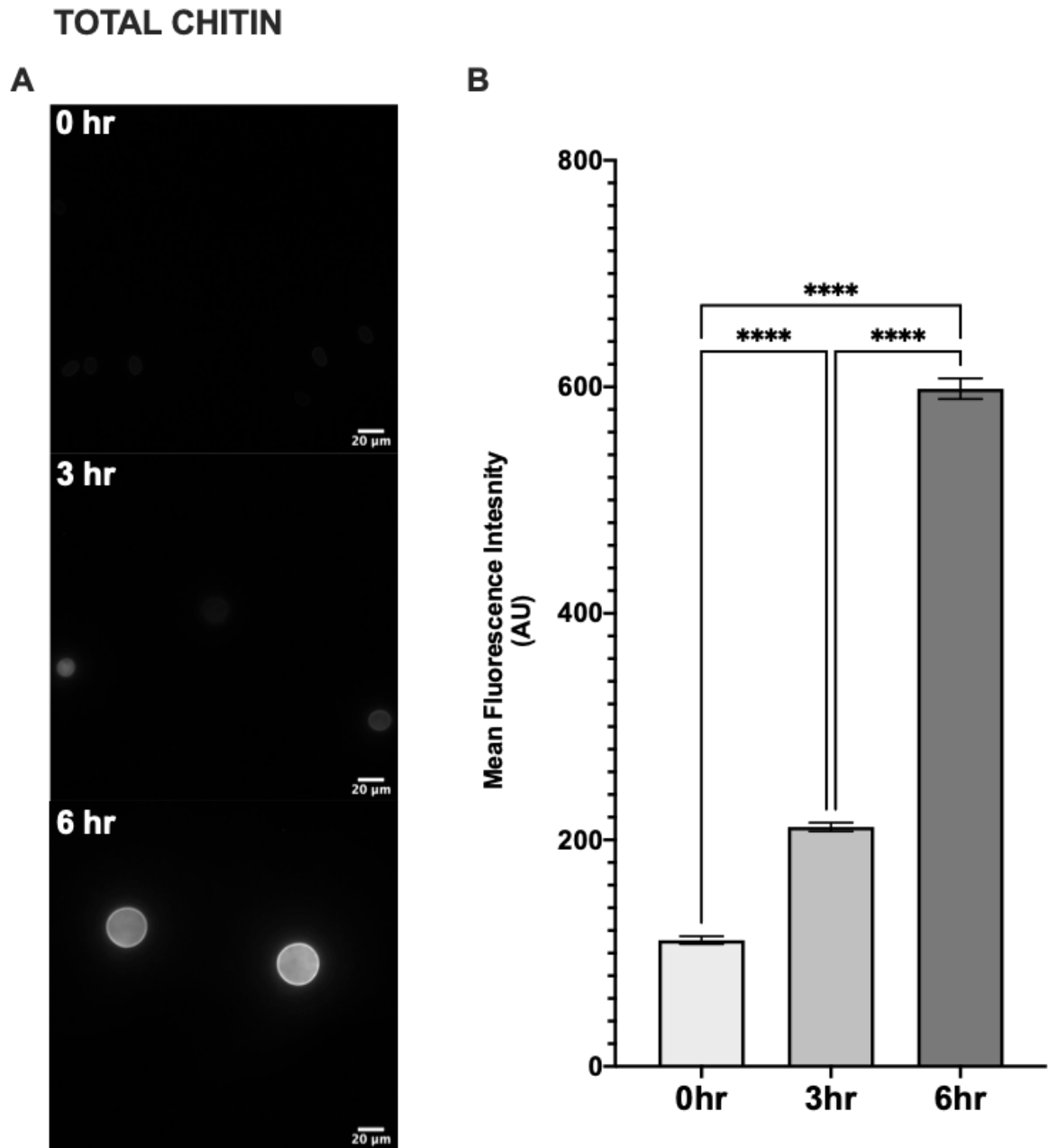


FIGURE 3.17 *M. CIRCINELLOIDES* TOTAL CHITIN CONTENT INCREASES DURING GERMINATION. *M. circinelloides* spores at 0, 3 and 6 hr germination were stained with Calcofluor White (CFW) to investigate total cell wall chitin by fluorescence microscopy. (A) fluorescence microscopy of spores stained with CFW shows an increase in fluorescence as spore germination progresses. Spores at 6 hr displayed uniform staining however intensity varied slightly between spores. (B) Pooled data shows as spores germinate chitin content increases significantly between each stage, 0, 3 and 6 hr. Data shown are mean \pm SEM of three independent experimental repeats; **** $p < 0.0001$. One-way ANOVA, Tukey's multiple comparisons.

EXPOSED CHITIN

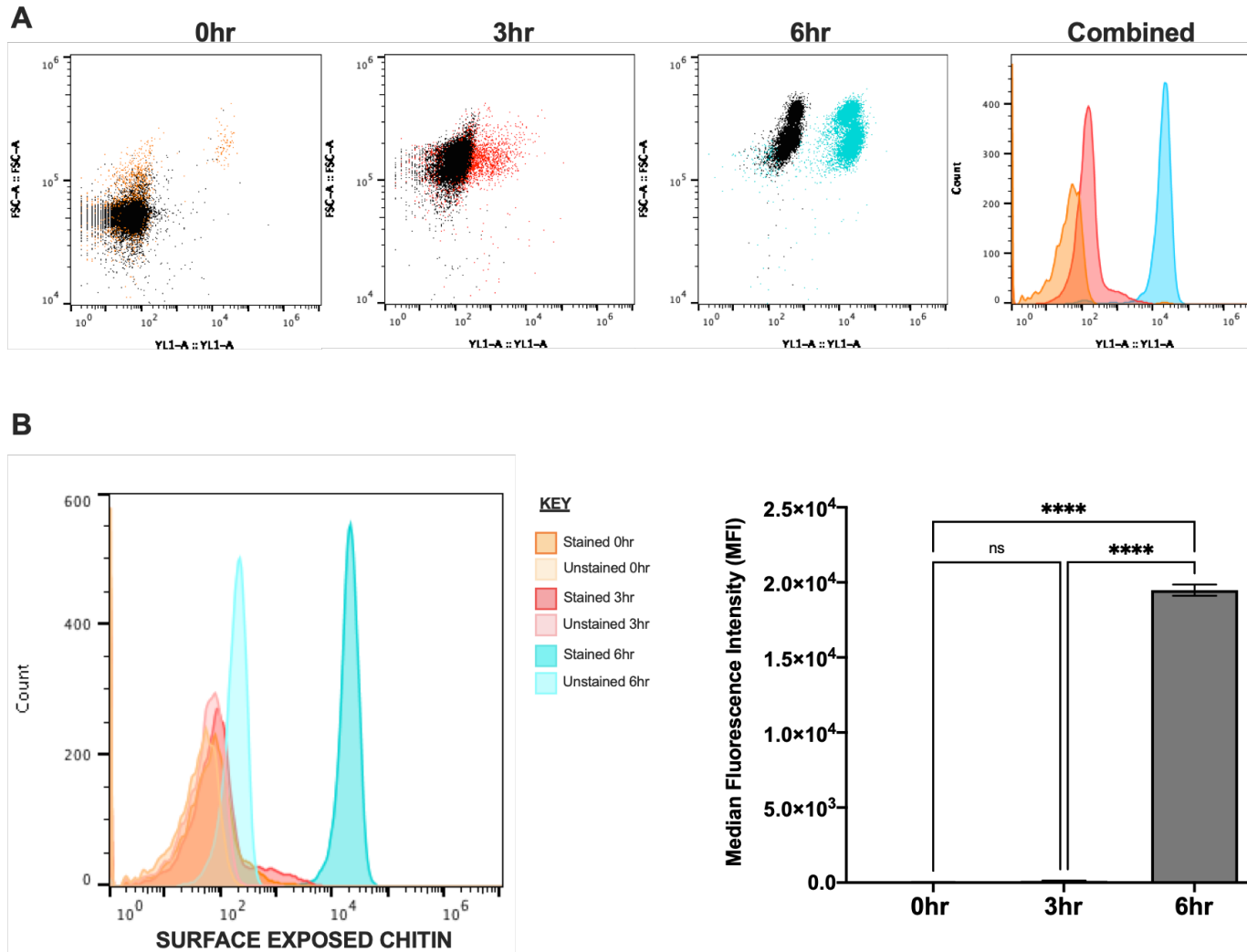


FIGURE 3.18 *M. CIRCINELLOIDES* SURFACE EXPOSED CHITIN CONTENT INCREASES DURING GERMINATION. *M. circinelloides* spores at 0, 3 and 6 hr germination were stained with WGA-TRITC to investigate surface exposed chitin by flow cytometry (WGA). (A) Singlet population against fluorescence for unstained (black) and stained (coloured) spores shows increase in fluorescence (WGA) is most prominent at 6 hr germination. (B) Pooled data shows significant increase in cell wall surface exposed chitin at 6 hr germination. Data shown are mean \pm SEM of three independent experimental repeats; **** p <0.0001. One-way ANOVA, Tukey's multiple comparisons.

3.2.7.3 Cell wall β -glucan levels increase late in germination

Fc-Dectin-1, is fusion protein consisting of the Dectin-1 receptor extracellular domain, and the Fc portion of immunoglobulin IgG1, which detects surface exposed β -glucan in the fungal cell wall (Graham *et al.*, 2006). Staining of *M. circinelloides* spores at 0 hr (resting), 3 hr (mid-point) and 6 hr (fully swollen) with Fc-Dectin-1-Alexa Fluor™488 confirmed that resting spores and mid-point spores hardly took up the dye, indicating low β -glucan content. However, spores that had been germinating for 6 hrs readily took up the dye (MFI 0hr: 12.7 ± 0.6 ; 3 hr: 51.0 ± 1.0 ; 6 hr: 654.3 ± 91.6) (Fig 3.19), suggesting that as germination progresses more β -glucan is synthesised. This cell wall staining supports the RNA-sequencing data where genes involved in β -glucan biosynthesis were identified as being significantly upregulated during *M. circinelloides* germination from resting (0 hr) spore to fully swollen (6 hr) spore (Table 3.5, Figure 3.15).

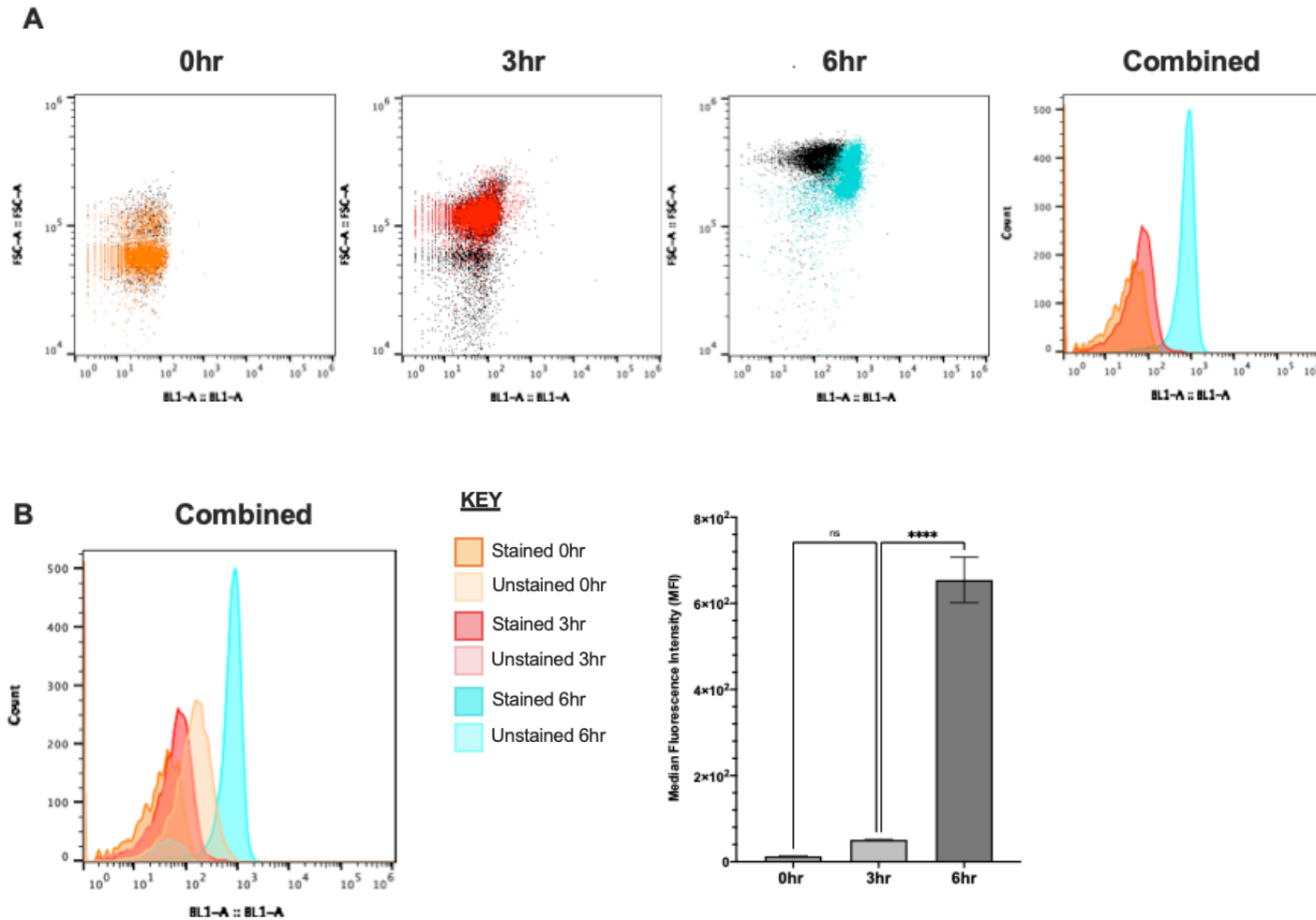


FIGURE 3.19. *M. CIRCINELLOIDES* β -GLUCAN CONTENT INCREASES DURING GERMINATION. *M. circinelloides* spores at 0,3 and 6 hr germination were stained with Fc-Dectin-1-Alexa Fluor™488 to determine cell wall β -glucan content by flow cytometry. (A) Singlet population against fluorescence for unstained (black) and Fc-Dectin-1 labelled (coloured) spores shows low Fc-Dectin-1 binding but significant increase at 6 hr germination. (B) Pooled data shows β -glucan increases significantly at 6hr germination. Data shown are mean \pm SEM of three independent experimental repeats; **** p <0.0001. One-way ANOVA, Tukey's multiple comparisons.

3.2.8 *M. CIRCINELLOIDES* ULTRASTRUCTURAL CHANGES DURING GERMINATION

The ultrastructure of the *M. circinelloides* spore at different stages of germination (0, 3 and 6 hr) was investigated by TEM. Images showed the complexity of the spore body increases as germination progresses. At 0 hr, resting spores displayed a nucleus and some vesicular structures (Figure 3.20). Upon reaching 3 hr, spores appeared to contain an increased abundance of vesicular bodies, with many approaching the periphery of the cell. The ultrastructure of the fully swollen (6 hr) spore body displayed mitochondria, in addition to the nucleus and some vesicle structures (Figure 3.20). When looking at the cell wall of the spores, resting (0 hr) spores had a thin, dense outer layer (layer B) and a significantly thicker but less dense inner layer (layer A) (Diameter: A: 74.03 ± 0.79 nm; B: 17.92 ± 0.23 nm) (Figure 3.19). At 3 hr, spores displayed a different cell wall structure to 0 hr spores, with a thin dense inner layer (layer C), an intermediate layer (layer D) that is significantly thicker than layer C, and an outermost layer (layer E) that is of intermediate density and thickness compared to layers C and D (Diameter: C: 19.10 ± 1.33 nm; D: 45.38 ± 1.32 nm; E: 38.80 ± 0.82 nm) (Figure 3.20). The ultrastructure of fully swollen (6 hr) spores is distinct from that of 3 hr and 0 hr spores. Spores displayed a thin dense outer layer (layer G), and a significantly thicker but less dense inner layer (layer F) (Diameter: F: 84.35 ± 2.16 nm; G: 26.46 ± 0.73 nm) (Figure 3.20). Furthermore, considering the complexity of layer F in fully swollen spores, there were variable regions of density, displaying a band-like organisation within this inner cell wall layer. Layer G of fully swollen spores was patchy, and there were regions where the layer was visibly absent (Figure 3.20).

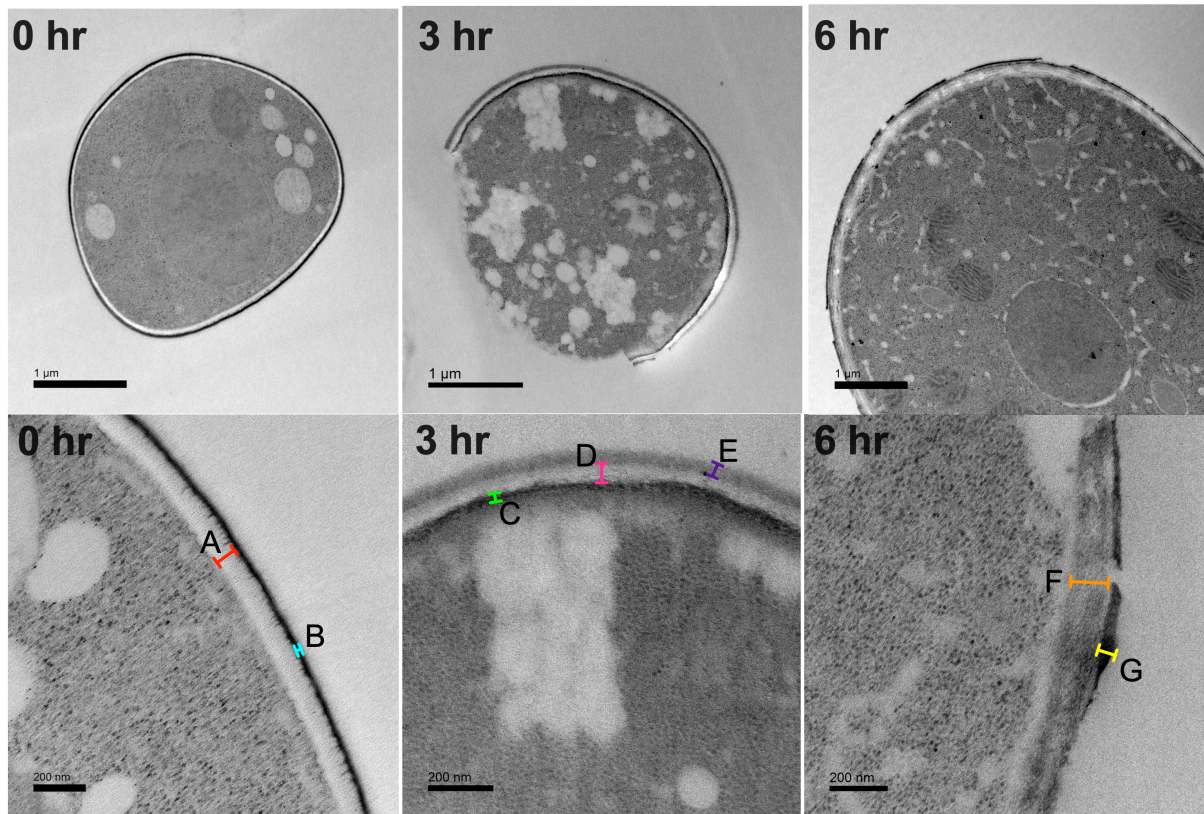
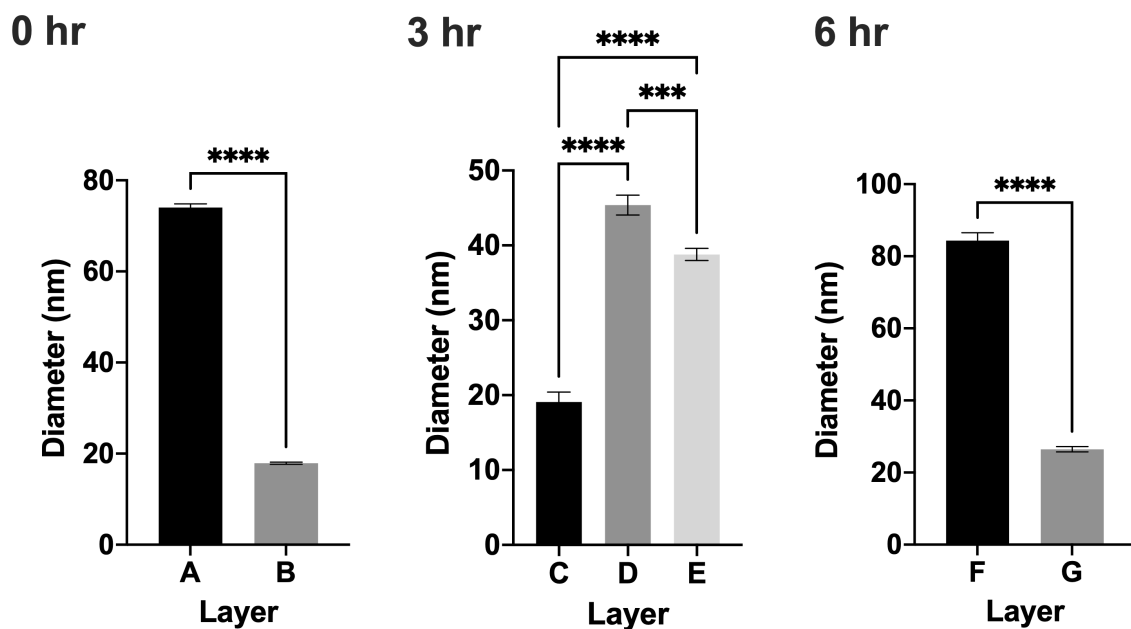
A**B**

FIGURE 3.20 *M. circinelloides* spore wall displays ultrastructural changes during germination. To visualise the ultrastructure of the *M. circinelloides* spore body and cell wall during germination, spores at 0, 3 and 6 hr germination were imaged by means of TEM. **(A)** Top panel, left to right: the 0 hr spore body displays a nucleus and some large vesicle bodies. The 3 hr spore body displays a large number of vesicular structures that approach the periphery of the spore. The complexity of 6 hr spore body is further increased, with visible mitochondria. Bottom panel, left to right: At 0 hr, the spore cell wall displays a thick inner layer (A) enclosed by a thin, dense outer layer (B). At 3 hr, the cell wall consists of a thin, dense inner layer (C), a thicker intermediate layer (D), and a thick outermost layer (E). The 6 hr spore has a thin, dense patchy outer layer (G) enclosing a thick inner layer (F). **(B)** Layers within the cell walls of 0, 3 and 6 hr display significant differences in thickness. Data shown for 0 hr and 6 hr spores are mean \pm SEM of five individual spores, **** $p < 0.0001$, Mann-Whitney U test. Data shown for 3 hr spores are mean \pm SEM of one spore, **** $p < 0.0001$, *** $p < 0.001$, One-way ANOVA, Tukey's multiple comparisons.

3.3 DISCUSSION

The underlying mechanisms of mucormycete spore germination are complex and poorly understood but the process can be broadly described as occurring in two stages: (1) the swelling of spores by isotropic growth, and (2) hyphae formation (Cano and Ruiz-Herrera, 1987; Medwid and Grant, 1984; Cano and Ruiz-Herrera, 1988). Transcriptional profiling of *M. circinelloides* spores at different stages of germination (0 hr vs 3 hr, 3 hr vs 6 hr and 0 hr vs 6 hr) was employed to elucidate key differentially regulated processes during the aforementioned stages. Data showed that the most transcriptional changes occur in the initial stages of germination (0 hr vs 3 hr), in comparison to the latter stages of germination (3 hr vs 6 hr).

As spores exit dormancy and germination follows, there was a heavy emphasis on the upregulation of genes associated with metabolic processes, protein synthesis and translation. This agrees with what is seen in transcriptional profiling of Mucorales *Rhizopus delemar* germination, where transcripts with predicted functions in metabolic processes, such as sugar metabolism, are enriched during the initiation of germination (Sephton-Clark, 2018). Previous research also shows *R. delemar* spores in the initial phase of isotropic phase of growth have enriched transcripts with predicted functions in protein synthesis and modification (Sephton-Clark *et al.*, 2018). The ability of *M. circinelloides* spores to rapidly initiate translation could be due to the presence of stored mRNA transcripts, as seen in *Aspergillus fumigatus*, where dormant conidia hold pre-packaged mRNA transcripts and undergo significant transcriptional changes in the first 30 minutes of germination (Lamarre *et al.*, 2008).

Between 0 hr and 3 hr, there was also a large proportion of downregulated genes that have functions associated with metabolism, suggesting spores undergo a phase of metabolic 'reshaping'. Genes with predicted roles in translation were also downregulated between 3 hr and 6 hr germination, agreeing with previous research showing the downregulation of transcripts with predicted functions in translation during the latter stages of *R. delemar* germination (Sephton-Clark *et al.*, 2018). Here, data suggests there is a switch in differential gene expression associated with translation. In the early

stages of germination upregulated genes associated with translation were enriched, whereas in the late stages of germination downregulated genes associated with translation were enriched. This suggests protein synthesis aiding spore growth is initiated in the initial stages of germination, and that in the latter stages of germination this is dampened. Previous research has shown a similar transcriptional profile in the germination of *Saccharomyces cerevisiae* spores, where metabolic processes such as RNA metabolism are upregulated concomitantly with downregulated metabolic processes such as amino acid metabolism (Geijer *et al.*, 2012).

Processes associated with autophagy, stress response, and peroxisome were enriched in the downregulated gene set in early *M. circinelloides* germination. Autophagy is conserved in eukaryotes and regulates intracellular homeostasis by the degradation of intracellular components such as damaged cell organelles and abnormal proteins (Kanayama and Shinohara, 2016). The process is induced by nutrient starvation, and can be described in stages: (1) induction, (2) autophagosome formation, (3) vacuole transport, and (4) degradation of autophagic bodies (Kikuma and Kitamoto, 2011). Little is known with regards to the role of autophagy in filamentous fungi, but it is believed to be important in growth and survival (Khan *et al.*, 2012). In *A. fumigatus*, autophagy mutants display reduced conidiation and growth, rescued by nitrogen supplementation (Richie *et al.*, 2007). Furthermore, depletion of cations by addition of EDTA, induced autophagy in wild-type *A. fumigatus* despite carbon and nitrogen abundance, suggesting autophagy is important in metal ion recycling under nutrient starvation (Richie *et al.*, 2007). The downregulation of autophagy in early *M. circinelloides* germination appears to be contradictory, however *Mucor* spores were cultured in nutrient rich media, suggesting a reduced requirement for breaking down internal components. As *M. circinelloides* enters the late phase of germination, between 3 hr and 6 hr, there was a shift from the downregulation of transcripts associated with autophagy to their upregulation. This could be as a result of limited nutrient availability and the need for macromolecule recycling to aid spore survival and the continuation of germination. During the latter stages of *M. circinelloides* spore germination, between 3 hr and 6 hr, genes associated with the response to stress were also upregulated. This

agrees with previous research showing an upregulation in transcripts with predicted stress response function in the latter stages of *R. delamar* germination, although this trend was seen after the isotropic growth phase during hyphal formation (Sephton-Clark *et al.*, 2018).

Peroxisomes are ubiquitous cell organelles consisting of a single membrane-enclosed protein matrix, containing a range of enzymes including enzymes that mediate fatty acid β -oxidation and the detoxification of ROS (Hynes *et al.*, 2008; van der Klei and Veenhuis, 2013; Peraza-Reyes and Berteaux-Lecellier, 2013). The role of peroxisomes in filamentous fungal growth and development has been explored in *Aspergillus* (Hynes *et al.*, 2008). Peroxins are encoded for by genes of the *PEX* family, and mutations of *pex* genes has implications in peroxisome biogenesis and matrix protein targeting (Hynes *et al.*, 2008). *pex* mutants of *A. nidulans* display delayed germination and impaired nuclear morphology (Hynes *et al.*, 2008). In early germination of *M. circinelloides* spores, between 0hr and 3hr, genes with functions associated with peroxisome biogenesis and matrix protein targeting were significantly downregulated, suggesting that they do not aid germination as is seen in *Aspergillus*. Genes with functions associated with response to stress and response to oxidative stress were also downregulated between 0 hr and 3 hr germination. This agrees with previous research showing decreased levels of stress response-associated transcripts in the early stages of *R. delamar* germination (Sephton-Clark *et al.*, 2018). The expression of catalase was shown to decrease upon the initiation of germination, and is coupled with an increase in ROS in the germinating spore body. Additionally, preventing the production of superoxide radicals significantly impaired germination, suggesting they are required for germination and thus the presence of superoxide dismutases and catalases needs to be dampened. The downregulation of stress response genes in *M. circinelloides* spores during the initial stages of germination, suggests this may aid germination through the dampening of catalase activity.

Transcriptional profiling of *M. circinelloides* spore germination between 0 hr and 6 hr provides an overview of processes that are differentially expressed over the course of spore germination. Data

showed processes such as protein translation, glycosylation and folding were upregulated, alongside cell wall organization/biogenesis. Supporting the notion that during germination, there is an upregulation in processes mediating protein synthesis that presumably partake in the reorganisation of the cell wall during germination. Similarly, previous research has shown transcripts with predicted functions in cell wall biogenesis are enriched during isotropic growth of *R. delemar* (Sephton-Clark *et al.*, 2018).

Genes with predicted roles in cell wall organization and cell wall biosynthesis were differentially expressed during *M. circinelloides* spore germination, suggesting a remodelling of the cell wall and increased chitin and β -glucan synthesis. This agrees with previous literature showing the cell wall of *Mucor* spores undergoes dynamic compositional changes during germination (Bartnicki-Garcia and Reyes, 1964, Bartnicki-Garcia and Reyes, 1968, Gachhi and Hungund, 1930). During germination, the abundance of chitin in the cell wall of *Rhizopus oryzae* has been shown to increase (Gachhi and Hungund, 1930). There are conflicting reports of β -glucan compositional changes during Mucorales spore germination. Whilst one study reports β -glucan composition in the cell wall of *M. circinelloides* decreases as germination progresses, the β -glucan content of *R. oryzae* increases during germination from spore to hyphae (Bartnicki-Garcia and Reyes, 1964, Chamilos *et al.*, 2010).

Analysis highlighted several upregulated genes with predicted chitin synthase products were differentially expressed during spore swelling. Chitin biosynthesis pathway(s) in *M. circinelloides* have not been reported. However, the functions of various chitin synthases in the cell wall chitin biosynthesis pathway have been reported in *C. albicans*, including: essential chitinase *CHS1* necessary for the formation of the primary septum, *CHS2* implicated in hyphal chitin deposition, *CHS3* which synthesises the majority of chitin in the lateral cell wall, *CHS7* a key regulator of chitin synthase III, and *CHS8* which mediates chitin deposition in hyphae (Munro and Gow, 2001, Sanz *et al.*, 2005, Lenardon, Munro and Gow, 2010). Here, data suggests that chitin synthase activity mediating cell wall chitin synthesis and deposition is upregulated during the early and late stages of *Mucor* germination, between 0 hr and 3 hr. This agrees with previous research on Mucorales *Rhizopus oryzae*, showing

chitin content increases during germination (Gachhi and Hungund, 1930). Analysis of terms assigned to the downregulated gene subset also highlighted a gene encoding a chitin synthase. Differential regulation of chitin synthase genes has previously been reported in the filamentous fungus *Trichoderma atroviride* (Kappel *et al.*, 2020). Within various stress conditions *CHS* genes are differentially regulated, suggesting their regulation is not required in tandem (Kappel *et al.*, 2020). It is plausible that there is differential regulation of chitin synthases during the latter stages of *M. circinelloides* germination where it appears cell wall organisation is heavily differentially regulated with a higher proportion of cell wall associated GO terms noted in comparison to early germination. Determination of cell wall chitin in germinating *M. circinelloides* spores by chitin labelling and microscopy supported the findings of RNA-sequencing analysis. Staining for total and surface exposed chitin with CFW and WGA, respectively, showed chitin content significantly increases in the *M. circinelloides* spore wall between resting (0 hr), mid-point (3 hr) and fully swollen (6 hr) spores. This data agrees with previous research that shows the chitin abundance in *R. oryzae* increases during germination (Gachhi and Hungund, 1930).

There are conflicting reports of the β -glucan composition in the Mucorales cell wall during germination. Whilst some have reported higher β -glucan content in spores than hyphae, others report an increase in β -glucan abundance during germination (Bartnicki-Garcia and Reyes, 1964, Chamilos *et al.*, 2010). Cell wall β -1,6-glucan has not previously been reported in the Mucorales cell wall, however, β -1,3-glucan has been identified in the cell wall of *R. oryzae* in the late stages of germination post-hyphal formation (Chamilos *et al.*, 2010). Analysis of upregulated genes highlighted, genes orthologous to *C. albicans* *PHR1*, *PHR2* and *PHR3*, *GSL1*, *GSL2* and *GSC1*, and *KRE5*. The biosynthesis pathway of cell wall β -glucan has not been described in Mucorales. However, In *C. albicans*, β -1,3-glucan biosynthesis has been shown to be mediated by *GSL1*, *GSL2* and *GSC1*, and whilst the biosynthesis pathway of β -1,6-glucan has not been fully characterised *KRE5* function has been shown to be necessary for β -1,6-glucan biosynthesis (Mio *et al.*, 1997, Herrero *et al.*, 2004). Genes *PHR1*, *PHR2* and *PHR3* have been implicated in β -1,3- and β -1,6- glucan crosslinking also (Fonzi 1999, Douglas

2001). Here, the upregulation of genes implicated in β -1,3-glucan biosynthesis agrees with previous reports of increased β -1,3-glucan in the cell wall of germinating Mucorales spores (Chamilos *et al.*, 2010). The upregulation of a gene orthologous to *KRE5*, alongside the upregulation of a gene orthologous to *PHR* genes, suggests β -1-6-glucan biosynthesis is also upregulated during germination. Analysis of downregulated genes during late germination highlighted genes orthologous to *C. albicans* *BGL2* and *UTR2*. In *C. albicans*, *BGL2*, encodes a 1,3- β -glucosyltransferase that transfers a β -1, 3-glucan chain to another to form a β -1, 6- linkage, playing a role in β -1,3-glucan remodelling (Hartland, Emerson and Sullivan, 1991). *UTR2* encodes a GPI-anchored cell wall glycosidase that binds chitin and is suggested to play a role in β -1,3-glucan crosslinking (Pardini *et al.*, 2006). Here, analysis suggests cell wall β -1,3-glucan remodelling by 1,6-linkages, may be downregulated during late *M. circinelloides* germination. Determination of cell wall β -1,3-glucan in germinating *M. circinelloides* spores by Fc-Dectin-1-Alexa Flour™ 488 labelling and fluorescence microscopy supported the findings of RNA-sequencing analysis. Data showed β -glucan content increases significantly in *M. circinelloides* spores between mid-point (3 hr) and fully swollen (6 hr) stages of germination. This data agrees with previous research showing the levels of β -1,3-glucan increase in the cell wall of *R. oryzae* in the late stages of germination (Chamilos *et al.*, 2010).

Analysis of upregulated genes showed several genes encoding mannosyltransferases, glucosyltransferases and glycosyltransferases were upregulated during *M. circinelloides* germination. Product descriptions indicated two of the products were predicted to be Alg6p and Alg8p, indicating a role in the assembly of the lipid-linked oligosaccharide in protein glycosylation. Ortholog analysis, also highlighted genes orthologous to genes of the *ALG* family, including *ALG1*, *ALG6* *ALG9* and *ALG14*. The assembly of the lipid-linked oligosaccharide has been characterised in *C. albicans*. Briefly, an enzyme complex comprised of Alg7/Alg13/Alg14, adds two N-GlcNAc from UDP-GlcNAc to form Dol-PP-GlcNAc₂. Next Alg1, Alg2 and Alg11 add five mannose residues. The pre-cursor is then flipped from the cytosol into the lumen by Rft1p, and then Alg3, Alg9 and Alg12 add a further four mannose residues. Finally, Alg6, Alg8 and Alg10 add three glucose units to form the Dol-PP-GlcNAc₂Man₉Glc₃

precursor (Mora-Montes et al., 2007). Data shows, that genes with predicted functions in lipid-linked oligosaccharide assembly were upregulated in the early stages of germination, suggesting the process of glycosylation is initiated early in *M. circinelloides* spore germination.

Genes predicted to be implicated in *N*- and *O*- linked mannoprotein glycosylation were also upregulated during spore germination. *C. albicans* orthologs include genes belonging to the *MNN1*, *MNT*, *PMT* and *DPM* family, *RFT1*, *OST1*, *MNS1* and *AMS1*. The *N*- and *O*- linked glycosylation pathways have been well characterised in *C. albicans* and *S. cerevisiae*. Briefly, following the assembly of the lipid-linked oligosaccharide, the precursor is transferred to an asparagine residue on nascent protein by the oligosaccharide (OST) complex. Subsequently, a terminal α 1,2-linked glucose unit is removed by α -glucosidase I, two α 1,3-linked glucose residues are cleaved by α -glucosidase II, and α -mannosidase (*MNS1*) removes a mannose residue to give Man₈GlcNAc₂ isomer B (Herscovics, 1999). In *Candida*, elongation of *N*-linked glycans occurs in the Golgi by Och1, and mannan polymerase I and II (Mora-Montes et al., 2021). Branching of the backbone is performed by Mnt3-5, Mnn2 and Mnn5, and capping of branches by Mnn1 and Mnn12-15. *N*-linked glycans can be further modified by phosphomannans, by Mnt3 and Mnt5 (Mora-Montes et al., 2021). In *O*-linked glycosylation, α 1,2-linked mannose residues are added to serine or threonine residues in the ER lumen by protein mannosyltransferases of the *PMT* family. In *C. albicans*, five Pmt enzymes have been identified (Pmt1-2, and Pmt4-6). Next, mannose residues are added by Mnt1 and Mnt2, and the *O*-linked glycan is extended by, Mnn5. The role of *AMS1* has not been defined in *C. albicans*, however in *S. cerevisiae* *AMS1* has been shown to catalyse the processing of free cytosolic *N*-glycans. DPM synthases are comprised of three subunits, Dpm1, Dpm2 and Dpm3, and have been implicated in both *N*- and *O*-linked glycosylation. Collectively, data showed the upregulation of genes with predicted functions in *N*- and *O*- linked mannoprotein glycosylation, suggesting glycosylation is initiated in the early stages of *M. circinelloides* germination and continues throughout spore swelling. Determination of cell wall mannan content in germinating *M. circinelloides* spores by ConA-TRITC labelling, flow cytometry and fluorescence microscopy, supported the findings of RNA-sequencing analysis. Flow cytometry data

showed mannan content increases significantly in *M. circinelloides* spore between resting (0 hr), mid-point (3 hr) and fully swollen (6 hr) stages of germination. Fluorescence microscopy corroborated this, but also showed staining not to be uniform in the spore once fully swollen, suggesting mannan is incorporated into the cell wall in 'patches'. This is in conflict with previous research showing the mannan content to decrease during germination from spore to hyphae in *M. rouxii* (Bartnicki-Garcia and Reyes, 1964).

During early *M. circinelloides* germination, analysis highlighted several upregulated genes with products implicated in GPI anchor protein biosynthesis, including genes orthologous to *GPI7*, *GPI1*, *GPI2* and *GWT1*. GPI proteins are found in the cell wall covalently linked to glucans and act as anchors for cell wall proteins. There have been no previous reports of GPI proteins in the cell wall of Mucorales. The biosynthesis of GPI lipids begins with GlcNAc being added to PI, a process mediated by a multi-subunit enzyme complex comprised of Gpi1-3, Gpi15, Gpi19 and Eri1 (Pittet and Conzelmann, 2007). Subsequently, Gpi12, removes GlcNH₂ from PI-GlcNAc, and Gwt1 performs inositol acylation of GlcN-PI. Next, mannose residues are added through the activity of several Gpi proteins (Gpi14, Gpi18, Gpi10, and Smp3 (Pittet and Conzelmann, 2007). Phosphorylethanolamine is added to the first three mannose residues by Mcd4, Gpi7, and Gpi13. The GPI lipid is then transferred to the GPI protein by a transamidase complex, composed of Gpi8, Gaa1, Gpi17, Gpi16 and Gab1. Subsequently, deacylation of inositol is performed by Bst1 and the GPI anchor is supposedly modified through the activity of Gup1 and Cwh43, the exact functions of which are yet to be characterised. Data suggests GPI protein biosynthesis is upregulated during *M. circinelloides* germination.

The ultrastructure of *M. circinelloides* spores at different stages of germination, resting (0 hr), mid-point (3 hr) and fully swollen (6 hr) was shown by TEM. When considering the main spore body, the complexity of structures increases during germination. At resting stage, 0 hr spores displayed a nucleus and some vesicular bodies. Upon reaching 3 hr germination, there were markedly more vesicular bodies seen. These appeared to be concentrated towards the periphery of the spore body, towards the cell wall. This may be indicative of trafficking cargo to the cell wall, which would support

the findings of RNA-sequencing showing an upregulation of genes associated with cell wall biosynthesis and organisation. At 6 hr, fully swollen spores displayed mitochondria and greater complexity of the spore body than that seen with 0 hr and 3 hr spores. Collectively, the increase in complexity agrees with transcriptional profiling data, showing significant increase in processes such as metabolism, translation, protein synthesis and cell wall biosynthesis.

TEM showed distinct differences in the cell wall of spores at 0 hr, 3 hr and 6 hr germination. In resting spores, there were two discernible cell wall layers: (i) a thin, dense outer layer (layer B) and (ii) a thicker less dense inner layer (layer A). Layer A, in resting *M. circinelloides* spores, could be a melanin outer coat, such as that shown in *R. oryzae* and *M. rouxii* (Andrianaki *et al.*, 2018, Bartnicki-Garcia and Reyes, 1964). 3 hr spores displayed a distinct cell wall to that of 0 hr spores, that is composed of: (i) a thin, dense inner layer (layer C), (ii) a thick outer layer of intermediate density (layer E), and (iii) a thick intermediate layer (layer D). The outer layers could be composed of mannan, β -glucan and chitin, abundances of which were shown to increase in 3 hr spores by means of cell wall staining. Layer D of 3 hr spores could be the same as layer A of 0 hr spores, and likewise layer C of 3 hr spores could be the same as layer B of 0 hr spores. It is also possible however, that spores undergo extensive cell wall remodelling, and that the composition of these layers is distinct between the 0 hr and 3 hr spores. It is not possible to discern this from data shown here without further means such as immunogold labelling and HPLC, which would identify the character of these layers. A cell wall layer of similar nature to layer E of 3 hr spores was not seen in 0 hr spores, suggesting this is a new layer of the cell wall synthesised soon after the initiation of germination. Collectively, the remodelling of the cell wall seen in the early stages of germination would agree with RNA-sequencing data showing an upregulation of cell wall biosynthesis genes during the early stages of germination (between 0 hr and 3 hr). Fully swollen spores (6 hr), displayed a distinct cell wall ultrastructure than that of 0 hr and 3 hr spores. The cell wall appeared to consist of two layers: (i) a dense, thin, patchy outer layer (Layer G) and (ii) a thick, complex inner layer of intermediate density (Layer F). Here, it could be postulated that layer G is of the same nature as layers B and C of 0 hr and 3 hr, respectively, and that layer F is the

same as layer E of 3 hr spores. It is also possible that there is extensive cell wall remodelling in the latter stages of germination, between 3 hr and 6 hr, and these are distinct from one another. Again, this would require further investigation to discern. The patchy nature of layer G in 6 hr spores could explain the patchy mannan staining noted in conA-TRITC staining by fluorescence microscopy. This outermost layer could be mannan itself, or an undefined layer that is masking the mannan beneath it – both are possible explanations for the patchy mannan staining that would require further investigation to determine.

In summary, *M. circinelloides* spores undergo large transcriptional changes during germination and, interestingly switch the differential expression of processes between the early and late stages of germination to aid their growth and survival. Throughout the process of germination, spores upregulate genes associated with mannoprotein glycosylation, chitin synthesis and β -glucan synthesis – the cell wall abundances of which increase during germination.

4 *M. CIRCINELLOIDES* SPORE DEVELOPMENT INFLUENCES ITS INTERACTION WITH MACROPHAGES

4.1 INTRODUCTION

Macrophages are the first line of defence in the innate immune response to pathogens. Successful clearance of pathogenic fungi by macrophages relies on a series of events; (i) fungal recognition, (ii) fungal internalisation and containment within a phagosome, and (iii) fungal killing within the phagosome.

Fungal recognition by macrophages is mediated by pathogen recognition receptors (PRRs) on the macrophage surface either (i) directly with pathogen associated-molecular patterns (PAMPs) on the fungal cell surface, or (ii) indirectly by opsonins. There are a variety of known PRRs and their respective fungal PAMP(s). These include receptor Dectin-1 that recognises fungal β -glucan, and CLR mannose receptor that recognises fungal mannan. Following successful recognition, macrophages internalise the fungal pathogen via a process known as phagocytosis. Here, the pathogen is uptaken and contained within an organelle known as a phagosome. Once contained within the phagosome, the phagosome then undergoes a process known as phagosome maturation, in which a series of fusion events with endosomes and lysosomes leads to the accumulation of antimicrobial effectors and acidification within the phagosome. Phagosome maturation is essential in the damage and degradation of macrophage-contained fungal pathogens. Some fungi are able to delay or even evade phagosome maturation. For example, *Cryptococcus neoformans* are successfully phagocytosed by macrophages but evade killing and modify the phagosome, so that early maturation markers are removed prematurely and acidification is dampened (Smith, Dixon and May, 2014). This enables *C. neoformans*, to hijack the macrophage, evade degradation, proliferate, and eventually escape to continue to cause disease.

RNA-sequencing and cell staining showed *M. circinelloides* spores undergo considerable cell wall compositional changes during spore swelling from resting to fully swollen spore. To elucidate

whether *M. circinelloides* spore uptake and killing by macrophages is influenced by spore swelling stage, phagocytosis of *M. circinelloides* spores at 0, 3 and 6 hr swelling by macrophages was investigated. By means of live imaging and fluorescence microscopy, various parameters were investigated including phagocytic indices, phagosome maturation and the effect of inhibition of mannose receptors on uptake.

4.2 RESULTS

4.2.1 MOI OPTIMISATION

To determine the optimal multiplicity of infection (MOI) for macrophage-*M. circinelloides* phagocytosis, *M. circinelloides* spores at 0, 3 and 6 hr germination were incubated with macrophages in serum-free DMEM (to limit opsonisation), and the following three phagocytic indices were analysed: (i) phagocytic index (PI), (ii) association index (AI) and (iii) %phagocytosis (%P). Analysis of PI and AI of *M. circinelloides* spores at an MOI of 1:1 (1 spore: 1 macrophage) showed low uptake and association (MOI 1:1: 0hr PI: 31.67 ± 5.49 , AI: 36.67 ± 7.22 ; 3hr PI: 29.33 ± 2.33 , AI: 30.33 ± 2.60 ; 6hr PI: 18.67 ± 2.33 , AI: 20.00 ± 3.06), which was marginally improved at an MOI of 2.5:1 (MOI 2.5:1: 0hr PI: 55.67 ± 12.81 , AI: 62.67 ± 11.62 ; 3hr PI: 61.33 ± 6.69 , AI: 62.00 ± 7.00 ; 6hr PI: 50.00 ± 1.00 , AI: 51.33 ± 1.20) (Figure 4.1). At an MOI of 5:1, there was a further increase in PI and AI particularly with 3 hr spores (MOI 5:1: 0hr PI: 85.33 ± 11.70 , AI: 102.70 ± 17.68 ; 3hr PI: 169.7 ± 8.09 , AI: 171.7 ± 7.42 ; 6hr PI: 92.33 ± 7.54 , AI: 93.33 ± 7.42) (Figure 4.1). As %P is essentially a ratio of PI:AI and the degree of association and phagocytosis are fairly uniform, %P is high and constant across the entire range of MOIs, and between the spores at different stages of swelling (Figure 4.1). An MOI of 5:1 was carried forward for all further investigations, and the PI was deemed the most appropriate indices for analysis.

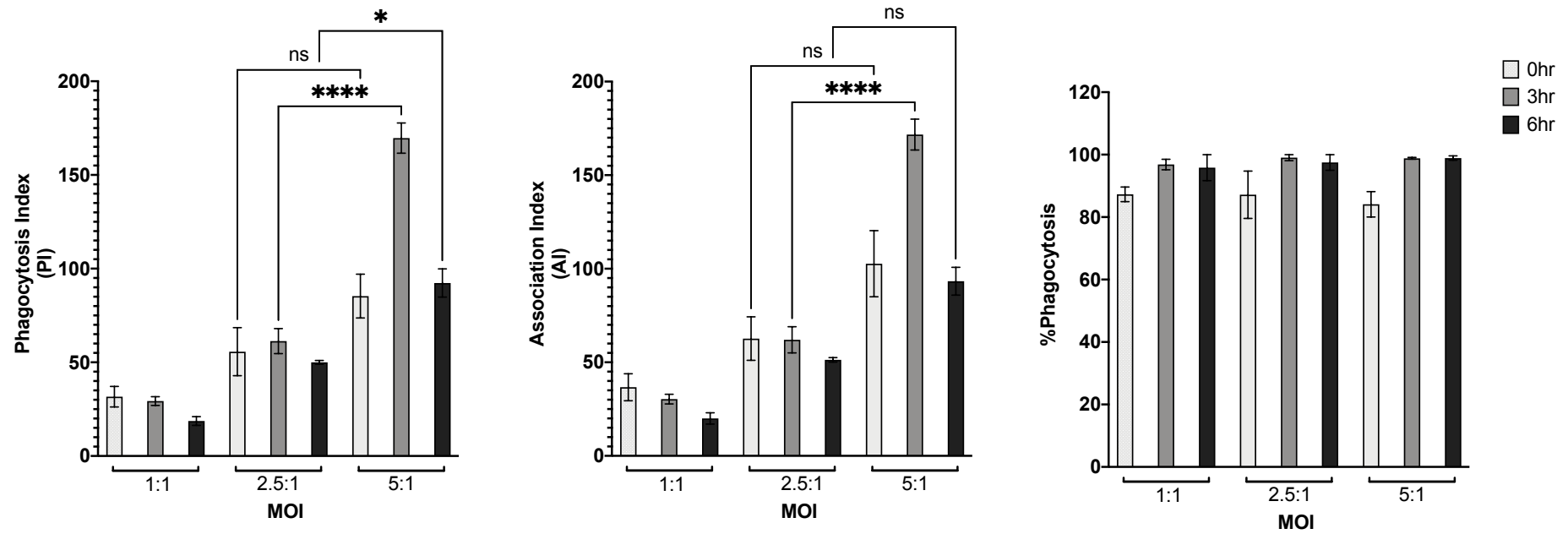


FIGURE 4.1 MOI OPTIMISATION The optimal MOI for *M. circinelloides* phagocytosis was determined through the analysis of phagocytosis of *M. circinelloides* spores cultured for 0, 3 or 6 hr by J774A.1 macrophages following 2 hr co-incubation at 37°C, 5% CO₂. At an MOI of 5:1, there was considerably increased phagocytosis (PI) and association (AI) across all stages of spore swelling, in comparison to at an MOI of 1:1 and 2.5:1. Data shown are mean \pm SEM of three independent experimental repeats. **** p <0.0001. * p <0.05, One-way ANOVA with Tukey's multiple comparisons.

4.2.2 *M. CIRCINELLOIDES* SPORE DEVELOPMENTAL STAGE INFLUENCES PHAGOCYTIC UPTAKE

Fluorescence microscopy showed fully swollen spores are considerably larger than 0 hr and 3 hr spores and occupy far greater space in the macrophage, and that macrophages that had phagocytosed fully swollen spores displayed a 'rounded' shape in comparison to those that had phagocytosed 0 hr and 3 hr spores that displayed normal morphology (Figure 4.2). Additionally, data showed that spores at 3 hr germination were phagocytosed significantly more than resting (0 hr) and fully swollen (6 hr) spores (PI 0 hr: 85.33 ± 11.70 ; PI 3 hr: 169.7 ± 8.09 ; PI 6 hr: 92.33 ± 7.54) (Figure 4.2B).

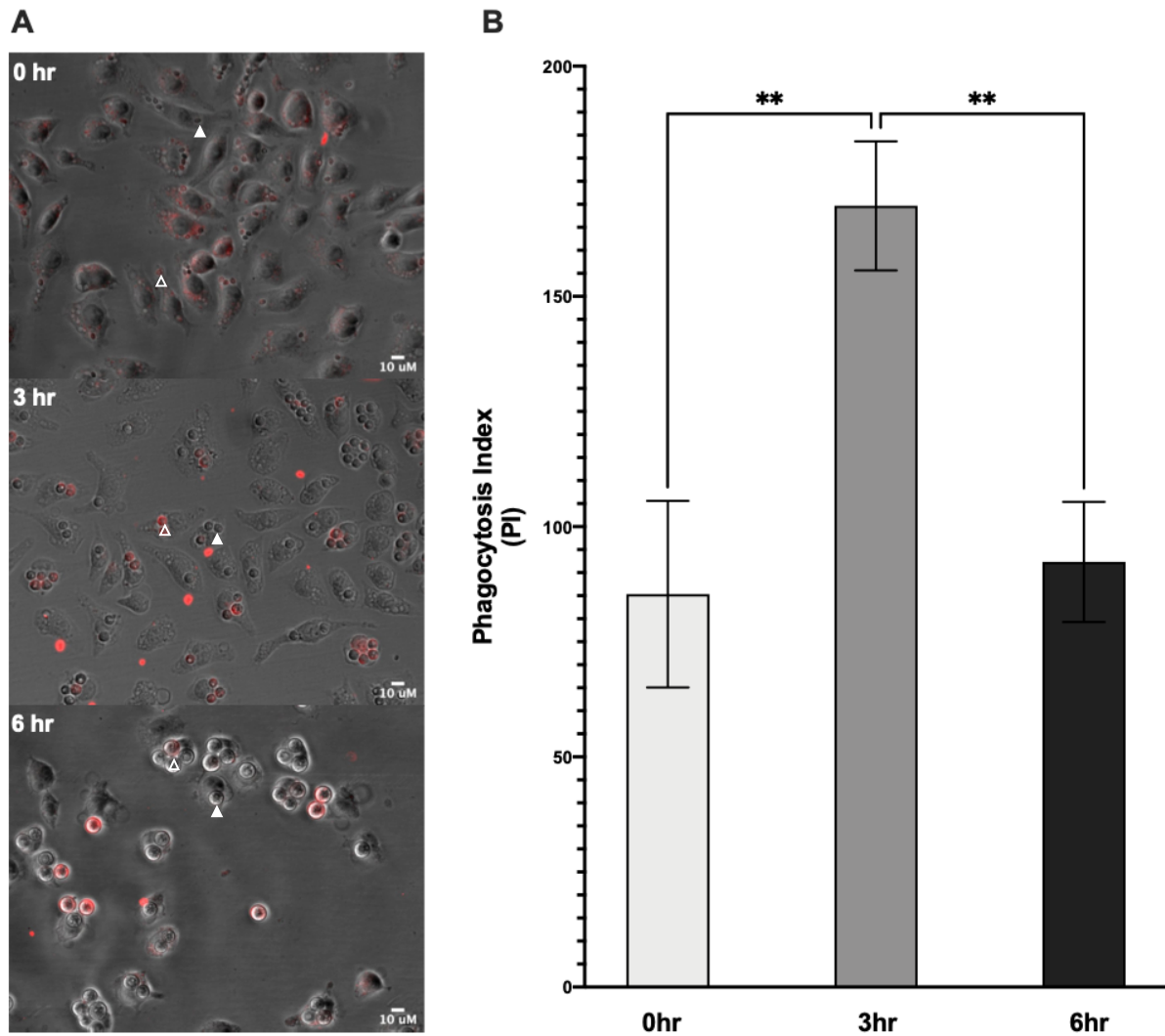


FIGURE 4.2 PHAGOCYTOSIS OF *M. CIRCINELLOIDES* SPORES IS DEPENDENT UPON SPORE DEVELOPMENT. The effect of *M. circinelloides* spore developmental stage on phagocytosis was investigated by co-incubating J774A.1 macrophages with spores at 0, 3 or 6 hr germination, and analysing phagocytosis after 2 hr incubation at 37°C, 5% CO₂. Spores were stained with ConA-TRITC to discern phagocytosed (filled arrowhead) and adhered/non-phagocytosed (unfilled arrowhead) spores. (A) Macrophages that had phagocytosed 0 and 3 hr spores displayed normal morphology, however macrophages that had phagocytosed 6 hr spores displayed a rounded shape. Furthermore, 6 hr spores occupied markedly greater area of the macrophage than 3 hr and 0 hr spores. (B) 3 hr spores displayed significantly increased uptake by macrophages in comparison to 0 hr and 6 hr spores. Data from Figure 4.1. Data shown are mean \pm SEM of three independent experimental repeats; ** p <0.01, One-way ANOVA, Tukey's multiple comparisons.

4.2.3 *M. CIRCINELLOIDES* SPORE GERMINATION STAGE INFLUENCES ITS VIABILITY POST-PHAGOCYTOSIS

M. circinelloides spores were readily phagocytosed by macrophages across all stages of spore swelling. To determine the efficacy of spore killing by macrophages, spore viability post-phagocytosis was investigated. To determine the effect of phagocytosis on spore viability, *M. circinelloides* spores at 0, 3 and 6 hr germination were co-incubated with macrophages for 0, 2 and 18 hr time periods, subsequently macrophages were lysed and spores plated for viability counts. Data shows *M. circinelloides* spore viability decreases as incubation time increases (Figure 4.3). Resting spores displayed a small but non-significant reduction in viability following 2 hr and 18 hr incubation with macrophages (0 hr CFU, T0: 98.33 ± 5.81 , T2: 93.67 ± 1.67 , T18: 87.33 ± 2.19) (Figure 4.3). Spores that had germinated for 3 hr displayed a significant reduction in viability by almost 50% after 18 hr incubation with macrophages (3 hr CFU, T0: 89.00 ± 2.65 , T2: 90.33 ± 3.48 , T18: 49.00 ± 4.16) (Figure 4.3). Spore viability of fully swollen spores was impaired significantly after 18 hr incubation with macrophages with a reduction of over 50% in viability (6 hr CFU, T0: 79.33 ± 6.33 , T2: 66.67 ± 2.33 , T18: 42.33 ± 4.602) (Figure 4.3). Here, data showed that the *M. circinelloides* spore developmental stage plays a significant role in spore viability post-phagocytosis, with spores in the early stages of germination displaying the greatest resistance to macrophage killing and fully swollen spores being the most susceptible to macrophage killing.

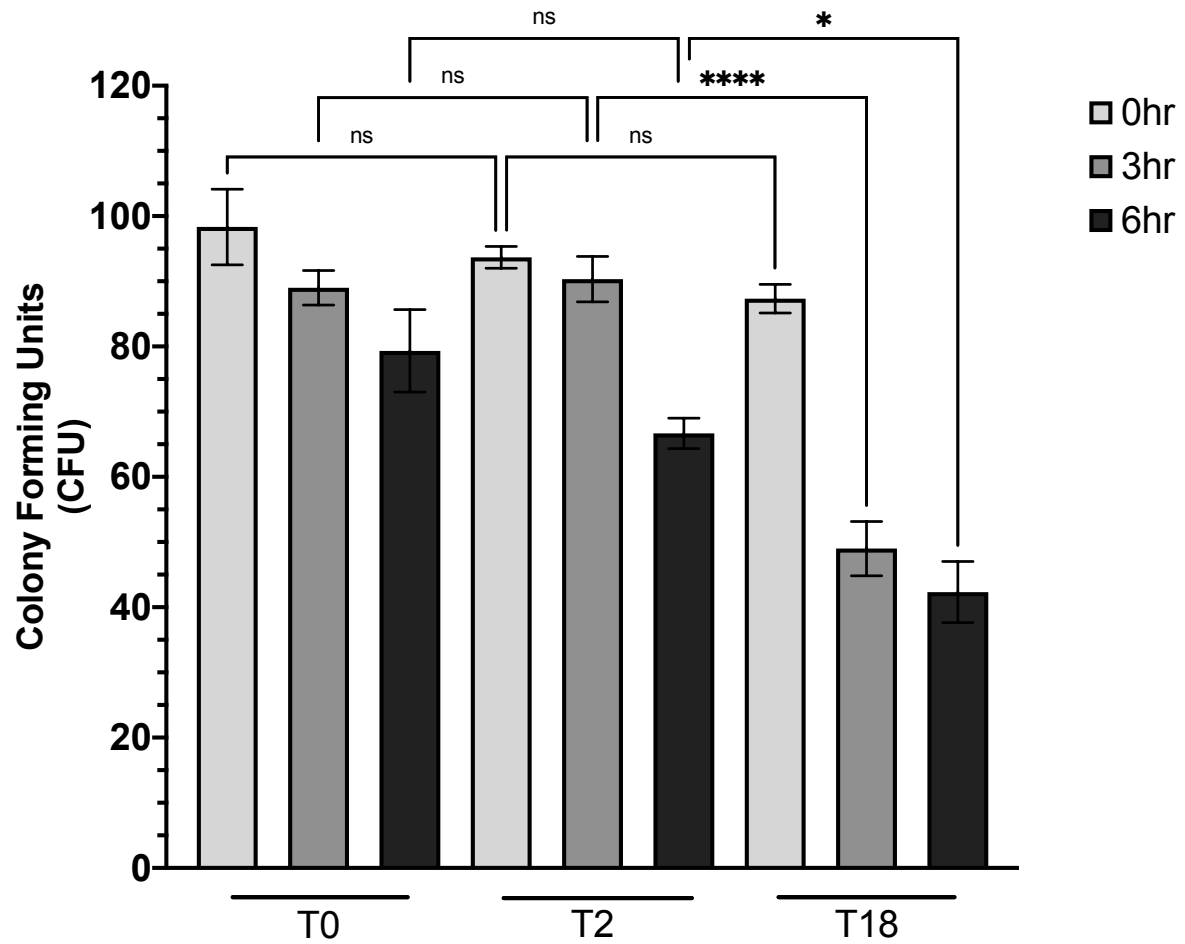


FIGURE 4.3 *M. CIRCINELLOIDES* SPORE VIABILITY POST-PHAGOCYTOSIS. Spores at 0, 3 and 6 hr germination were co-incubated with J774.A1 macrophages for 0, 2 and 18 hr. Following co-incubation macrophages were lysed and spores plated for viability. As incubation time increases, spore viability decreases with those co-incubated with macrophages for 18 hr displaying the lowest viability. Furthermore, spore developmental age influences its viability post-phagocytosis, with those at fully swollen state (6 hr) being less viable than those at 3 hr germination, and those at the mid-point (3 hr) being less viable than resting (0 hr) spores. Data shown are mean \pm SEM of three independent experimental repeats. **** p <0.0001, * p <0.05, One-way ANOVA with Tukey's multiple comparisons.

4.2.4 *M. CIRCINELLOIDES* SPORES DO NOT INDUCE PHAGOSOME MATURATION

Spore viability of 3 hr and 6 hr *M. circinelloides* spores was significantly impaired between 2 hr and 18 hr phagocytosis, with those at the latter stages of swelling (6 hr) being the least viable, and resting (0 hr) spores being able to withstand phagocytic killing the best. To investigate whether phagosome maturation was in part responsible for spore killing, macrophages were stained with LysoTracker™ Red, a stain for acidic organelles and incubated with live or heat-killed *M. circinelloides* 0, 3 and 6 hr spores. Phagosome maturation was tracked using live-cell fluorescence microscopy and % phagosome maturation (%PM) of 100 phagosomes per condition calculated as ((number of lysotracker-red positive phagosomes/total number of phagosomes) x100).

Analysis showed macrophages were able to ingest heat-killed *M. circinelloides* spores across all developmental stages, and %PM exceeded 90% across all conditions (%PM, 0 hr: $92.67 \pm 1.20\%$, 3 hr: $96.00 \pm 1.16\%$, 6 hr: $95.67 \pm 0.67\%$) (Figure 4.4). However, the converse was seen with live *M. circinelloides* spores, whereby spores across all three germination stages (0, 3 and 6 hr) were phagocytosed but phagosome maturation was absent (%PM, 0 hr: $7.67 \pm 0.88\%$, 3 hr: $5.67 \pm 2.60\%$, 6 hr $5.00 \pm 1.16\%$) (Figure 4.4).

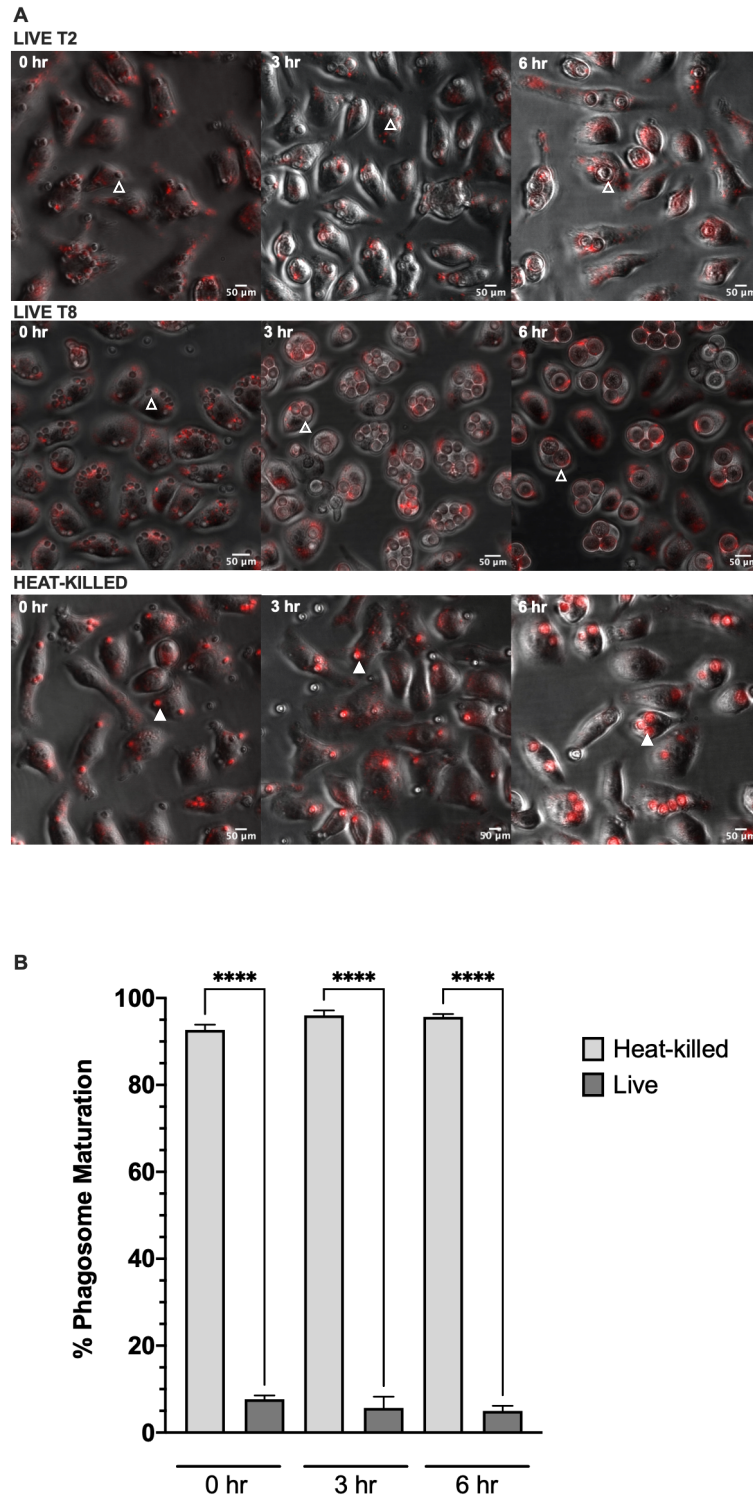


FIGURE 4.4. *M. CIRCINELLOIDES* SPORES DO NOT INDUCE PHAGOSOME MATURATION IN MACROPHAGES. Heat-killed and live *M. circinelloides* spores across the three stages of swelling (0, 3 and 6 hr) were co-incubated with J774A.1 macrophages. Phagosome maturation was tracked using LysoTracker™ Red and live fluorescence microscopy (phagosome maturation positive: filled arrowhead, phagosome maturation negative: unfilled arrowhead). (A) Live spores across all stages of germination, at T2 and T8, did not induce phagosome maturation in macrophages, whereas heat-killed spores were ingested and triggered phagosome maturation. (B) Phagosome maturation was significantly reduced in response to live *M. circinelloides* spores compared to heat-killed spores. **** $p < 0.0001$, One-way ANOVA with Šidák's multiple comparisons.

4.2.5 *M. CIRCINELLOIDES* PHAGOCYTOSIS IS MEDIATED BY MACROPHAGE MANNOSE RECEPTORS

RNA-sequencing data indicated mannan biosynthesis pathways are upregulated during *M. circinelloides* spore swelling, and cell wall staining confirmed cell wall mannan content increases from resting (0 hr) to fully swollen (6 hr) spore stage. Macrophages have a repertoire of mannose receptors shown to bind fungal mannan, these include DC-SIGN, Dectin-2 and the mannose receptor. To investigate whether mannose receptors play a role in the phagocytosis of *M. circinelloides* spores, macrophages were pre-treated with exogenous mannan from *S. cerevisiae* - a competitive inhibitor of mannose receptors DC-SIGN, mannose receptor and Dectin-2 - at a range of concentrations, from 10 µg/mL up to 500 µg/mL (Vendele *et al.*, 2020). Following competitive inhibition of mannose receptors, 3 hr spores were co-incubated with macrophages, and phagocytosis analysed using fluorescence microscopy. Data showed phagocytosis was significantly reduced when macrophages were pre-treated with exogenous mannan at the lowest concentration of 10 µg/mL (PI: 0 µg/mL: 124.7 ± 9.87 , 10 µg/mL: 64.00 ± 9.45) (Figure 4.5). The effect of mannose receptor inhibition was fairly consistent across all higher concentrations of mannan (PI: 50 µg/mL: 60.67 ± 4.98 , 100 µg/mL: 66.33 ± 10.90 , 250 µg/mL: 72.67 ± 9.40 , 500 µg/mL: 60.67 ± 7.22) (Figure 4.5).

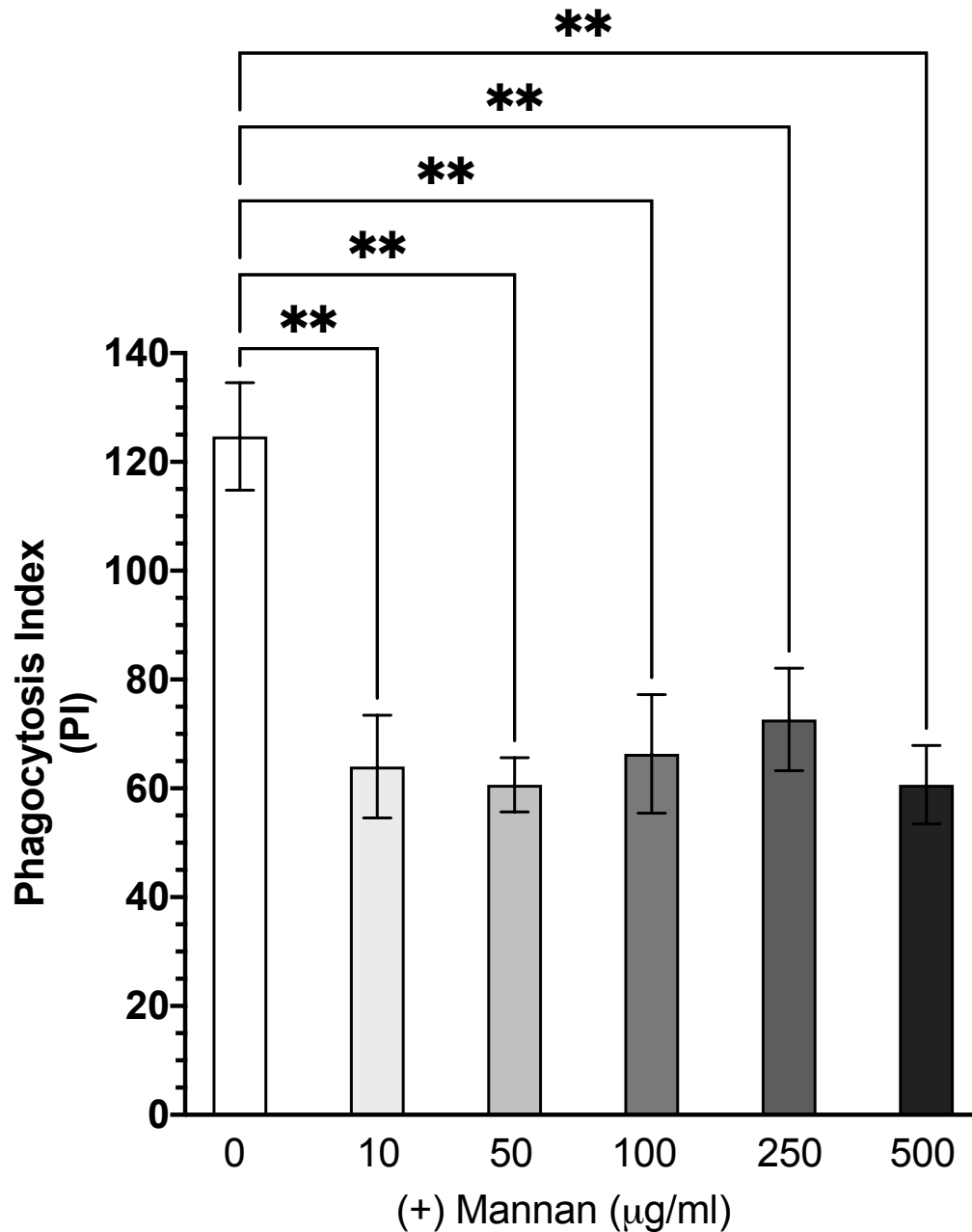


FIGURE 4.5. INHIBITION OF MANNANOSE RECEPTORS SIGNIFICANTLY INHIBITS *M. CIRCINELLOIDES* SPORE PHAGOCYTOSIS. *M. circinelloides* spores at the mid-point of swelling (3 hr) were co-incubated with J774A.1 macrophages that had no mannann treatment prior to fungal spore exposure, or that had been pre-treated with exogenous mannann at ranging concentrations, from 10 - 500 µg/mL. Pre-treatment of macrophages with mannann significantly decreases spore phagocytosis, across all concentrations investigated. ** $p < 0.01$ Data shown are mean \pm SEM of three independent experimental repeats. One-way ANOVA. Dunnett's multiple comparisons to 0 µg/mL control.

4.3 DISCUSSION

The ability of Mucorales to evade phagocytosis enables their dissemination and pathogenic success as an invasive filamentous fungal pathogen. Macrophages eradicate pathogenic microorganisms through the recognition of pathogen-associated molecular patterns via pattern recognition receptors, enabling subsequent pathogen engulfment, degradation and antigen presentation (Ghuman and Voelz, 2017).

Investigation of the influence of *M. circinelloides* spore germination on phagocytic uptake showed the developmental stage of the spore influences its phagocytosis by macrophages. Resting (0 hr) and fully swollen (6 hr) spores were readily phagocytosed by macrophages, however there was significantly increased uptake of spores at the mid-point (3 hr). During spore germination, the cell wall of Mucorales spores undergo considerable compositional changes. Previous research shows dormant spores have a melanin outer layer, which is shed upon germination to reveal an inner layer comprised primarily of chitin, glucan and mannan (Bartnicki-Garcia and Reyes, 1964, Bartnicki-Garcia and Reyes, 1968). Cell wall staining data showed that, as germination proceeds, the abundance of *M. circinelloides* cell wall glucan, chitin and mannan increases. Considering this, the significantly increased uptake of 3 hr spores in comparison to 0 hr spores could be due to the loss of the melanin layer and unmasking of the glucan, chitin and mannan rich inner layer. This, does not explain the reduced phagocytosis of 6 hr *M. circinelloides* spores in comparison to 3 hr spores. Itabangi *et al.*, showed that the phagocytosis of swollen *Rhizopus microsporus* spores is impaired compared to resting spores, and that the supernatant of swollen spores exerts an inhibitory effect on the phagocytosis of resting *R. microsporus* spores and other fungi such as *C. albicans* (Itabangi *et al.*, 2022). This inhibitory effect was shown to be a result of bacterial endosymbiont, *Ralstonia pickettii*, which is contained within resting *R. microsporus* spores and released upon spore swelling (Itabangi *et al.*, 2022). Data here shows swollen 3 hr and 6 hr *M. circinelloides* spores are phagocytosed more readily than resting spores; no inhibitory effect such as that seen with *R. microsporus* swollen spores is shown. Microscopy

showed *M. circinellodites* 6 hr spores are considerably larger than 3 hr spores, and occupy a larger space in the macrophage, and therefore size could be the limiting factor here to explain the reduced phagocytosis of these fully swollen spores.

M. circinellodites spore developmental stage was shown to influence its viability post-phagocytosis. Resting (0 hr) spores were resistant to macrophage killing, however 3 hr spores were less viable than resting spores, and 6 hr spores less than 3 hr spores. This suggests spore viability decreases as developmental stage increases. Previous research has shown resting *Rhizopus* spores are resistant to macrophage killing (Levitz *et al.*, 1986). Additionally, swollen conidia of *Aspergillus fumigatus* are more susceptible to macrophage killing than resting conidia, and this is correlated with increased reactive oxygen intermediate production (Philippe *et al.*, 2003). The outer layer of resting *A. fumigatus* conidia contains hydrophobins, primarily RodA (Valsecchi *et al.*, 2020). The loss of RodA confers increased susceptibility to macrophage killing (Paris *et al.*, 2003). Considering this, there are two plausible explanations for the reduced viability of 3 hr and 6 hr *M. circinelloides* spores: (i) there is an increased production of reactive oxygen species in response to swollen spores, and/or (ii) the melanin outer layer of *Mucor* spores offers protection to resting spores, which upon its loss during germination renders swollen spores more susceptible to macrophage killing.

Data showed an absence of macrophage phagosome maturation in response to 0, 3 and 6 hr spores. Macrophages displayed acidification in response to heat-killed spores, however when live spores were phagocytosed phagosome maturation was notably absent. This agrees with previous research, that shows *M. circinelloides* resting spores block or delay phagosome maturation in macrophages (Lee *et al.*, 2016). When considering the enhanced efficacy of macrophage killing of swollen *M. circinelloides* spores, it is interesting that phagosome maturation is absent when these spores are phagocytosed. Initial investigations probed for phagosome maturation over a 2 hr time period. Investigations of phagosome maturation in response to *M. circinelloides* spores across all three developmental stages over 8 hr still showed an absence of phagosome maturation. Collectively, data suggests *M. circinelloides* spores arrest macrophage phagosome maturation enabling their

persistence within in the cell, and that there are likely other factors contributing to fungal killing of swollen spores' post-phagocytosis. A similar phenomenon has been shown in *Cryptococcus neoformans*-macrophage interaction, whereby phagosome maturation is arrested through the premature removal of Rab5 and Rab11 from early phagosomes, preventing acidification of the phagosome and enabling *C. neoformans* persistence (Smith *et al.*, 2014).

Cell wall staining data showed *M. circinelloides* cell wall mannan content increases significantly at 3 hr and 6 hr germination. Fungal mannan is a known ligand of various macrophage mannose receptors, including DC-SIGN and Dectin-2 (Vendele *et al.*, 2020). Considering the loss of the melanin layer and increase of cell wall mannan, the role of mannose receptors in *M. circinelloides* phagocytosis was investigated. To ensure opsonisation driven uptake through the complement system was not taking place and enable the investigation of PAMP-PRR recognition, macrophages and spores were co-incubated in sfDMEM. Data showed pre-treatment of macrophages with exogenous mannan from *S. cerevisiae* (a competitive inhibitor of DC-SIGN, mannose receptor and Dectin-2) significantly reduced the uptake of 3 hr spores. Receptors, Dectin-2, DC-SIGN and mannose receptor, have been shown to recognise fungal mannan of species including, *C. albicans*, *C. neoformans* and *A. fumigatus* (Serrano-Gómez *et al.*, 2004, Dan *et al.*, 2008, Cambi *et al.*, 2008, van de Veerdonk *et al.*, 2009, Saijo *et al.*, 2010, Loures *et al.*, 2015). Here data suggests *M. circinelloides* phagocytosis is mediated through mannose receptors, also indicating that fungal cell wall mannan is key in its phagocytosis.

In summary, the spore developmental stage of *M. circinelloides* spores significantly affects its phagocytosis by macrophages. Resting and fully swollen spores are phagocytosed to a significantly lesser degree than those at the mid-point of swelling. This may in part owe to a size limitation factor of 6 hr spores, and/or the melanin layer of resting spores shielding fungal PAMPS, such as mannan. Although less readily phagocytosed, fully swollen spores are less viable to phagocytic killing upon internalisation than spores at the mid-point of swelling and resting spores. Phagosome maturation is notably absent in response to spores across all developmental stages and does not contribute to fungal killing, hence there are likely to be other factors owing to the increased susceptibility of swollen

spores to phagocytic killing that are yet to be determined. Finally, although it is known that macrophages phagocytose Mucorales spores, the receptors mediating the process had not been previously described. Here, data shows mannose receptors play a key role in the uptake of *M. circinelloides* spores.

5 *M. CIRCINELLOIDES* INDUCES PLATELET AGGREGATION THROUGH INTEGRIN

α IIb β 3 AND IgG RECEPTOR Fc γ RIIA

5.1 INTRODUCTION

Platelet surface integrin, α IIb β 3, and IgG receptor, Fc γ RIIA, are essential in platelet activation and aggregation in response to bacteria, suggesting a common pathway to bacterial-induced platelet activation (Arman *et al.*, 2014). Inhibiting either α IIb β 3 or Fc γ RIIA, led to significantly impaired platelet aggregation as recorded via light-transmission aggregometry, and a failure to activate platelets as measured by dense granule secretion (ATP release) and PF-4 secretion (Arman *et al.*, 2014; Watson *et al.*, 2016). Furthermore, downstream activation of the Src and Syk tyrosine kinases, and the release of secondary mediators ADP and TxA₂ are also essential for platelet aggregation to bacteria (Arman *et al.*, 2014, Watson *et al.*, 2016).

Thrombosis is a hallmark of mucormycosis, indicating a role for platelets during infection. To elucidate whether platelets are activated by *M. circinelloides* and whether the pathway is similar to that seen with bacteria, the platelet aggregation potential of, and activation pathway in response to, *M. circinelloides* was investigated. Aggregation and inhibition studies were used to identify the key platelet receptor(s) and downstream signalling molecules involved in *M. circinelloides*-induced platelet aggregation. Furthermore, fluorescence microscopy was employed to visualise *M. circinelloides*-platelet thrombi.

5.2 RESULTS

Results in this chapter have been published (Ghuman *et al.*, 2019), and/or submitted as part of an MSc project by Harlene Ghuman as denoted in text and figure legends (*MSc; ^ΔGhuman *et al.*, 2019). Figures denoted (*) are to be considered for contextual purposes only and not for credit.

5.2.1 *M. CIRCINELLOIDES* INDUCES PLATELET AGGREGATION IN WHOLE HUMAN BLOOD AND PRP

It has previously been shown that *M. circinelloides* platelet aggregation potential in platelet-rich plasma (PRP) is dependent upon spore developmental stage and is dose-dependent (Figure 5.1A-B^Δ). Using light-transmission aggregometry to record platelet aggregation over 30 minutes in response to *M. circinelloides* spores at different stages of germination (0 hr, 3 hr, 6 hr) and hyphae (48 hr), it was shown that platelets exposed to resting spores exhibit significant but low platelet aggregation (0 hr: 15.6 ± 10.2%; $p < 0.05$), but when exposed to 3 hr spores aggregation was strikingly increased (3 hr: 1:10: 56.0 ± 12.3%; $p < 0.01$) (Figure 5.1A^{*Δ}). When platelets were incubated with fully swollen spores, platelet aggregation markedly declined (6 hr: 1:10: 32.6 ± 14.3%), and this decline in aggregation was further exaggerated in response to *M. circinelloides* hyphae, with negligible platelet aggregation noted (48 hr: 1:10: 2.80 ± 1.11%) (Figure 5.1A^{*Δ}). Additionally, the platelet aggregation potential of *M. circinelloides* spores was shown to be dose-dependent (Figure 5.1B^{*Δ}). Using a range of spore:platelet concentrations, ranging from 1:10 to 1:500, platelet aggregation was recorded over 30 minutes using light-transmission aggregometry. Significant platelet aggregation was induced by 3 hr spores at 1:10 and 1:20 spore:platelet ratios (1:10: 56.0 ± 12.3%; 1:20: 52.8 ± 14.6%; $p < 0.01$) but declined to negligible levels at 1:100 and 1:500 spore:platelet ratios (1:100: 2.6 ± 0.5%; 1:500: 2.6 ± 0.4%) (Figure 5.1B^{*Δ}). As *M. circinelloides* spores at 3 hr germination displayed the greatest platelet aggregation potential (1:10 and 1:20 spore:platelet concentration), all subsequent investigations were conducted using spores at this stage of spore development. To provide more clinical context and determine whether spores induce aggregation in the presence of other blood cells and components, platelet aggregation induced by *M. circinelloides* in whole human blood was investigated. Using

multiple-electrode aggregometry, platelet aggregation in whole human blood was recorded over 30 minutes in response to spores. Spores induced significant platelet aggregation in whole human blood ($180 \pm 16U$; $p < 0.05$) (Figure 5.1C^A).

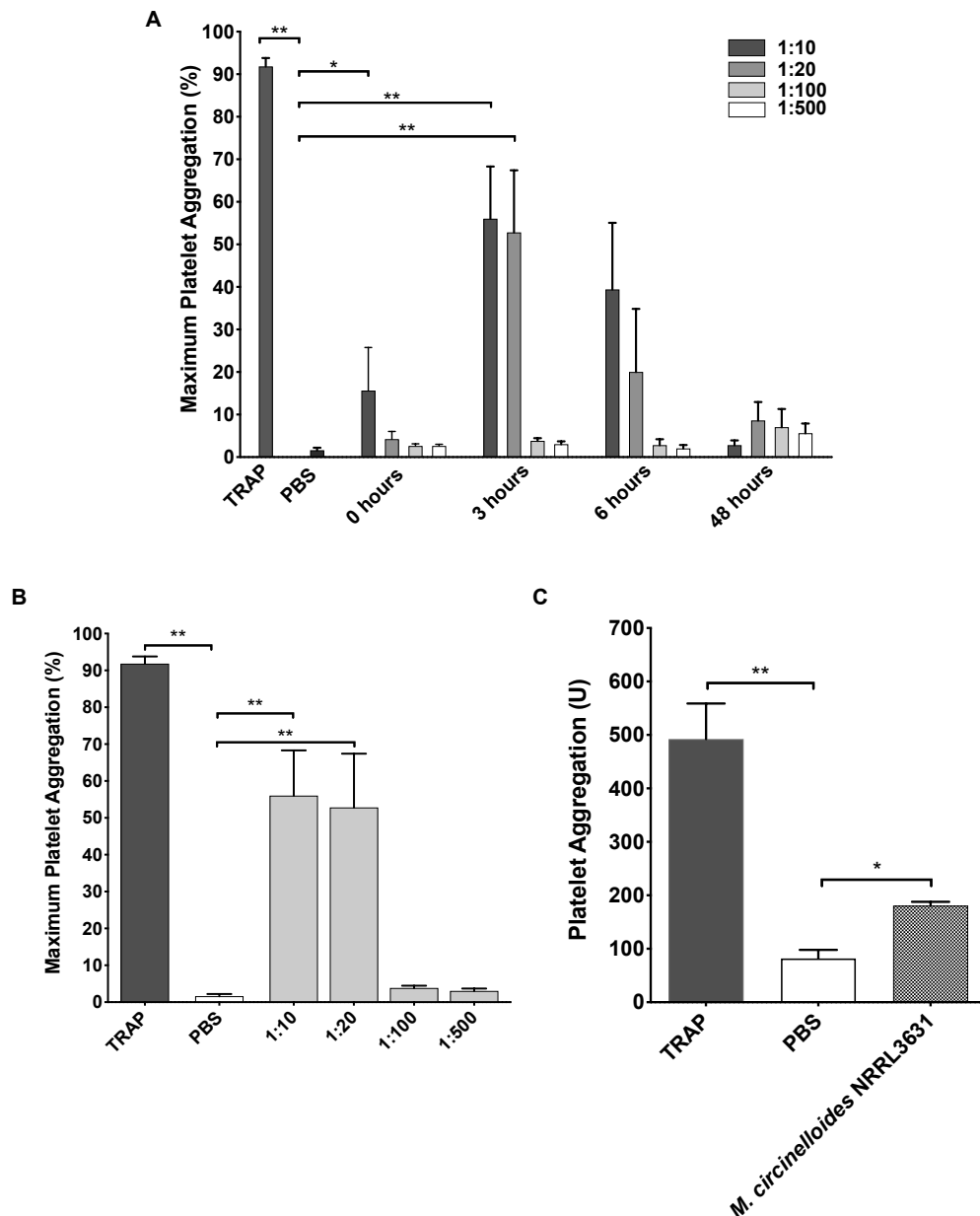


FIGURE 5.1. *M. CIRCINELLOIDES* INDUCES PLATELET AGGREGATION IN PRP AND WHOLE BLOOD. (A^Δ) Platelet aggregation was recorded via light-transmission aggregometry over 30 minutes in response to TRAP, PBS and *M. circinelloides* at different stages of germination (0, 3, 6 and 48 hr). Significant platelet aggregation was seen with spores at 0 hr germination (1:10 spore:platelet ratio). Aggregation increased with 3 hr spores (1:10 and 1:20 spore:platelet ratio). Platelet aggregation potential declined with 6 hr spores and 48 hr hyphae. Data shown are mean \pm SEM of five independent experimental repeats; * p <0.05, ** p <0.01, One-way ANOVA, Kruskal-Wallis multiple comparisons. (B^Δ) Platelet aggregation was recorded via light-transmission aggregometry over 30 minutes in response to TRAP, PBS and *M. circinelloides* 3 hr spores at decreasing spore:platelet ratios. Spores induced significant platelet aggregation at a 1:10 spore:platelet ratio, decreasing slightly at a 1:20 spore:platelet ratio, after which platelet aggregation declines to negligible levels at 1:100 and 1:500 spore:platelet ratios. Data shown are mean \pm SEM of five independent experimental repeats; ** p <0.01, Mann-Whitney U test. (C^Δ) Platelet aggregation in response to TRAP, PBS and *M. circinelloides* 3 hr spores in whole human blood was recorded via multiple-electrode aggregometry over 30min. Spores induced significant platelet aggregation in whole blood. Data shown are mean \pm SEM of five independent experimental repeats; * p <0.05, ** p <0.01, Mann-Whitney U test.

5.2.2 *M. CIRCINELLOIDES* SPORES FORM LARGE COMPLEX AGGREGATES WITH HUMAN PLATELETS

To visualise *M. circinelloides*-induced platelet thrombi, dual inverted Selective Plane Illumination fluorescence microscopy (diSPIM) was used. *M. circinelloides* spores were stained with ConA - Alexa Fluor™ 488, and platelets were stained with CellMask Deep Red Plasma Membrane Stain. Spores were added to PRP and incubated at 37°C for 30 min. Following incubation, aggregates were fixed onto glass coverslips and imaged. Microscopy showed the formation of large complex structures, with numerous spores contained within a single platelet thrombus (Figure 5.2^A).

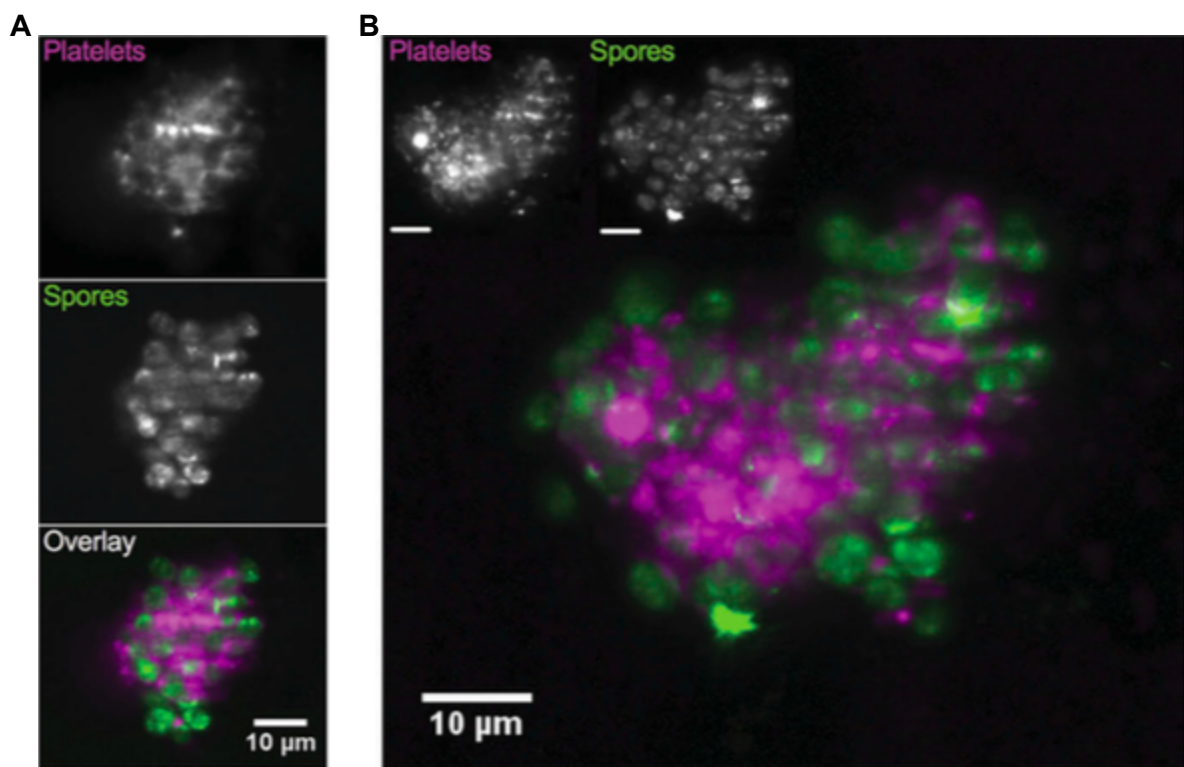


FIGURE 5.2 *M. CIRCINELLOIDES* SPORES FROM LARGE, COMPLEX AGGREGATES WITH HUMAN PLATELETS. Platelet-spore aggregates were visualised by diSPIM. *M. circinelloides* spores (green) interact with platelets (magenta) to form large complex aggregate structures. (A^Δ) optical section through a spore-platelet aggregate. (B^Δ) maximal intensity projection of the 3D volume of the spore-platelet aggregate. Aggregates were visualised with a 40x objective and analysed on FIJI.

5.2.3 PLATELET AGGREGATION IN RESPONSE TO *M. CIRCINELLOIDES* IS SUPPORTED BY INTEGRIN α IIb β 3, IgG RECEPTOR Fc γ RIIA, AND DOWNSTREAM SRC AND SYK TYROSINE KINASES

Platelet integrin α IIb β 3 is key to platelet activation in response to bacteria. To investigate the role of α IIb β 3 in platelet aggregation to *M. circinelloides*, the integrin was inhibited by pre-treatment with eptifibatide and aggregation recorded in the presence and absence of α IIb β 3 inhibition, by light-transmission aggregometry over 30 min. Platelets treated with eptifibatide prior to the exposure of *M. circinelloides* spores failed to aggregate in response to spores (+eptifibatide: 1:10: 0.60 \pm 0.25%; 1:20: 0.60 \pm 0.2%; -eptifibatide: 1:10: 58.0 \pm 7.46%, 1:20: 43.4 \pm 11.4%) (Figure 5.3A*^A).

In addition to α IIb β 3, platelet IgG receptor Fc γ RIIA has been shown to be necessary for bacterial-induced platelet aggregation. To determine the role of Fc γ RIIA in *M. circinelloides*-induced platelet aggregation, the receptor was inhibited with mAb IV.3 prior to spore exposure, and aggregation was recorded over 30 minutes using light-transmission aggregometry. Platelets treated with Fc γ RIIA inhibitor mAb IV.3 did not aggregate in response to *M. circinelloides* spores (+mAb IV.3: 1:10: 12.8 \pm 10.57%; 1:20: 2.2 \pm 0.4%; - mAb IV.3: 1:10: 48.8 \pm 9.58%, 1:20: 37.0 \pm 13.0%) (Figure 5.3B^A).

Activation of α IIb β 3 and/or Fc γ RIIA results in the activation of downstream tyrosine kinases Src and Syk, and is key to platelet activation by bacteria. To identify the role of Src and Syk tyrosine kinases in *M. circinelloides*-induced platelet aggregation, the effect of Src inhibition by Dasatinib and Syk inhibition by PRT-060318 was determined. Platelets were treated with Dasatinib or PRT-060318 prior to the addition of *M. circinelloides*, and aggregation recorded via light-transmission aggregometry. Platelets treated with Dasatinib and PRT-060318 displayed negligible aggregation in response to spores (+Dasatinib: 0.8 \pm 0.2%; +PRT-060318: 2.0 \pm 0.3%); -inhibitor: 56.2 \pm 6.3%) (Figure 5.3C*^A).

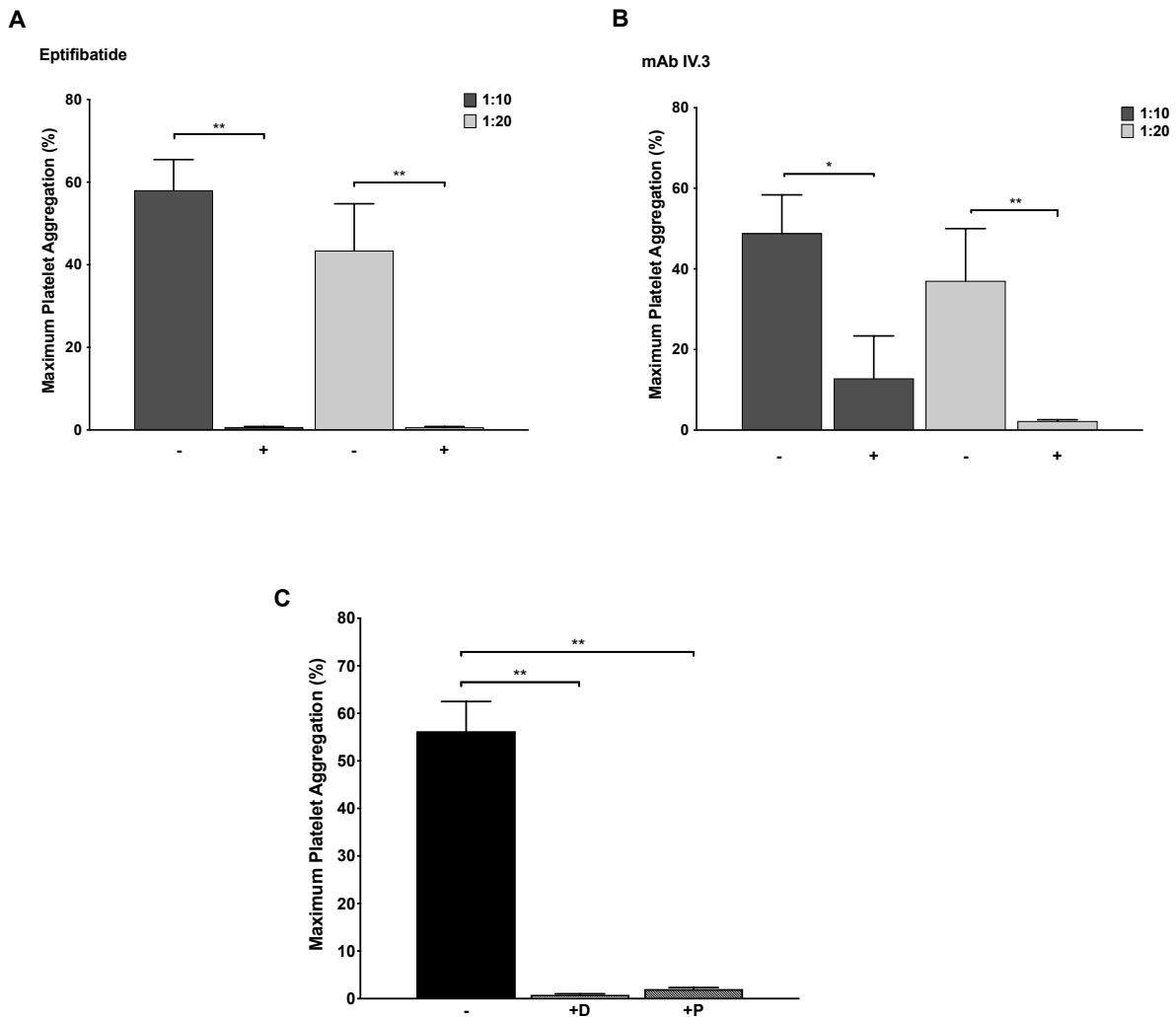


FIGURE 5.3. PLATELET AGGREGATION INDUCED BY *M. CIRCINELLOIDES* IS FACILITATED BY AIIBB3, FCγRIIA AND DOWNSTREAM SRC AND SYK TYROSINE KINASES. (A^Δ) Platelet aggregation in response to *M. circinelloides* spores in the presence and absence of αIIbβ3 inhibitor, eptifibatide, was recorded via light-transmission aggregometry over 30 min. Platelet aggregation to spores was significantly inhibited by eptifibatide. Data shown are mean ± SEM of five independent experimental repeats; ** $p < 0.01$; Mann-Whitney *U*. (B^Δ) Platelet aggregation in response to *M. circinelloides* spores in the presence and absence of FcγRIIA inhibitor, mAb IV.3, was recorded via light-transmission aggregometry over 30 min. mAb IV.3 significantly inhibited platelet aggregation to spores. Data shown are mean ± SEM of five independent experimental repeats; * $p < 0.05$, ** $p < 0.01$; Mann-Whitney *U*. (C^Δ) Platelet aggregation in response to *M. circinelloides* spores in the presence and absence of Src inhibitor Dasatanib and Syk inhibitor PRT-060318, was recorded via light-transmission aggregometry over 30 min. Platelet aggregation to *M. circinelloides* spores was significantly inhibited by Dasatanib and PRT-060318. Data shown are mean ± SEM of five independent experimental repeats; ** $p < 0.01$; Mann-Whitney *U*.

5.2.4. SECONDARY MEDIATORS TxA_2 AND ADP SUPPORT *M. CIRCINELLOIDES*-INDUCED PLATELET AGGREGATION

Secondary mediators TxA_2 and ADP are released upon platelet activation to support aggregate formation, and are key in aggregation to bacteria. The profile of *M. circinelloides*-induced aggregation was investigated by light-transmission aggregometry. *M. circinelloides* spores were added to platelets in PRP at a 1:10 spore:platelet ratio and aggregation recorded over 30 min. The *M. circinelloides*-induced platelet aggregation profile displayed a lag phase prior to rapid aggregation and finally plateau, in comparison to the rapid aggregation seen with TRAP (Figure 5.4A^Δ). The lag phase suggests secondary mediators TxA_2 and ADP may play a key role in platelet aggregation to *M. circinelloides*. To determine the role of TxA_2 and ADP in *M. circinelloides*-induced aggregation, platelets were treated with TxA_2 inhibitor Indomethacin and ADP inhibitor Apyrase. Platelet aggregation to *M. circinelloides* was then recorded in the presence and absence of inhibitors via light-transmission aggregometry over 30 min. Platelet aggregation to spores was significantly inhibited when treated with Indomethacin independently and when in combination with Apyrase (-Indomethacin -Apyrase: $70.0 \pm 6.0\%$; +Indomethacin: $24.3 \pm 6.8\%$; +Indomethacin +Apyrase: $18.3 \pm 6.1\%$) (Figure 5.4B^Δ).

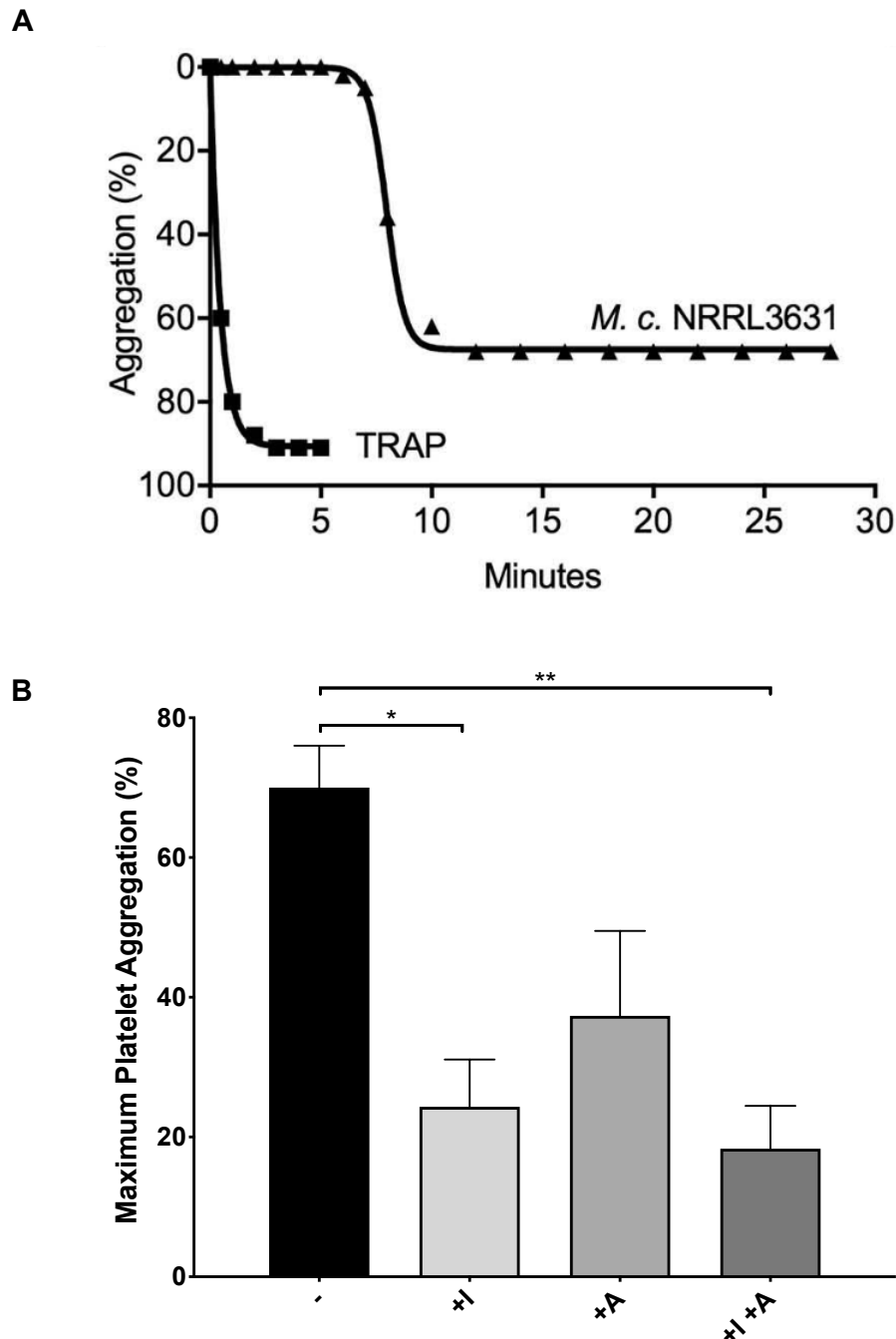


FIGURE 5.4 *M. CIRCINELLOIDES* INDUCED PLATELET AGGREGATION IS SUPPORTED BY SECONDARY MEDIATORS TxA_2 AND ADP. (A^Δ) Platelet aggregation in response to TRAP and *M. circinelloides* spores was recorded via light-transmission aggregometry over 30min. TRAP induced rapid platelet aggregation whilst aggregation to *M. circinelloides* spores displayed a lag-phase, followed by rapid aggregation and then plateau. (B^Δ) Platelet aggregation in response to *M. circinelloides* spores in the absence or presence of TxA_2 inhibitor, indomethacin (I), and ADP inhibitor, apyrase (A), was recorded using light-transmission aggregometry over 30 min. Indomethacin significantly inhibited platelet aggregation to *M. circinelloides* independently and in combination with Apyrase. Data shown are mean \pm SEM of three independent experimental repeats; * p < 0.05, ** p < 0.01; One-way ANOVA, Dunnett's multiple comparison test.

5.2.5 *M. CIRCINELLOIDES* SPORES ACTIVATE PLATELETS

Upon activation, platelets express the α -granule released activation marker CD62P (P-Selectin) on their surface. To elucidate whether platelets are activated by *M. circinelloides*, spores were incubated with platelets under aggregating and non-aggregating conditions for 30 minutes at 37°C. For non-aggregating conditions platelets were pre-treated with α IIb β 3 inhibitor, eptifibatide, whilst for aggregating conditions no inhibitor treatment was performed. Following incubation, platelets were labelled for P-Selectin using CD62P-FITC, and platelet surface expression recorded via flow cytometry. Platelets exposed to *M. circinelloides* spores under aggregating conditions displayed increased P-selectin surface expression, whilst under non-aggregating conditions platelet P-Selectin surface expression did not increase, indicating that platelets are activated by *M. circinelloides* spores under aggregating conditions (Figure 5.5^A).

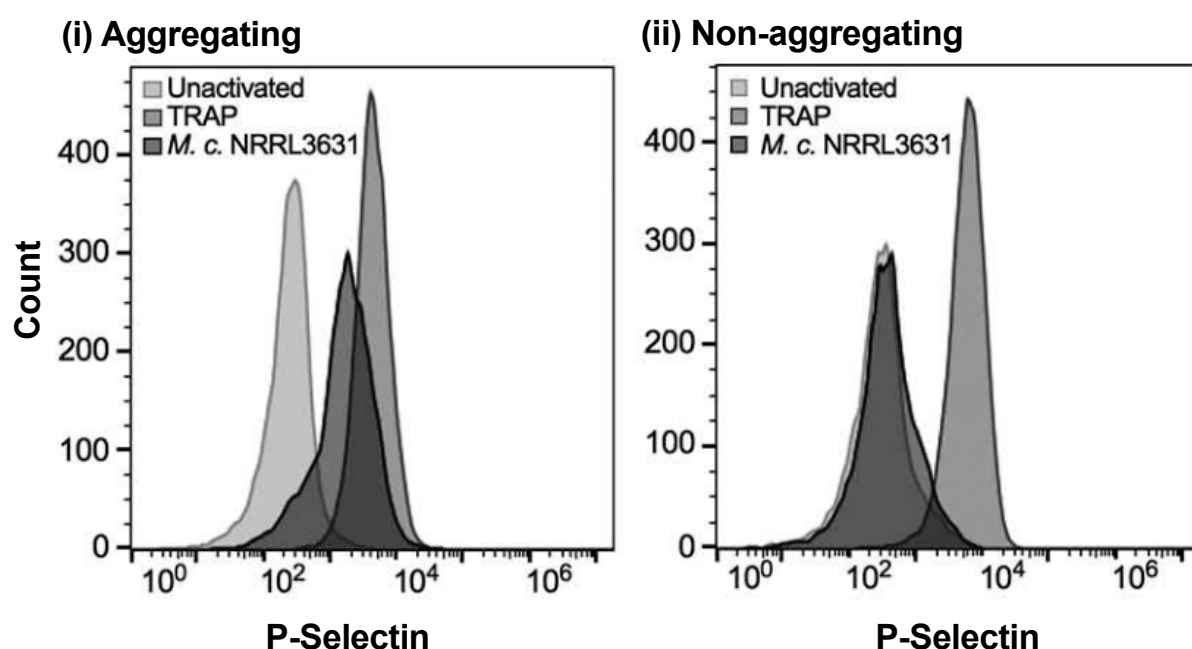


FIGURE 5.5^A *M. CIRCINELLOIDES* ACTIVATES PLATELETS UNDER AGGREGATING CONDITIONS. Platelet surface expression of activation marker P-selectin (using CD62P-FITC) following incubation with *M. circinelloides* spores under (i) aggregating (-eptifibatide) and (ii) non-aggregating (+eptifibatide) conditions, was determined using flow cytometry. (i) CD62P expression increases following *M. circinelloides* exposure under aggregating conditions, but not under (ii) non-aggregating conditions.

5.2.6 PLATELET SURFACE α IIb β 3 EXPRESSION INCREASES FOLLOWING *M. CIRCINELLOIDES* EXPOSURE

α IIb β 3 stores are found within α -granules and released to the platelet surface upon platelet activation, consolidating thrombus formation. Upregulation of α IIb β 3 surface expression on activated platelets is seen in response to bacteria. Platelet surface expression levels of Fc γ RIIA are expected to remain stable. To investigate the platelet surface expression levels of integrin α IIb β 3 and receptor Fc γ RIIA following exposure to *M. circinelloides* spores, platelets were incubated with *M. circinelloides* spores under aggregating and non-aggregating conditions, and incubated at 37°C for 30 min. For non-aggregating conditions platelets were pre-treated with α IIb β 3 inhibitor eptifibatide prior to spore exposure, whilst for aggregating conditions no inhibitor treatment was performed. Following spore-platelet incubation, platelets were labelled for surface α IIb β 3 using APC-Mouse Anti-Human CD41a, and Fc γ RIIA using conjugated anti-human CD32 + anti-mouse 2° Alexa Fluor™ 488, and surface expression recorded by flow cytometry.

Under aggregating conditions, platelets exposed to *M. circinelloides* spores displayed increased α IIb β 3 surface expression when compared to non-aggregating conditions (Figure 5.6A^Δ). Expectedly, platelet surface expression levels of Fc γ RIIA remained stable under both non-aggregating and aggregating conditions as levels are stable and not affected by platelet activation (Figure 5.6B^Δ).

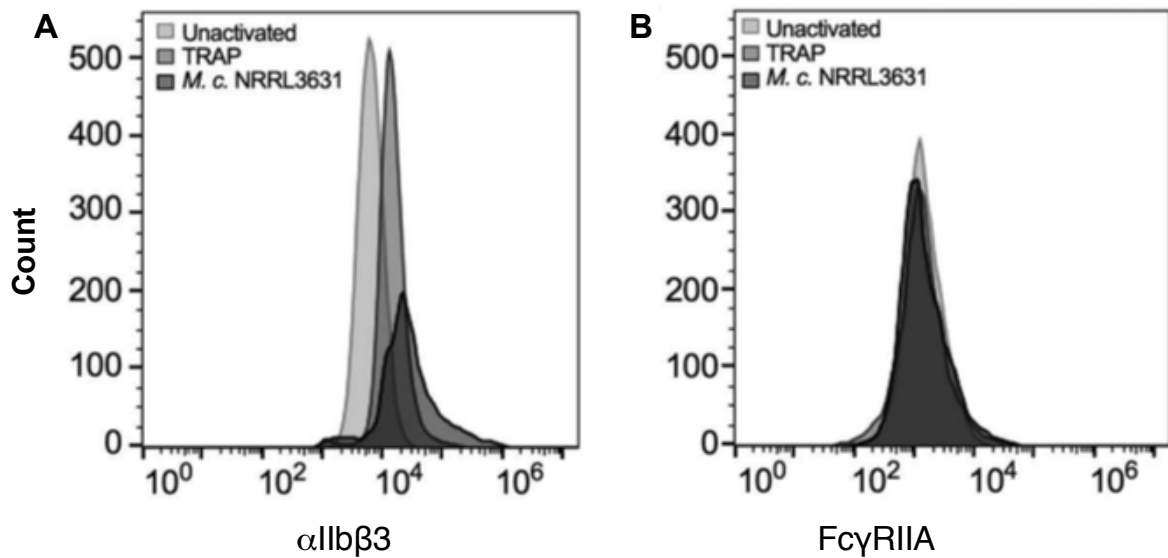


FIGURE 5.6^A. *M. CIRCINELLOIDES* INDUCES INCREASED SURFACE $\alpha\text{IIb}\beta\text{3}$ EXPRESSION BUT SURFACE Fc γ RIIA EXPRESSION REMAINS STABLE. *M. circinelloides* spores were incubated with platelets following treatment with or without eptifibatide for 30 minutes at 37°C. TRAP was used as a positive control. Following incubation, platelet surface $\alpha\text{IIb}\beta\text{3}$ expression was labelled using APC-Mouse Anti-Human CD41a, and Fc γ RIIA using conjugated anti-human CD32 + anti-mouse 2° Alexa Fluor™ 488 and recorded by flow cytometry. (A^A) Platelet surface $\alpha\text{IIb}\beta\text{3}$ expression increases following spore exposure in the absence of eptifibatide. (B^A) Platelet surface expression levels of Fc γ RIIA remain stable following *M. circinelloides* exposure in the presence or absence of eptifibatide.

5.3 DISCUSSION

Platelets are responsible for maintaining haemostasis and thrombosis, and sealing damaged vasculature, but recently platelets have been recognised as key immune effectors, displaying antimicrobial properties, such as the release of PF-4 shown to have microbicidal properties against *C. albicans* (Tang, Yeaman and Selsted, 2002). Thrombosis is a hallmark of mucormycosis, and therefore suggests platelets may play a role in infection (Spellberg, Edwards and Ibrahim, 2005). Understanding the mechanistic underpinnings of platelet-*Mucor* interaction is key to our understanding of thrombosis in mucormycosis, and could elucidate novel therapeutic strategies to aid treatment of this infection.

Data showed, *M. circinelloides* spores induce platelet aggregation in a dose-dependent manner, with higher spore concentrations inducing greater platelet aggregation. Furthermore, platelet aggregation was dependent upon spore developmental stage. Resting (0 hr) spores induced

low, albeit significant, aggregation. Platelet aggregation in response to spores at the mid-point of maximal spore swelling (3 hr) was strikingly higher, with significant aggregation at 1:10 and 1:20 spore:platelet concentrations. Upon spores reaching maximal swelling (6 hr) platelet aggregation was markedly reduced, and the decline was exaggerated further in response to *M. circinelloides* hyphae (48 hr). This suggests the developmental stage of *M. circinelloides* spores plays a key role in the induction of platelet aggregation, with swollen spores at the mid-point of swelling inducing the greatest platelet aggregation, and those with hyphal structures inducing negligible aggregation. Additionally, spores at the mid-point induced significant platelet aggregation in whole human blood, indicating their strong aggregation potential was retained in the presence of other blood cells and components, as would be seen in a clinical context. Additionally, fluorescence microscopy showed, *M. circinelloides* spores induced the formation of large complex platelet aggregates, containing numerous spores, supporting the data showing significant induction of platelet aggregation in response to swelling spores. The decline in platelet aggregation potential of *M. circinelloides* spores in the latter stages of germination and hyphal formation, is somewhat in conflict with previous research showing the adherence and activation of platelets to mucormycetes conidia and hyphae, although aggregation was not recorded in this study (Perkhofer *et al.*, 2009). The effect of germination on platelet activation has also been explored in *Aspergillus fumigatus* conidia and hyphae, where it has been shown that platelet activation is significantly increased in response to hyphae compared to resting and swollen conidia (Rødland *et al.*, 2010). The distinct aggregation profile seen in response to *M. circinelloides* spores at different developmental stages suggests there is an inhibitory effect exerted on platelet aggregation in the latter stages of *M. circinelloides* germination. A plausible explanation of this could be the release of an inhibitory factor, such as that seen in *C. albicans*, through its metabolite, gliotoxin, shown to significantly inhibit platelet aggregation (Bertling *et al.*, 2010).

Investigation of the molecular underpinnings of platelet aggregation in response to *M. circinelloides* spores, highlighted two key platelet receptors in this process, surface integrin $\alpha\text{IIb}\beta\text{3}$ and IgG receptor Fc γ RIIA. Inhibition of these receptors, resulted in the loss of platelet aggregation in

response to *M. circinelloides* spores. This agrees with previous research showing platelet receptors $\alpha\text{IIb}\beta 3$ and Fc γ RIIA are crucial in the platelet activation pathway in response to bacteria (Arman *et al.*, 2014). Research showed platelet activation in response to bacterial species, including *Streptococcus gordonii* and *Staphylococcus aureus* is dependent upon Fc γ RIIA activation (Arman *et al.*, 2014). The activation of Fc γ RIIA was also shown to be dependent upon IgG and $\alpha\text{IIb}\beta 3$ interaction. Here it appears *M. circinelloides* spores induce platelet aggregation through a common activation pathway to that seen with bacteria, although the role of IgG was not explored.

Fc γ RIIA signals through downstream Src and Syk tyrosine kinases (Oberfell *et al.*, 2002; Boylan *et al.*, 2008). Data showed that the activation of Src and Syk is essential in platelet aggregation in response to *M. circinelloides* spores. This agrees with previous research showing inhibition of Src and Syk tyrosine kinases results in the loss of platelet aggregation in response to bacteria (Arman *et al.*, 2014). Additionally, a pronounced lag phase was noted in the aggregation profile of *M. circinelloides* spores suggesting secondary mediators may be required in the aggregation in response to spores. Secondary mediators, such as TxA₂ and ADP, partake in a positive feedback loop whereby they recruit further platelets to the thrombus and generate their own release and activation. Data showed inhibition of secondary mediators, TxA₂ and ADP significantly reduced platelet aggregation, suggesting secondary platelet mediators are necessary for aggregation in response to *M. circinelloides* spores. This again agrees with previous research showing ADP and TxA₂ support platelet aggregation to bacteria, suggesting *M. circinelloides* spores employ a common pathway to platelet activation as seen in bacteria (Arman *et al.*, 2014).

Data discussed above indicates platelet activation in response to *M. circinelloides* spores. Labelling of platelet activation marker, CD62P, showed platelets are activated in response to *M. circinelloides* spores under aggregating conditions. This agrees with previous research showing platelet activation in response to Mucorales spores (Perkhofer *et al.*, 2009). Additionally, surface expression of surface integrin $\alpha\text{IIb}\beta 3$ was shown to significantly increase upon exposure to *M. circinelloides* under aggregating conditions. This is also suggestive of activation and α -granule release,

as α -granules contain α IIb β 3, which are trafficked to the platelet surface through granule release upon activation (Blair and Flaumenhaft, 2009).

In summary, *M. circinelloides* induces platelet activation in a dose-dependent manner and aggregation is dependent upon spore developmental stage. Here, the first elucidation of fungal-induced platelet activation pathway is made. Platelet surface IgG receptor, Fc γ RIIA, surface integrin, α IIb β 3, and downstream tyrosine kinases, Src and Syk, mediate the activation of platelets in response to *M. circinelloides* spores, and aggregation is supported by secondary mediators ADP and TxA₂. This elucidation highlights a common platelet activation pathway amongst bacteria and fungi and offers foundational research to further tease apart the role of thrombosis in mucormycosis.

6.0 DISCUSSION

Mucormycosis has drawn considerable attention over the last two years, owing to its prominence in co-infections of COVID-19 patients. Colloquially termed the ‘black fungus’, this rare but fatal opportunistic infection is poorly understood, and until recently was paid little attention. The invasive fungal infection is caused by filamentous fungi of the Mucorales order, and includes species such as *Rhizopus*, *Mucor* and *Lichtheimia*. The hallmarks of mucormycosis are considered to be angioinvasion, tissue necrosis and thrombosis, and the germination process is at the crux of mucormycetes’ pathogenicity. Hyphal structures can penetrate the endothelial lining allowing the fungus to enter the bloodstream, enabling dissemination and widespread infection (Liu *et al.*, 2010). The failure of phagocytes to successfully clear resting spores is an important factor in mucormycosis, as it ultimately enables the pathogen to escape killing by the usually robust innate immune system, and for spores to germinate and cause extensive tissue damage (Levitz *et al.*, 1986). Angioinvasion exposes the pathogenic fungus to components of the blood including platelets, and as thrombosis is a hallmark of mucormycosis, it suggests that there is platelet activation during infection (Spellberg, Edwards and Ibrahim, 2005). Ultimately, Mucorales are able to circumvent the innate immune system, germinate and cause thrombosis and extensive tissue damage. There are three factors to consider here: (i) the process of germination and associated cell wall changes, (ii) the interaction between Mucorales and macrophage, and (iii) the platelet activation pathway in response to Mucorales - each of which are discussed in this concluding chapter.

6.1 ENHANCING OUR UNDERSTANDING OF *M. CIRCINELLOIDES* GERMINATION

The germination of Mucorales spores encompasses exiting dormancy, swelling by isotropic growth, and forming hyphal structures by apical growth (Cano and Ruiz-Herrera, 1987; Medwid and Grant, 1984; Cano and Ruiz-Herrera, 1988). The underlying processes of mucormycete spore germination are complex and poorly understood. TEM showed the complexity of the *M. circinelloides* spore body increases during germination, with more vesicular bodies and mitochondria visible as

germination progresses. To enhance our understanding of *Mucor* spore swelling, from a state of dormancy up to the maximal point of swelling prior to hyphal emergence, RNA-sequencing was employed. RNA was extracted from spores at resting (0 hr), maximal swelling mid-point (3 hr) and maximal swelling (6 hr), sequenced, and differential gene expression analysed and compared in the following conditions: (i) 0 hr vs 3 hr (early germination), (ii) 3 hr vs 6 hr (late germination) and (iii) 0 hr vs 6 hr (complete germination).

Transcriptional profiling of early *M. circinelloides* germination showed that, as spores exit dormancy and begin the process of germination, there is a high degree of transcriptional change that occurs. A large proportion of biological processes assigned to upregulated genes are predicted to be involved in metabolism. This is indicative of spores exiting a state of dormancy and becoming metabolically active. A similar profile is seen in the early stages of *Rhizopus delemar* germination, where transcripts with predicted functions in metabolic processes are enriched (Sephton-Clark, 2018). Processes associated with protein synthesis are also heavily enriched in the 0 hr vs 3 hr profile, including translation and protein folding. Coupled with the upregulation of metabolic processes, it appears that *M. circinelloides* spores initiate protein synthesis soon after exiting dormancy, enabling rapid growth. In *R. delemar*, transcripts with predicted functions in protein synthesis and modification, and metabolism are also enriched during germination initiation (Sephton-Clark *et al.*, 2018). There are also a large proportion of downregulated genes that have functions predicted to be associated with metabolism in early *M. circinelloides* germination, suggesting there is a metabolic ‘reshaping’ during the initial stages of germination. A similar transcriptional profile is noted in the germination of *S. cerevisiae* spores, where metabolic processes are upregulated and downregulated concomitantly (Geijer *et al.*, 2012). Furthermore, processes associated with autophagy and stress response are downregulated during early *M. circinelloides* germination. Autophagy is induced by nutrient starvation and has been shown to be important in the germination of *A. fumigatus* under nutrient and metal ion starvation conditions, however the role of autophagy in filamentous fungi is not well understood (Richie *et al.*, 2007, Kikuma and Kitamoto, 2011). When considering the optimal growth conditions *M.*

circinelloides spores were exposed to, it seems reasonable that autophagy genes are downregulated, as spores were not under a state of nutrient starvation. Furthermore, data showed that genes with predicted roles in response to stress and response to oxidative stress are also downregulated in the early stages of *M. circinelloides* germination. During early *R. delamar* germination, decreased catalase expression is coupled with increased ROS expression, and furthermore, preventing superoxide radical generation significantly impairs germination (Sephton-Clark *et al.*, 2018). Catalases detoxify hydrogen peroxide and ROS generation has been shown to be important for Mucorales germination. Therefore, the downregulation of catalase expression noted in the transcriptional profiling of *M. circinelloides* spores between 0 hr and 3 hr, suggests ROS generation is important for early fungal growth in this Mucorales species also.

Transcriptional profiling of late *M. circinelloides* spore germination showed that, there is a lesser degree of transcriptional change compared to that seen in early germination, and the majority of genes are upregulated. Comparing the transcriptional profiles of early and late *M. circinelloides* germination, suggests that there is a 'switch' in gene expression, whereby genes that are downregulated in early germination are upregulated in late germination, and genes that are downregulated in late germination are upregulated during early germination. *M. circinelloides* spores between 3 hr and 6 hr upregulate genes associated with autophagy. Although associated with nutrient starvation, autophagic vacuoles have been shown in swollen conidia and hyphae of *Aspergillus oryzae* cultured in nutrient-rich growth conditions, suggesting autophagy is required for germination in filamentous fungi (Kikuma *et al.*, 2006). Considering this, it appears that autophagy may aid the process of late *M. circinelloides* germination. In addition, genes associated with stress response are upregulated during the late phase of germination. Transcripts with predicted stress response functions are also upregulated in the latter stages of *R. delamar* germination (Sephton-Clark *et al.*, 2018). Stress response has been shown to be important for hyphal growth in various filamentous fungi, including *Fusarium graminearum* (Zheng *et al.*, 2012). *M. circinelloides* spores at 6 hr are approaching the filamentation stage of growth. Considering this, the upregulation in stress response

genes prior to germ tube emergence may aid hyphal growth of *M. circinelloides* as shown in other filamentous fungi. Furthermore, genes associated with translation are downregulated in late *M. circinelloides* spore germination. Translation is also shown to be downregulated in the latter stages of *R. delamar* germination (Sephton-Clark *et al.*, 2018). From this, it seems protein synthesis is primarily upregulated in the initial stages of Mucorales spore germination where there are the majority of transcriptional changes, and as spores approach the hyphal growth stage, protein synthesis is downregulated. This suggests the majority of protein synthesis required for growth occurs soon after breaking dormancy.

Enhancing our understanding of Mucorales spore germination – a process enabling extensive tissue damage in the host – could elude novel anti-therapeutic strategies. For example, considering the emphasis on protein synthesis in the initial stages of germination, it would be useful to investigate the efficacy of protein synthesis inhibitors, such as sordarins (Botet *et al.*, 2008). Sordarin is an antifungal compound that targets translation elongation factor 2 production, inhibiting translocation and protein synthesis (Botet *et al.*, 2008). A recent study investigating the *in vitro* effects of the sordarin and its derivative hypoxysordarin, showed promising antifungal activity of the compounds against *Mucor miehei*, although sordarin is not yet approved for clinical use (Daferner *et al.*, 1999).

6.2 CELL WALL REMODELLING IN *M. CIRCINELLOIDES* DURING SPORE DEVELOPMENT

The fungal cell wall is the target of many antifungals, such as echinocandins targeting β -glucan, yet antifungal efficacy against Mucorales is low. This is perhaps unsurprising considering the cell wall composition of Mucorales is understudied, raising questions of drug specificity. The frontline antifungal employed in mucormycosis treatment is L-AMB, a polyene contained within a liposome. Upon trafficking of the liposome through the cell wall, the polyene is released and binds to plasma membrane ergosterol, forms pores and resulting in ion leakage (Scorzoni *et al.*, 2017). Ergosterol abundance varies between Mucorales species. For example, in *Rhizopus pusillus* hyphae the relative abundance of ergosterol is 38%, whilst in *M. circinelloides* is 65.8% (Müller *et al.*, 2018). Considering

the inefficacy of L-AMB, enhancing our knowledge of the cell wall composition and compositional changes during *M. circinelloides* spore development, could elucidate novel antifungal cell wall targets.

During germination, *M. circinelloides* spores display phenotypic changes, swelling significantly from resting to fully swollen spores. TEM shows distinct differences in the cell walls of spores at 0, 3 and 6 hr germination. In resting spores, there are two discernible cell wall layers, in 3 hr spores there are three discernible layers, and in 6 hr spores there are two discernible layers. This indicates that the cell wall undergoes considerable cell wall remodelling during germination, with each stage of spore swelling displaying distinct cell wall profiles. Probing DEGs associated with cell wall synthesis during early (0 hr vs 3 hr) and late (3 hr vs 6 hr) germination supported these findings. Genes implicated in glycosylation, chitin synthesis and β -glucan synthesis were shown to be upregulated during both early and late stages of *M. circinelloides* spore germination.

During early *M. circinelloides* germination, analysis highlighted the upregulation of genes with predicted chitin synthase products orthologous to *C. albicans* *CHS1*, *CHS2*, *CHS3*, *CHS7* and *CHS8*. Analysis of late *M. circinelloides* germination showed chitin synthases are differentially regulated in the latter stages of germination. Considering chitin synthases have distinct roles, synthesising chitin of differing structures, in particular locations, during certain stages of germination, this is unsurprising (Leonardon *et al.*, 2007). For example, in *C. albicans*, *CHS2* and *CHS3* expression increases during hyphal formation, whereas *CHS1* expression remains low in yeast and hyphal growth (Munro *et al.*, 1998). Furthermore, cell wall chitin content was shown to increase in germinating *M. circinelloides* spores, as shown by total and surface exposed chitin staining with CFW and WGA, respectively. Chitin content significantly increases in the *M. circinelloides* cell wall between resting (0 hr), mid-point (3 hr) and fully swollen (6 hr) spores, supporting RNA-seq analysis showing the upregulation of chitin synthase expression in early and late germination. Considering the expression of chitin in the *M. circinelloides* cell wall and the expression of chitin synthases during germination, investigation of chitin synthase inhibitors against *M. circinelloides* could be effective in the development of novel therapeutic strategies targeting mucormycosis. *In vitro* investigation shows the inhibition of chitin synthase

activity in *Mucor mucedo*, by phenylpropene derivative, anethole. Furthermore, anethole inhibits *M. mucedo* growth and induces morphological changes in hyphal structures impairing cell wall rigidity (Yutani *et al.*, 2011). Currently chitin synthase inhibitors are not used clinically, however Nikkomycin B is currently in clinical trial and may offer an alternative antifungal for mucormycosis treatment than LAmB (Shubitz *et al.* 2014).

Genes encoding 1,3- β -glucan synthases (and orthologous to *C. albicans* *GSL1*, *GSL2* and *GSC1*) were shown to be upregulated during early and late *M. circinelloides* germination. Additionally, determination of β -1,3-glucan in germinating *M. circinelloides* spores by Fc-Dectin-1-Alexa Fluor™ 488 labelling and fluorescence microscopy supported the findings of RNA-sequencing analysis. β -1,3-glucan content increases slightly between resting (0 hr) and mid-point (3 hr) spores, and significantly between mid-point and fully swollen (6 hr) spores, supporting RNA-sequencing analysis showing the upregulation of β -1,3-glucan synthase expression in early and late germination. Considering this, β -1,3-glucan and/or β -1,3-glucan synthase targeting antifungals would seem like a favourable alternative to L-AMB. However, due to the inefficacy of echinocandins against mucormycetes *in vitro*, Mucorales are considered to be resistant to the antifungal class (Walsh and Kontoyiannis, 2008). However, *in vivo* research has shown echinocandin, caspofungin, inhibits 1,3- β -D-glucan synthase in *Rhizopus oryzae* and reduces mortality in a diabetic murine model of mucormycosis (Ibrahim *et al.*, 2005). Although not the preferentially recommended treatment strategy, a retrospective study on L-AMB-caspofungin combination therapy of rhinocerebral mucormycosis patients showed combination therapy is more effective than L-AMB monotherapy in mucormycosis treatment (Reed *et al.*, 2008). Considering the upregulation of β -1,3-glucan synthase during *M. circinelloides* germination, and the potential increased efficacy of combination polyene-echinocandin therapy, further research into combination therapy in a clinical setting could offer a more effective approach to mucormycosis treatment than current recommendations.

In addition to the upregulation of genes associated with β -1,3-glucan biosynthesis, RNA-sequencing analysis highlighted several upregulated genes during *M. circinelloides* germination that

are orthologous to *C. albicans* genes such as *BGL2* and *KRE5*. Such genes have been implicated in β -1,3- β -1,6-glucan linkage formation, suggesting β -1,3- β -1,6- glucan crosslinking is upregulated during *M. circinelloides* germination. β -1,6-glucan linkages have not been identified in the mucormycete cell wall, however determination of β -1,6-glucan linkages could be useful in identifying novel targets for mucormycosis antifungals. An investigation that screened small compounds for antifungal activity identified a pyridobenzimidazole derivative, D75-4590, that targets β -1,6-glucan synthase Kre6p in *Saccharomyces cerevisiae* (Kitamura *et al.*, 2009). The β -1,6-glucan synthase inhibitor prevented *C. albicans* hyphal formation and displayed fungistatic properties against a range of fungal pathogens (Kitamura *et al.*, 2009). Considering this, investigation of β -1,6-glucan cell wall content in mucormycetes could offer a new target for antifungal drug design targeting mucormycosis.

RNA-sequencing analysis showed that during *M. circinelloides* germination, a plethora of genes implicated in glycosylation are upregulated. These include genes encoding mannosyltransferases and mannan polymerases. Genes were shown to be orthologous to *C. albicans* genes of the *ALG*, *GPI*, *MNN1*, *MNT* and *PMT* families, such as *GPI14*, *ALG6*, *MNN1*, *MNT3* and *PMT4*. Collectively, RNA-sequencing analysis indicated *N*-linked and *O*-linked glycosylation is upregulated during *M. circinelloides* spore swelling from resting state to fully swollen state. Determination of cell wall mannan by ConA-TRITC staining and flow cytometry supported the findings of RNA-sequencing analysis. Cell wall mannan significantly increases in *M. circinelloides* spores between resting (0 hr), mid-point (3 hr) and fully swollen (6 hr) stages of germination. Fluorescence microscopy showed staining to be patchy in fully swollen spores, suggesting mannan is not incorporated in the cell wall uniformly. Additionally, TEM showed 6 hr spores have a dense, patchy outer layer, which could explain the patchy staining of ConA-TRITC noted. Considering cell wall mannan is upregulated from the initiation of germination through to maximal spore swelling stage, and that spores across all stages display mannan in their cell walls, it offers an attractive cell wall target for antifungal drug design combatting mucormycosis. Currently there are no approved mannoprotein-targeting antifungals for clinical use, however research has identified several promising prospects. These include, gepinacin, a

monocarboxylic acid amide that targets Gwt1 (McLellan *et al.*, 2012). Gwt1 catalyses the inositol acylation of GlcN-PI prior to the addition of mannose residues during GPI biosynthesis (Pittet and Conzelmann, 2007). Gepinacin has been shown to inhibit the growth of *C. albicans* and unmask cell wall β -glucan (McLellan *et al.*, 2012). Furthermore, β -glucan unmasking resulted in increased release of the pro-inflammatory cytokine TNF- α in response to gepinacin-treated *C. albicans*, offering a desirable knock on effect of the GPI synthesis targeting molecule. Considering this, mannoproteins may be a desirable cell wall target in the design of novel antifungals against mucormycosis.

In summary, the *M. circinelloides* spore cell wall displays dynamic cell wall remodelling during the spore swelling stages of germination. Increases in cell wall mannan, chitin and β -1,3-glucan are noted during the germination of *M. circinelloides* spores. The current recommended antifungal approach to mucormycosis treatment is through the use of L-AMB, targeting plasma membrane ergosterol, however this has low efficacy against this fatal invasive fungal infection. Here we highlight several components of the *M. circinelloides* cell wall that may offer more attractive targets in the design of novel antifungal drug design against mucormycetes.

6.3 ENHANCING OUR UNDERSTANDING OF THE INTERACTION BETWEEN *M. CIRCINELLOIDES* AND MACROPHAGES

The inefficiency of phagocytes to clear mucormycete spores, enables the fungal pathogen to persist and germinate, resulting in angioinvasion, dissemination and tissue necrosis. The ability of mucormycetes to evade phagocytic killing underlies their pathogenic success. Enhancing our understanding of Mucorales-macrophage interaction is necessary to decipher how this invasive fungal pathogen is able to circumvent the usually robust clearance mechanisms of this innate immune cell, and could prove fruitful in the design of novel therapeutic strategies. Considering the evident changes in the *Mucor* cell wall, the influence of spore developmental stage on macrophage interaction was investigated.

M. circinelloides spore developmental stage was shown to influence phagocytic uptake by macrophages. Interestingly, resting (0 hr) and fully swollen (6 hr) spores are readily phagocytosed, but to a significantly lesser degree than spores at the mid-point (3 hr) of swelling. Macrophage interaction of fungi is mediated by PPR interaction with fungal PAMPs. When considering the compositional changes in the germinating *M. circinelloides* spore cell wall, the differences in phagocytic uptake seen between germinating spores may be due to changes in *M. circinelloides* surface exposed PAMPs during germination. Cell wall staining showed cell wall mannan, β -1,3-glucan and chitin increase during spore swelling. A possible explanation for the increased uptake of 3 hr spores compared to resting spores could be that the outer melanin layer of resting spores is shed, exposing the inner cell wall. This unmasking of the cell wall could expose a range of *M. circinelloides* cell wall PAMPs, such as mannan and β -glucan. When considering cell wall staining, data showed that β -1,3-glucan content in 3 hr spores only increases marginally in comparison to resting spores, whilst mannan content increases significantly. Fungal mannan is recognised by macrophage mannose receptors, including DC-SIGN and Dectin-2 (Vendele *et al.*, 2020). It is plausible that the increase in cell wall mannan of swollen spores, results in increased recognition and uptake via mannose receptors. To pursue this hypothesis, the effect of inhibiting mannose receptors on *M. circinelloides* phagocytosis was investigated. Inhibiting mannose receptors by exogenous fungal mannan prior to fungal exposure, significantly decreases spore uptake. Here data suggests that mannose receptors play a key role in mediating *M. circinelloides* phagocytosis. Mannose receptors, DC-SIGN and Dectin-2 have been shown to play a pivotal role in the clearance of invasive fungal infections. Single nucleotide polymorphisms (SNPs) in mannose binding lectin, DC-SIGN, is associated with increased susceptibility to invasive pulmonary aspergillosis, and similarly SNPs in Dectin-2 has been associated with increased susceptibility to pulmonary cryptococcosis (Sainz *et al.*, 2012, Hu *et al.*, 2015). There are currently no associations with SNPs of PRRs and mucormycosis, however investigation of genetic polymorphisms could determine populations at increased risk to mucormycosis.

Increased phagocytic uptake of swollen spores, is coupled with a decrease in viability post-phagocytosis. Resting spores are seemingly resistant to macrophage killing and display high viability following up to 18 hr phagocytosis, however, 3 hr spores are less viable than resting spores, and 6 hr spores less than 3 hr spores. This indicates that spore developmental stage influences spore viability post-phagocytosis. Furthermore, increased periods of phagocytosis, displays a further decline in spore viability, suggesting the macrophage environment is not favourable to swollen *M. circinelloides* spore survival. Although there are no reports on macrophage spore killing efficacy of swollen mucormycete spores, the efficacy of macrophage killing on swollen conidia of filamentous fungi *A. fumigatus* has been reported (Phillippe *et al.*, 2003). Swollen conidia are shown to be more susceptible to macrophage killing than resting conidia, which is correlated with an increase in macrophages reactive oxygen intermediate production (Philippe *et al.*, 2003). Considering this, a plausible explanation for the reduced viability of 3 hr and 6 hr *M. circinelloides* spores, is an increased production of reactive oxygen species in response to swollen spores. However, this was not shown and phagosome maturation was absent in response to live 0, 3 and 6 hr spores, whilst heat-killed spores triggered phagosome maturation. This could indicate *M. circinelloides* spores inhibit phagosome maturation, in a similar fashion to *C. neoformans*, which has been shown to arrest phagosome maturation through the premature removal of early phagosome markers Rab5 and Rab7, and to *Rhizopus oryzae*, which arrests phagosome maturation through the impairment of Rab5 recruitment to the phagosome (Smith *et al.*, 2014, Andrianaki *et al.*, 2018).

In summary, *M. circinelloides* spore developmental stage influences spore-macrophage interaction and the efficacy of phagocytic killing. Swollen spores are phagocytosed more readily than resting spores, whilst being more susceptible to phagocytic killing. The underlying mechanisms facilitating *M. circinelloides*-macrophage interaction have not been reported. However, here data shows mannose receptors play a key role in *M. circinelloides* spore phagocytosis. As spore cell wall mannan content increases during germination, this could be at a detriment to *M. circinelloides*. Increasing mannan exposure is likely driving increased uptake of spores through mannose receptors,

seemingly placing swollen spores in an environment where they are more susceptible to killing, although swollen spore viability is still relatively high post-phagocytosis, so perhaps this is a means of hijacking the macrophage for survival and dissemination. Additionally, live *M. circinelloides* spores appear to arrest phagosome maturation aiding their persistence within the phagosome. When considering the resistance of resting spores to phagocytic killing, investigating the mechanisms behind phagosome maturation arrest by *M. circinelloides* could enhance our understanding of how mucormycetes circumvent phagocytic killing.

6.4 ELUCIDATING THE PLATELET ACTIVATION PATHWAY IN RESPONSE TO *M. CIRCINELLOIDES*

M. circinelloides spores induce platelet aggregation in a spore developmental and dose-dependent manner. Resting (0 hr) spores induce mild aggregation, however, spores at the mid-point of maximal swelling (3 hr) induce platelet aggregation to a strikingly higher degree. Interestingly, platelet aggregation in response to fully swollen (6 hr) spores declines from that seen with 3 hr spores, and platelet aggregation in response to hyphae (48 hr) is negligible. Interestingly, previous research has shown platelet activation in response to mucormycetes spores and hyphae, although the study did not specify species. *M. circinelloides* spores are shown to induce platelet activation and aggregation, perhaps highlighting species and strain-specific differences in platelet activation potential. The distinct aggregation profile of *M. circinelloides* at different developmental stages has not been shown in other fungi. In fact, with the filamentous fungus *Aspergillus fumigatus*, platelet activation is significantly increased in response to hyphae compared to resting and swollen conidia (Rødland *et al.*, 2010). As the cell wall of *M. circinelloides* undergoes considerable compositional change during germination, this could explain the increased platelet aggregation in response to 3 hr spores compared with resting spores. As the resting spore loses the outer melanin layer upon initiating spore swelling, an inner layer comprised of glucan, mannan and chitin is exposed which may unmask ligands for platelet receptors, inducing their activation and aggregation. Chitin purified from the cell

wall of *C. albicans*, has been shown to impair platelet activation, aggregation and adhesion in response to *C. albicans*, and similarly *S. cerevisiae* β -1,3-glucan has been shown to impair platelet activation and decrease ATP release (Leroy *et al.*, 2019). Considering the inhibitory effects of chitin and glucan on platelet activation, it seems unlikely that these are the fungal ligands of *M. circinelloides* that are responsible for inducing platelet activation. The effect of mannan on platelets has not yet been reported, however when considering mannan content increases significantly during *M. circinelloides* spore germination, and that platelet aggregation is increased in response to swollen spores compared to resting spores, it offers a promising fungal ligand to investigate in the characterisation of platelet activation in response to mucormycetes.

To determine the platelet activation pathway in response to *M. circinelloides* spores, the roles of receptors known to mediate platelet activation in response to bacteria were investigated. Previous research shows platelet surface integrin α IIb β 3 and IgG receptor Fc γ RIIA are necessary for platelet activation in response to bacteria (Arman *et al.*, 2014). Furthermore, the activation of Fc γ RIIA is dependent upon IgG and α IIb β 3 interaction (Arman *et al.*, 2014). Platelet aggregation in response to *M. circinelloides* is also dependent upon platelet receptors α IIb β 3 and Fc γ RIIA, with the inhibition of both resulting in loss of aggregation in response to spores. Fc γ RIIA signals through Src and Syk tyrosine kinases, both shown to be crucial for bacterial-induced platelet aggregation (Arman *et al.*, 2014). Src and Syk are essential in platelet aggregation in response to *M. circinelloides* spores, with inhibition of these tyrosine kinases resulting in platelet inhibition. This agrees with previous research showing inhibition of Src and Syk tyrosine kinases results in the loss of platelet aggregation in response to bacteria (Arman *et al.*, 2014). The aggregation profile of *M. circinelloides* displays a pronounced lag phase suggesting secondary mediators may be required. Secondary mediators, such as TxA₂ and ADP, aid thrombus formation by means of a positive feedback loop whereby they recruit further platelets to the thrombus, and further generate their own release. TxA₂ and ADP inhibition significantly reduces platelet aggregation in response to *M. circinelloides*, suggesting secondary platelet mediators support *Mucor*-induced platelet aggregation. ADP and TxA₂ have been shown to support platelet aggregation

to bacteria also. Platelets are activated in response to *M. circinelloides* spores, with platelet surface expression levels of activation marker, P-selectin, increasing in response to spores under aggregating conditions. Additionally, surface integrin $\alpha\text{IIb}\beta\text{3}$ expression is also increased in response to *M. circinelloides* under aggregating conditions, indicative of α -granule release (Blair and Flaumenhaft, 2009).

In summary, *M. circinelloides* induces platelet activation in a dose-dependent manner and aggregation is dependent upon spore developmental age. The elucidation of the platelet activation pathway in response to *M. circinelloides* highlights a common pathway to platelet activation as seen in bacteria (Arman *et al.*, 2014). Aggregation is dependent on the activation of surface receptors, Fc γ RIIA and $\alpha\text{IIb}\beta\text{3}$, and downstream Src and Syk tyrosine kinases, supported by the secondary mediators ADP and TxA₂. The fungal ligand(s) of *M. circinelloides* spores that mediate platelet activation has yet to be determined, however based on previous research showing the platelet inhibitory effects of major fungal cell wall components chitin and β -1,3-glucan, mannan seems to be a promising cell wall component to investigate further.

6.5 LIMITATIONS

The use of RNA sequencing elucidated key processes that are differentially expressed during spore germination and highlighted numerous cell wall associated pathways. Initial analysis of DEGs resulted in a large proportion of uncharacterized and unspecified gene products, thus the genome of *C. albicans* was used as a reference genome. Whilst *C. albicans* ortholog analysis can indicate gene function, gene function has not been validated in *M. circinelloides*. Data could be more robust here by adding functional validity. For example, by creating gene knockout strains and investigating the effect of genetic manipulation on *M. circinelloides* function. Although gene knockout strains for *M. circinelloides* are not readily available and genetic mutation protocols for Mucorales are not well established, employment of these methods would be beneficial in determining gene function(s). Additionally, stringent parameters were applied to filter genes of interest ($P_{\text{adj}} \leq 0.05$ and Log2fold

change ≥ 1 (upregulated) or ≤ 1 (downregulated). Although this narrowed the genes of interest to highlight those that were most prominent, those falling outside these parameters would have been missed. Analysis with less stringent parameters could be employed to capture further differentially expressed genes that may be of interest.

TEM was employed to show differences in the spore body and cell wall architecture of *M. circinelloides* spores at different stages of germination. During the process of sample preparation, high-pressure freezing resulted fractured/damaged 3 hr spores that were not suitable for analysis, limiting the number of 3 hr spore samples available to just one. Optimization of the high-pressure freezing preparation of *M. circinelloides* spores is necessary to improve the quality of samples for TEM, and to increase the number of samples for analysis and integrity of analyses. Additionally, the identification of cell wall components could not be determined by TEM. Investigation of the cell wall architecture of *M. circinelloides* spores by TEM imaging would have been more fruitful had there been a more targeted approach employed, such as the use of HPLC/immunogold labelling for cell wall characterization.

The investigation of spore-macrophage interaction employed spore cell wall staining by ConA-TRITC. This method relied on the principle that ConA-TRITC cannot enter the macrophage and can only stain mannan found in external spores. A proof of principle assay such as spore staining prior to phagocytosis would be useful here to show that the J774A.1 cell membrane is impermeable to ConA-TRITC, and to add to the robustness of phagocytosis assay data. Competitive inhibition of mannose receptors by exogenous mannan was used to determine the role of mannose receptors in *M. circinelloides* phagocytosis. There are numerous mannose-binding receptors that are not decipherable in this method. A more targeted approach to determine the specific macrophage receptors recruited in spore phagocytosis would be beneficial. For example, by utilizing murine receptor knockout lines (Dectin-2^{-/-}, MR^{-/-}) or specific antibody blocking of receptors to determine their function in spore phagocytosis. The use of cytokine profiling would also have been useful in enhancing our understanding of *M. circinelloides*-macrophage interaction. The murine macrophage cell line J774A.1

is not best suited for this investigation as elicited cytokine profiles are weak and difficult to determine using standardising ELISA-based assays. Here, the use of human peripheral blood mononuclear cells to determine cytokine profiling upon spore exposure could be beneficial. Previous study of *R. microsporus* showed that spores contained a *R. pickettii* endosymbiont and that secreted activity induces an inhibitory effect on spore phagocytosis. Whilst data here indicates *M. circinelloides* spores are readily phagocytosed by macrophages, the presence or absence of *R. pickettii*, or the potential inhibitory effect of secreted activity was not investigated. The inhibitory potential of *M. circinelloides* spore swelling supernatant and determination of *R. pickettii* presence by means such as RNA-sequencing would be valuable in further elucidating the spore-macrophage interaction.

6.6 FUTURE PERSPECTIVES

This research enhances our current understanding of *M. circinelloides* germination and how spore development influences host interaction. The cell wall of the *M. circinelloides* spore at different stages of germination has been shown to display distinct ultrastructural profiles. RNA-sequencing highlighted the upregulation of genes associated with the synthesis of major fungal cell wall components, mannan, chitin and β -1,3-glucan. Additionally, the composition of the cell wall was shown to undergo significant changes as spores develop, with increases in mannan, β -1,3-glucan and chitin noted during germination. The current recommended antifungal approach is L-AMB monotherapy targeting fungal ergosterol, however efficacy is poor and mortality rates associated with mucormycosis are astonishingly high. Here, findings offer potentially novel drug targets that may enhance the efficacy of antifungal mucormycosis treatment. These may include chitin synthases and mannoproteins, which currently have no approved antifungals targeting them in clinical use. Additionally, based on our findings and supporting literature, the current guidelines around the use of echinocandins targeting β -1,3-glucan synthases in clinical practice could be considered for revision.

M. circinelloides spore development was shown to influence spore interaction with macrophages, whereby swollen spores are more readily phagocytosed by macrophages than resting spores. Additionally, mannose receptors were shown to mediate phagocytic uptake of *M. circinelloides*, and when considering the increase in cell wall mannan of swollen spores, these findings offer promising scope to develop our understanding of the mechanistic underpinnings of *M. circinelloides* phagocytosis. Enhanced exposure of cell wall mannan may result in swollen spores being more susceptible to phagocytosis and subsequent phagocytic killing. However, phagosome maturation is not triggered by *M. circinelloides* spores, and the viability of swollen spores is still fairly high. This could suggest the enhanced uptake of germinating spores aids their survival and dissemination, by providing them an environment in which they can persist. When considering the resistance of resting spores to phagocytic killing, investigating the mechanisms behind phagosome maturation arrest by *M. circinelloides* spores could would enhance our understanding of how mucormycetes circumvent phagocytic killing.

Investigation of platelet activation by *M. circinelloides* showed strong platelet aggregation in response to swollen *M. circinelloides* spores. The role of thrombosis in mucormycosis has not been determined, however, considering the induction of platelet aggregation by *M. circinelloides* spores and that thrombocytopenia is a known risk of mucormycosis, it may suggest excessive thrombosis is detrimental to infection prognosis. Here, the platelet activation pathway in response to *M. circinelloides* was elucidated and offers a potential target for novel therapeutic strategies. The fungal ligands of *M. circinelloides* mediating platelet activation are yet to be determined. Considering our findings on *M. circinelloides* spore cell wall composition and previous research that shows fungal cell wall chitin and β -1,3-glucan have inhibitory effects on platelet activation, investigating the role of cell wall mannan in *M. circinelloides*-induced platelet activation could also elucidate a target for therapeutic intervention.

REFERENCES

- Abeijon, C., & Chen, L. Y. (1998) The role of glucosidase I (Cwh41p) in the biosynthesis of cell wall β -1, 6-glucan is indirect. *Molecular biology of the cell*, 9(10), 2729-2738. doi:10.1091/mbc.9.10.2729
- Abo Elsoud, M.M. and El Kady, E.M. (2019) Current trends in fungal biosynthesis of chitin and chitosan. *Bulletin of the National Research Centre*, 43(1), pp.1-12
- Aebi, M. (2013) N-linked protein glycosylation in the ER. *Biochimica et Biophysica Acta (BBA)-Molecular Cell Research*, 1833(11), pp.2430-2437. doi: 10.1016/j.bbamcr.2013.04.001
- Afshar, P., Larijani, L.V. and Rouhanizadeh, H. (2018) A comparison of conventional rapid methods in diagnosis of superficial and cutaneous mycoses based on KOH, Chicago sky blue 6B and calcofluor white stains. *Iranian journal of microbiology*, 10(6), p.433.
- Ahmadikia, K., Hashemi, S.J., Khodavaisy, S., Getso, M.I., Alijani, N., Badali, H., Mirhendi, H., Salehi, M., Tabari, A., Mohammadi Ardehali, M. and Kord, M. (2021) The double-edged sword of systemic corticosteroid therapy in viral pneumonia: A case report and comparative review of influenza-associated mucormycosis versus COVID-19 associated mucormycosis. *Mycoses*, 64(8), pp.798-808. doi: 10.1111/myc.13256.
- Almyroudīs, N.G., Sutton, D.A., Linden, P., Rinaldi, M.G., Fung, J. and Kusne, S. (2006) Zygomycosis in solid organ transplant recipients in a tertiary transplant center and review of the literature. *American Journal of Transplantation*, 6(10), pp.2365-2374. doi: 10.1111/j.1600-6143.2006.01496.x.
- Ambrosio, A. L., & Di Pietro, S. M. (2017). Storage pool diseases illuminate platelet dense granule biogenesis. *Platelets*, 28(2), 138-146.
- Ambrosio, A.L., Boyle, J.A. and Di Pietro, S.M. (2012) Mechanism of platelet dense granule biogenesis: study of cargo transport and function of Rab32 and Rab38 in a model system. *Blood, The Journal of the American Society of Hematology*, 120(19), pp.4072-4081.
- Andrianaki, A.M., Kyrnizi, I., Thanopoulou, K., Baldin, C., Drakos, E., Soliman, S.S., Shetty, A.C., McCracken, C., Akoumianaki, T., Stylianou, K. and Ioannou, P. (2018). Iron restriction inside macrophages regulates pulmonary host defense against *Rhizopus* species. *Nature communications*, 9(1), pp.1-17. doi: 10.1038/s41467-018-05820-2.
- Aranjani, J.M., Manuel, A., Abdul Razack, H.I. and Mathew, S.T. (2021) COVID-19–associated mucormycosis: Evidence-based critical review of an emerging infection burden during the pandemic’s second wave in India. *PLoS neglected tropical diseases*, 15(11), p.e0009921. doi: 10.1371/journal.pntd.0009921.
- Arias, L.S., Butcher, M.C., Short, B., McKloud, E., Delaney, C., Kean, R., Monteiro, D.R., Williams, C., Ramage, G. and Brown, J.L. (2020) Chitosan ameliorates *Candida auris* virulence in a *Galleria mellonella* infection model. *Antimicrobial agents and chemotherapy*, 64(8), pp.e00476-20. doi: 10.1128/AAC.00476-20.

- Arman, M., Krauel, K., Tilley, D.O., Weber, C., Cox, D., Greinacher, A., Kerrigan, S.W. and Watson, S.P. (2014) Amplification of bacteria-induced platelet activation is triggered by FcγRIIA, integrin αIIbβ3, and platelet factor 4. *Blood, The Journal of the American Society of Hematology*, 123(20), pp.3166-3174. doi: 10.1182/blood-2013-11-540526. Epub 2014 Mar 18. PMID: 24642751; PMCID: PMC4023422.
- Arroyo, J., Farkaš, V., Sanz, A. B., & Cabib, E. (2016). Strengthening the fungal cell wall through chitin–glucan cross-links: effects on morphogenesis and cell integrity. *Cellular Microbiology*, 18(9), 1239-1250.
- Baltussen, T. J., Zoll, J., Verweij, P. E., & Melchers, W. J. (2020). Molecular mechanisms of conidial germination in *Aspergillus* spp. *Microbiology and Molecular Biology Reviews*, 84(1), e00049-19. doi: 10.1128/MMBR.00049-19.
- Bartnicki-Garcia, S. and Reyes, E. (1964) Chemistry of spore wall differentiation in *Mucor rouxii*. *Archives of Biochemistry and Biophysics*, 108(1), pp.125-133. doi: 10.1016/0003-9861(64)90363-7.
- Bartnicki-Garcia, S. and Reyes, E. (1968) Polyuronides in the cell walls of *Mucor rouxii*. *Biochimica et Biophysica Acta (BBA)-General Subjects*, 170(1), pp.54-62. doi: 10.1016/0304-4165(68)90160-8.
- Bates, S., Hall, R.A., Cheetham, J., Netea, M.G., MacCallum, D.M., Brown, A.J., Odds, F.C. and Gow, N.A. (2013) Role of the *Candida albicans* MNN1 gene family in cell wall structure and virulence. *BMC research notes*, 6(1), pp.1-9. <https://doi.org/10.1186/1756-0500-6-294>
- Bates, S., Hughes, H.B., Munro, C.A., Thomas, W.P., MacCallum, D.M., Bertram, G., Atrih, A., Ferguson, M.A., Brown, A.J., Odds, F.C. and Gow, N.A. (2006) Outer chain N-glycans are required for cell wall integrity and virulence of *Candida albicans*. *Journal of Biological Chemistry*, 281(1), pp.90-98. doi: 10.1074/jbc.M510360200.
- Bemena, L.D., Min, K., Konopka, J.B. and Neiman, A.M. (2021) A conserved machinery underlies the synthesis of a chitosan layer in the *Candida* chlamydospore cell wall. *Mosphere*, 6(2), pp.e00080-21.
- Benham, A.M. (2009) Protein folding and disulfide bond formation in the eukaryotic cell: Meeting report based on the presentations at the European Network Meeting on Protein Folding and Disulfide Bond Formation 2009 (Elsinore, Denmark). doi: 10.1111/j.1742-4658.2009.07409.x.
- Bertling, A., Niemann, S., Uekötter, A., Fegeler, W., Lass-Flörl, C., von Eiff, C. and Kehrel, B.E. (2010) *Candida albicans* and its metabolite gliotoxin inhibit platelet function via interaction with thiols. *Thrombosis and haemostasis*, 104(08), pp.270-278. doi: 10.1160/TH09-11-0769.
- Bigby, M., Jick, S., Jick, H. and Arndt, K. (1986) Drug-induced cutaneous reactions: a report from the Boston Collaborative Drug Surveillance Program on 15 438 consecutive inpatients, 1975 to 1982. *Jama*, 256(24), pp.3358-3363. doi: 10.1001/jama.256.24.3358.

Blair, P., & Flaumenhaft, R. (2009). Platelet α -granules: Basic biology and clinical correlates. *Blood reviews*, 23(4), 177-189.

Boelaert, J.R., Van Cutsem, J., de Locht, M., Schneider, Y.J. and Crichton, R.R. (1994) Deferoxamine augments growth and pathogenicity of *Rhizopus*, while hydroxypyridinone chelators have no effect. *Kidney international*, 45(3), pp.667-671. doi: 10.1038/ki.1994.89.

Bojang, E., Ghuman, H., Kumwenda, P. and Hall, R.A. (2021) Immune sensing of *Candida albicans*. *Journal of Fungi*, 7(2), p.119. doi: 10.3390/jof7020119.

Boone, C., Sommer, S. S., Hensel, A., & Bussey, H. (1990) Yeast KRE genes provide evidence for a pathway of cell wall β -glucan assembly. *The Journal of cell biology*, 110(5), 1833-1843.

Botet, J., Rodríguez-Mateos, M., Ballesta, J.P., Revuelta, J.L. and Remacha, M. (2008) A chemical genomic screen in *Saccharomyces cerevisiae* reveals a role for diphthamidation of translation elongation factor 2 in inhibition of protein synthesis by sordarin. *Antimicrobial agents and chemotherapy*, 52(5), pp.1623-1629

Boylan B., Gao C., Rathore V., Gill J.C., Newman D.K., Newman P.J. Identification of Fc γ RIIa as the ITAM-bearing receptor mediating α IIb β 3 outside-in integrin signaling in human platelets. *Blood*. 2008;112:2780–2786. doi: 10.1182/blood-2008-02-142125.

Bulawa, C. E., Miller, D. W., Henry, L. K., & Becker, J. M. (1995). Attenuated virulence of chitin-deficient mutants of *Candida albicans*. *Proceedings of the National Academy of Sciences*, 92(23), 10570-10574.

Burda, P. and Aebi, M. (1999) The dolichol pathway of N-linked glycosylation. *Biochimica et Biophysica Acta (BBA)-General Subjects*, 1426(2), pp.239-257. doi: 10.1016/s0304-4165(98)00127-5. PMID: 9878760.

Cagas, S.E., Jain, M.R., Li, H. and Perlin, D.S. (2011) The proteomic signature of *Aspergillus fumigatus* during early development. *Molecular & Cellular Proteomics*, 10(11) doi: 10.1074/mcp.M111.010108.

Camara-Lemarroy, C.R., González-Moreno, E.I., Rodríguez-Gutiérrez, R., Rendón-Ramírez, E.J., Ayala-Cortés, A.S., Fraga-Hernández, M.L., García-Labastida, L. and Galarza-Delgado, D.Á. (2014) Clinical features and outcome of mucormycosis. *Interdiscip Perspect Infect Dis*. 2014;2014:562610. doi: 10.1155/2014/562610.

Cambi, A., Netea, M.G., Mora-Montes, H.M., Gow, N.A., Hato, S.V., Lowman, D.W., Kullberg, B.J., Torensma, R., Williams, D.L. and Figdor, C.G. (2008) Dendritic cell interaction with *Candida albicans* critically depends on N-linked mannan. *Journal of Biological Chemistry*, 283(29), pp.20590-20599. doi: 10.1074/jbc.M709334200.

Campos-Takaki, G. M., & Dietrich, S. M. (2009). Characterization of cell walls from mucoralean fungi by biochemical composition, transmission electron microscopy and X-ray microanalysis. In *Current Research Topics In Applied Microbiology And Microbial Biotechnology* (pp. 121-125).

Cano, C. and Ruiz-Herrera, J. (1988) Developmental stages during the germination of *Mucor* sporangiospores. *Experimental mycology*, 12(1), pp.47-59. doi: 10.1016/0147-5975(88)90015-1

- Caron, E. and Hall, A. (1998) Identification of two distinct mechanisms of phagocytosis controlled by different Rho GTPases. *Science*, 282(5394), pp.1717-1721. doi: 10.1126/science.282.5394.1717. PMID: 9831565.
- Carroll, C.S., Grieve, C.L., Murugathasan, I., Bennet, A.J., Czekster, C.M., Liu, H., Naismith, J. and Moore, M.M. (2017) The rhizoferrin biosynthetic gene in the fungal pathogen *Rhizopus deleamar* is a novel member of the NIS gene family. *The international journal of biochemistry & cell biology*, 89, pp.136-146. doi: 10.1016/j.biocel.2017.06.005.
- Castellano, F., Chavrier, P., & Caron, E. (2001, December). Actin dynamics during phagocytosis. In *Seminars in immunology* (Vol. 13, No. 6, pp. 347-355). Academic Press.
- Chai, L.Y., Kullberg, B.J., Vonk, A.G., Warris, A., Cambi, A., Latgé, J.P., Joosten, L.A., van der Meer, J.W. and Netea, M.G. (2009). Modulation of Toll-like receptor 2 (TLR2) and TLR4 responses by *Aspergillus fumigatus*. *Infection and immunity*, 77(5), 2184-2192.
- Chakrabarti, A., Das, A., Mandal, J., Shivaprakash, M.R., George, V.K., Tarai, B., Rao, P., Panda, N., Verma, S.C. and Sakhuja, V. (2006) The rising trend of invasive zygomycosis in patients with uncontrolled diabetes mellitus. *Sabouraudia*, 44(4), pp.335-342. doi: 10.1080/13693780500464930.
- Chamilos, G., Ganguly, D., Lande, R., Gregorio, J., Meller, S., Goldman, W.E., Gilliet, M. and Kontoyiannis, D.P. (2010) Generation of IL-23 producing dendritic cells (DCs) by airborne fungi regulates fungal pathogenicity via the induction of TH-17 responses. *PloS one*, 5(9), p.e12955. doi: 10.1371/journal.pone.0012955.
- Chamilos, G., Lewis, R.E. and Kontoyiannis, D.P. (2008) Delaying amphotericin B-based frontline therapy significantly increases mortality among patients with hematologic malignancy who have zygomycosis. *Clinical Infectious Diseases*, 47(4), pp.503-509. doi: 10.1086/590004.
- Chen, X., Zhang, R., Takada, A., Iwatani, S., Oka, C., Kitamoto, T. and Kajiwarra, S. (2017) The role of Bgl2p in the transition to filamentous cells during biofilm formation by *Candida albicans*. *Mycoses*, 60(2), pp.96-103. doi: 10.1111/myc.12554.
- Chen, Y., Yuan, Y., & Li, W. (2018). Sorting machineries: how platelet-dense granules differ from α -granules. *Bioscience reports*, 38(5).
- Cornely, O.A., Alastruey-Izquierdo, A., Arenz, D., Chen, S.C., Dannaoui, E., Hochhegger, B., Hoenigl, M., Jensen, H.E., Lagrou, K., Lewis, R.E. and Mellinshoff, S.C. (2019) Global guideline for the diagnosis and management of mucormycosis: an initiative of the European Confederation of Medical Mycology in cooperation with the Mycoses Study Group Education and Research Consortium. *The Lancet infectious diseases*, 19(12), pp.e405-e421. doi: 10.1016/S1473-3099(19)30312-3.
- Walther, G., Wagner, L. and Kurzai, O. (2019) Updates on the taxonomy of Mucorales with an emphasis on clinically important taxa. *Journal of fungi*, 5(4), p.106. doi: 10.3390/jof5040106.
- Cortez, J., Gomes, B.C., Speidel, A., Peixoto, C., Selicka, E., Valente, C., Figueiredo, P. and Vieira, A. (2013) Mind the gap: Management of an emergent and threatening invasive fungal infection—a case report of rhino-orbital-cerebral and pulmonary mucormycosis. *Medical mycology case reports*, 2, pp.79-84. doi: 10.1016/j.mmcr.2013.02.008..

Corzo-León, D.E., Chora-Hernández, L.D., Rodríguez-Zulueta, A.P. and Walsh, T.J. (2018) Diabetes mellitus as the major risk factor for mucormycosis in Mexico: epidemiology, diagnosis, and outcomes of reported cases. *Medical mycology*, 56(1), pp.29-43. doi: 10.1093/mmy/myx017.

Daferner, M., Mensch, S., Anke, T. and Sterner, O. (1999) Hypoxysordarin, a new sordarin derivative from *Hypoxylon croceum*. *Zeitschrift für Naturforschung C*, 54(7-8), pp.474-480.

Dan, J.M., Kelly, R.M., Lee, C.K. and Levitz, S.M. (2008) Role of the mannose receptor in a murine model of *Cryptococcus neoformans* infection. *Infection and immunity*, 76(6), pp.2362-2367. doi: 10.1128/IAI.00095-08.

Dorsam, R.T. and Kunapuli, S.P. (2004) Central role of the P2Y₁₂ receptor in platelet activation. *The Journal of clinical investigation*, 113(3), pp.340-345

Douglas, C.M. (2001) Fungal β (1, 3)-D-glucan synthesis. *Sabouraudia*, 39(1), pp.55-66. doi: 10.1080/mmy.39.1.55.66.

Dutton, L.C., Nobbs, A.H., Jepson, K., Jepson, M.A., Vickerman, M.M., Aqeel Alawfi, S., Munro, C.A., Lamont, R.J. and Jenkinson, H.F. (2014) O-mannosylation in *Candida albicans* enables development of interkingdom biofilm communities. *MBio*, 5(2), pp.e00911-14. doi: 10.1128/mBio.00911-14.

Eisenman, H.C. and Casadevall, A. (2012) Synthesis and assembly of fungal melanin. *Applied microbiology and biotechnology*, 93(3), pp.931-940. doi: 10.1007/s00253-011-3777-2.

Eisenman, H.C., Mues, M., Weber, S.E., Frases, S., Chaskes, S., Gerfen, G. and Casadevall, A. (2007) *Cryptococcus neoformans* laccase catalyses melanin synthesis from both D- and L-DOPA. *Microbiology*, 153(12), pp.3954-3962. doi: 10.1099/mic.0.2007/011049-0.

Esher, S.K., Ost, K.S., Kohlbrenner, M.A., Pianalto, K.M., Telzrow, C.L., Campuzano, A., Nichols, C.B., Munro, C., Wormley Jr, F.L. and Alspaugh, J.A. (2018) Defects in intracellular trafficking of fungal cell wall synthases lead to aberrant host immune recognition. *PLoS pathogens*, 14(6), p.e1007126. doi: 10.1371/journal.ppat.1007126.

Esteban, A., Popp, M.W., Vyas, V.K., Strijbis, K., Ploegh, H.L. and Fink, G.R. (2011) Fungal recognition is mediated by the association of dectin-1 and galectin-3 in macrophages. *Proceedings of the National Academy of Sciences*, 108(34), pp.14270-14275. doi: 10.1073/pnas.1111415108.

Ferling, I., Dunn, J.D., Ferling, A., Soldati, T. and Hillmann, F. (2020) Conidial melanin of the human-pathogenic fungus *Aspergillus fumigatus* disrupts cell autonomous defenses in amoebae. *MBio*, 11(3), pp.e00862-20. doi: 10.1128/mBio.00862-20.

Ferwerda, G., Meyer-Wentrup, F., Kullberg, B.J., Netea, M.G. and Adema, G.J. (2008) Dectin-1 synergizes with TLR2 and TLR4 for cytokine production in human primary monocytes and macrophages. *Cellular microbiology*, 10(10), pp.2058-2066. doi: 10.1111/j.1462-5822.2008.01188.x.

Fonzi, W.A. (1999) PHR1 and PHR2 of *Candida albicans* encode putative glycosidases required for proper cross-linking of β -1, 3-and β -1, 6-glucans. *Journal of bacteriology*, 181(22), pp.7070-7079. doi:10.1128/JB.181.22.7070-7079.1999

Free, S.J. (2013) Fungal cell wall organization and biosynthesis. *Advances in genetics*, 81, pp.33-82. doi: 10.1016/B978-0-12-407677-8.00002-6.

Frost, D.J., Brandt, K., Capobianco, J. and Goldman, R. (1994) Characterization of (1, 3)- β -glucan synthase in *Candida albicans*: microsomal assay from the yeast or mycelial morphological forms and a permeabilized whole-cell assay. *Microbiology*, 140(9), pp.2239-2246. doi: 10.1099/13500872-140-9-2239. PMID: 7952175.

Gachhi, D.B. and Hungund, B.S., (1930) Two-phase extraction, characterization, and biological evaluation of chitin and chitosan from *Rhizopus oryzae*. *Journal of Applied Pharmaceutical Science*, 8(11), pp.116-122.

Garcia-Rubio, R., de Oliveira, H.C., Rivera, J. and Trevijano-Contador, N. (2020) The fungal cell wall: *Candida*, *Cryptococcus*, and *Aspergillus* species. *Frontiers in Microbiology*, p.2993.

Geib, E., Gressler, M., Viedernikova, I., Hillmann, F., Jacobsen, I.D., Nietzsche, S., Hertweck, C. and Brock, M. (2016) A non-canonical melanin biosynthesis pathway protects *Aspergillus terreus* conidia from environmental stress. *Cell chemical biology*, 23(5), pp.587-597. doi: 10.1016/j.chembiol.2016.03.014.

Geijer, C., Pirkov, I., Vongsangnak, W., Ericsson, A., Nielsen, J., Krantz, M. and Hohmann, S. (2012) Time course gene expression profiling of yeast spore germination reveals a network of transcription factors orchestrating the global response. *BMC genomics*, 13(1), pp.1-15. doi: 10.1186/1471-2164-13-554.

Gersuk, G.M., Underhill, D.M., Zhu, L. and Marr, K.A. (2006). Dectin-1 and TLRs permit macrophages to distinguish between different *Aspergillus fumigatus* cellular states. *The Journal of Immunology*, 176(6), pp.3717-3724. doi: 10.4049/jimmunol.176.6.3717.

Ghuman, H. and Voelz, K. (2017) Innate and adaptive immunity to mucorales. *Journal of Fungi*, 3(3), p.48. doi: 10.3390/jof3030048. PMID: 29371565; PMCID: PMC5715954.

Ghuman, H., Shepherd-Roberts, A., Watson, S., Zuidschewoude, M., Watson, S. P., & Voelz, K. (2019). *Mucor circinelloides* induces platelet aggregation through integrin α IIb β 3 and Fc γ RIIA. *Platelets*, 30(2), 256-263.

Golebiewska, E. M., & Poole, A. W. (2015). Platelet secretion: From haemostasis to wound healing and beyond. *Blood reviews*, 29(3), 153-162

Gómez-Gaviria, M., Vargas-Macías, A.P., García-Carnero, L.C., Martínez-Duncker, I. and Mora-Montes, H.M. (2021) Role of Protein Glycosylation in Interactions of Medically Relevant Fungi with the Host. *Journal of Fungi*, 7(10), p.875. doi:10.3390/jof7100875

Goto, M. (2007) Protein O-glycosylation in fungi: diverse structures and multiple functions. *Bioscience, biotechnology, and biochemistry*, 71(6), pp.1415-1427.

- Graham, L.M., Tsoni, S.V., Willment, J.A., Williams, D.L., Taylor, P.R., Gordon, S., Dennehy, K. and Brown, G.D. (2006) Soluble Dectin-1 as a tool to detect β -glucans. *Journal of immunological methods*, 314(1-2), pp.164-169. doi: 10.1016/j.jim.2006.05.013
- Griffin Jr, F.M., Griffin, J.A., Leider, J.E. and Silverstein, S.C. (1975) Studies on the mechanism of phagocytosis. I. Requirements for circumferential attachment of particle-bound ligands to specific receptors on the macrophage plasma membrane. *The Journal of experimental medicine*, 142(5), pp.1263-1282. doi: 10.1084/jem.142.5.1263.
- Hall, R.A. and Gow, N.A. (2013) Mannosylation in *Candida albicans*: role in cell wall function and immune recognition. *Molecular microbiology*, 90(6), pp.1147-1161. doi: 10.1111/mmi.12426.
- Hamada, K., Terashima, H., Arisawa, M., Yabuki, N. and Kitada, K. (1999) Amino acid residues in the ω -minus region participate in cellular localization of yeast glycosylphosphatidylinositol-attached proteins. *Journal of Bacteriology*, 181(13), pp.3886-3889. doi: 10.1128/JB.181.13.3886-3889.1999.
- Hammond, S.P., Bialek, R., Milner, D.A., Petschnigg, E.M., Baden, L.R. and Marty, F.M. (2011) Molecular methods to improve diagnosis and identification of mucormycosis. *Journal of Clinical Microbiology*, 49(6), pp.2151-2153. doi: 10.1128/JCM.00256-11.
- Hamzeh-Cognasse, H., Damien, P., Chabert, A., Pozzetto, B., Cognasse, F. and Garraud, O. (2015) Platelets and infections—complex interactions with bacteria. *Frontiers in immunology*, 6, p.82.
- Harrasser, N., Banke, I.J., Hauschild, M., Lenze, U., Prodinger, P.M., Toepfer, A., Peschel, C., von Eisenhart-Rothe, R., Ringshausen, I. and Verbeek, M. (2014) Clinical challenge: fatal mucormycotic osteomyelitis caused by *Rhizopus microsporus* despite aggressive multimodal treatment. *BMC Infectious Diseases*, 14(1), pp.1-6. doi: 10.1186/1471-2334-14-488.
- Hartland, R.P., Emerson, G.W. and Sullivan, P.A. (1991) A secreted β -glucan-branching enzyme from *Candida albicans*. *Proceedings of the Royal Society of London. Series B: Biological Sciences*, 246(1316), pp.155-160. doi: 10.1098/rspb.1991.0138. PMID: 1685240.
- Hassan, M.I.A. and Voigt, K. (2019) Pathogenicity patterns of mucormycosis: epidemiology, interaction with immune cells and virulence factors. *Medical mycology*, 57(Supplement_2), pp.S245-S256. doi: 10.1093/mmy/myz011.
- Hayward, C.P., Furmaniak-Kazmierczak, E., Cieutat, A.M., Moore, J.C., Bainton, D.F., Nesheim, M.E., Kelton, J.G. and Côté, G. (1995) Factor V is complexed with multimerin in resting platelet lysates and colocalizes with multimerin in platelet α -granules. *Journal of Biological Chemistry*, 270(33), pp.19217-19224.
- Heijnen, H. and Van der Sluijs, P. (2015) Platelet secretory behaviour: as diverse as the granules... or not?. *Journal of thrombosis and haemostasis*, 13(12), pp.2141-2151.
- Heinekamp, T., Thywißen, A., Macheleidt, J., Keller, S., Valiante, V. and Brakhage, A.A. (2013) *Aspergillus fumigatus* melanins: interference with the host endocytosis pathway and impact on virulence. *Frontiers in microbiology*, 3, p.440. doi: 10.3389/fmicb.2012.00440.

Henry, C., Fontaine, T., Heddergott, C., Robinet, P., Aïmanianda, V., Beau, R., Beauvais, A., Mouyna, I., Prevost, M.C., Fekkar, A. and Zhao, Y. (2016) Biosynthesis of cell wall mannan in the conidium and the mycelium of *Aspergillus fumigatus*. *Cellular microbiology*, 18(12), pp.1881-1891

Herrero, A.B., Magnelli, P., Mansour, M.K., Levitz, S.M., Bussey, H. and Abeijon, C. (2004) KRE5 gene null mutant strains of *Candida albicans* are avirulent and have altered cell wall composition and hypha formation properties. *Eukaryotic cell*, 3(6), pp.1423-1432. doi:10.1128/EC.3.6.1423-1432.2004

Herscovics, A. (1999) Processing glycosidases of *Saccharomyces cerevisiae*. *Biochimica et Biophysica Acta (BBA)-General Subjects*, 1426(2), pp.275-285. doi: 10.1016/s0304-4165(98)00129-9.

Herscovics, A. (1999). Importance of glycosidases in mammalian glycoprotein biosynthesis. *Biochimica et Biophysica Acta (BBA)-General Subjects*, 1473(1), 96-107.

Hewitt, G. and Korolchuk, V.I. (2017) Repair, reuse, recycle: the expanding role of autophagy in genome maintenance. *Trends in cell biology*, 27(5), pp.340-351. doi: 10.1016/j.tcb.2016.11.011.

Hiasa, M., Togawa, N., Miyaji, T., Omote, H., Yamamoto, A. and Moriyama, Y. (2014) Essential role of vesicular nucleotide transporter in vesicular storage and release of nucleotides in platelets. *Physiological Reports*, 2(6), p.e12034.

Hong, H. L., Lee, Y. M., Kim, T., Lee, J. Y., Chung, Y. S., Kim, M. N., Kim, S. H., Choi, S. H., Kim, Y. S., Woo, J. H., & Lee, S. O. (2013). Risk factors for mortality in patients with invasive mucormycosis. *Infection & chemotherapy*, 45(3), 292–298. <https://doi.org/10.3947/ic.2013.45.3.292>

Hrdlickova, R., Toloue, M. and Tian, B. (2017) RNA-Seq methods for transcriptome analysis. *Wiley Interdisciplinary Reviews: RNA*, 8(1), p.e1364.

Hu, X.P., Wang, R.Y., Wang, X., Cao, Y.H., Chen, Y.Q., Zhao, H.Z., Wu, J.Q., Weng, X.H., Gao, X.H., Sun, R.H. and Zhu, L.P. (2015) Dectin-2 polymorphism associated with pulmonary cryptococcosis in HIV-uninfected Chinese patients. *Medical mycology*, 53(8), pp.810-816.

Hynes, M.J., Murray, S.L., Khew, G.S. and Davis, M.A. (2008) Genetic analysis of the role of peroxisomes in the utilization of acetate and fatty acids in *Aspergillus nidulans*. *Genetics*, 178(3), pp.1355-1369. doi: 10.1534/genetics.107.085795.

Ibrahim, A.S., Gebermariam, T., Fu, Y., Lin, L., Hussein, M.I., French, S.W., Schwartz, J., Skory, C.D., Edwards, J.E. and Spellberg, B.J. (2007) The iron chelator deferasirox protects mice from mucormycosis through iron starvation. *The Journal of clinical investigation*, 117(9), pp.2649-2657. doi: 10.1172/JCI32338.

Ibrahim, A.S., Spellberg, B., Walsh, T.J. and Kontoyiannis, D.P. (2012) Pathogenesis of mucormycosis. *Clinical Infectious Diseases*, 54(suppl_1), pp.S16-S22. doi: 10.1097/QCO.0b013e3283165fd1.

Ibrahim, A.S., Spellberg, B., Walsh, T.J. and Kontoyiannis, D.P. (2012) Pathogenesis of mucormycosis. *Clinical Infectious Diseases*, 54(suppl_1), pp.S16-S22. doi: 10.1093/cid/cir865.

Ibrahim, A. S., & Voelz, K. (2017). The mucormycete–host interface. *Current opinion in microbiology*, 40, 40-45.

Ibrahim, A. S., Bowman, J. C., Avanesian, V., Brown, K., Spellberg, B., Edwards Jr, J. E., & Douglas, C. M. (2005). Caspofungin inhibits *Rhizopus oryzae* 1, 3- β -D-glucan synthase, lowers burden in brain measured by quantitative PCR, and improves survival at a low but not a high dose during murine disseminated zygomycosis. *Antimicrobial agents and chemotherapy*, 49(2), 721-727

Inglesfield, S., Jasiulewicz, A., Hopwood, M., Tyrrell, J., Youlden, G., Mazon-Moya, M., Millington, O. R., Mostowy, S., Jabbari, S., & Voelz, K. (2018). Robust Phagocyte Recruitment Controls the Opportunistic Fungal Pathogen *Mucor circinelloides* in Innate Granulomas In Vivo. *mBio*, 9(2), e02010-17. <https://doi.org/10.1128/mBio.02010-17>

Inoue, S. B., N. Takewaki, T. Takasuka, T. Mio, M. Adachi, Y. Fujii, C. Miyamoto, M. Arisawa, Y. Furuichi, and T. Watanabe. (1995) Characterization and gene cloning of 1,3--D-glucan synthase from *Saccharomyces cerevisiae*. *Eur. J. Biochem.* 231:845–854.

Inoue, S.B., Qadota, H., Arisawa, M., Anraku, Y., Watanabe, T. and Ohya, Y. (1996) Signaling toward yeast 1, 3- β -glucan synthesis. *Cell structure and function*, 21(5), pp.395-402. doi: 10.1247/csf.21.395.

Itabangi, H., Sephton-Clark, P.C., Tamayo, D.P., Zhou, X., Starling, G.P., Mahamoud, Z., Insua, I., Probert, M., Correia, J., Moynihan, P.J. and Gebremariam, T. (2022) A bacterial endosymbiont of the fungus *Rhizopus microsporus* drives phagocyte evasion and opportunistic virulence. *Current Biology*, 32(5), pp.1115-1130

Italiano Jr, J.E., Richardson, J.L., Patel-Hett, S., Battinelli, E., Zaslavsky, A., Short, S., Ryeom, S., Folkman, J. and Klement, G.L. (2008) Angiogenesis is regulated by a novel mechanism: pro-and antiangiogenic proteins are organized into separate platelet α granules and differentially released. *Blood, The Journal of the American Society of Hematology*, 111(3), pp.1227-1233.

Jackson, R.J., Hellen, C.U. and Pestova, T.V. (2010) The mechanism of eukaryotic translation initiation and principles of its regulation. *Nature reviews Molecular cell biology*, 11(2), pp.113-127. doi: 10.1038/nrm2838.

Jantzen, H.M., Gousset, L., Bhaskar, V., Vincent, D., Tai, A., Reynolds, E.E. and Conley, P.B. (1999) Evidence for two distinct G-protein-coupled ADP receptors mediating platelet activation. *Thrombosis and haemostasis*, 81(01), pp.111-117.

Jeong, W., Keighley, C., Wolfe, R., Lee, W.L., Slavin, M.A., Kong, D.C.M. and Chen, S.A. (2019) The epidemiology and clinical manifestations of mucormycosis: a systematic review and meta-analysis of case reports. *Clinical Microbiology and Infection*, 25(1), pp.26-34. doi: 10.1016/j.cmi.2018.07.011.

Jin, C. (2012) Protein glycosylation in *Aspergillus fumigatus* is essential for cell wall synthesis and serves as a promising model of multicellular eukaryotic development. *International Journal of Microbiology*, 2012. doi: 10.1155/2012/654251

Jouault, T., Ibata-Ombetta, S., Takeuchi, O., Trinel, P.A., Sacchetti, P., Lefebvre, P., Akira, S. and Poulain, D. (2003) *Candida albicans* phospholipomannan is sensed through toll-like receptors. *The Journal of infectious diseases*, 188(1), pp.165-172. doi: 10.1086/375784.

Juchimiuk, M., Kruszewska, J. and Palamarczyk, G. (2015) Dolichol phosphate mannose synthase from the pathogenic yeast *Candida albicans* is a multimeric enzyme. *Biochimica et Biophysica Acta (BBA)-General Subjects*, 1850(11), pp.2265-2275. doi: 10.1016/j.bbagen.2015.08.012.

Kanayama, M. and Shinohara, M.L. (2016) Roles of autophagy and autophagy-related proteins in antifungal immunity. *Frontiers in immunology*, 7, p.47. doi: 10.3389/fimmu.2016.00047.

Kannan, K., Divers, S.G., Lurie, A.A., Chervenak, R., Fukuda, M. and Holcombe, R.F. (1995) Cell surface expression of lysosome-associated membrane protein-2 (lamp2) and CD63 as markers of in vivo platelet activation in malignancy. *European journal of haematology*, 55(3), pp.145-151.

Kappel, L., Münsterkötter, M., Sipos, G., Escobar Rodriguez, C. and Gruber, S. (2020) Chitin and chitosan remodeling defines vegetative development and Trichoderma biocontrol. *PLoS pathogens*, 16(2), p.e1008320. doi: 10.1371/journal.ppat.1008320.

Kapteyn, J. C., Van Den Ende, H., & Klis, F. M. (1999). The contribution of cell wall proteins to the organization of the yeast cell wall. *Biochimica et Biophysica Acta (BBA)-General Subjects*, 1426(2), 373-383.

Kerrigan, S.W., Douglas, I., Wray, A., Heath, J., Byrne, M.F., Fitzgerald, D. and Cox, D. (2002) A role for glycoprotein Ib in *Streptococcus sanguis*-induced platelet aggregation. *Blood, The Journal of the American Society of Hematology*, 100(2), pp.509-516.

Khan, I.A., Lu, J.P., Liu, X.H., Rehman, A. and Lin, F.C. (2012) Multifunction of autophagy-related genes in filamentous fungi. *Microbiological research*, 167(6), pp.339-345. doi: 10.1016/j.micres.2012.01.004.

Kikuma, T., Ohneda, M., Arioka, M. and Kitamoto, K. (2006) Functional analysis of the ATG8 homologue Ao atg8 and role of autophagy in differentiation and germination in *Aspergillus oryzae*. *Eukaryotic cell*, 5(8), pp.1328-1336. doi: 10.1128/EC.00024-06.

Kitamura, A., Someya, K., Hata, M., Nakajima, R. and Takemura, M. (2009) Discovery of a small-molecule inhibitor of β -1, 6-glucan synthesis. *Antimicrobial agents and chemotherapy*, 53(2), pp.670-677

Kollár, R., Reinhold, B.B., Petráková, E., Yeh, H.J., Ashwell, G., Drgonová, J., et al (1997) Architecture of the yeast cell wall. β (1 \rightarrow 6)-glucan interconnects mannoprotein, β (1 \rightarrow 3)-glucan, and chitin. *J Biol Chem* 272: 17762–17775.

Kousser, C., Clark, C., Sherrington, S., Voelz, K., & Hall, R. A. (2019). *Pseudomonas aeruginosa* inhibits *Rhizopus microsporus* germination through sequestration of free environmental iron. *Scientific reports*, 9(1), 1-14. doi: 10.1038/s41598-019-42175-0.

- Kraibooj, K., Park, H.R., Dahse, H.M., Skerka, C., Voigt, K. and Figge, M.T. (2014) Virulent strain of *Lichtheimia corymbifera* shows increased phagocytosis by macrophages as revealed by automated microscopy image analysis. *Mycoses*, 57, pp.56-66. doi: 10.1111/myc.12237
- Lamarre, C., Sokol, S., Debeaupuis, J.P., Henry, C., Lacroix, C., Glaser, P., Coppée, J.Y., François, J.M. and Latgé, J.P. (2008) Transcriptomic analysis of the exit from dormancy of *Aspergillus fumigatus* conidia. *BMC genomics*, 9(1), pp.1-15. doi: 10.1186/1471-2164-9-417.
- Lanternier, F., Poiree, S., Elie, C., Garcia-Hermoso, D., Bakouboula, P., Sitbon, K., Herbrecht, R., Wolff, M., Ribaud, P., Lortholary, O. and French Mycosis Study Group (2015) Prospective pilot study of high-dose (10 mg/kg/day) liposomal amphotericin B (L-AMB) for the initial treatment of mucormycosis. *Journal of Antimicrobial Chemotherapy*, 70(11), pp.3116-3123. doi: 10.1093/jac/dkv236.
- Lanternier, F., Dannaoui, E., Morizot, G., Elie, C., Garcia-Hermoso, D., Huerre, M., Bitar, D., Dromer, F., Lortholary, O. and French Mycosis Study Group (2012) A global analysis of mucormycosis in France: the RetroZygo Study (2005–2007). *Clinical Infectious Diseases*, 54(suppl_1), pp.S35-S43.
- Lass-Flörl, C. (2009) Zygomycosis: conventional laboratory diagnosis. *Clinical Microbiology and Infection*, 15, pp.60-65. doi: 10.1111/j.1469-0691.2009.02999.x.
- Lecointe, K., Cornu, M., Leroy, J., Coulon, P. and Sendid, B. (2019). Polysaccharides cell wall architecture of Mucorales. *Frontiers in microbiology*, 10, p.469. doi: 10.3389/fmicb.2019.00469.
- Lee, H.J., Ko, H.J., Song, D.K. and Jung, Y.J. (2018) Lysophosphatidylcholine promotes phagosome maturation and regulates inflammatory mediator production through the protein kinase a–phosphatidylinositol 3 kinase–p38 mitogen-activated protein kinase signaling pathway during mycobacterium tuberculosis infection in mouse macrophages. *Frontiers in immunology*, 9, p.920. doi: 10.3389/fimmu.2018.00920.
- Lee, H.J., Woo, Y., Hahn, T.W., Jung, Y.M. and Jung, Y.J. (2020) Formation and maturation of the phagosome: a key mechanism in innate immunity against intracellular bacterial infection. *Microorganisms*, 8(9), p.1298. doi: 10.3390/microorganisms8091298. PMID: 32854338; PMCID: PMC7564318.
- Lee S.C., Li A., Calo S., Heitman J. (2013) Calcineurin plays key roles in the dimorphic transition and virulence of the human pathogenic zygomycete *Mucor circinelloides*. *PLoS Pathog.* 9(9):e1003625. doi: 10.1371/journal.ppat.1003625. Epub 2013 Sep 5. PMID: 24039585; PMCID: PMC3764228.
- Lenardon, M.D., Munro, C.A. and Gow, N.A. (2010) Chitin synthesis and fungal pathogenesis. *Current opinion in microbiology*, 13(4), pp.416-423. doi:10.1016/j.mib.2010.05.002
- Levitz, S.M., Selsted, M.E., Ganz, T., Lehrer, R.I. and Diamond, R.D. (1986) In vitro killing of spores and hyphae of *Aspergillus fumigatus* and *Rhizopus oryzae* by rabbit neutrophil cationic peptides and bronchoalveolar macrophages. *Journal of Infectious Diseases*, 154(3), pp.483-489.

- Li, C.H., Cervantes, M., Springer, D.J., Boekhout, T., Ruiz-Vazquez, R.M., Torres-Martinez, S.R., Heitman, J. and Lee, S.C. (2011) Sporangiospore size dimorphism is linked to virulence of *Mucor circinelloides*. *PLoS Pathogens*, 7(6), p.e1002086. doi: 10.1371/journal.ppat.1002086.
- Liu, M., Spellberg, B., Phan, Q.T., Fu, Y., Fu, Y., Lee, A.S., Edwards, J.E., Filler, S.G. and Ibrahim, A.S. (2010) The endothelial cell receptor GRP78 is required for mucormycosis pathogenesis in diabetic mice. *The Journal of clinical investigation*, 120(6), pp.1914-1924. doi: 10.1172/JCI42164.
- Lo, R. W., Li, L., Leung, R., Pluthero, F. G., & Kahr, W. H. (2018). NBEAL2 (Neurobeachin-Like 2) is required for retention of cargo proteins by α -granules during their production by megakaryocytes. *Arteriosclerosis, thrombosis, and vascular biology*, 38(10), 2435-2447.
- López-Fernández, L., Sanchis, M., Navarro-Rodríguez, P., Nicolás, F.E., Silva-Franco, F., Guarro, J., Garre, V., Navarro-Mendoza, M.I., Pérez-Arques, C. and Capilla, J., 2018. Understanding *Mucor circinelloides* pathogenesis by comparative genomics and phenotypical studies. *Virulence*, 9(1), pp.707-720. doi: 10.1080/21505594.2018.1435249.
- Lourbakos, A., Potempa, J., Travis, J., D'Andrea, M.R., Andrade-Gordon, P., Santulli, R., Mackie, E.J. and Pike, R.N. (2001) Arginine-specific protease from *Porphyromonas gingivalis* activates protease-activated receptors on human oral epithelial cells and induces interleukin-6 secretion. *Infection and immunity*, 69(8), pp.5121-5130.
- Loures, F.V., Röhm, M., Lee, C.K., Santos, E., Wang, J.P., Specht, C.A., Calich, V.L., Urban, C.F. and Levitz, S.M. (2015) Recognition of *Aspergillus fumigatus* hyphae by human plasmacytoid dendritic cells is mediated by dectin-2 and results in formation of extracellular traps. *PLoS pathogens*, 11(2), p.e1004643. doi: 10.1371/journal.ppat.1004643.
- Lu, X.L., Najafzadeh, M.J., Dolatabadi, S., Ran, Y.P., Gerrits van den Ende, A.H.G., Shen, Y.N., Li, C.Y., Xi, L.Y., Hao, F., Li, R.Y. and Hu, Z.M. (2013) Taxonomy and epidemiology of *Mucor irregularis*, agent of chronic cutaneous mucormycosis. *Persoonia-Molecular Phylogeny and Evolution of Fungi*, 30(1), pp.48-56. doi: 10.3767/003158513X665539.
- Maertens, J., Demuyne, H., Verbeken, E.K., Zachee, P., Verhoef, G.E.G., Vandenberghe, P. and Boogaerts, M.A. (1999) Mucormycosis in allogeneic bone marrow transplant recipients: report of five cases and review of the role of iron overload in the pathogenesis. *Bone marrow transplantation*, 24(3), pp.307-312. doi: 10.1038/sj.bmt.1701885.
- Manzoni, L., Zucal, C., Maio, D.D., D'Agostino, V.G., Thongon, N., Bonomo, I., Lal, P., Miceli, M., Baj, V., Brambilla, M. and Cerofolini, L. (2018) Interfering with HuR-RNA interaction: design, synthesis and biological characterization of tanshinone mimics as novel, effective HuR inhibitors. *Journal of medicinal chemistry*, 61(4), pp.1483-1498
- Marty, F.M., Ostrosky-Zeichner, L., Cornely, O.A., Mullane, K.M., Perfect, J.R., Thompson 3rd, G.R., Alangaden, G.J., Brown, J.M., Fredricks, D.N. and Heinz, W.J. (2016) VITAL and FungiScope Mucormycosis Investigators Isavuconazole treatment for mucormycosis: a single-arm open-label trial and case-control analysis. *Lancet Infect Dis*, 16(7), pp.828-837. doi: 10.1016/S1473-3099(16)00071-2.
- May, R. C., Caron, E., Hall, A., & Machesky, L. M. (2000). Involvement of the Arp2/3 complex in phagocytosis mediated by Fc γ R or CR3. *Nature cell biology*, 2(4), 246-248.

- McLellan, C.A., Whitesell, L., King, O.D., Lancaster, A.K., Mazitschek, R. and Lindquist, S. (2012) Inhibiting GPI anchor biosynthesis in fungi stresses the endoplasmic reticulum and enhances immunogenicity. *ACS chemical biology*, 7(9), pp.1520-1528.
- Medwid, R.D. and Grant, D.W. (1984) Germination of *Rhizopus oligosporus* sporangiospores. *Applied and environmental microbiology*, 48(6), pp.1067-1071. doi: 10.1128/aem.48.6.1067-1071.1984.
- Meng, R., Wu, J., Harper, D.C., Wang, Y., Kowalska, M.A., Abrams, C.S., Brass, L.F., Poncz, M., Stalker, T.J. and Marks, M.S. (2015) Defective release of α granule and lysosome contents from platelets in mouse Hermansky-Pudlak syndrome models. *Blood, The Journal of the American Society of Hematology*, 125(10), pp.1623-1632.
- Miajlovic, H., Zapotoczna, M., Geoghegan, J.A., Kerrigan, S.W., Speziale, P. and Foster, T.J. (2010) Direct interaction of iron-regulated surface determinant IsdB of *Staphylococcus aureus* with the GPIIb/IIIa receptor on platelets. *Microbiology*, 156(3), pp.920-928.
- Mio, T., Adachi-Shimizu, M., Tachibana, Y., Tabuchi, H., Inoue, S.B., Yabe, T., Yamada-Okabe, T., Arisawa, M., Watanabe, T. and Yamada-Okabe, H. (1997) Cloning of the *Candida albicans* homolog of *Saccharomyces cerevisiae* GSC1/FKS1 and its involvement in beta-1, 3-glucan synthesis. *Journal of Bacteriology*, 179(13), pp.4096-4105. doi: 10.1128/jb.179.13.4096-4105.1997.
- Mohammadi, R., Nazeri, M., Sayedayn, S.M.A. and Ehteram, H. (2014) A successful treatment of rhinocerebral mucormycosis due to *Rhizopus oryzae*. *Journal of research in medical sciences: the official journal of Isfahan University of Medical Sciences*, 19(1), p.72.
- Mora-Montes, H.M., Bates, S., Netea, M.G., Castillo, L., Brand, A., Buurman, E.T., Díaz-Jiménez, D.F., Kullberg, B.J., Brown, A.J., Odds, F.C. and Gow, N.A. (2010) A multifunctional mannosyltransferase family in *Candida albicans* determines cell wall mannan structure and host-fungus interactions. *Journal of Biological Chemistry*, 285(16), pp.12087-12095. doi:10.1074/jbc.M109.081513
- Mora-Montes, H. M., Bates, S., Netea, M. G., Díaz-Jiménez, D. F., López-Romero, E., Zinker, S., ... & Gow, N. A. (2007). Endoplasmic reticulum α -glycosidases of *Candida albicans* are required for N glycosylation, cell wall integrity, and normal host-fungus interaction. *Eukaryotic cell*, 6(12), 2184-2193.
- Mora-Montes, H. M., Netea, M. G., Ferwerda, G., Lenardon, M. D., Brown, G. D., Mistry, A. R., ... & Gow, N. A. (2011). Recognition and blocking of innate immunity cells by *Candida albicans* chitin. *Infection and immunity*, 79(5), 1961-1970.
- Mougeot, J.C., Stevens, C.B., Paster, B.J., Brennan, M.T., Lockhart, P.B. and Mougeot, F.B. (2017) *Porphyromonas gingivalis* is the most abundant species detected in coronary and femoral arteries. *Journal of oral microbiology*, 9(1), p.1281562.
- Munro, C.A. and Gow, N.A.R. (2001) Chitin synthesis in human pathogenic fungi. *Medical mycology*, 39(1), pp.41-53

Munro, C.A., Schofield, D.A., Gooday, G.W. and Gow, N.A.R. (1998) Regulation of chitin synthesis during dimorphic growth of *Candida albicans*. *Microbiology*, 144(2), pp.391-401.

Nakamura, K., Miyazato, A., Xiao, G., Hatta, M., Inden, K., Aoyagi, T., Shiratori, K., Takeda, K., Akira, S., Saijo, S. and Iwakura, Y. (2008) Deoxynucleic acids from *Cryptococcus neoformans* activate myeloid dendritic cells via a TLR9-dependent pathway. *The Journal of Immunology*, 180(6), pp.4067-4074. doi: 10.4049/jimmunol.180.6.4067.

Netea, M.G., Brown, G.D., Kullberg, B.J. and Gow, N.A. (2008) An integrated model of the recognition of *Candida albicans* by the innate immune system. *Nature Reviews Microbiology*, 6(1), pp.67-78. <https://doi.org/10.1038/nrmicro1815>

Ngamskulrungron, P., Price, J., Sorrell, T., Perfect, J.R. and Meyer, W. (2011) *Cryptococcus gattii* virulence composite: candidate genes revealed by microarray analysis of high and less virulent Vancouver Island outbreak strains. *PloS one*, 6(1), p.e16076. doi: 10.1371/journal.pone.0016076.

Nishibori, M., Cham, B., McNicol, A., Shalev, A., Jain, N. and Gerrard, J.M. (1993) The protein CD63 is in platelet dense granules, is deficient in a patient with Hermansky-Pudlak syndrome, and appears identical to granulophysin. *The Journal of clinical investigation*, 91(4), pp.1775-1782.

Nosanchuk, J.D., Stark, R.E. and Casadevall, A. (2015) Fungal melanin: what do we know about structure?. *Frontiers in microbiology*, 6, p.1463. doi: 10.3389/fmicb.2015.01463.

Nurden, A. T. (2018). The biology of the platelet with special reference to inflammation, wound healing and immunity. *Front Biosci (Landmark Ed)*, 23(2), 726-751.

Nurden, P., Jandrot-Perrus, M., Combri  , R., Winckler, J., Aroc  s, V., Lecut, C., Pasquet, J.M., Kunicki, T.J. and Nurden, A.T. (2004) Severe deficiency of glycoprotein VI in a patient with gray platelet syndrome. *Blood*, 104(1), pp.107-114.

Obergfell A., Eto K., Mocsai A., Buensuceso C., Moores S.L., Brugge J.S., Lowell C.A., Shattil S.J. Coordinate interactions of Csk, Src, and Syk kinases with $\alpha\text{IIb}\beta\text{3}$ initiate integrin signaling to the cytoskeleton. *J. Cell Biol.* 2002;157:265–275. doi: 10.1083/jcb.200112113.

Offermanns, S. (2006) Activation of platelet function through G protein–coupled receptors. *Circulation research*, 99(12), pp.1293-1304. doi: 10.1161/01.RES.0000251742.71301.16.

Oshero, N. and May, G. (2000) Conidial germination in *Aspergillus nidulans* requires RAS signaling and protein synthesis. *Genetics*, 155(2), pp.647-656. doi: 10.1093/genetics/155.2.647.

Pagano, L., Ricci, P., Tonso, A., Nosari, A., Cudillo, L., Montillo, M., Cenacchi, A., Pacilli, L., Fabbiano, F., Del Favero, A. and GIMEMA Infection Program (1997) Mucormycosis in patients with haematological malignancies: a retrospective clinical study of 37 cases. *British journal of haematology*, 99(2), pp.331-336. doi: 10.1046/j.1365-2141.1997.3983214.x.

Pardini, G., De Groot, P.W., Coste, A.T., Karababa, M., Klis, F.M., de Koster, C.G. and Sanglard, D. (2006) The CRH family coding for cell wall glycosylphosphatidylinositol proteins with a predicted transglycosidase domain affects cell wall organization and virulence of *Candida albicans*. *Journal of Biological Chemistry*, 281(52), pp.40399-40411. doi: 10.1074/jbc.M606361200.

Paris, S., Wysong, D., Debeaupuis, J.P., Shibuya, K., Philippe, B., Diamond, R.D. and Latgé, J.P. (2003) Catalases of *Aspergillus fumigatus*. *Infection and immunity*, 71(6), pp.3551-3562. doi:10.1128/IAI.71.6.3551-3562.2003

Patel, A., Kaur, H., Xess, I., Michael, J.S., Savio, J., Rudramurthy, S., Singh, R., Shastri, P., Umabala, P., Sardana, R. and Kindo, A. (2020) A multicentre observational study on the epidemiology, risk factors, management and outcomes of mucormycosis in India. *Clinical Microbiology and Infection*, 26(7), pp.944-e9. doi: 10.1016/j.cmi.2019.11.021..

Patin, E.C., Thompson, A. and Orr, S.J. (2019) May. Pattern recognition receptors in fungal immunity. In *Seminars in cell & developmental biology* (Vol. 89, pp. 24-33). Academic Press. doi: 10.1016/j.semcdb.2018.03.003.

Paul, B.Z., Jin, J. and Kunapuli, S.P. (1999) Molecular Mechanism of Thromboxane A₂-induced Platelet Aggregation: ESSENTIAL ROLE FOR P2TAC and α 2ARECEPTORS. *Journal of Biological Chemistry*, 274(41), pp.29108-29114.

Peraza Reyes, L. and Berteaux-Lecellier, V. (2013) Peroxisomes and sexual development in fungi. *Frontiers in physiology*, p.244. doi:10.3389/fphys.2013.00244

Perkhofer, S., Kainzner, B., Kehrel, B. E., Dierich, M. P., Nussbaumer, W., & Lass-Flörl, C. (2009). Potential antifungal effects of human platelets against zygomycetes in vitro. *The Journal of infectious diseases*, 200(7), 1176–1179. <https://doi.org/10.1086/605607>

Petrikkos, G., Skiada, A., Lortholary, O., Roilides, E., Walsh, T.J. and Kontoyiannis, D.P. (2012) Epidemiology and clinical manifestations of mucormycosis. *Clinical Infectious Diseases*, 54(suppl_1), pp.S23-S34. doi: 10.1093/cid/cir866..

Philippe, B., Ibrahim-Granet, O., Prevost, M.C., Gougerot-Pocidalo, M.A., Sanchez Perez, M., Van der Meeren, A. and Latge, J.P. (2003) Killing of *Aspergillus fumigatus* by alveolar macrophages is mediated by reactive oxidant intermediates. *Infection and immunity*, 71(6), pp.3034-3042 doi: 10.1128/IAI.71.6.3034-3042.2003.

Pittet, M. and Conzelmann, A. (2007) Biosynthesis and function of GPI proteins in the yeast *Saccharomyces cerevisiae*. *Biochimica et Biophysica Acta (BBA)-Molecular and Cell Biology of Lipids*, 1771(3), pp.405-420. doi: 10.1016/j.bbalip.2006.05.015.

Plummer, C., Wu, H., Kerrigan, S.W., Meade, G., Cox, D. and Ian Douglas, C.W. (2005) A serine-rich glycoprotein of *Streptococcus sanguis* mediates adhesion to platelets via GPIb. *British journal of haematology*, 129(1), pp.101-109.

Pollack, J.K., Harris, S.D. and Marten, M.R. (2009) Autophagy in filamentous fungi. *Fungal Genetics and Biology*, 46(1), pp.1-8. doi: 10.1016/j.fgb.2008.10.010. Epub 2008 Nov 5. PMID: 19010432.

Prakash, H. and Chakrabarti, A. (2019) Global epidemiology of mucormycosis. *Journal of Fungi*, 5(1), p.26. doi: 10.3390/jof5010026.

- Prill, S.K.H., Klinkert, B., Timpel, C., Gale, C.A., Schröppel, K., and Ernst, J.F. (2005) PMT family of *Candida albicans*: five protein mannosyltransferase isoforms affect growth, morphogenesis and antifungal resistance. *Mol Microbiol* **55**: 546–560.
- Ramirez-Ortiz, Z.G., Specht, C.A., Wang, J.P., Lee, C.K., Bartholomeu, D.C., Gazzinelli, R.T. and Levitz, S.M. (2008) Toll-like receptor 9-dependent immune activation by unmethylated CpG motifs in *Aspergillus fumigatus* DNA. *Infection and immunity*, *76*(5), pp.2123-2129. doi: 10.1128/IAI.00047-08. Epub 2008 Mar 10.
- Reed, C., Bryant, R., Ibrahim, A.S., Edwards Jr, J., Filler, S.G., Goldberg, R. and Spellberg, B. (2008) Combination polyene-caspofungin treatment of rhino-orbital-cerebral mucormycosis. *Clinical Infectious Diseases*, *47*(3), pp.364-371.
- Rees, J.R., Pinner, R.W., Hajjeh, R.A., Brandt, M.E. and Reingold, A.L. (1998) The epidemiological features of invasive mycotic infections in the San Francisco Bay area, 1992–1993: results of population-based laboratory active surveillance. *Clinical Infectious Diseases*, *27*(5), pp.1138-1147.
- Reid, G., Lynch III, J.P., Fishbein, M.C. and Clark, N.M. (2020) February. Mucormycosis. In *Seminars in respiratory and critical care medicine* (Vol. 41, No. 01, pp. 099-114). Thieme Medical Publishers. doi: 10.1055/s-0039-3401992.
- Rendu, F. and Brohard-Bohn, B. (2001) The platelet release reaction: granules' constituents, secretion and functions. *Platelets*, *12*(5), pp.261-273.
- Ribes, J.A., Vanover-Sams, C.L. and Baker, D.J. (2000) Zygomycetes in human disease. *Clinical microbiology reviews*, *13*(2), pp.236-301. doi: 10.1128/CMR.13.2.236.
- Richardson, M. and Page, I. (2018) Role of serological tests in the diagnosis of mold infections. *Current fungal infection reports*, *12*(3), pp.127-136. doi: 10.1007/s12281-018-0321-1.
- Richie, D.L., Fuller, K.K., Fortwendel, J., Miley, M.D., McCarthy, J.W., Feldmesser, M., Rhodes, J.C. and Askew, D.S. (2007) Unexpected link between metal ion deficiency and autophagy in *Aspergillus fumigatus*. *Eukaryotic cell*, *6*(12), pp.2437-2447. doi:10.1128/EC.00224-07
- Roden, M.M., Zaoutis, T.E., Buchanan, W.L., Knudsen, T.A., Sarkisova, T.A., Schaufele, R.L., Sein, M., Sein, T., Chiou, C.C., Chu, J.H. and Kontoyiannis, D.P. (2005) Epidemiology and outcome of zygomycosis: a review of 929 reported cases. *Clinical infectious diseases*, *41*(5), pp.634-653. doi: 10.1086/432579.
- Rødland, E.K., Ueland, T., Pedersen, T.M., Halvorsen, B., Muller, F., Aukrust, P. and Frøland, S.S. (2010) Activation of platelets by *Aspergillus fumigatus* and potential role of platelets in the immunopathogenesis of *Aspergillosis*. *Infection and immunity*, *78*(3), pp.1269-1275. doi: 10.1128/IAI.01091-09
- Roh, D.H., Bowers, B., Riezman, H. and Cabib, E. (2002) Rho1p mutations specific for regulation of β (1 \rightarrow 3) glucan synthesis and the order of assembly of the yeast cell wall. *Molecular microbiology*, *44*(5), pp.1167-1183. doi: 10.1046/j.1365-2958.2002.02955.x.

Romero, P.A., Dijkgraaf, G.J.P., Shahinian, S., Herscovics, A., and Bussey, H. (1997) The yeast CWH41 gene encodes glucosidase I. *Glycobiology* 7: 997– 1004.

Ruiz-Herrera, J., & Ortiz-Castellanos, L. (2019). Cell wall glucans of fungi. A review. *The Cell Surface*, 5, 100022.

Saijo, S., Ikeda, S., Yamabe, K., Kakuta, S., Ishigame, H., Akitsu, A., Fujikado, N., Kusaka, T., Kubo, S., Chung, S.H. and Komatsu, R. (2010) Dectin-2 recognition of α -mannans and induction of Th17 cell differentiation is essential for host defense against *Candida albicans*. *Immunity*, 32(5), pp.681-691. doi: 10.1016/j.immuni.2010.05.001.

Sainz, J., Lupiáñez, C.B., Segura-Catena, J., Vazquez, L., Ríos, R., Oyonarte, S., Hemminki, K., Försti, A. and Jurado, M. (2012). Dectin-1 and DC-SIGN polymorphisms associated with invasive pulmonary Aspergillosis infection. *PloS one*, 7(2), p.e32273.

Sanz, M., Carrano, L., Jimenez, C., Candiani, G., Trilla, J.A., Duran, A. and Roncero, C. (2005) *Candida albicans* strains deficient in CHS7, a key regulator of chitin synthase III, exhibit morphogenetic alterations and attenuated virulence. *Microbiology*, 151(8), pp.2623-2636. doi: 10.1099/mic.0.28093-0.

Schrettl, M., Bignell, E., Kragl, C., Sabiha, Y., Loss, O., Eisendle, M., Wallner, A., Arst Jr, H.N., Haynes, K. and Haas, H. (2007) Distinct roles for intra-and extracellular siderophores during *Aspergillus fumigatus* infection. *PLoS pathogens*, 3(9), p.e128. doi: 10.1371/journal.ppat.0030128.

Schultz, C.M., Goel, A., Dunn, A., Knauss, H., Huss, C., Launder, D., Wuescher, L.M., Conti, H.R. and Worth, R.G. (2020) Stepping Up to the Plate (let) against *Candida albicans*. *Infection and Immunity*, 88(4), pp.e00784-19. doi: 10.1128/IAI.00784-19.

Scorzoni, L., de Paula e Silva, A.C., Marcos, C.M., Assato, P.A., de Melo, W.C., de Oliveira, H.C., Costa-Orlandi, C.B., Mendes-Giannini, M.J. and Fusco-Almeida, A.M. (2017) Antifungal therapy: new advances in the understanding and treatment of mycosis. *Frontiers in microbiology*, p.36.

Sen, M., Lahane, S., Lahane, T.P., Parekh, R. and Honavar, S.G. (2021) *Mucor* in a viral land: a tale of two pathogens. *Indian journal of ophthalmology*, 69(2), p.244. doi: 10.4103/ijo.IJO_3774_20.

Sephton-Clark, P.C., Muñoz, J.F., Ballou, E.R., Cuomo, C.A. and Voelz, K. (2018) Pathways of pathogenicity: Transcriptional stages of germination in the fatal fungal pathogen *Rhizopus delemar*. *Msphere*, 3(5), pp.e00403-18. doi:10.1128/mSphere.00403-18

Serrano-Gómez, D., Domínguez-Soto, A., Ancochea, J., Jimenez-Heffernan, J. A., Leal, J. A., & Corbí, A. L. (2004). Dendritic cell-specific intercellular adhesion molecule 3-grabbing nonintegrin mediates binding and internalization of *Aspergillus fumigatus* conidia by dendritic cells and macrophages. *The Journal of Immunology*, 173(9), 5635-5643.

Seyoum, M., Enawgaw, B. and Melku, M. (2018) Human blood platelets and viruses: defense mechanism and role in the removal of viral pathogens. *Thrombosis journal*, 16(1), pp.1-6.

Sharda, A., & Flaumenhaft, R. (2018). The life cycle of platelet granules. *F1000Research*, 7.

Shematek, E. M., & Cabib, E. (1980). Biosynthesis of the yeast cell wall. II. Regulation of β -(1to3) glucan synthetase by ATP and GTP. *Journal of Biological Chemistry*

Shrimal, S., & Gilmore, R. (2019). Oligosaccharyltransferase structures provide novel insight into the mechanism of asparagine-linked glycosylation in prokaryotic and eukaryotic cells. *Glycobiology*, 29(4), 288-297.

Shubitz, L.F., Trinh, H.T., Perrill, R.H., Thompson, C.M., Hanan, N.J., Galgiani, J.N. and Nix, D.E. (2014) Modeling nikkomycin Z dosing and pharmacology in murine pulmonary coccidioidomycosis preparatory to phase 2 clinical trials. *The Journal of infectious diseases*, 209(12), pp.1949-1954

Silverstein, R.L. and Febbraio, M. (1992) Identification of lysosome-associated membrane protein-2 as an activation-dependent platelet surface glycoprotein. *Blood*, 80(6), pp.1470-5.

Skiada, A., Lanternier, F., Groll, A.H., Pagano, L., Zimmerli, S., Herbrecht, R., Lortholary, O. and Petrikos, G.L. (2013) Diagnosis and treatment of mucormycosis in patients with hematological malignancies: guidelines from the 3rd European Conference on Infections in Leukemia (ECIL 3). *haematologica*, 98(4), p.492. doi: 10.3324/haematol.2012.065110.

Skiada, A., Lass-Floerl, C., Klimko, N., Ibrahim, A., Roilides, E. and Petrikos, G. (2018) Challenges in the diagnosis and treatment of mucormycosis. *Medical mycology*, 56(suppl_1), pp.S93-S101. doi: 10.1093/mmy/myx101.

Skiada, A., Pagano, L.I.V.I.O., Groll, A., Zimmerli, S., Dupont, B., Lagrou, K., Lass-Florl, C., Bouza, E., Klimko, N., Gaustad, P. and Richardson, M. (2011) Zygomycosis in Europe: analysis of 230 cases accrued by the registry of the European Confederation of Medical Mycology (ECMM) Working Group on Zygomycosis between 2005 and 2007. *Clinical Microbiology and Infection*, 17(12), pp.1859-1867. doi: 10.1111/j.1469-0691.2010.03456.x.

Skiada, A., Pavleas, I., & Drogari-Apiranthitou, M. (2020) Epidemiology and Diagnosis of Mucormycosis: An Update. *Journal of fungi (Basel, Switzerland)*, 6(4), 265. <https://doi.org/10.3390/jof6040265>

Slatko, B.E., Gardner, A.F. and Ausubel, F.M. (2018) 'Overview of next-generation sequencing technologies'. *Current protocols in molecular biology*, 122(1), p.e59.

Smith, L.M., Dixon, E.F. and May, R.C., 2015. The fungal pathogen *Cryptococcus neoformans* manipulates macrophage phagosome maturation. *Cellular microbiology*, 17(5), pp.702-713. doi: 10.1111/cmi.12394. Epub 2014 Dec 19.

Spellberg, B., Edwards Jr, J. and Ibrahim, A. (2005) Novel perspectives on mucormycosis: pathophysiology, presentation, and management. *Clinical microbiology reviews*, 18(3), pp.556-569. doi: 10.1128/CMR.18.3.556-569.2005.

Spellberg, B. and Ibrahim, A.S. (2010) Recent advances in the treatment of mucormycosis. *Current infectious disease reports*, 12(6), pp.423-429. doi: 10.1007/s11908-010-0129-9.

Stappers, M., Clark, A. E., Aimaniananda, V., Bidula, S., Reid, D. M., Asamaphan, P., Hardison, S. E., Dambuza, I. M., Valsecchi, I., Kerscher, B., Plato, A., Wallace, C. A., Yuecel, R., Hebecker, B., da Glória

Teixeira Sousa, M., Cunha, C., Liu, Y., Feizi, T., Brakhage, A. A., Kwon-Chung, K. J., ... Brown, G. D. (2018). Recognition of DHN-melanin by a C-type lectin receptor is required for immunity to *Aspergillus*. *Nature*, 555(7696), 382–386. <https://doi.org/10.1038/nature25974>

Tada, H., Nemoto, E., Shimauchi, H., Watanabe, T., Mikami, T., Matsumoto, T., Ohno, N., Tamura, H., Shibata, K.I., Akashi, S. and Miyake, K. (2002) *Saccharomyces cerevisiae*- and *Candida albicans*-derived mannan induced production of tumor necrosis factor alpha by human monocytes in a CD14- and Toll-like receptor 4-dependent manner. *Microbiology and immunology*, 46(7), pp.503-512. doi: 10.1111/j.1348-0421.2002.tb02727.x.

Kikuma, T. and Kitamoto, K. (2011) Analysis of autophagy in *Aspergillus oryzae* by disruption of *Aoatg13*, *Aoatg4*, and *Aoatg15* genes. *FEMS microbiology letters*, 316(1), pp.61-6. <https://doi.org/10.1111/j.1574-6968.2010.02192.x>

Tang, Y.Q., Yeaman, M.R. and Selsted, M.E. (2002) Antimicrobial peptides from human platelets. *Infection and immunity*, 70(12), pp.6524-6533. doi: 10.1128/IAI.70.12.6524-6533.2002.

Tchernychev, B., Furie, B. and Furie, B.C. (2003) Peritoneal macrophages express both P-selectin and PSGL-1. *The Journal of cell biology*, 163(5), pp.1145-1155.

Thanh, N.V., Rombouts, F.M. and Nout, M.J.R. (2005) Effect of individual amino acids and glucose on activation and germination of *Rhizopus oligosporus* sporangiospores in tempe starter. *Journal of applied microbiology*, 99(5), pp.1204-1214. doi: 10.1111/j.1365-2672.2005.02692.x.

T Thompson, A., Griffiths, J.S., Walker, L., Da Fonseca, D.M., Lee, K.K., Taylor, P.R., Gow, N.A. and Orr, S.J. (2019) Dependence on Dectin-1 varies with multiple *Candida* species. *Frontiers in Microbiology*, p.1800. doi: 10.3389/fmicb.2019.01800.

Tischler, B.Y., Tosini, N.L., Cramer, R.A. and Hohl, T.M. (2020) Platelets are critical for survival and tissue integrity during murine pulmonary *Aspergillus fumigatus* infection. *PLoS pathogens*, 16(5), p.e1008544. doi: 10.1371/journal.ppat.1008544.

Tkacz, J.S., Cybulska, E.B. and Lampen, J.O. (1971) Specific staining of wall mannan in yeast cells with fluorescein-conjugated concanavalin A. *Journal of Bacteriology*, 105(1), pp.1-5. doi: 10.1128/jb.105.1.1-5.1971. PMID: 5541005; PMCID: PMC248315.

Trombetta, E.S., Simons, J.F., and Helenius, A. (1996) Endoplasmic reticulum glucosidase II is composed of a catalytic subunit, conserved from yeast to mammals, and a tightly bound noncatalytic HDEL-containing subunit. *J Biol Chem* 271: 27509– 27516.

Tsai, H.F., Chang, Y.C., Washburn, R.G., Wheeler, M.H. and Kwon-Chung, K. (1998) The developmentally regulated *alb1* gene of *Aspergillus fumigatus*: its role in modulation of conidial morphology and virulence. *Journal of bacteriology*, 180(12), pp.3031-3038. doi: 10.1128/JB.180.12.3031-3038.1998.

- Umeyama, T., Kaneko, A., Watanabe, H., Hirai, A., Uehara, Y., Niimi, M. and Azuma, M. (2006) Deletion of the Ca BIG1 gene reduces β -1, 6-glucan synthesis, filamentation, adhesion, and virulence in *Candida albicans*. *Infection and immunity*, 74(4), pp.2373-2381. doi:10.1128/IAI.74.4.2373-2381.2006
- Uwamahoro, N., Verma-Gaur, J., Shen, H.H., Qu, Y., Lewis, R., Lu, J., Bamberg, K., Masters, S.L., Vince, J.E., Naderer, T. and Traven, A. (2014) The pathogen *Candida albicans* hijacks pyroptosis for escape from macrophages. *MBio*, 5(2), pp.e00003-14. doi: 10.1128/mBio.00003-14.
- Valsecchi, I., Dupres, V., Stephen-Victor, E., Guijarro, J.I., Gibbons, J., Beau, R., Bayry, J., Coppee, J.Y., Lafont, F., Latgé, J.P. and Beauvais, A. (2017) Role of hydrophobins in *Aspergillus fumigatus*. *Journal of fungi*, 4(1), p.2. doi: 10.3390/jof4010002. PMID: 29371496; PMCID: PMC5872305.
- Valsecchi, I., Stephen-Victor, E., Wong, S.S.W., Karnam, A., Sunde, M., Guijarro, J.I., Rodríguez de Francisco, B., Krüger, T., Kniemeyer, O., Brown, G.D. and Willment, J.A. (2020) The role of rodA-conserved cysteine residues in the *Aspergillus fumigatus* conidial surface organization. *Journal of Fungi*, 6(3), p.151. doi: 10.3390/jof6030151.
- van de Veerdonk, F.L., Marijnissen, R.J., Kullberg, B.J., Koenen, H.J., Cheng, S.C., Joosten, I., van den Berg, W.B., Williams, D.L., van der Meer, J.W., Joosten, L.A. and Netea, M.G. (2009) The macrophage mannose receptor induces IL-17 in response to *Candida albicans*. *Cell host & microbe*, 5(4), pp.329-340. doi: 10.1016/j.chom.2009.02.006.
- Klei, I.J. and Veenhuis, M. (2013) The versatility of peroxisome function in filamentous fungi. *Peroxisomes and their key role in cellular signaling and metabolism*, pp.135-152. doi: 10.1007/978-94-007-6889-5_8. PMID: 23821147.
- van Leeuwen, M.R., Krijgheld, P., Bleichrodt, R., Menke, H., Stam, H., Stark, J., Wösten, H.A.B. and Dijksterhuis, J. (2008) Germination of conidia of *Aspergillus niger* is accompanied by major changes in RNA profiles. *Studies in mycology*, 61(1), pp.iii-iii. doi: 10.3114/sim0009.
- Vendele, I., Willment, J.A., Silva, L.M., Palma, A.S., Chai, W., Liu, Y., Feizi, T., Spyrou, M., Stappers, M.H., Brown, G.D. and Gow, N.A. (2020) Mannan detecting C-type lectin receptor probes recognise immune epitopes with diverse chemical, spatial and phylogenetic heterogeneity in fungal cell walls. *PLoS pathogens*, 16(1), p.e1007927
- Vieira, O.V., Bucci, C., Harrison, R.E., Trimble, W.S., Lanzetti, L., Gruenberg, J., Schreiber, A.D., Stahl, P.D. and Grinstein, S. (2003) Modulation of Rab5 and Rab7 recruitment to phagosomes by phosphatidylinositol 3-kinase. *Molecular and cellular biology*, 23(7), pp.2501-2514. doi: 10.1128/MCB.23.7.2501-2514.2003. PMID: 12640132; PMCID: PMC150733.
- Voelz K., Gratacap R.L., Wheeler R.T. (2015) A zebrafish larval model reveals early tissue-specific innate immune responses to *Mucor circinelloides*. *Dis Model Mech*. Nov;8(11):1375-88. doi: 10.1242/dmm.019992. Epub 2015 Aug 20. PMID: 26398938; PMCID: PMC4631785.
- Wagener, J., Malireddi, R.S., Lenardon, M.D., Köberle, M., Vautier, S., MacCallum, D.M., Biedermann, T., Schaller, M., Netea, M.G., Kanneganti, T.D. and Brown, G.D. (2014) Fungal chitin dampens inflammation through IL-10 induction mediated by NOD2 and TLR9 activation. *PLoS pathogens*, 10(4), p.e1004050. doi: 10.1371/journal.ppat.1004050.

Waldorf, A.R., Levitz, S.M. and Diamond, R.D. (1984) In vivo bronchoalveolar macrophage defense against *Rhizopus oryzae* and *Aspergillus fumigatus*. *Journal of Infectious Diseases*, 150(5), pp.752-760. doi: 10.1093/infdis/150.5.752.

Walsh, T.J., Gamaletsou, M.N., McGinnis, M.R., Hayden, R.T. and Kontoyiannis, D.P., (2012) Early clinical and laboratory diagnosis of invasive pulmonary, extrapulmonary, and disseminated mucormycosis (zygomycosis). *Clinical Infectious Diseases*, 54(suppl_1), pp.S55-S60. doi: 10.1093/cid/cir868.

Walsh, T.J. and Kontoyiannis, D.P. (2008) What is the role of combination therapy in management of zygomycosis?. *Clinical Infectious Diseases*, 47(3), pp.372-374.

Wang, X.M., Guo, L.C., Xue, S.L. and Chen, Y.B. (2016) Pulmonary mucormycosis: a case report and review of the literature. *Oncology letters*, 11(5), pp.3049-3053. doi: 10.3892/ol.2016.4370.

Wang, Z., Gerstein, M. and Snyder, M. (2009) RNA-Seq: a revolutionary tool for transcriptomics. *Nature reviews genetics*, 10(1), pp.57-63

Watson, C.N., Kerrigan, S.W., Cox, D., Henderson, I.R., Watson, S.P. and Arman, M. (2016) Human platelet activation by *Escherichia coli*: roles for FcγRIIA and integrin αIIbβ3. *Platelets*, 27(6), pp.535-540. doi: 10.3109/09537104.2016.1148129.

Woods Jr, V. L., Wolff, L. E., & Keller, D. M. (1986). Resting platelets contain a substantial centrally located pool of glycoprotein IIb-IIIa complex which may be accessible to some but not other extracellular proteins. *Journal of Biological Chemistry*, 261(32), 15242-15251.

Yalamanchili, H.K., Wan, Y.W. and Liu, Z. (2017) Data Analysis Pipeline for RNA-seq Experiments: From Differential Expression to Cryptic Splicing. *Current protocols in bioinformatics*, 59(1), pp.11-15.

Yeaman, M.R., Tang, Y.Q., Shen, A.J., Bayer, A.S. and Selsted, M.E. (1997) Purification and in vitro activities of rabbit platelet microbicidal proteins. *Infection and immunity*, 65(3), pp.1023-1031.

Youssef, J., Novosad, S.A. and Winthrop, K.L. (2016) Infection risk and safety of corticosteroid use. *Rheumatic Disease Clinics*, 42(1), pp.157-176. doi: 10.1016/j.rdc.2015.08.004.

Youssefian, T., Drouin, A., Massé, J.M., Guichard, J. and Cramer, E.M. (2002) Host defense role of platelets: engulfment of HIV and *Staphylococcus aureus* occurs in a specific subcellular compartment and is enhanced by platelet activation. *Blood, The Journal of the American Society of Hematology*, 99(11), pp.4021-4029.

Zander, D.M. and Klinger, M. (2009) The blood platelets contribution to innate host defense—what they have learned from their big brothers. *Biotechnology Journal: Healthcare Nutrition Technology*, 4(6), pp.914-926.

Zhu, L.L., Zhao, X.Q., Jiang, C., You, Y., Chen, X.P., Jiang, Y.Y., Jia, X.M. and Lin, X. (2013) C-type lectin receptors Dectin-3 and Dectin-2 form a heterodimeric pattern-recognition receptor for host defense against fungal infection. *Immunity*, 39(2), pp.324-334. doi: 10.1016/j.immuni.2013.05.017.

APPENDIX I: PUBLICATIONS


This appendix contains a publication to which research from my PhD has been contributed. Published research included in this thesis has been referenced and noted in text.

- I. Ghuman, H., Shepherd-Roberts, A., Watson, S., Zuidsherwoude, M., Watson, S. P., & Voelz, K. (2019). *Mucor circinelloides* induces platelet aggregation through integrin $\alpha\text{IIb}\beta 3$ and Fc γ RIIA. *Platelets*, 30(2), 256-263.

ORIGINAL ARTICLE



Mucor circinelloides induces platelet aggregation through integrin α IIb β 3 and Fc γ RIIA

Harlene Ghuman¹, Alicia Shepherd-Roberts¹, Stephanie Watson², Malou Zuidschewoude ^{2,3}, Steve P. Watson^{2,3}, & Kerstin Voelz¹

¹School of Biosciences and Institute of Microbiology and Infection, College of Life and Environmental Sciences, University of Birmingham, Birmingham UK, ²Institute of Cardiovascular Sciences, College of Medical and Dental Sciences, University of Birmingham, Birmingham UK, and ³Centre of Membrane Proteins and Receptors (COMPARE), Universities of Birmingham and Nottingham, Midlands, UK

Abstract

Thrombosis is a hallmark of the fatal fungal infection mucormycosis. Yet, the platelet activation pathway in response to mucormycetes is unknown. In this study we determined the platelet aggregation potential of *Mucor circinelloides* (*M. circinelloides*) NRRL3631, characterized the signaling pathway facilitating aggregation in response to fungal spores, and identified the influence of the spore developmental stage upon platelet aggregation potential. Using impedance and light-transmission aggregometry, we showed that *M. circinelloides* induced platelet aggregation in whole blood and in platelet-rich plasma, respectively. The formation of large spore-platelet aggregates was confirmed by light-sheet microscopy, which showed spores dispersed throughout the aggregate. Aggregation potential was dependent on the spore's developmental stage, with the strongest platelet aggregation by spores in mid-germination. Inhibitor studies revealed platelet aggregation was mediated by the low affinity IgG receptor Fc γ RIIA and integrin α IIb β 3; Src and Syk tyrosine kinase signaling; and the secondary mediators TxA₂ and ADP. Flow cytometry of antibody stained platelets showed that interaction with spores increased expression of platelet surface integrin α IIb β 3 and the platelet activation marker CD62P. Together, this is the first elucidation of the signaling pathways underlying thrombosis formation during a fungal infection, highlighting targets for therapeutic intervention.

Keywords

Fc γ RIIA, *Mucor circinelloides*, mucormycetes, mucormycosis, platelets, thrombosis

History

Received 15 February 2017
Revised 26 November 2017
Accepted 13 December 2017
Published online 4 January 2018

Introduction

The incidence of invasive fungal infections is on the rise, and this is attributed to the increasing population of immunosuppressed individuals under the influence of modern medicine [1–4]. Mucormycosis—a previously uncommon infection—has grown in occurrence to become the third most common invasive fungal infection after aspergillosis and candidiasis, respectively [5]. Infection is caused by species of the Mucorales order, with *Rhizopus* spp. and *Mucor* spp. being the most common causative agents [1–4]. Prognosis for this severe fungal infection is poor, with studies reporting mortality rates in the range of 60–100% [4]. This staggeringly high mortality rate is reflective of the aggressive nature of infection, and the poor efficacy of antifungal therapeutics currently employed [2,3]. Risk factors identified for mucormycosis include uncontrolled diabetes mellitus, diabetes mellitus with ketoacidosis, organ transplantation, and neutropenia [3,4,6].

The hallmarks of mucormycosis are considered to be angioinvasion, tissue necrosis, and thrombosis, the latter indicating a potential role of platelets [6]. Platelets have been identified as

major players of the innate immune system with the onset of thrombocytopenia common during infectious diseases. Infective endocarditis and septicemia in particular have sparked interest into the interaction between pathogens and platelets [7–9]. It is unknown if thrombus formation protects from mucormycosis or exaggerates symptoms by inducing excessive inflammation and tissue necrosis.

The platelet IgG receptor Fc γ RIIA and integrin α IIb β 3 have been highlighted as crucial to platelet activation in response to both Gram-negative and Gram-positive bacteria [7–9]. While the proteins that give rise to bacterial–platelet interaction are strain-specific, platelet activation is mediated by a common pathway consisting of Fc γ RIIA, Src and Syk tyrosine kinase activation, α IIb β 3 engagement and the secondary mediators thromboxane A₂ (TxA₂) and adenosine 5'-diphosphate (ADP) [8,9].

There is currently little information on the interaction between platelets and mucormycetes under physiological conditions and the molecular signaling pathways underlying this interaction. An improved understanding of the signaling underlying thrombus formation during mucormycosis might offer novel therapeutic targets to improve current treatment approaches and thus patient outcome. Hence, we investigated the interaction between the clinical isolate *Mucor circinelloides* NRRL3631 and platelets. We show that platelets form aggregates with fungal spores dependent on the spore developmental stage. Spore aggregation is

Color versions of one or more of the figures in the article can be found online at www.tandfonline.com/IPLT.

Correspondence: K. Voelz k.voelz@bham.ac.uk, School of Biosciences, University of Birmingham, Edgbaston, Birmingham, B15 2TT

mediated through the platelet IgG receptor FcγRIIA, integrin αIIbβ3 and Src and Syk tyrosine kinases, and secondary mediators TxA₂ and ADP. Platelet activation is also associated with increased expression of platelet surface integrin αIIbβ3 and the platelet activation marker CD62P. Together, this provides the first elucidation of the signaling pathways underlying thrombosis formation during mucormycosis highlighting potential strategies to interfere with thrombus formation.

Methods

Fungal strains and growth conditions

The *Mucor circinelloides* strain used was *Mucor circinelloides* f. sp. *lusitanicus* strain NRRL3631, a clinical isolate [10]. The strain was grown on Sabouraud dextrose agar (Merck-Millipore, Billerica, MA, USA) at room temperature for 7 days prior to use.

Spore preparation for aggregation assays

Spores were collected in phosphate buffered saline (PBS) and centrifuged at 1811 \times g for three min. The spore pellet was washed twice with PBS and then re-suspended in Sabouraud broth (Sigma-Aldrich, St. Louis, MO, USA). Spores were cultured at 37°C with shaking at 45 rpm, over 0, 3, 6, and 48 h. Following incubation, spore suspensions were centrifuged at 1811 \times g for three min. The spore pellet was washed twice, and re-suspended in PBS at concentrations to allow for 1:10, 1:20, 1:100, and 1:500 spore:platelet ratios. Spore suspensions were kept on ice until used for aggregometry.

Blood preparation

Blood samples were collected from healthy human donors into 4% (w/v) citrate (Sigma-Aldrich, St. Louis, MO, USA). The study design was approved by the University of Birmingham's research ethics committee (ERN_11-0175). Blood was centrifuged at 200 \times g for 20 min and platelet-rich plasma (PRP) collected. For light-transmission aggregometry, a PRP platelet count was taken using Coulter® Z2 Particle Counter in triplicate and averaged. For multiple-electrode aggregometry, a whole blood platelet count was taken using Sysmex XN-1000 Hematology Analyzer.

Platelet aggregometry in PRP

PRP was incubated at 37°C for 1 min and then stirred for 1 min. *M. circinelloides* NRRL3631 suspension containing appropriate spore numbers for 1:10, 1:20, 1:100, and 1:500 spore:platelet ratios was added to the PRP, and platelet aggregation recorded over 30 min using light-transmission aggregometer PAP-8E (Bio/Data Corporation, Horsham, PA, USA). As a positive control, Thrombin Receptor-Activating Peptide (TRAP; Severn Biotech, Kidderminster, UK) (100 μM) was added to PRP, and as a negative control PBS was added.

Platelet aggregometry in whole blood

Whole blood was added to sodium chloride and incubated for 3 min at 37°C. *M. circinelloides* NRRL3631 at 3 h germination, and at a spore concentration allowing for a spore:platelet ratio of 1:10, was added and platelet aggregation recorded over 30 min using multiple electrode aggregometer, Multiplate® Analyzer (Roche, Basel, Switzerland). TRAP was added to PRP and used as a positive control, and PBS was used as a negative control.

Cell staining and microscopy

Platelets were stained with CellMask Deep Red Plasma Membrane Stain (1:2000, Thermo Fisher Scientific, Waltham, MA, USA), and *M. circinelloides* NRRL3631 spores with Concanavalin A, Alexa fluor™ 488 conjugate (300 μg ml⁻¹, Thermo Fisher Scientific, Waltham, MA, USA). Formed aggregates were immobilized on poly-L-lysine (Sigma) coated rectangular coverslips (25x50 mm), fixed using 4% PFA, washed and placed in the imaging chamber filled with PBS. Orthogonal views of the aggregates were acquired on a Marianas LightSheet (Intelligent Imaging Innovations, Denver, CO, USA), a dual inverted Selective Plane Illumination Microscope (diSPIM) which uses two perpendicular 0.8 NA, 40x water immersion objectives to excite and detect fluorescence in an alternating duty cycle.

Volumes of 200 image planes were captured using both arms sequentially in slice scan mode, with a step size of 0.5 μm, for both 488 nm and 640 nm excitation wavelengths, on ORCA-Flash4.0 V3 sCMOS cameras (Hamamatsu), driven by SlideBook 6.0 software (Intelligent Imaging Innovations, Denver, CO, USA).

Image analysis was performed using Fiji software [11], and a maximal intensity projection was made of a single volume view. For the supplementary movie, the two orthogonal volumes were registered and deconvolved (joint-deconvolution) using the multi-view Reconstruction plugin [12] and visualized by rotating the 3D volume around the y-axis.

Inhibitor treatments

Inhibition of αIIbβ3 was achieved by pre-incubating platelets with 9 μM eptifibatide (GlaxoSmithKline, Coventry, UK) for 1 min at room temperature. FcγRIIA was blocked with 10 μM mAbIV.3 (hybridoma from American Tissue Culture Corporation (Manassas, Virginia), Src and Syk tyrosine kinases with 4 μM dasatinib (D-3307, LC Laboratories, Woburn, MA, USA) and 10 μM PRT-060318 (AdipoGen Life Sciences, Liestal, Switzerland) respectively, and secondary mediators TxA₂ and ADP with 30 μM Indomethacin (I7378, Sigma-Aldrich, St. Louis, MO, USA) and 2 U Apyrase (A6535, Sigma-Aldrich, St. Louis, MO, USA) respectively. Platelet aggregation was assessed by light-transmission in a PAP-8E aggregometer over 30 min.

Platelet receptor labeling

Conjugated anti-human CD32 (#60012; mouse; StemCell Technologies, Vancouver, Canada) and anti-mouse 2° Alexa Fluor® 488 conjugate (A10680; goat; Invitrogen, Carlsbad, CA, USA) was used to label FcγRIIA. Anti-Human CD41a-APC (BD559777; mouse; BD Biosciences, San Jose, CA, USA) was used to label αIIbβ3. CD62P-FITC (BC A07790; mouse; Beckman Coulter, Brea, CA, USA) was used to label CD62P. Platelet aggregation was assessed by light-transmission in a PAP-8E aggregometer over 30 min. Receptor antibody labels were added to samples for 30 min prior to flow cytometry assays. Flow cytometry analysis was conducted using BD Accuri™ C6 Plus (BD Biosciences, Oxford, UK). Samples were run for 10000 events, and cell count vs fluorescence recorded.

Statistical analysis

Statistical analysis was conducted using GraphPad Prism 6.0. Data are presented as mean ± SEM, unless stated otherwise. Data was analysed using the one-way analysis of variance (ANOVA) with post hoc Dunnett's multiple comparison test, Mann-Whitney *U*-test or Kruskal-Wallis test with post-hoc

Dunn's multiple comparison test, as indicated in the figure legends. $p < 0.05$ was deemed to be statistically significant. Technical repeats were conducted at $n = 3$, and biological repeats at $n = 5$ unless otherwise stated.

Results

Mucor circinelloides NRRL3631 induces platelet aggregation in whole human blood and PRP

Thrombus formation during mucormycosis might be induced by fungal invasion of blood vessels, and thus formation of a platelet-reactive surface, or direct interaction between platelets and the fungus. Therefore, we investigated the potential of the clinical isolate *Mucor circinelloides* NRRL3631 to induce platelet aggregation qualitatively and quantitatively.

Initially, we visualized spore-platelet interaction by dual inverted Selective Plane Illumination fluorescence microscopy (diSPIM), which gives isotropic resolution in three dimensions. *M. circinelloides* spores were stained with Concanavalin A, Alexa Fluor™ 488 conjugate and platelets in platelet-rich plasma (PRP) with CellMask Deep Red Plasma Membrane Stain. *M. circinelloides* spores were incubated in PRP at a 1:10 spore:platelet ratio under stirring conditions in the PAP-8E aggregometer and formed aggregates were fixed onto glass coverslips. Fluorescence

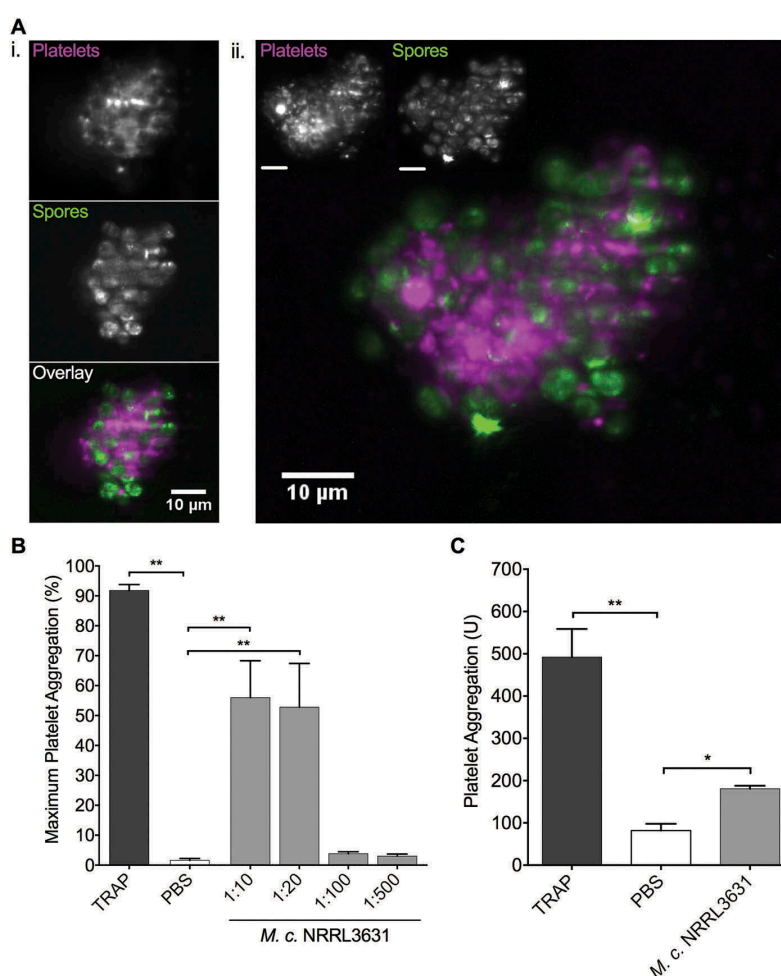
microscopy revealed *M. circinelloides* NRRL3631 spores to be contained within large platelet aggregates with individual spores being surrounded by platelets (Figure 1 Ai & ii and Supplementary Movie 1).

We then quantified this interaction by light transmission aggregometry. Experiments were performed in PRP using 1:10, 1:20, 1:100, and 1:500 spore:platelet ratios. The agonist thrombin-related-activating peptide (TRAP) induced maximal platelet aggregation ($91.8 \pm 2.0\%$). *M. circinelloides* NRRL3631 induced platelet aggregation in a concentration-dependent manner, with significant platelet aggregation occurring at 1:10 and 1:20 spore:platelet ratios (1:10: $56.0 \pm 12.3\%$ and 1:20: $52.8\% \pm 14.6\%$ platelet aggregation; $p < 0.01$) (Figure 1B).

To examine the physiological relevance of platelet aggregation in response to mucormycetes, we determined the platelet aggregation potential of *M. circinelloides* NRRL3631 in whole blood using impedance aggregometry. *M. circinelloides* NRRL3631 was added to whole blood at a spore:platelet ratio of 1:10, and platelet aggregation assessed. *M. circinelloides* NRRL3631 induced significant platelet aggregation ($180 \pm 16U$; $p < 0.05$) in comparison to PBS ($81 \pm 16U$) (Figure 1C).

In summary, these data show that platelets interact with mucormycete spores to form large platelet-spore aggregates. This indicates that thrombus formation during mucormycosis can be mediated by a direct platelet response to fungal spores.

Figure 1. *Mucor circinelloides* NRRL3631 induces platelet aggregation in whole blood and PRP. (A) *M. circinelloides* NRRL3631 spores (green) interact with human platelets (magenta) to form large complex structures. We imaged a total of 17 aggregates and show here images for two of those. These images show (i) an optical section through a platelet and spore aggregate and (ii) the maximal intensity projection of the (single view diSPIM) 3D volume of the spore-induced platelet aggregate. Images are representative of 17 aggregates from two independent experiments. Complexes were visualized by dual inverted Selective Plane Illumination Microscopy (diSPIM) using 40x objectives and analysed on Image J (Fiji); scale bar: 10µm. (B) Platelet aggregation in response to TRAP, PBS and *M. circinelloides* NRRL3631 over increasing spore:platelet ratios was measured in PRP using light-transmission aggregometry over 30 min. Significant platelet aggregation was induced by *M. circinelloides* NRRL3631 at a 1:10 and 1:20 spore:platelet ratio. Notably *M. circinelloides* NRRL3631 induced platelet aggregation in a concentration-dependent manner. Data shown are mean±SEM of five independent experimental repeats; ** $p < 0.01$, Mann–Whitney *U* test. (C) Platelet aggregation in response to TRAP, PBS and *Mucor circinelloides* NRRL3631 spores was measured in whole blood using multiple-electrode aggregometry over 30 min. *M. circinelloides* NRRL3631 spores induced significant platelet aggregation in whole blood. Data shown are mean±SEM of five independent experimental repeats; * $p < 0.05$, Mann–Whitney *U* test.



Platelet aggregation in response to *Mucor circinelloides* NRRL3631 is supported by the $\text{Fc}\gamma\text{RIIA}$ receptor and integrin $\alpha\text{IIb}\beta 3$

Having shown that platelets form aggregates with mucormycete spores, we next wanted to identify the receptor(s) and downstream signaling components mediating this interaction. Aggregation studies with washed platelets did not induce aggregation suggesting the requirement of a serum factor. Therefore, this study performed aggregations in PRP with the focus to elucidate the receptors and downstream signaling mediators. The platelet low affinity immune receptor, $\text{Fc}\gamma\text{RIIA}$ has been identified as a key receptor in platelet activation in response to bacterial pathogen through the result of antibody-pathogen interaction [8,9,13,14]. We hypothesized that $\text{Fc}\gamma\text{RIIA}$ plays a key role in the induction of platelet aggregation by *M. circinelloides* NRRL3631 in view of the dependency on plasma. In addition, platelet integrin $\alpha\text{IIb}\beta 3$, the most abundant platelet surface glycoprotein, has been shown to be essential for platelet activation by bacteria [13–16]. To investigate whether platelet aggregation in response to *M. circinelloides* NRRL3631 is supported by $\text{Fc}\gamma\text{RIIA}$ and $\alpha\text{IIb}\beta 3$ engagement, platelets were treated with the $\text{Fc}\gamma\text{RIIA}$ blocking mAb IV.3 or $\alpha\text{IIb}\beta 3$ inhibitor eptifibatide, prior to *M. circinelloides* NRRL3631 exposure. Blocking $\text{Fc}\gamma\text{RIIA}$ significantly decreased platelet aggregation in response to *M. circinelloides* NRRL3631 (1:10 (-)mAb IV.3: $48.8 \pm 9.58\%$; (+) mAb IV.3: $12.8 \pm 10.57\%$; $p < 0.05$) (Figure 2A). Platelet aggregation was abrogated by eptifibatide (1:10 (-)eptifibatide: $58.0 \pm 7.46\%$; (+) eptifibatide: $0.60 \pm 0.25\%$; $p < 0.01$) and (Figure 2B).

Upon platelet activation, expression of surface $\alpha\text{IIb}\beta 3$ is upregulated, further supporting platelet-platelet interaction and therefore aggregation [7,13,15], including during bacterial infection [8,9]. Platelet surface integrin $\alpha\text{IIb}\beta 3$ expression levels are enhanced as a result of platelet activation by means of α -granule release [17]. We thus investigated the expression patterns of

$\text{Fc}\gamma\text{RIIA}$ and $\alpha\text{IIb}\beta 3$ by flow cytometry after antibody labeling. Platelet expression levels of $\text{Fc}\gamma\text{RIIA}$ were not altered in response to *M. circinelloides* NRRL3631 spores under aggregating conditions (Figure 2C). In contrast, surface $\alpha\text{IIb}\beta 3$ levels were increased in response to *M. circinelloides* NRRL3631 spores under the same conditions (Figure 2D).

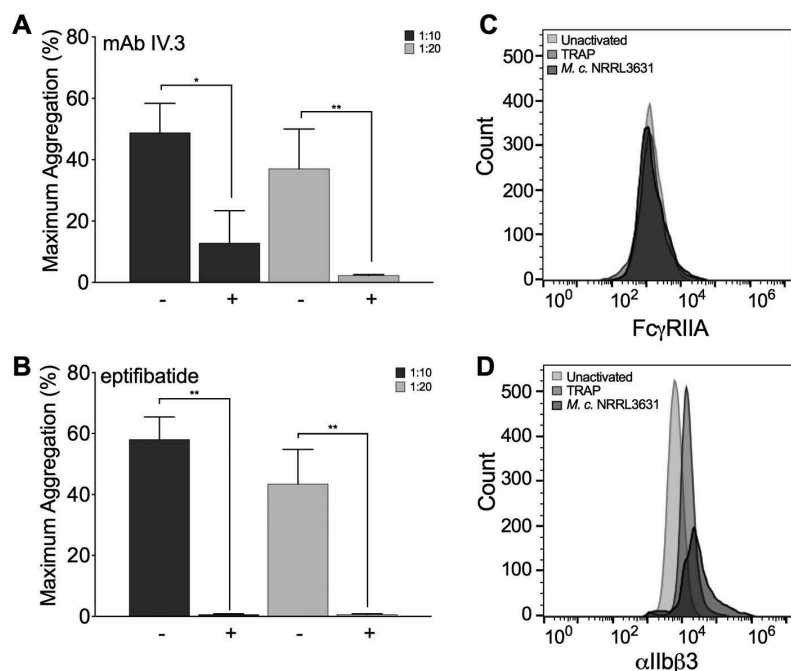
Thus, this shows that platelets respond to fungal spores through interaction with the IgG receptor $\text{Fc}\gamma\text{RIIA}$ and integrin $\alpha\text{IIb}\beta 3$. Subsequently, $\alpha\text{IIb}\beta 3$ surface levels are upregulated to further support platelet aggregation.

Mucor circinelloides NRRL3631 activates Src and Syk signaling cascades and induces platelet activation supported by secondary mediators TxA_2 and ADP

The two identified interaction platelet receptors $\text{Fc}\gamma\text{RIIA}$ and $\alpha\text{IIb}\beta 3$ both activate downstream Src and Syk tyrosine kinases [16]. To test if the interaction of *M. circinelloides* NRRL3631 with platelets also results in the activation of Src and Syk, platelets were treated with Src inhibitor Dasatinib, and Syk inhibitor PRT-060318 prior to *M. circinelloides* NRRL3631 exposure. Dasatinib and PRT-060318 inhibited platelet aggregation in response to *M. circinelloides* NRRL3631 (Figure 3A).

The platelet α -granules activation marker CD62P (P-selectin) is expressed on the platelet surface upon platelet activation [18]. Platelets were antibody-labeled for P-selectin, and expression levels measured pre- and postexposure to *M. circinelloides* NRRL3631 spores using flow cytometry. P-selectin expression levels were markedly increased following exposure to *M. circinelloides* spores indicating that platelets are activated by *M. circinelloides* NRRL3631 under aggregating conditions (Figure 3Bi). Under non-aggregating conditions by means of eptifibatide platelet pre-treatment, P-selectin expression was negligible, suggesting that $\alpha\text{IIb}\beta 3$ activation is crucial to platelet activation by *M. circinelloides* NRRL3631 interaction (3Bii).

Figure 2. Platelet aggregation in response to *Mucor circinelloides* NRRL3631 is supported by the $\text{Fc}\gamma\text{RIIA}$ receptor and integrin $\alpha\text{IIb}\beta 3$ (A) *Mucor circinelloides* NRRL3631 is recognized by the $\text{Fc}\gamma\text{RIIA}$ receptor. Platelet aggregation in response to *M. circinelloides* NRRL3631 in the presence and absence of $\text{Fc}\gamma\text{RIIA}$ blocking mAb IV.3 was measured in PRP using light-transmission aggregometry over 30 min. mAb IV.3 significantly inhibited platelet aggregation in response to *M. circinelloides* NRRL3631. Data shown are mean \pm SEM of five independent experimental repeats; $**p < 0.01$, Mann–Whitney U test. (B) Platelet aggregation in response to *Mucor circinelloides* NRRL3631 is supported by the $\alpha\text{IIb}\beta 3$ integrin. Platelet aggregation in response to *M. circinelloides* NRRL3631 spores in the presence and absence of $\alpha\text{IIb}\beta 3$ inhibitor, eptifibatide, was measured in PRP using light-transmission aggregometry over 30 min. Eptifibatide significantly inhibited platelet aggregation in response to *M. circinelloides* NRRL3631. Data shown are mean \pm SEM of five independent experimental repeats; $*p < 0.05$, $**p < 0.01$, Mann–Whitney U test. (C) *Mucor circinelloides* NRRL3631-platelet interaction does not affect $\text{Fc}\gamma\text{RIIA}$ platelet surface expression but does (D) increase $\alpha\text{IIb}\beta 3$ platelet surface expression. Platelets were labeled for $\text{Fc}\gamma\text{RIIA}$, using conjugated anti-human CD32 + anti-mouse 2° Alexa 488, and $\alpha\text{IIb}\beta 3$, using APC-Mouse Anti-Human CD41a. Platelet surface expression of $\text{Fc}\gamma\text{RIIA}$ and $\alpha\text{IIb}\beta 3$ were read using flow cytometry.



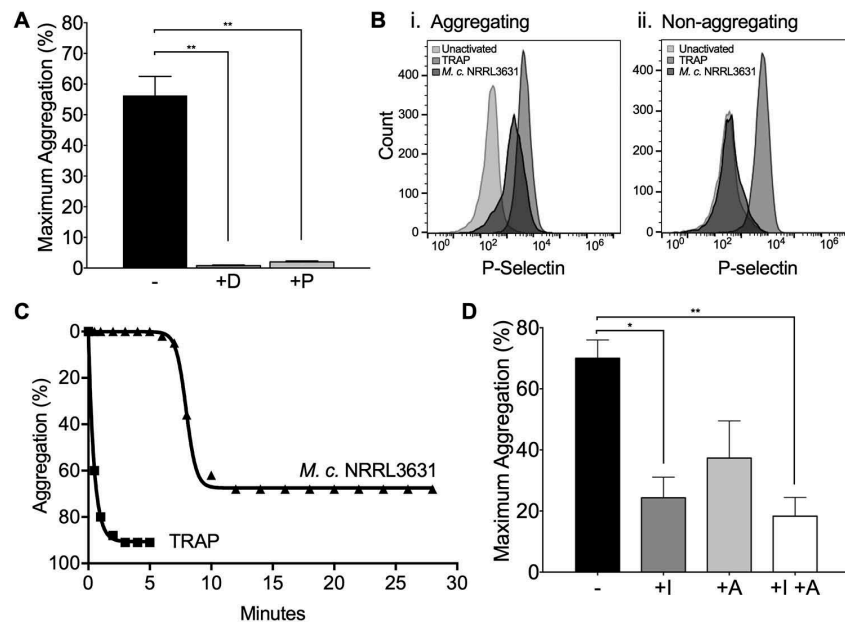


Figure 3. *Mucor circinelloides* NRRL3631 activates Src and Syk signaling cascades and induces platelet activation supported by secondary mediators TxA_2 and ADP (A) *Mucor circinelloides* NRRL3631 activates the Src and Syk signaling cascades. Platelet aggregation in response to *M. circinelloides* NRRL3631 in the presence and absence of Src receptor inhibitor, dasatinib (4 μM), and Syk inhibitor, PRT-060318 (10 μM), was measured in PRP using light-transmission aggregometry over 30 min. Dasatinib significantly inhibited platelet aggregation in response to *M. circinelloides* NRRL3631. PRT-060318 also significantly inhibited platelet aggregation in response to *M. circinelloides* NRRL3631. Data shown are mean \pm SEM of five independent experimental repeats; $^{**}p < 0.01$, Mann-Whitney U test. (B) *M. circinelloides* NRRL3631 activates platelets under (i) aggregating conditions but not under (ii) non-aggregating conditions. Platelet aggregation in response to *M. circinelloides* NRRL3631 in the presence and absence of $\alpha\text{IIb}\beta_3$ inhibitor, eptifibatide, and was measured in PRP using light-transmission aggregometry over 30 min. Platelets were labelled for CD62P activation marker using CD62P-FITC and surface expression read using flow cytometry. (i) Under aggregating conditions CD62P expression is enhanced following *M. circinelloides* NRRL3631 exposure. (ii) Under non-aggregating conditions, change in CD62P expression is undetectable following *M. circinelloides* NRRL3631 exposure. (C) Example aggregation traces showing fast initiation of platelet aggregation in response to the agonist TRAP and a lag phase before induction of platelet activation in response to fungal spores. (D) Secondary mediators TxA_2 and ADP play a role in *M. circinelloides* NRRL3631-induced platelet aggregation. Platelet aggregation in response to *M. circinelloides* NRRL3631 in the presence and absence of TxA_2 inhibitor, indomethacin (30 μM), and ADP inhibitor, apyrase (2 U), was measured in PRP using light-transmission aggregometry over 30 min. Indomethacin significantly inhibited platelet aggregation in response to *M. circinelloides* NRRL3631, and apyrase markedly reduced platelet aggregation in response to *M. circinelloides* NRRL3631. Combined indomethacin and apyrase treatment significantly further reduced platelet aggregation in response to *M. circinelloides* NRRL3631. Data shown are mean \pm SEM of three independent experimental repeats; $^*p < 0.05$, $^{**}p < 0.01$, One-way ANOVA with post hoc Dunnett's multiple comparison test.

While platelet aggregation in response to the agonist TRAP occurs rapidly within minutes, platelet aggregation in response to spores is characterised by a lag-phase (Figure 3C). This long incubation time needed to detect spore-induced platelet aggregation suggests that secondary mediators might be required for the platelet response. The secondary mediators, thromboxane A_2 (TxA_2) and adenosine 5'-diphosphate (ADP), are released upon platelet activation and act to support clot consolidation [19,20]. Platelets were treated with TxA_2 inhibitor, indomethacin, and ADP inhibitor, apyrase, prior to *M. circinelloides* NRRL3631 spore exposure. TxA_2 and ADP inhibition independently (e.g. at 1:10 spore:platelet ratio: 70.0 \pm 6.0%; (+)indomethacin: 24.3 \pm 6.8%; (+)apyrase: 37.3 \pm 12.2%) and in combination (e.g. at 1:10 spore: platelet ratio (+)indomethacin(+apyrase: 18.3 \pm 6.1%) reduced *M. circinelloides* NRRL3631-induced platelet aggregation (Figure 3D).

In summary, these data demonstrate that spore interaction with platelet receptors activates downstream Src and Syk tyrosine kinases leading to platelet activation including the release of α -granules shown by increased surface expression of the activation marker P-selectin and by increased expression of integrin $\alpha\text{IIb}\beta_3$. Activation is supported by secondary mediators TxA_2 and ADP.

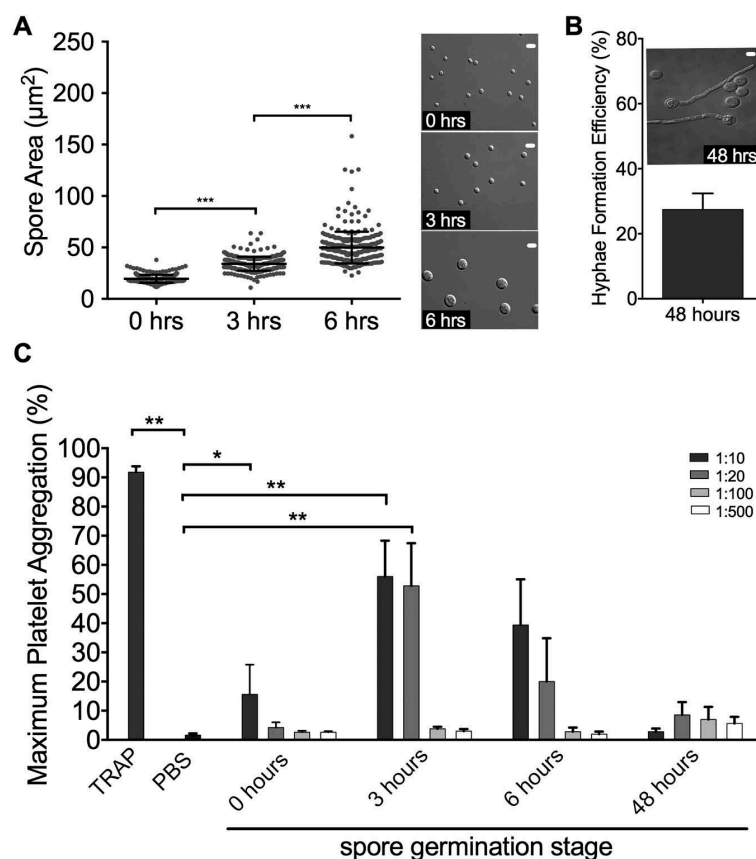
Mucor circinelloides NRRL3631 spore developmental stage impacts on platelet aggregation

Mucormycete spores undergo both metabolic and structural changes during development from spore to hyphae [21]. The host encounters these different developmental stages during infection, thus requiring a dynamic response. We hypothesized that the developmental stage of the *M. circinelloides* NRRL3631 spore would influence its platelet aggregation potential.

We first identified stages of germination at which a significant increase in spore size occurs. Resting spores at the start of germination, displayed a surface area of 19.8 \pm 3.0 μm^2 (Figure 4A). Spores significantly increased in size at 3 h germination (34.1 \pm 6.8 μm^2 ; $p < 0.05$), and furthermore at 6 h germination (49.9 \pm 15.4 μm^2 ; $p < 0.05$). Hyphae formation was observed on spores at 48 h germination (hyphae formation efficiency: 27.5 \pm 8.5%) (Figure 4B).

We investigated *M. circinelloides* NRRL3631 spores at 0, 3, and 6 h germination, and hyphae at 48 h germination in PRP, and showed that the developmental stage of *M. circinelloides* NRRL3631 influences its platelet aggregation potential (Figure 4C).

Figure 4. *Mucor circinelloides* NRRL3631 spore developmental stage impacts on platelet aggregation (A) *Mucor circinelloides* spore development. *M. circinelloides* NRRL3631 spore swelling was investigated over 0, 3, and 6 h. Spores were visualized by DIC light microscopy at 60x magnification; scale bar: 5µm. 100 spores from each time point were analysed on ImageJ: a length and width measurement (in µm) was taken from each spore and the spore area calculated ((length/2)*(width/2)*π). *M. circinelloides* NRRL3631 spores exhibited significant increase in size from 0 to 3 h germination, and from 3 to 6 h germination. Data shown are pooled data points with mean±SD of three independent experimental repeats, each analysing the surface area of 100 spores per incubation period; *** $p < 0.001$, one-way ANOVA with post hoc Dunnett's multiple comparison test. (B) *M. circinelloides* hyphae formation efficiency. *M. circinelloides* NRRL3631 hyphae formation was studied at 48 h germination. Spores were visualized by DIC light microscopy at 60x magnification; scale bar: 10µm. 100 spores at 48 h germination were analysed on ImageJ to determine the percentage of hyphae per 100 spores. Data shown are mean±SEM from three independent experimental repeats; scale bar: 10µm. (C) Platelet aggregation potential is dependent on the developmental stage of *Mucor circinelloides* NRRL3631. Platelet aggregation in response to *M. circinelloides* NRRL3631 spores over progressive developmental stages, was measured in PRP using light-transmission aggregometry over 30 min. *M. circinelloides* NRRL3631 spores at time zero germination induced significant platelet aggregation at a 1:10 spore:platelet ratio. *M. circinelloides* NRRL3631 spores at 3 hours germination induced significant platelet aggregation at a 1:10 and 1:20 spore:platelet ratio (data from Figure 2B). *M. circinelloides* NRRL3631 spores at 6 h induced aggregation to a lesser degree than those at 3 hours germination, and spores at 48 hours germination induced negligible platelet aggregation. Data shown are mean±SEM of five independent experimental repeats; * $p < 0.05$, ** $p < 0.01$, Kruskal-Wallis test.



At the beginning of germination, *M. circinelloides* NRRL3631 induced significant platelet aggregation (1:10: $15.6 \pm 10.2\%$; $p < 0.05$), however to a lesser degree than spores at 3 h germination (1:10: $56.0 \pm 12.3\%$; $p < 0.01$). As *M. circinelloides* NRRL3631 spore development progressed beyond 3 h germination, platelet aggregation potential declined (6 h germination; 1:10: $32.6 \pm 14.3\%$). Moreover, *M. circinelloides* NRRL3631 spores exhibiting hyphae formation at 48 h germination induced negligible platelet aggregation (1:10: $2.80 \pm 1.11\%$).

Together, this shows that the platelet response to *M. circinelloides* varies with the spore developmental stage, indicating a dynamic interaction pattern that needs to be considered for mucormycosis treatment approaches.

Discussion

Clinical management of mucormycosis remains a challenge while the disease incidence is on the rise. Many of our antifungal agents are ineffective against mucormycetes and associated with toxic side effects. The gold standard therapy still is surgical debridement often leading to long-term disability. Together, this results in

extremely high mortality in patients with mucormycosis and highlights the need for more effective therapeutic strategies.

Thrombosis is a hallmark of mucormycosis. It is currently not clear if thrombus formation is beneficial for the patient by containing the fungus or detrimental due to reduced oxygen supply and subsequent tissue necrosis. Ability to manipulate the platelet—spore interaction, either by enhancing or inhibiting, might be a promising medical approach to improve patient outcome.

To identify potential targets for medical intervention, we here elucidated components of the signaling pathway underlying platelet—spore interaction. Our data demonstrate that platelets form aggregates surrounding mucormycete spores, the infectious agent of mucormycosis. This aggregation is dose-dependent. Platelet activation by spores is mediated through the platelet receptors FcγRIIA and αIIbβ3 and, the Syk/Src signaling cascade to induces α-granules release. This activation is supported by the secondary mediators TxA₂ and ADP. The dose-dependent nature of platelet aggregation (Figure 1B) mimics the all-or-nothing response previously described for *E. coli* and Gram-positive bacteria [8,9] suggesting a positive feedback mechanism supporting platelet aggregation. Inhibitor studies suggest that FcγRIIA is an essential receptor for platelet activation in response to fungal

spores (Figure 2A). As no aggregation was observed in washed platelets, this suggests that one or more plasma factor(s) mediate this interaction. The current literature suggests these are IgG, by forming an immune complex with spores, to interact with FcγRIIA and fibrinogen as a bridging molecule to interact with αIIbβ3 [9]. While we currently do not know the fungal cell wall components interacting with platelets and whether this interaction is direct or indirect, binding of fibrinogen has been reported to *Candida albicans* cell wall [22]. Due to the constant exposure of humans to these environmentally ubiquitous fungal spores, it is also highly likely that humans have circulating antibodies to support the platelet-spore interaction. Research on bacterial interaction with platelets has shown that several platelet receptors are required for efficient platelet activation [8,9,23–25]. Similarly, platelet activation after spore encounter also requires integrin αIIbβ3 (Figure 2B) and secondary mediators TxA₂ and ADP supporting the notion of positive feedback mechanisms reinforcing initial FcγRIIA activation. Inside-out signaling has previously been reported for αIIbβ3 to induce secondary platelet-platelet aggregation after initial activation in response to a stimulus through FcγRIIA [8,26,27]. Thus both receptors might have dual functionality in initiating as well as amplifying thrombus formation. Together, these signaling events correspond to those reported previously for a range of bacterial interaction with platelets [8,9] and thus indicate that the platelet response to infectious particles is conserved.

The conserved nature of the platelet activation pathway in response to pathogens might be indicative of a protective innate immune function performed by platelets. Attachment of platelets to fungal hyphae has shown to result in hyphal damage and reduced viability [6,28]. Yet, a potential detrimental outcome due to excessive platelet aggregation causing tissue necrosis, similar to exaggerated inflammatory responses needs to be considered. The release of immune-stimulatory effectors such as pro-inflammatory and pro-necrotic factor TNF-α and phagocyte chemoattractant TGF-β in α-granules [29] would support this idea. In the context of mucormycosis, thrombocytopenia has been suggested as factor for severe disease and poor patient outcome [30,31] suggesting that thrombus formation contributes to disease pathology.

During filamentous fungal infections, platelets encounter a range of morphological structures. While initial infection often occurs through inhalation of spores, the propagules then undergo a developmental program of metabolic and physiological changes to form invasive hyphae. During this germination process, water uptake causes the spore to ‘swell’ and undergo a change in both size and structural composition. As mucormycete spores germinate, there is a depletion of melanin from the outer surface exposing a glucan-rich outer wall [32]. In the latter stages of germination hyphae are formed, the outer wall of which is chitosan-rich and formed by the germinating spore’s inner wall [32]. During the preliminary stages of *M. circinelloides* NRRL3631 germination we saw a stark increase in platelet aggregation potential, reaching a peak at 3 h germination, where spores are between resting and maximal swelling stage. Surprisingly, platelet aggregation potential of *M. circinelloides* NRRL3631 declined toward the latter stages of germination as spores reach their maximal swelling stage, and *M. circinelloides* hyphal structures appeared to induce negligible platelet aggregation altogether. Two plausible explanations for the change in mucormycete spore platelet aggregation potential during germination are: (I) compositional changes of the germinating mucormycete spore; and (II) the secretion of platelet inhibitory fungal secretory factors. The secretion of platelet inhibitory fungal secretory factor has been shown in *Candida albicans* [33]. *C. albicans* activates platelets but inhibits aggregation to fibrinogen, in part via the fungal secretory factor gliotoxin [33].

In summary, this is the first analysis of the signaling underlying platelet aggregation in response to fungi and thus providing a better understanding of this interaction. The interaction with fungi is dependent on the developmental stage of the fungus, which might lead to different outcomes of this interaction that can be beneficial as well as detrimental to the host. This needs to be carefully considered for the clinical management of patients. During mucormycosis, platelets have the potential to inhibit the germination process of mucormycetes [6]. We identify several receptors and the downstream signaling components that could be targeted with already available medical interventions as preventative measures inhibiting disease onset (i.e. spore germination) or by targeting thrombus formation to improve current disease outcome.

Acknowledgments

We would like to thank Soo Chan Lee for providing the mucormycete strain NRRL3631 used in this study.

Declaration of Interests

The authors report no declarations of interest.

Funding

This work was supported by Wellcome ISSF grant [175ISSFPP to KV] and the British Heart Foundation [CH03/03 to SPW]. HG is supported by MRC doctoral training partnership: Integrated Midlands Partnership for Biomedical Training (MR/N013913/1).

Supplemental data

Supplemental data for this article can be access on the [publisher's website](#).

Notes on contributor

Conceived and designed the experiments: KV, SPW, HG, MZ. Performed the experiments: HG, AS-R, MZ. Analyzed the data: HG, SW, KV. Wrote the paper: HG, KV. Critically reviewed the manuscript: KV, SPW.

ORCID

Malou Zuidschewoude  <http://orcid.org/0000-0002-5071-9000>

References

- [1] Chayakulkeeree M, Ghannoum MA, Perfect JR. Zygomycosis: the re-emerging fungal infection. *Eur J Clin Microbiol Infect Dis*. 2006;25(4):215–229.
- [2] Greenberg RN, Scott LJ, Vaughn HH, Ribes JA. zygomycosis (mucormycosis): emerging clinical importance and new treatments. *Curr Opin Infect Dis*. 2004;17(6):517–525.
- [3] Spellberg B, Edwards J Jr., Ibrahim A. Novel perspectives on mucormycosis: pathophysiology, presentation, and management. *Clin Microbiol Rev*. 2005;18(3):556–569.
- [4] Roden MM, Zaoutis TE, Buchanan WL, Knudsen TA, Sarkisova TA, Schaufele RL, Sein M, Sein T, Chiou CC, Chu JH, et al. Epidemiology and outcome of zygomycosis: a review of 929 reported cases. *Clin Infect Dis*. 2005;41(5):634–653.
- [5] Brown GD, Denning DW, Gow NA, Levitz SM, Netea MG, White TC. Hidden killers: human fungal infections. *Sci Transl Med*. 2012;4(165):165rv113.
- [6] Perkhof S, Kainzner B, Kehrel BE, Dierich MP, Nussbaumer W, Lass-Flörl C. Potential antifungal effects of human platelets against zygomycetes *in vitro*. *J Infect Dis*. 2009;200(7):1176–1179.
- [7] Keane C, Petersen H, Reynolds K, Newman DK, Cox D, Jenkinson HF, Newman PJ, Kerrigan SW. Mechanism of outside-in {alpha}IIb {beta}3-mediated activation of human platelets by the colonizing

- Bacterium, *Streptococcus gordonii*. *Arterioscler Thromb Vasc Biol*. 2010;30(12):2408–2415.
- [8] Arman M, Krauel K, Tilley DO, Weber C, Cox D, Greinacher A, Kerrigan SW, Watson SP. Amplification of bacteria-induced platelet activation is triggered by FcgammaRIIA, integrin alphaIIb beta3, and platelet factor 4. *Blood*. 2014;123(20):3166–3174.
- [9] Watson CN, Kerrigan SW, Cox D, Henderson IR, Watson SP, Arman M. Human platelet activation by *Escherichia coli*: roles for FcgammaRIIA and integrin alphaIIb beta3. *Platelets*. 2016;27(6):535–40. doi: 10.3109/09537104.2016.1148129.
- [10] Li CH, Cervantes M, Springer DJ, Boekhout T, Ruiz-Vazquez RM, Torres-Martinez SR, Heitman J, Lee SC. Sporangiospore size dimorphism is linked to virulence of *Mucor circinelloides*. *PLoS Pathog*. 2011;7(6):e1002086.
- [11] Schindelin J, Arganda-Carreras I, Frise E, Kaynig V, Longair M, Pietzsch T, Preibisch S, Rueden C, Saalfeld S, Schmid B, et al. Fiji: an open-source platform for biological-image analysis. *Nat Methods*. 2012;9(7):676–682.
- [12] Preibisch S, Amat F, Stamatakis E, Sarov M, Singer RH, Myers E, Tomancak P. Efficient Bayesian-based multiview deconvolution. *Nat Methods*. 2014;11(6):645–648.
- [13] Cox D, Kerrigan SW, Watson SP. Platelets and the innate immune system: mechanisms of bacterial-induced platelet activation. *J Thromb Haemost*. 2011;9(6):1097–1107.
- [14] Qiao J, Al-Tamimi M, Baker RI, Andrews RK, Gardiner EE. The platelet Fc receptor, FcgammaRIIa. *Immunol Rev*. 2015;268(1):241–252.
- [15] Deppermann C, Kubes P. Platelets and infection. *Semin Immunol*. 2016;28(6):536–545.
- [16] Senis YA, Mazharian A, Mori J. Src family kinases: at the forefront of platelet activation. *Blood*. 2014;124(13):2013–2024.
- [17] Thornber K, McCarty OJ, Watson SP, Pears CJ. Distinct but critical roles for integrin alphaIIb beta3 in platelet lamellipodia formation on fibrinogen, collagen-related peptide and thrombin. *Febs J*. 2006;273(22):5032–5043.
- [18] Wasiluk A, Kemona H, Mantur M, Polewko A, Ozmirski A, Milewski R. Expression of P-selectin (CD62P) on platelets after thrombin and ADP in hypotrophic and healthy, full-term newborns. *J Matern Fetal Neonatal Med*. 2013;26(13):1321–1324.
- [19] Paul BZ, Jin J, Kunapuli SP. Molecular mechanism of thromboxane A(2)-induced platelet aggregation. Essential role for p2t(ac) and alpha(2a) receptors. *J Biol Chem*. 1999;274(41):29108–29114.
- [20] Woulfe D, Yang J, Brass L. ADP and platelets: the end of the beginning. *J Clin Invest*. 2001;107(12):1503–1505.
- [21] Petraitis V, Petraitiene R, Antachopoulos C, Hughes JE, Cotton MP, Kasai M, Harrington S, Gamaletsou MN, Bacher JD, Kontoyiannis DP, et al. Increased virulence of *Cunninghamella bertholletiae* in experimental pulmonary mucormycosis: correlation with circulating molecular biomarkers, sporangiospore germination and hyphal metabolism. *Med Mycol*. 2013;51(1):72–82.
- [22] Senet JM. *Candida* adherence phenomena, from commensalism to pathogenicity. *Int Microbiol*. 1998;1(2):117–122.
- [23] Kerrigan SW. The expanding field of platelet-bacterial interconnections. *Platelets*. 2015;26(4):293–301.
- [24] Fitzgerald JR, Foster TJ, Cox D. The interaction of bacterial pathogens with platelets. *Nat Rev Microbiol*. 2006;4(6):445–457.
- [25] Pampolina C, McNicol A. *Streptococcus sanguis*-induced platelet activation involves two waves of tyrosine phosphorylation mediated by FcgammaRIIA and alphaIIb beta3. *Thromb Haemost*. 2005;93(5):932–939.
- [26] Boylan B, Gao C, Rathore V, Gill JC, Newman DK, Newman PJ. Identification of FcgammaRIIa as the ITAM-bearing receptor mediating alphaIIb beta3 outside-in integrin signaling in human platelets. *Blood*. 2008;112(7):2780–2786.
- [27] Zhi H, Rauova L, Hayes V, Gao C, Boylan B, Newman DK, McKenzie SE, Cooley BC, Poncz M, Newman PJ. Cooperative integrin/ITAM signaling in platelets enhances thrombus formation *in vitro* and *in vivo*. *Blood*. 2013;121(10):1858–1867.
- [28] Perkhofer S, Kehrel BE, Dierich MP, Donnelly JP, Nussbaumer W, Hofmann J, Von Eiff C, Lass-Flörl C. Human platelets attenuate *Aspergillus* species via granule-dependent mechanisms. *J Infect Dis*. 2008;198(8):1243–1246.
- [29] Whiteheart SW. Platelet granules: surprise packages. *Blood*. 2011;118(5):1190–1191.
- [30] Chang FY, Singh N, Gayowski T, Wagener MM, Mietzner SM, Stout JE, Marino IR. Thrombocytopenia in liver transplant recipients: predictors, impact on fungal infections, and role of endogenous thrombopoietin. *Transplantation*. 2000;69(1):70–75.
- [31] Bloxham CA, Carr S, Ryan DW, Kesteven PJ, Bexton RS, Griffiths ID, Richards J. Disseminated zygomycosis and systemic lupus erythematosus. *Intensive Care Med*. 1990;16(3):201–207.
- [32] Bartnickigarcia S, Reyes E. Chemistry of spore wall differentiation in *Mucor Rouxii*. *Arch Biochem Biophys*. 1964;108(1):125.
- [33] Bertling A, Niemann S, Uekotter A, Fegeler W, Lass-Flörl C, Von Eiff C, Kehrel BE. *Candida albicans* and its metabolite gliotoxin inhibit platelet function via interaction with thiols. *Thromb Haemost*. 2010;104(2):270–278.

APPENDIX II: RNA-SEQUENCING SUPPLEMENTARY DATA

I. SEQUENCE QUALITY

TABLE S1. SAMPLE SEQUENCE STATISTICS

Sample ID	# Reads	Yield (Mbases)	Mean Quality Score	% Bases >= 30
HGH01_0hr-n-1	18581013	5574	35.95	93.96
HGH01_0hr-n-2	18249854	5475	35.99	94.14
HGH01_0hr-n-3	19392437	5818	36.01	94.26
HGH01_0hr-n-4	22076064	6623	35.96	94.01
HGH01_3hr-n-1	34362150	10309	36.01	94.25
HGH01_3hr-n-2	29347764	8804	35.98	94.16
HGH01_3hr-n-3	32128084	9638	35.95	93.91
HGH01_3hr-n-4	56055335	16817	36.01	94.21
HGH01_6hr-n-1	62608480	18783	35.81	93.2
HGH01_6hr-n-2	36638521	10992	35.99	94.08
HGH01_6hr-n-3	27372837	8212	35.99	94.09
HGH01_6hr-n-4	36800091	11040	35.92	93.71
TOTAL	393612630	118085	35.96	94.00

II. TRANSCRIPTIONAL PROFILING OF *M. CIRCINELLOIDES* GERMINATION

TABLE S2. BIOLOGICAL PROCESS GO TERMS ASSOCIATED WITH METABOLIC PROCESSES: 0 HR VS 3 HR, UPREGULATED GENES

GO ID	GO TERM	Gene Count	Benjamini
GO:0006139	nucleobase-containing compound metabolic process	386	1.27E-13
GO:0034660	ncRNA metabolic process	116	3.68E-13
GO:0046483	heterocycle metabolic process	411	4.77E-12
GO:0006725	cellular aromatic compound metabolic process	411	4.77E-12
GO:1901360	organic cyclic compound metabolic process	420	8.77E-11
GO:0016070	RNA metabolic process	221	1.09E-09
GO:0006399	tRNA metabolic process	78	6.07E-09
GO:1901135	carbohydrate derivative metabolic process	164	1.05E-08
GO:0055086	nucleobase-containing small molecule metabolic process	112	1.14E-08
GO:0009117	nucleotide metabolic process	93	3.35E-08
GO:0006753	nucleoside phosphate metabolic process	93	3.35E-08
GO:0090304	nucleic acid metabolic process	273	9.52E-08
GO:0034641	cellular nitrogen compound metabolic process	513	2.85E-07
GO:0009259	ribonucleotide metabolic process	71	5.51E-07
GO:0019693	ribose phosphate metabolic process	71	5.51E-07
GO:0009150	purine ribonucleotide metabolic process	64	4.17E-06
GO:0019637	organophosphate metabolic process	147	4.93E-06
GO:0006163	purine nucleotide metabolic process	63	6.40E-06
GO:0009141	nucleoside triphosphate metabolic process	27	1.10E-05
GO:0071704	organic substance metabolic process	1003	4.18E-05

GO:0009205	purine ribonucleoside triphosphate metabolic process	25	4.18E-05
GO:0009167	purine ribonucleoside monophosphate metabolic process	24	7.83E-05
GO:0009199	ribonucleoside triphosphate metabolic process	24	7.83E-05
GO:0016072	rRNA metabolic process	38	0.000125166
GO:0044281	small molecule metabolic process	251	0.000140486
GO:0044237	cellular metabolic process	904	0.000147964
GO:0072521	purine-containing compound metabolic process	63	0.000177362
GO:0009123	nucleoside monophosphate metabolic process	27	0.000340142
GO:0009144	purine nucleoside triphosphate metabolic process	21	0.000564002
GO:0046034	ATP metabolic process	40	0.000618933
GO:0044238	primary metabolic process	931	0.001048
GO:0009161	ribonucleoside monophosphate metabolic process	25	0.001055833
GO:0006807	nitrogen compound metabolic process	812	0.003858412
GO:0043170	macromolecule metabolic process	659	0.005064713
GO:0072527	pyrimidine-containing compound metabolic process	20	0.005157375
GO:0008152	metabolic process	1157	0.006290335
GO:0006220	pyrimidine nucleotide metabolic process	16	0.006290335
GO:0046128	purine ribonucleoside metabolic process	14	0.010063782
GO:0009225	nucleotide-sugar metabolic process	15	0.012018469
GO:0009126	purine nucleoside monophosphate metabolic process	15	0.026145831
GO:0043094	cellular metabolic compound salvage	11	0.031393939
GO:0006743	ubiquinone metabolic process	7	0.06753381
GO:1901661	quinone metabolic process	7	0.06753381
GO:0009100	glycoprotein metabolic process	34	0.073201204
GO:0044255	cellular lipid metabolic process	79	0.07954415
GO:0046500	S-adenosylmethionine metabolic process	5	0.085314788
GO:0009129	pyrimidine nucleoside monophosphate metabolic process	8	0.089137297
GO:0009218	pyrimidine ribonucleotide metabolic process	11	0.121876749
GO:0006544	glycine metabolic process	6	0.135720168
GO:0046033	AMP metabolic process	6	0.135720168
GO:0006259	DNA metabolic process	82	0.136399274
GO:0009132	nucleoside diphosphate metabolic process	21	0.142473471
GO:0006644	phospholipid metabolic process	44	0.1562274
GO:0019752	carboxylic acid metabolic process	134	0.1765703
GO:0006629	lipid metabolic process	107	0.180884221
GO:0009147	pyrimidine nucleoside triphosphate metabolic process	8	0.180884221
GO:0006084	acetyl-CoA metabolic process	8	0.180884221
GO:0019692	deoxyribose phosphate metabolic process	4	0.180884221
GO:0009069	serine family amino acid metabolic process	13	0.182011992
GO:0006720	isoprenoid metabolic process	13	0.182011992
GO:0006730	one-carbon metabolic process	10	0.184790042
GO:0006650	glycerophospholipid metabolic process	29	0.185926241
GO:0043436	oxoacid metabolic process	134	0.193839362
GO:0006090	pyruvate metabolic process	18	0.208243762
GO:0046031	ADP metabolic process	17	0.217341899
GO:0009185	ribonucleoside diphosphate metabolic process	17	0.217341899

GO:0009135	purine nucleoside diphosphate metabolic process	17	0.217341899
GO:0009179	purine ribonucleoside diphosphate metabolic process	17	0.217341899
GO:0006082	organic acid metabolic process	134	0.24724448
GO:0006520	cellular amino acid metabolic process	91	0.252627518
GO:0042157	lipoprotein metabolic process	13	0.252627518
GO:0009116	nucleoside metabolic process	13	0.252627518
GO:1901657	glycosyl compound metabolic process	13	0.252627518
GO:0006505	GPI anchor metabolic process	12	0.252627518
GO:1903509	liposaccharide metabolic process	12	0.252627518
GO:0006664	glycolipid metabolic process	12	0.252627518
GO:0046049	UMP metabolic process	6	0.252627518
GO:0009262	deoxyribonucleotide metabolic process	6	0.252627518
GO:0006547	histidine metabolic process	6	0.252627518
GO:0009173	pyrimidine ribonucleoside monophosphate metabolic process	6	0.252627518
GO:0006047	UDP-N-acetylglucosamine metabolic process	7	0.257008231
GO:0046040	IMP metabolic process	8	0.257142876
GO:0006793	phosphorus metabolic process	243	0.292265999
GO:0046486	glycerolipid metabolic process	29	0.301797596

Table S3. BIOLOGICAL PROCESS GO TERMS: 0 HR VS 3 HR, UPREGULATED GENES

GO ID	GO TERM	Gene Count	Benjamini
GO:0006139	nucleobase-containing compound metabolic process	386	1.27E-13
GO:0034660	ncRNA metabolic process	116	3.68E-13
GO:0046483	heterocycle metabolic process	411	4.77E-12
GO:0006725	cellular aromatic compound metabolic process	411	4.77E-12
GO:1901360	organic cyclic compound metabolic process	420	8.77E-11
GO:0022613	ribonucleoprotein complex biogenesis	79	1.97E-10
GO:0043038	amino acid activation	39	6.49E-10
GO:0043039	tRNA aminoacylation	39	6.49E-10
GO:0016070	RNA metabolic process	221	1.09E-09
GO:1901137	carbohydrate derivative biosynthetic process	115	1.66E-09
GO:0044249	cellular biosynthetic process	464	5.68E-09
GO:0006418	tRNA aminoacylation for protein translation	36	5.68E-09
GO:0006399	tRNA metabolic process	78	6.07E-09
GO:0006260	DNA replication	47	6.07E-09
GO:0009058	biosynthetic process	493	8.64E-09
GO:1901135	carbohydrate derivative metabolic process	164	1.05E-08
GO:1901576	organic substance biosynthetic process	476	1.07E-08
GO:0055086	nucleobase-containing small molecule metabolic process	112	1.14E-08
GO:1902600	proton transmembrane transport	35	3.35E-08
GO:0009117	nucleotide metabolic process	93	3.35E-08
GO:0006753	nucleoside phosphate metabolic process	93	3.35E-08
GO:0090304	nucleic acid metabolic process	273	9.52E-08
GO:0090407	organophosphate biosynthetic process	108	1.54E-07

GO:0042254	ribosome biogenesis	59	1.96E-07
GO:0034641	cellular nitrogen compound metabolic process	513	2.85E-07
GO:0009165	nucleotide biosynthetic process	67	5.35E-07
GO:1901293	nucleoside phosphate biosynthetic process	67	5.35E-07
GO:0009259	ribonucleotide metabolic process	71	5.51E-07
GO:0019693	ribose phosphate metabolic process	71	5.51E-07
GO:0009987	cellular process	1390	1.57E-06
GO:0006396	RNA processing	129	1.93E-06
GO:0034470	ncRNA processing	77	2.46E-06
GO:0009150	purine ribonucleotide metabolic process	64	4.17E-06
GO:0046390	ribose phosphate biosynthetic process	50	4.28E-06
GO:0009260	ribonucleotide biosynthetic process	50	4.28E-06
GO:0019637	organophosphate metabolic process	147	4.93E-06
GO:0006163	purine nucleotide metabolic process	63	6.40E-06
GO:0044085	cellular component biogenesis	113	7.91E-06
GO:0034654	nucleobase-containing compound biosynthetic process	125	1.01E-05
GO:0009141	nucleoside triphosphate metabolic process	27	1.10E-05
GO:0006457	protein folding	40	1.23E-05
GO:0009142	nucleoside triphosphate biosynthetic process	25	1.50E-05
GO:0071840	cellular component organization or biogenesis	183	1.86E-05
GO:0098662	inorganic cation transmembrane transport	42	2.80E-05
GO:0098655	cation transmembrane transport	42	2.80E-05
GO:0098660	inorganic ion transmembrane transport	42	2.80E-05
GO:0009201	ribonucleoside triphosphate biosynthetic process	24	2.99E-05
GO:0019438	aromatic compound biosynthetic process	147	3.49E-05
GO:0071704	organic substance metabolic process	1003	4.18E-05
GO:0009205	purine ribonucleoside triphosphate metabolic process	25	4.18E-05
GO:0034220	ion transmembrane transport	45	5.66E-05
GO:0006754	ATP biosynthetic process	18	5.66E-05
GO:0015985	energy coupled proton transport, down electrochemical gradient	18	5.66E-05
GO:0015986	ATP synthesis coupled proton transport	18	5.66E-05
GO:0006364	rRNA processing	38	6.89E-05
GO:0009167	purine ribonucleoside monophosphate metabolic process	24	7.83E-05
GO:0009199	ribonucleoside triphosphate metabolic process	24	7.83E-05
GO:0009152	purine ribonucleotide biosynthetic process	41	7.83E-05
GO:0006164	purine nucleotide biosynthetic process	41	7.83E-05
GO:0016072	rRNA metabolic process	38	0.000125166
GO:0018130	heterocycle biosynthetic process	146	0.000135279
GO:0044281	small molecule metabolic process	251	0.000140486
GO:0044237	cellular metabolic process	904	0.000147964
GO:0072521	purine-containing compound metabolic process	63	0.000177362
GO:0002181	cytoplasmic translation	12	0.000208048
GO:0009145	purine nucleoside triphosphate biosynthetic process	21	0.000221218
GO:0009206	purine ribonucleoside triphosphate biosynthetic process	21	0.000221218
GO:0009123	nucleoside monophosphate metabolic process	27	0.000340142
GO:1901362	organic cyclic compound biosynthetic process	157	0.00035192
GO:0009451	RNA modification	37	0.000366997
GO:0072522	purine-containing compound biosynthetic process	41	0.000394791

GO:0002183	cytoplasmic translational initiation	11	0.000497804
GO:0007018	microtubule-based movement	25	0.000520743
GO:0006928	movement of cell or subcellular component	25	0.000520743
GO:0009124	nucleoside monophosphate biosynthetic process	25	0.000520743
GO:0009144	purine nucleoside triphosphate metabolic process	21	0.000564002
GO:0008150	biological process	1702	0.000618933
GO:0046034	ATP metabolic process	40	0.000618933
GO:0022618	ribonucleoprotein complex assembly	23	0.000821986
GO:0071826	ribonucleoprotein complex subunit organization	23	0.000821986
GO:0007017	microtubule-based process	34	0.000969419
GO:0044238	primary metabolic process	931	0.001048
GO:0009161	ribonucleoside monophosphate metabolic process	25	0.001055833
GO:0001732	formation of cytoplasmic translation initiation complex	10	0.00113067
GO:0032543	mitochondrial translation	12	0.001332397
GO:0140053	mitochondrial gene expression	12	0.001332397
GO:0009059	macromolecule biosynthetic process	271	0.001412383
GO:0032259	methylation	44	0.001412383
GO:0043414	macromolecule methylation	22	0.001469488
GO:0034645	cellular macromolecule biosynthetic process	268	0.0016502
GO:0009156	ribonucleoside monophosphate biosynthetic process	23	0.0016502
GO:0010467	gene expression	315	0.002129114
GO:0072528	pyrimidine-containing compound biosynthetic process	20	0.002383856
GO:0006807	nitrogen compound metabolic process	812	0.003858412
GO:0044271	cellular nitrogen compound biosynthetic process	280	0.004999943
GO:0043170	macromolecule metabolic process	659	0.005064713
GO:0072527	pyrimidine-containing compound metabolic process	20	0.005157375
GO:0008152	metabolic process	1157	0.006290335
GO:0006220	pyrimidine nucleotide metabolic process	16	0.006290335
GO:0006221	pyrimidine nucleotide biosynthetic process	16	0.006290335
GO:0006270	DNA replication initiation	8	0.006598928
GO:0006261	DNA-dependent DNA replication	13	0.007717735
GO:1901566	organonitrogen compound biosynthetic process	299	0.008619763
GO:0046128	purine ribonucleoside metabolic process	14	0.010063782
GO:0008610	lipid biosynthetic process	67	0.010642643
GO:0018193	peptidyl-amino acid modification	30	0.011010053
GO:0009225	nucleotide-sugar metabolic process	15	0.012018469
GO:0009226	nucleotide-sugar biosynthetic process	12	0.01585544
GO:0006812	cation transport	68	0.016318398
GO:0006413	translational initiation	18	0.016537783
GO:0006487	protein N-linked glycosylation	10	0.024425043
GO:0009126	purine nucleoside monophosphate metabolic process	15	0.026145831
GO:0008654	phospholipid biosynthetic process	37	0.026985639
GO:0051169	nuclear transport	19	0.031393939
GO:0006913	nucleocytoplasmic transport	19	0.031393939
GO:0001522	pseudouridine synthesis	11	0.031393939
GO:0043094	cellular metabolic compound salvage	11	0.031393939
GO:0008104	protein localization	101	0.031944496

GO:0008033	tRNA processing	39	0.032429857
GO:0045184	establishment of protein localization	99	0.035922724
GO:0001510	RNA methylation	12	0.037090273
GO:0009127	purine nucleoside monophosphate biosynthetic process	13	0.041794986
GO:0009168	purine ribonucleoside monophosphate biosynthetic process	13	0.041794986
GO:0048193	Golgi vesicle transport	24	0.046111129
GO:0034622	cellular protein-containing complex assembly	47	0.046263541
GO:0015031	protein transport	97	0.046907589
GO:0051028	mRNA transport	16	0.048267202
GO:0050657	nucleic acid transport	17	0.048267202
GO:0050658	RNA transport	17	0.048267202
GO:0051128	regulation of cellular component organization	17	0.048267202
GO:0006403	RNA localization	17	0.048267202
GO:0051236	establishment of RNA localization	17	0.048267202
GO:0033036	macromolecule localization	120	0.052750055
GO:0043933	protein-containing complex subunit organization	57	0.060420217
GO:0044272	sulfur compound biosynthetic process	25	0.062912933
GO:0042181	ketone biosynthetic process	7	0.06753381
GO:0006743	ubiquinone metabolic process	7	0.06753381
GO:1901663	quinone biosynthetic process	7	0.06753381
GO:1901661	quinone metabolic process	7	0.06753381
GO:0006744	ubiquinone biosynthetic process	7	0.06753381
GO:0009100	glycoprotein metabolic process	34	0.073201204
GO:0033043	regulation of organelle organization	15	0.079229025
GO:0071705	nitrogen compound transport	117	0.07954415
GO:0044255	cellular lipid metabolic process	79	0.07954415
GO:0046500	S-adenosylmethionine metabolic process	5	0.085314788
GO:0051649	establishment of localization in cell	88	0.087559465
GO:0009130	pyrimidine nucleoside monophosphate biosynthetic process	8	0.089137297
GO:0009129	pyrimidine nucleoside monophosphate metabolic process	8	0.089137297
GO:0030488	tRNA methylation	8	0.089137297
GO:0009101	glycoprotein biosynthetic process	33	0.099637302
GO:0043413	macromolecule glycosylation	33	0.099637302
GO:0006486	protein glycosylation	33	0.099637302
GO:0065003	protein-containing complex assembly	51	0.102042406
GO:0016043	cellular component organization	128	0.102042406
GO:0009218	pyrimidine ribonucleotide metabolic process	11	0.121876749
GO:0009220	pyrimidine ribonucleotide biosynthetic process	11	0.121876749
GO:0006414	translational elongation	11	0.121876749
GO:0046474	glycerophospholipid biosynthetic process	24	0.124240984
GO:0051641	cellular localization	96	0.126007888
GO:0046907	intracellular transport	85	0.135306526
GO:0006544	glycine metabolic process	6	0.135720168
GO:0006813	potassium ion transport	6	0.135720168
GO:0046033	AMP metabolic process	6	0.135720168
GO:0006259	DNA metabolic process	82	0.136399274
GO:0009132	nucleoside diphosphate metabolic process	21	0.142473471

GO:0006644	phospholipid metabolic process	44	0.1562274
GO:0070085	glycosylation	33	0.162685293
GO:0071702	organic substance transport	129	0.166315375
GO:0034613	cellular protein localization	63	0.166315375
GO:0070727	cellular macromolecule localization	63	0.166315375
GO:0006490	oligosaccharide-lipid intermediate biosynthetic process	7	0.167235367
GO:0019752	carboxylic acid metabolic process	134	0.1765703
GO:0006629	lipid metabolic process	107	0.180884221
GO:0015833	peptide transport	47	0.180884221
GO:0009147	pyrimidine nucleoside triphosphate metabolic process	8	0.180884221
GO:0006084	acetyl-CoA metabolic process	8	0.180884221
GO:0051130	positive regulation of cellular component organization	4	0.180884221
GO:0019692	deoxyribose phosphate metabolic process	4	0.180884221
GO:0018216	peptidyl-arginine methylation	4	0.180884221
GO:0006167	AMP biosynthetic process	4	0.180884221
GO:0018195	peptidyl-arginine modification	4	0.180884221
GO:0006497	protein lipidation	13	0.182011992
GO:0009069	serine family amino acid metabolic process	13	0.182011992
GO:0006888	endoplasmic reticulum to Golgi vesicle-mediated transport	13	0.182011992
GO:0042158	lipoprotein biosynthetic process	13	0.182011992
GO:0006720	isoprenoid metabolic process	13	0.182011992
GO:1902903	regulation of supramolecular fiber organization	9	0.182011992
GO:0008213	protein alkylation	9	0.182011992
GO:0110053	regulation of actin filament organization	9	0.182011992
GO:0009070	serine family amino acid biosynthetic process	9	0.182011992
GO:0006479	protein methylation	9	0.182011992
GO:0008299	isoprenoid biosynthetic process	12	0.184290602
GO:0006730	one-carbon metabolic process	10	0.184790042
GO:0000097	sulfur amino acid biosynthetic process	11	0.184790042
GO:0006650	glycerophospholipid metabolic process	29	0.185926241
GO:0006400	tRNA modification	20	0.185926241
GO:0043436	oxoacid metabolic process	134	0.193839362
GO:0006811	ion transport	82	0.208243762
GO:0006090	pyruvate metabolic process	18	0.208243762
GO:0046031	ADP metabolic process	17	0.217341899
GO:0009185	ribonucleoside diphosphate metabolic process	17	0.217341899
GO:0009135	purine nucleoside diphosphate metabolic process	17	0.217341899
GO:0009179	purine ribonucleoside diphosphate metabolic process	17	0.217341899
GO:0006886	intracellular protein transport	58	0.232700829
GO:0006325	chromatin organization	15	0.239895191
GO:0009263	deoxyribonucleotide biosynthetic process	5	0.239895191
GO:0034314	Arp2/3 complex-mediated actin nucleation	5	0.239895191
GO:0019344	cysteine biosynthetic process	5	0.239895191
GO:0009266	response to temperature stimulus	5	0.239895191
GO:0000154	rRNA modification	5	0.239895191
GO:0009408	response to heat	5	0.239895191
GO:0006448	regulation of translational elongation	5	0.239895191
GO:0045017	glycerolipid biosynthetic process	24	0.247175529
GO:0006082	organic acid metabolic process	134	0.24724448

GO:0006520	cellular amino acid metabolic process	91	0.252627518
GO:0042157	lipoprotein metabolic process	13	0.252627518
GO:0009116	nucleoside metabolic process	13	0.252627518
GO:1901657	glycosyl compound metabolic process	13	0.252627518
GO:0022607	cellular component assembly	58	0.252627518
GO:0009247	glycolipid biosynthetic process	12	0.252627518
GO:0046467	membrane lipid biosynthetic process	12	0.252627518
GO:0006505	GPI anchor metabolic process	12	0.252627518
GO:1903509	liposaccharide metabolic process	12	0.252627518
GO:0006664	glycolipid metabolic process	12	0.252627518
GO:0006506	GPI anchor biosynthetic process	12	0.252627518
GO:0006165	nucleoside diphosphate phosphorylation	18	0.252627518
GO:0046939	nucleotide phosphorylation	18	0.252627518
GO:0045010	actin nucleation	6	0.252627518
GO:0009174	pyrimidine ribonucleoside monophosphate biosynthetic process	6	0.252627518
GO:0000105	histidine biosynthetic process	6	0.252627518
GO:0006488	dolichol-linked oligosaccharide biosynthetic process	6	0.252627518
GO:0046049	UMP metabolic process	6	0.252627518
GO:0006222	UMP biosynthetic process	6	0.252627518
GO:0009262	deoxyribonucleotide metabolic process	6	0.252627518
GO:0006547	histidine metabolic process	6	0.252627518
GO:0043173	nucleotide salvage	6	0.252627518
GO:0009173	pyrimidine ribonucleoside monophosphate metabolic process	6	0.252627518
GO:0006189	'de novo' IMP biosynthetic process	6	0.252627518
GO:0046349	amino sugar biosynthetic process	10	0.257008231
GO:0006048	UDP-N-acetylglucosamine biosynthetic process	7	0.257008231
GO:0009148	pyrimidine nucleoside triphosphate biosynthetic process	7	0.257008231
GO:0032271	regulation of protein polymerization	7	0.257008231
GO:0090066	regulation of anatomical structure size	7	0.257008231
GO:0008064	regulation of actin polymerization or depolymerization	7	0.257008231
GO:0030832	regulation of actin filament length	7	0.257008231
GO:0030833	regulation of actin filament polymerization	7	0.257008231
GO:0006047	UDP-N-acetylglucosamine metabolic process	7	0.257008231
GO:0032535	regulation of cellular component size	7	0.257008231
GO:0051168	nuclear export	9	0.257008231
GO:0032970	regulation of actin filament-based process	9	0.257008231
GO:0051493	regulation of cytoskeleton organization	9	0.257008231
GO:0042398	cellular modified amino acid biosynthetic process	9	0.257008231
GO:0032956	regulation of actin cytoskeleton organization	9	0.257008231
GO:0006188	IMP biosynthetic process	8	0.257142876
GO:0046040	IMP metabolic process	8	0.257142876
GO:0008380	RNA splicing	28	0.260784397
GO:0051276	chromosome organization	27	0.280404006
GO:0006757	ATP generation from ADP	15	0.284220843
GO:0006096	glycolytic process	15	0.284220843
GO:0006793	phosphorus metabolic process	243	0.292265999
GO:0046486	glycerolipid metabolic process	29	0.301797596

TABLE S4. BIOLOGICAL PROCESS GO TERMS ASSOCIATED WITH METABOLIC PROCESSES: 0 HR VS 3 HR, DOWNREGULATED GENES

ID	Name	Gene count	Benjamini
GO:0043603	cellular amide metabolic process	166	5.52E-07
GO:0006518	peptide metabolic process	154	5.52E-07
GO:0009081	branched-chain amino acid metabolic process	18	0.000674089
GO:1901564	organonitrogen compound metabolic process	469	0.022854074
GO:0044267	cellular protein metabolic process	300	0.033201289
GO:1901605	alpha-amino acid metabolic process	53	0.033201289
GO:0019538	protein metabolic process	339	0.040750565
GO:0006549	isoleucine metabolic process	7	0.040750565
GO:0009072	aromatic amino acid family metabolic process	16	0.053386843
GO:0051252	regulation of RNA metabolic process	118	0.078548983
GO:0019219	regulation of nucleobase-containing compound metabolic process	118	0.086233682
GO:0006553	lysine metabolic process	7	0.08884042
GO:0006012	galactose metabolic process	4	0.159833362
GO:0006573	valine metabolic process	8	0.161265714
GO:0080090	regulation of primary metabolic process	134	0.175871138
GO:0031323	regulation of cellular metabolic process	134	0.181284051
GO:1902221	erythrose 4-phosphate/phosphoenolpyruvate family amino acid metabolic process	5	0.181284051
GO:0006558	L-phenylalanine metabolic process	5	0.181284051
GO:0051171	regulation of nitrogen compound metabolic process	133	0.192187601
GO:0006082	organic acid metabolic process	107	0.269596955
GO:0006520	cellular amino acid metabolic process	73	0.294011752
GO:0019222	regulation of metabolic process	137	0.294011752
GO:0060255	regulation of macromolecule metabolic process	136	0.294011752
GO:0008152	metabolic process	861	0.294011752
GO:0019752	carboxylic acid metabolic process	104	0.294011752
GO:0044260	cellular macromolecule metabolic process	378	0.294011752
GO:0006641	triglyceride metabolic process	3	0.294011752
GO:0006639	acylglycerol metabolic process	3	0.294011752
GO:0006638	neutral lipid metabolic process	3	0.294011752
GO:0006551	leucine metabolic process	3	0.294011752
GO:0006570	tyrosine metabolic process	4	0.308335702
GO:0043436	oxoacid metabolic process	104	0.316460657
GO:0009066	aspartate family amino acid metabolic process	15	0.421488045
GO:0019751	polyol metabolic process	9	0.488158787
GO:0006144	purine nucleobase metabolic process	5	0.512422404

TABLE S5. BIOLOGICAL PROCESS GO TERMS: 0 HR VS 3 HR, DOWNREGULATED GENES

ID	Name	Gene count	Benjamini
GO:0006412	translation	150	3.64E-07
GO:0043604	amide biosynthetic process	157	3.64E-07
GO:0043043	peptide biosynthetic process	151	3.95E-07

GO:0043603	cellular amide metabolic process	166	5.52E-07
GO:0006518	peptide metabolic process	154	5.52E-07
GO:0009081	branched-chain amino acid metabolic process	18	0.000674089
GO:0009082	branched-chain amino acid biosynthetic process	12	0.002616492
GO:0061919	process utilizing autophagic mechanism	14	0.00832714
GO:0006914	autophagy	14	0.00832714
GO:0050896	response to stimulus	142	0.01010085
GO:0044282	small molecule catabolic process	30	0.018986528
GO:1901564	organonitrogen compound metabolic process	469	0.022854074
GO:0055114	obsolete oxidation-reduction process	167	0.026997844
GO:0051716	cellular response to stimulus	131	0.028922967
GO:0016054	organic acid catabolic process	22	0.031504221
GO:0046395	carboxylic acid catabolic process	22	0.031504221
GO:0044267	cellular protein metabolic process	300	0.033201289
GO:0019878	lysine biosynthetic process via aminoadipic acid	6	0.033201289
GO:0044271	cellular nitrogen compound biosynthetic process	217	0.033201289
GO:0044248	cellular catabolic process	81	0.033201289
GO:0023052	signaling	87	0.033201289
GO:0007165	signal transduction	87	0.033201289
GO:1901605	alpha-amino acid metabolic process	53	0.033201289
GO:0050794	regulation of cellular process	235	0.034527538
GO:0007154	cell communication	87	0.035995587
GO:0019538	protein metabolic process	339	0.040750565
GO:0006549	isoleucine metabolic process	7	0.040750565
GO:0009085	lysine biosynthetic process	7	0.040750565
GO:0009097	isoleucine biosynthetic process	7	0.040750565
GO:0009056	catabolic process	103	0.042444377
GO:0050789	regulation of biological process	239	0.048650255
GO:0016042	lipid catabolic process	14	0.048650255
GO:0065007	biological regulation	251	0.051024471
GO:0009072	aromatic amino acid family metabolic process	16	0.053386843
GO:1902222	erythrose 4-phosphate/phosphoenolpyruvate family amino acid catabolic process	5	0.065353085
GO:0009099	valine biosynthetic process	5	0.065353085
GO:0006559	L-phenylalanine catabolic process	5	0.065353085
GO:0006468	protein phosphorylation	92	0.066096235
GO:0007031	peroxisome organization	11	0.06801617
GO:0044242	cellular lipid catabolic process	10	0.07728047
GO:1901566	organonitrogen compound biosynthetic process	228	0.078548983
GO:0051252	regulation of RNA metabolic process	118	0.078548983
GO:0019219	regulation of nucleobase-containing compound metabolic process	118	0.086233682
GO:1901607	alpha-amino acid biosynthetic process	33	0.087210281
GO:0006553	lysine metabolic process	7	0.08884042
GO:0009063	cellular amino acid catabolic process	16	0.102525181
GO:0006355	regulation of transcription, DNA-templated	113	0.103858787

GO:1903506	regulation of nucleic acid-templated transcription	113	0.103858787
GO:2001141	regulation of RNA biosynthetic process	113	0.103858787
GO:0035556	intracellular signal transduction	48	0.112634989
GO:0016310	phosphorylation	102	0.15194138
GO:0006012	galactose metabolic process	4	0.159833362
GO:0097720	calcineurin-mediated signaling	4	0.159833362
GO:0006573	valine metabolic process	8	0.161265714
GO:0080090	regulation of primary metabolic process	134	0.175871138
GO:0034645	cellular macromolecule biosynthetic process	196	0.181284051
GO:0031323	regulation of cellular metabolic process	134	0.181284051
GO:0043574	peroxisomal transport	6	0.181284051
GO:1902221	erythrose 4-phosphate/phosphoenolpyruvate family amino acid metabolic process	5	0.181284051
GO:0015919	peroxisomal membrane transport	5	0.181284051
GO:0006558	L-phenylalanine metabolic process	5	0.181284051
GO:0051171	regulation of nitrogen compound metabolic process	133	0.192187601
GO:0009059	macromolecule biosynthetic process	197	0.20162729
GO:0008652	cellular amino acid biosynthetic process	34	0.245237104
GO:0007034	vacuolar transport	8	0.254488839
GO:0031326	regulation of cellular biosynthetic process	120	0.254488839
GO:0009889	regulation of biosynthetic process	120	0.254488839
GO:0006082	organic acid metabolic process	107	0.269596955
GO:0019932	second-messenger-mediated signaling	7	0.286429765
GO:0009074	aromatic amino acid family catabolic process	7	0.286429765
GO:0019722	calcium-mediated signaling	7	0.286429765
GO:2000112	regulation of cellular macromolecule biosynthetic process	119	0.286429765
GO:0010556	regulation of macromolecule biosynthetic process	119	0.286429765
GO:0006520	cellular amino acid metabolic process	73	0.294011752
GO:0000160	phosphorelay signal transduction system	9	0.294011752
GO:0019222	regulation of metabolic process	137	0.294011752
GO:0034440	lipid oxidation	6	0.294011752
GO:0019395	fatty acid oxidation	6	0.294011752
GO:0009062	fatty acid catabolic process	6	0.294011752
GO:0006635	fatty acid β -oxidation	6	0.294011752
GO:0060255	regulation of macromolecule metabolic process	136	0.294011752
GO:0008152	metabolic process	861	0.294011752
GO:0019752	carboxylic acid metabolic process	104	0.294011752
GO:0044260	cellular macromolecule metabolic process	378	0.294011752
GO:0035303	regulation of dephosphorylation	5	0.294011752
GO:0072663	establishment of protein localization to peroxisome	5	0.294011752
GO:0072662	protein localization to peroxisome	5	0.294011752
GO:0006625	protein targeting to peroxisome	5	0.294011752
GO:0035304	regulation of protein dephosphorylation	5	0.294011752

GO:0006641	triglyceride metabolic process	3	0.294011752
GO:0006639	acylglycerol metabolic process	3	0.294011752
GO:0006638	neutral lipid metabolic process	3	0.294011752
GO:0030149	sphingolipid catabolic process	3	0.294011752
GO:0006551	leucine metabolic process	3	0.294011752
GO:0006572	tyrosine catabolic process	3	0.294011752
GO:0009098	leucine biosynthetic process	3	0.294011752
GO:0046460	neutral lipid biosynthetic process	3	0.294011752
GO:0046463	acylglycerol biosynthetic process	3	0.294011752
GO:0019432	triglyceride biosynthetic process	3	0.294011752
GO:0046466	membrane lipid catabolic process	3	0.294011752
GO:0010468	regulation of gene expression	123	0.294011752
GO:1901606	alpha-amino acid catabolic process	13	0.301674483
GO:0016558	protein import into peroxisome matrix	4	0.308335702
GO:0036297	interstrand cross-link repair	4	0.308335702
GO:0016560	protein import into peroxisome matrix, docking	4	0.308335702
GO:0006570	tyrosine metabolic process	4	0.308335702
GO:0016053	organic acid biosynthetic process	48	0.316460657
GO:0043436	oxoacid metabolic process	104	0.316460657
GO:1901565	organonitrogen compound catabolic process	52	0.338448669
GO:0030258	lipid modification	9	0.342370589
GO:0006979	response to oxidative stress	10	0.395390662
GO:0006950	response to stress	56	0.395390662
GO:1901575	organic substance catabolic process	86	0.402717768
GO:0072329	monocarboxylic acid catabolic process	6	0.419636315
GO:0009066	aspartate family amino acid metabolic process	15	0.421488045
GO:0019751	polyol metabolic process	9	0.488158787
GO:0033540	fatty acid β -oxidation using acyl-CoA oxidase	5	0.512422404
GO:0006144	purine nucleobase metabolic process	5	0.512422404

TABLE S6. BIOLOGICAL PROCESS GO TERMS: 3 HR VS 6 HR, UPREGULATED GENES

ID	Name	Gene Count	Benjamini
GO:0005975	carbohydrate metabolic process	66	1.18E-07
GO:0009081	branched-chain amino acid metabolic process	16	7.67E-07
GO:0009082	branched-chain amino acid biosynthetic process	11	1.31E-05
GO:0055114	obsolete oxidation-reduction process	100	4.39E-05
GO:0009097	isoleucine biosynthetic process	7	0.000639855
GO:0006549	isoleucine metabolic process	7	0.000639855
GO:0006082	organic acid metabolic process	69	0.000658775
GO:0019752	carboxylic acid metabolic process	68	0.000658775
GO:1901605	alpha-amino acid metabolic process	35	0.000658775
GO:0043436	oxoacid metabolic process	68	0.000686888
GO:0006520	cellular amino acid metabolic process	49	0.001371977
GO:0009099	valine biosynthetic process	5	0.002631807

GO:0044281	small molecule metabolic process	102	0.002639934
GO:0019318	hexose metabolic process	14	0.005596344
GO:0045229	external encapsulating structure organization	6	0.005710084
GO:0071555	cell wall organization	6	0.005710084
GO:0005996	monosaccharide metabolic process	14	0.006526222
GO:0006031	chitin biosynthetic process	5	0.008439816
GO:0006023	aminoglycan biosynthetic process	5	0.008439816
GO:1901073	glucosamine-containing compound biosynthetic process	5	0.008439816
GO:0006573	valine metabolic process	7	0.011067257
GO:0071554	cell wall organization or biogenesis	6	0.011067257
GO:1901607	alpha-amino acid biosynthetic process	21	0.016910674
GO:0016042	lipid catabolic process	9	0.055699879
GO:0009098	leucine biosynthetic process	3	0.070027295
GO:0006551	leucine metabolic process	3	0.070027295
GO:0008652	cellular amino acid biosynthetic process	21	0.070027295
GO:0046349	amino sugar biosynthetic process	7	0.072270477
GO:0044282	small molecule catabolic process	16	0.072270477
GO:0044262	cellular carbohydrate metabolic process	13	0.089617089
GO:0019878	lysine biosynthetic process via aminoadipic acid	4	0.093396766
GO:0009063	cellular amino acid catabolic process	10	0.093632402
GO:0016054	organic acid catabolic process	12	0.09776714
GO:0046395	carboxylic acid catabolic process	12	0.09776714
GO:0016052	carbohydrate catabolic process	16	0.168158763
GO:0006004	fucose metabolic process	4	0.168158763
GO:0042743	hydrogen peroxide metabolic process	3	0.174081998
GO:0042744	hydrogen peroxide catabolic process	3	0.174081998
GO:0006006	glucose metabolic process	6	0.184151065
GO:0007018	microtubule-based movement	10	0.195280819
GO:0006928	movement of cell or subcellular component	10	0.195280819
GO:0006979	response to oxidative stress	7	0.202850576
GO:0007165	signal transduction	42	0.202850576
GO:0023052	signaling	42	0.202850576
GO:0007154	cell communication	42	0.213682025
GO:0044275	cellular carbohydrate catabolic process	6	0.222470851
GO:0051273	β -glucan metabolic process	4	0.226161084
GO:0009085	lysine biosynthetic process	4	0.226161084
GO:0006030	chitin metabolic process	7	0.235599794
GO:0006022	aminoglycan metabolic process	7	0.235599794
GO:0055085	transmembrane transport	76	0.253870442
GO:0009056	catabolic process	49	0.253870442
GO:0030259	lipid glycosylation	2	0.253870442
GO:0035023	regulation of Rho protein signal transduction	2	0.253870442
GO:0009448	gamma-aminobutyric acid metabolic process	2	0.253870442
GO:0006083	acetate metabolic process	3	0.266452565
GO:0016053	organic acid biosynthetic process	26	0.277618856

GO:0044283	small molecule biosynthetic process	34	0.28275386
GO:0006094	gluconeogenesis	4	0.28275386
GO:0006553	lysine metabolic process	4	0.28275386
GO:0019319	hexose biosynthetic process	4	0.28275386
GO:0046364	monosaccharide biosynthetic process	4	0.28275386
GO:0016051	carbohydrate biosynthetic process	8	0.30348899
GO:0009072	aromatic amino acid family metabolic process	8	0.30348899
GO:0046394	carboxylic acid biosynthetic process	24	0.30348899
GO:0009066	aspartate family amino acid metabolic process	9	0.319539131
GO:0044042	glucan metabolic process	5	0.319539131
GO:0006073	cellular glucan metabolic process	5	0.319539131
GO:0044264	cellular polysaccharide metabolic process	5	0.319539131
GO:0005991	trehalose metabolic process	5	0.319539131
GO:0005984	disaccharide metabolic process	5	0.319539131
GO:0061919	process utilizing autophagic mechanism	6	0.336298195
GO:0006914	autophagy	6	0.336298195
GO:0015693	magnesium ion transport	4	0.354448783
GO:0046473	phosphatidic acid metabolic process	3	0.354570889
GO:0006654	phosphatidic acid biosynthetic process	3	0.354570889
GO:0007017	microtubule-based process	12	0.361767102
GO:0009067	aspartate family amino acid biosynthetic process	8	0.370947357
GO:0009311	oligosaccharide metabolic process	5	0.380499646
GO:0044242	cellular lipid catabolic process	5	0.380499646
GO:0005976	polysaccharide metabolic process	8	0.424665307
GO:0019722	calcium-mediated signaling	4	0.424665307
GO:0019932	second-messenger-mediated signaling	4	0.424665307
GO:0009074	aromatic amino acid family catabolic process	4	0.424665307
GO:0046466	membrane lipid catabolic process	2	0.424665307
GO:0006572	tyrosine catabolic process	2	0.424665307
GO:0019441	tryptophan catabolic process to kynurenine	2	0.424665307
GO:0030149	sphingolipid catabolic process	2	0.424665307
GO:0006075	(1->3)- β -D-glucan biosynthetic process	2	0.424665307
GO:0006074	(1->3)- β -D-glucan metabolic process	2	0.424665307

TABLE S7. BIOLOGICAL PROCESS GO TERMS: 3 HR VS 6 HR, DOWNREGULATED GENES

ID	Name	Gene count	Benjamini
GO:0005975	carbohydrate metabolic process	14	0.000388654
GO:0055085	transmembrane transport	18	0.003281349
GO:0006810	transport	22	0.075846218
GO:0051234	establishment of localization	22	0.075846218
GO:0051179	localization	22	0.075846218
GO:1902475	L-alpha-amino acid transmembrane transport	1	0.3569828
GO:0015810	aspartate transmembrane transport	1	0.3569828
GO:0008612	peptidyl-lysine modification to peptidyl-hypusine	1	0.3569828

GO:0003333	amino acid transmembrane transport	1	0.3569828
GO:0045901	positive regulation of translational elongation	1	0.3569828
GO:0015813	L-glutamate transmembrane transport	1	0.3569828
GO:0015800	acidic amino acid transport	1	0.3569828
GO:0006449	regulation of translational termination	1	0.3569828

TABLE S8. BIOLOGICAL PROCESS GO TERMS: 0 HR VS 6 HR, UPREGULATED GENES

ID	Name	Gene count	Benjamini
GO:1901137	carbohydrate derivative biosynthetic process	116	6.53E-08
GO:0043038	amino acid activation	38	6.53E-08
GO:0043039	tRNA aminoacylation	38	6.53E-08
GO:0006418	tRNA aminoacylation for protein translation	35	4.26E-07
GO:1902600	proton transmembrane transport	35	4.26E-07
GO:1901135	carbohydrate derivative metabolic process	162	2.69E-06
GO:0006260	DNA replication	44	7.43E-06
GO:0009141	nucleoside triphosphate metabolic process	28	1.69E-05
GO:0009142	nucleoside triphosphate biosynthetic process	26	1.83E-05
GO:0034660	ncRNA metabolic process	100	2.16E-05
GO:0009201	ribonucleoside triphosphate biosynthetic process	25	3.34E-05
GO:0090407	organophosphate biosynthetic process	105	3.36E-05
GO:0006399	tRNA metabolic process	72	3.36E-05
GO:0009205	purine ribonucleoside triphosphate metabolic process	26	4.57E-05
GO:0098655	cation transmembrane transport	43	6.25E-05
GO:0098662	inorganic cation transmembrane transport	43	6.25E-05
GO:0098660	inorganic ion transmembrane transport	43	6.25E-05
GO:0009199	ribonucleoside triphosphate metabolic process	25	7.67E-05
GO:0007018	microtubule-based movement	27	0.00015395
GO:0006928	movement of cell or subcellular component	27	0.00015395
GO:0009206	purine ribonucleoside triphosphate biosynthetic process	22	0.000179118
GO:0009145	purine nucleoside triphosphate biosynthetic process	22	0.000179118
GO:0009165	nucleotide biosynthetic process	63	0.000196401
GO:1901293	nucleoside phosphate biosynthetic process	63	0.000196401
GO:0006457	protein folding	39	0.000215458
GO:0009260	ribonucleotide biosynthetic process	48	0.000215458
GO:0046390	ribose phosphate biosynthetic process	48	0.000215458
GO:0055086	nucleobase-containing small molecule metabolic process	102	0.000271404
GO:0034220	ion transmembrane transport	45	0.000311342
GO:0006139	nucleobase-containing compound metabolic process	346	0.000417771
GO:0009144	purine nucleoside triphosphate metabolic process	22	0.000417771

GO:0072528	pyrimidine-containing compound biosynthetic process	22	0.000417771
GO:0007017	microtubule-based process	36	0.000507837
GO:0044281	small molecule metabolic process	255	0.001098412
GO:0072527	pyrimidine-containing compound metabolic process	22	0.001115481
GO:0009152	purine ribonucleotide biosynthetic process	40	0.001115481
GO:0006164	purine nucleotide biosynthetic process	40	0.001115481
GO:0006725	cellular aromatic compound metabolic process	374	0.001312808
GO:0015986	ATP synthesis coupled proton transport	17	0.001312808
GO:0006754	ATP biosynthetic process	17	0.001312808
GO:0015985	energy coupled proton transport, down electrochemical gradient	17	0.001312808
GO:0006753	nucleoside phosphate metabolic process	82	0.001515751
GO:0009117	nucleotide metabolic process	82	0.001515751
GO:0046483	heterocycle metabolic process	372	0.001878607
GO:0022613	ribonucleoprotein complex biogenesis	64	0.002008622
GO:0009058	biosynthetic process	468	0.003511377
GO:0006221	pyrimidine nucleotide biosynthetic process	17	0.003726328
GO:0006220	pyrimidine nucleotide metabolic process	17	0.003726328
GO:1901576	organic substance biosynthetic process	451	0.004123543
GO:0072522	purine-containing compound biosynthetic process	40	0.004123543
GO:1901360	organic cyclic compound metabolic process	383	0.004747866
GO:0044249	cellular biosynthetic process	436	0.004948199
GO:0019637	organophosphate metabolic process	138	0.005042346
GO:0009259	ribonucleotide metabolic process	62	0.00522296
GO:0019693	ribose phosphate metabolic process	62	0.00522296
GO:0009226	nucleotide-sugar biosynthetic process	13	0.006112131
GO:0009225	nucleotide-sugar metabolic process	16	0.006554617
GO:0034654	nucleobase-containing compound biosynthetic process	116	0.010033747
GO:0009150	purine ribonucleotide metabolic process	56	0.01227274
GO:0019438	aromatic compound biosynthetic process	139	0.013257333
GO:0042181	ketone biosynthetic process	8	0.013257333
GO:0006270	DNA replication initiation	8	0.013257333
GO:1901663	quinone biosynthetic process	8	0.013257333
GO:0006744	ubiquinone biosynthetic process	8	0.013257333
GO:0006743	ubiquinone metabolic process	8	0.013257333
GO:1901661	quinone metabolic process	8	0.013257333
GO:0009147	pyrimidine nucleoside triphosphate metabolic process	10	0.014177732
GO:0009167	purine ribonucleoside monophosphate metabolic process	21	0.014185962
GO:0006163	purine nucleotide metabolic process	55	0.015304863
GO:0032543	mitochondrial translation	11	0.023751934
GO:0140053	mitochondrial gene expression	11	0.023751934

GO:0016070	RNA metabolic process	190	0.028651759
GO:0009148	pyrimidine nucleoside triphosphate biosynthetic process	9	0.030391639
GO:0018130	heterocycle biosynthetic process	138	0.034379581
GO:0042254	ribosome biogenesis	47	0.038359059
GO:0051128	regulation of cellular component organization	18	0.038359059
GO:0006812	cation transport	69	0.038522311
GO:1901362	organic cyclic compound biosynthetic process	150	0.045818436
GO:0006487	protein N-linked glycosylation	10	0.046462595
GO:0006040	amino sugar metabolic process	24	0.046462595
GO:0033043	regulation of organelle organization	16	0.06008448
GO:0006241	CTP biosynthetic process	8	0.060411483
GO:0046036	CTP metabolic process	8	0.060411483
GO:0009209	pyrimidine ribonucleoside triphosphate biosynthetic process	8	0.060411483
GO:0009208	pyrimidine ribonucleoside triphosphate metabolic process	8	0.060411483
GO:0008610	lipid biosynthetic process	66	0.066377639
GO:0022618	ribonucleoprotein complex assembly	20	0.067620562
GO:0071826	ribonucleoprotein complex subunit organization	20	0.067620562
GO:0008654	phospholipid biosynthetic process	37	0.067697549
GO:0009220	pyrimidine ribonucleotide biosynthetic process	12	0.067697549
GO:0009218	pyrimidine ribonucleotide metabolic process	12	0.067697549
GO:0046349	amino sugar biosynthetic process	12	0.067697549
GO:0006261	DNA-dependent DNA replication	12	0.067697549
GO:0046128	purine ribonucleoside metabolic process	13	0.077958878
GO:0009451	RNA modification	32	0.079955728
GO:0002183	cytoplasmic translational initiation	9	0.08257976
GO:0009100	glycoprotein metabolic process	35	0.098500992
GO:0009987	cellular process	1374	0.104536859
GO:0090304	nucleic acid metabolic process	242	0.104536859
GO:0072521	purine-containing compound metabolic process	55	0.104588132
GO:0006730	one-carbon metabolic process	11	0.121565312
GO:0009101	glycoprotein biosynthetic process	34	0.133730338
GO:0006486	protein glycosylation	34	0.133730338
GO:0043413	macromolecule glycosylation	34	0.133730338
GO:0042723	thiamine-containing compound metabolic process	5	0.136202638
GO:0006772	thiamine metabolic process	5	0.136202638
GO:0042724	thiamine-containing compound biosynthetic process	5	0.136202638
GO:0009123	nucleoside monophosphate metabolic process	22	0.144153796
GO:0009069	serine family amino acid metabolic process	14	0.144153796
GO:0008150	biological process	1725	0.145563517
GO:0006811	ion transport	87	0.147372999
GO:0006048	UDP-N-acetylglucosamine biosynthetic process	8	0.147372999
GO:0006047	UDP-N-acetylglucosamine metabolic process	8	0.147372999

GO:0001732	formation of cytoplasmic translation initiation complex	8	0.147372999
GO:0034470	ncRNA processing	62	0.152267077
GO:0071840	cellular component organization or biogenesis	164	0.156502315
GO:0006396	RNA processing	109	0.159360448
GO:0044085	cellular component biogenesis	96	0.167956076
GO:0044255	cellular lipid metabolic process	80	0.170569283
GO:0002181	cytoplasmic translation	9	0.172223215
GO:0032970	regulation of actin filament-based process	10	0.184276584
GO:0051493	regulation of cytoskeleton organization	10	0.184276584
GO:0044042	glucan metabolic process	10	0.184276584
GO:0001522	pseudouridine synthesis	10	0.184276584
GO:0006073	cellular glucan metabolic process	10	0.184276584
GO:0032956	regulation of actin cytoskeleton organization	10	0.184276584
GO:0044264	cellular polysaccharide metabolic process	10	0.184276584
GO:0015833	peptide transport	49	0.184276584
GO:0007264	small GTPase mediated signal transduction	21	0.188496
GO:0009124	nucleoside monophosphate biosynthetic process	20	0.193194489
GO:0070085	glycosylation	34	0.194968479
GO:0006544	glycine metabolic process	6	0.201092884
GO:0008104	protein localization	99	0.201849516
GO:0018193	peptidyl-amino acid modification	27	0.201940257
GO:0045184	establishment of protein localization	97	0.220348902
GO:0071704	organic substance metabolic process	983	0.252129869
GO:0071554	cell wall organization or biogenesis	7	0.25236292
GO:0006490	oligosaccharide-lipid intermediate biosynthetic process	7	0.25236292
GO:0009228	thiamine biosynthetic process	4	0.25236292
GO:0051130	positive regulation of cellular component organization	4	0.25236292
GO:0140115	export across plasma membrane	4	0.25236292
GO:0018216	peptidyl-arginine methylation	4	0.25236292
GO:0120029	proton export across plasma membrane	4	0.25236292
GO:0051274	β -glucan biosynthetic process	4	0.25236292
GO:0018195	peptidyl-arginine modification	4	0.25236292
GO:0019692	deoxyribose phosphate metabolic process	4	0.25236292
GO:0034309	primary alcohol biosynthetic process	4	0.25236292
GO:0009161	ribonucleoside monophosphate metabolic process	20	0.25236292
GO:0015031	protein transport	95	0.255450339
GO:0005976	polysaccharide metabolic process	18	0.26795692
GO:0006084	acetyl-CoA metabolic process	8	0.26795692
GO:0051169	nuclear transport	17	0.274111706
GO:0006913	nucleocytoplasmic transport	17	0.274111706
GO:0044087	regulation of cellular component biogenesis	9	0.281554309
GO:0110053	regulation of actin filament organization	9	0.281554309
GO:1902903	regulation of supramolecular fiber organization	9	0.281554309

GO:0006364	rRNA processing	29	0.285242601
GO:0042158	lipoprotein biosynthetic process	13	0.288942974
GO:0009126	purine nucleoside monophosphate metabolic process	13	0.288942974
GO:0006888	endoplasmic reticulum to Golgi vesicle-mediated transport	13	0.288942974
GO:0006497	protein lipidation	13	0.288942974
GO:0032259	methylation	37	0.291080276
GO:0048193	Golgi vesicle transport	22	0.296365318
GO:0006629	lipid metabolic process	109	0.296365318
GO:0006644	phospholipid metabolic process	44	0.297025621
GO:0016072	rRNA metabolic process	29	0.336359846
GO:0006228	UTP biosynthetic process	5	0.336359846
GO:0034314	Arp2/3 complex-mediated actin nucleation	5	0.336359846
GO:0034308	primary alcohol metabolic process	5	0.336359846
GO:0006183	GTP biosynthetic process	5	0.336359846
GO:0009408	response to heat	5	0.336359846
GO:0046051	UTP metabolic process	5	0.336359846
GO:0000154	rRNA modification	5	0.336359846
GO:0009266	response to temperature stimulus	5	0.336359846
GO:0009263	deoxyribonucleotide biosynthetic process	5	0.336359846
GO:0009156	ribonucleoside monophosphate biosynthetic process	18	0.336359846
GO:0046474	glycerophospholipid biosynthetic process	23	0.353742517
GO:0044272	sulfur compound biosynthetic process	23	0.353742517
GO:0046034	ATP metabolic process	32	0.354142478
GO:1901071	glucosamine-containing compound metabolic process	16	0.36115318
GO:0050658	RNA transport	15	0.361796495
GO:0006403	RNA localization	15	0.361796495
GO:0051236	establishment of RNA localization	15	0.361796495
GO:0050657	nucleic acid transport	15	0.361796495
GO:0006413	translational initiation	15	0.361796495
GO:0051028	mRNA transport	14	0.361796495
GO:0009262	deoxyribonucleotide metabolic process	6	0.361796495
GO:0006189	'de novo' IMP biosynthetic process	6	0.361796495
GO:0045229	external encapsulating structure organization	6	0.361796495
GO:0000271	polysaccharide biosynthetic process	6	0.361796495
GO:0033692	cellular polysaccharide biosynthetic process	6	0.361796495
GO:0009250	glucan biosynthetic process	6	0.361796495
GO:0071555	cell wall organization	6	0.361796495
GO:0045010	actin nucleation	6	0.361796495
GO:0051273	β -glucan metabolic process	6	0.361796495
GO:0006488	dolichol-linked oligosaccharide biosynthetic process	6	0.361796495
GO:0006520	cellular amino acid metabolic process	93	0.364223476

GO:0042157	lipoprotein metabolic process	13	0.364223476
GO:0009247	glycolipid biosynthetic process	12	0.364223476
GO:1903509	liposaccharide metabolic process	12	0.364223476
GO:0006506	GPI anchor biosynthetic process	12	0.364223476
GO:0046467	membrane lipid biosynthetic process	12	0.364223476
GO:0006664	glycolipid metabolic process	12	0.364223476
GO:0006505	GPI anchor metabolic process	12	0.364223476
GO:0032535	regulation of cellular component size	7	0.364223476
GO:0030832	regulation of actin filament length	7	0.364223476
GO:0032271	regulation of protein polymerization	7	0.364223476
GO:0030833	regulation of actin filament polymerization	7	0.364223476
GO:0009130	pyrimidine nucleoside monophosphate biosynthetic process	7	0.364223476
GO:0090066	regulation of anatomical structure size	7	0.364223476
GO:0009129	pyrimidine nucleoside monophosphate metabolic process	7	0.364223476
GO:0008064	regulation of actin polymerization or depolymerization	7	0.364223476
GO:0009127	purine nucleoside monophosphate biosynthetic process	11	0.366170213
GO:0009168	purine ribonucleoside monophosphate biosynthetic process	11	0.366170213

TABLE S9. BIOLOGICAL PROCESS GO TERMS: 0 HR VS 6 HR, DOWNREGULATED GENES

ID	Name	Gene count	Benjamini
GO:0006412	translation	159	8.99E-12
GO:0043043	peptide biosynthetic process	160	1.25E-11
GO:0006518	peptide metabolic process	163	2.50E-11
GO:0043604	amide biosynthetic process	163	4.56E-11
GO:0043603	cellular amide metabolic process	171	3.54E-10
GO:0044267	cellular protein metabolic process	309	0.00013128
GO:0019538	protein metabolic process	345	0.000595821
GO:0044271	cellular nitrogen compound biosynthetic process	221	0.001276027
GO:0009059	macromolecule biosynthetic process	209	0.002589021
GO:0034645	cellular macromolecule biosynthetic process	207	0.002589021
GO:0051252	regulation of RNA metabolic process	124	0.003342546
GO:0019219	regulation of nucleobase-containing compound metabolic process	124	0.003598184
GO:0044260	cellular macromolecule metabolic process	389	0.006735657
GO:2001141	regulation of RNA biosynthetic process	118	0.006735657
GO:0006355	regulation of transcription, DNA-templated	118	0.006735657
GO:1903506	regulation of nucleic acid-templated transcription	118	0.006735657
GO:0050794	regulation of cellular process	231	0.010982194
GO:0080090	regulation of primary metabolic process	139	0.013713162

GO:0006914	autophagy	13	0.013713162
GO:0061919	process utilizing autophagic mechanism	13	0.013713162
GO:0031323	regulation of cellular metabolic process	139	0.013713162
GO:0051171	regulation of nitrogen compound metabolic process	138	0.013713162
GO:0065007	biological regulation	247	0.013713162
GO:1901564	organonitrogen compound metabolic process	450	0.013713162
GO:0050789	regulation of biological process	235	0.013713162
GO:0031326	regulation of cellular biosynthetic process	126	0.013713162
GO:0009889	regulation of biosynthetic process	126	0.013713162
GO:0009081	branched-chain amino acid metabolic process	15	0.014763074
GO:1901566	organonitrogen compound biosynthetic process	226	0.016009032
GO:2000112	regulation of cellular macromolecule biosynthetic process	125	0.016009032
GO:0010556	regulation of macromolecule biosynthetic process	125	0.016009032
GO:0019878	lysine biosynthetic process via aminoadipic acid	6	0.016409841
GO:0010467	gene expression	233	0.019985916
GO:0010468	regulation of gene expression	129	0.024507528
GO:0009085	lysine biosynthetic process	7	0.024966745
GO:0019222	regulation of metabolic process	142	0.02511422
GO:0009082	branched-chain amino acid biosynthetic process	10	0.025437391
GO:0060255	regulation of macromolecule metabolic process	141	0.027513401
GO:0050896	response to stimulus	131	0.032463628
GO:0006468	protein phosphorylation	90	0.03641916
GO:0051716	cellular response to stimulus	123	0.039367917
GO:0007031	peroxisome organization	11	0.042350805
GO:0006559	L-phenylalanine catabolic process	5	0.043639522
GO:1902222	erythrose 4-phosphate/phosphoenolpyruvate family amino acid catabolic process	5	0.043639522
GO:0006553	lysine metabolic process	7	0.066589259
GO:0032958	inositol phosphate biosynthetic process	4	0.149337502
GO:0097720	calcineurin-mediated signaling	4	0.149337502
GO:0043574	peroxisomal transport	6	0.167835079
GO:0006549	isoleucine metabolic process	6	0.167835079
GO:0009097	isoleucine biosynthetic process	6	0.167835079
GO:0006558	L-phenylalanine metabolic process	5	0.167835079
GO:0015919	peroxisomal membrane transport	5	0.167835079
GO:1902221	erythrose 4-phosphate/phosphoenolpyruvate family amino acid metabolic process	5	0.167835079
GO:0044248	cellular catabolic process	73	0.168020891
GO:0007165	signal transduction	78	0.203198272
GO:0023052	signaling	78	0.203198272
GO:0016310	phosphorylation	97	0.216260586
GO:0007154	cell communication	78	0.221042665
GO:0016054	organic acid catabolic process	18	0.260560551
GO:0046395	carboxylic acid catabolic process	18	0.260560551

GO:0006974	cellular response to DNA damage stimulus	45	0.273652936
GO:0046173	polyol biosynthetic process	6	0.321222824
GO:0006281	DNA repair	42	0.333001858
GO:0006289	nucleotide-excision repair	10	0.333800221
GO:0009056	catabolic process	92	0.333800221
GO:0033554	cellular response to stress	49	0.33939842
GO:0035303	regulation of dephosphorylation	5	0.33939842
GO:0072663	establishment of protein localization to peroxisome	5	0.33939842
GO:0072662	protein localization to peroxisome	5	0.33939842
GO:0006625	protein targeting to peroxisome	5	0.33939842
GO:0035304	regulation of protein dephosphorylation	5	0.33939842
GO:0006572	tyrosine catabolic process	3	0.34197583
GO:0009098	leucine biosynthetic process	3	0.34197583
GO:0006551	leucine metabolic process	3	0.34197583
GO:0000289	nuclear-transcribed mRNA poly(A) tail shortening	3	0.34197583
GO:0016558	protein import into peroxisome matrix	4	0.342671965
GO:0036297	interstrand cross-link repair	4	0.342671965
GO:0009099	valine biosynthetic process	4	0.342671965
GO:0016560	protein import into peroxisome matrix, docking	4	0.342671965
GO:0006570	tyrosine metabolic process	4	0.342671965
GO:0030258	lipid modification	9	0.347699978
GO:0006950	response to stress	55	0.354997523
GO:0006573	valine metabolic process	7	0.354997523
GO:0044282	small molecule catabolic process	23	0.421990668
GO:0016042	lipid catabolic process	11	0.425010767
GO:1901607	alpha-amino acid biosynthetic process	28	0.552894827
GO:0007034	vacuolar transport	7	0.55406255
GO:0035556	intracellular signal transduction	42	0.55406255
GO:0033540	fatty acid β -oxidation using acyl-CoA oxidase	5	0.55406255
GO:0006144	purine nucleobase metabolic process	5	0.55406255
GO:0009063	cellular amino acid catabolic process	13	0.599938938
GO:0015698	inorganic anion transport	9	0.641726084

TABLE S10. CELLULAR COMPONENT GO TERMS: 0 HR VS 3 HR, UPREGULATED GENES

ID	Name	Gene count	Benjamini
GO:0032991	protein-containing complex	410	2.73E-23
GO:0005622	intracellular anatomical structure	1016	9.94E-22
GO:0043227	membrane-bounded organelle	726	6.14E-20
GO:0043231	intracellular membrane-bounded organelle	726	6.14E-20
GO:0005737	cytoplasm	531	1.10E-17
GO:0043226	organelle	841	1.80E-12
GO:0043229	intracellular organelle	841	1.80E-12
GO:0044424	obsolete intracellular part	194	2.78E-12

GO:0005634	nucleus	427	1.27E-11
GO:0044428	obsolete nuclear part	53	7.60E-11
GO:0005730	nucleolus	54	2.87E-10
GO:0031981	nuclear lumen	90	1.73E-09
GO:1905368	peptidase complex	40	3.77E-09
GO:1905369	endopeptidase complex	32	8.64E-09
GO:0000502	proteasome complex	28	4.88E-08
GO:0098796	membrane protein complex	92	9.56E-08
GO:0043233	organelle lumen	113	1.51E-07
GO:0031974	membrane-enclosed lumen	113	1.51E-07
GO:0070013	intracellular organelle lumen	113	1.51E-07
GO:0016469	proton-transporting two-sector ATPase complex	30	1.51E-07
GO:0033178	proton-transporting two-sector ATPase complex, catalytic domain	18	5.18E-07
GO:1902494	catalytic complex	117	5.18E-07
GO:0031975	envelope	106	2.56E-06
GO:0031967	organelle envelope	106	2.56E-06
GO:0005739	mitochondrion	162	3.04E-06
GO:0012505	endomembrane system	149	9.32E-06
GO:0140535	intracellular protein-containing complex	86	1.32E-05
GO:0005839	proteasome core complex	14	1.95E-05
GO:0005852	eukaryotic translation initiation factor 3 complex	13	4.99E-05
GO:0045259	proton-transporting ATP synthase complex	17	6.92E-05
GO:0005575	cellular component	1651	8.30E-05
GO:0044444	obsolete cytoplasmic part	109	8.30E-05
GO:0005856	cytoskeleton	59	0.00010967
GO:0031090	organelle membrane	190	0.00010967
GO:0005875	microtubule associated complex	12	0.00010967
GO:0140513	nuclear protein-containing complex	110	0.000122654
GO:0032993	protein-DNA complex	16	0.00013378
GO:0110165	cellular anatomical entity	1626	0.000140077
GO:0005740	mitochondrial envelope	86	0.000158567
GO:0005783	endoplasmic reticulum	87	0.000200428
GO:0000785	chromatin	20	0.000221484
GO:0045261	proton-transporting ATP synthase complex, catalytic core F(1)	11	0.000242225
GO:0031966	mitochondrial membrane	80	0.000286898
GO:0005743	mitochondrial inner membrane	66	0.000312805
GO:0031984	organelle subcompartment	73	0.000417531
GO:0019866	organelle inner membrane	66	0.000430735
GO:0005789	endoplasmic reticulum membrane	70	0.000466931
GO:0098827	endoplasmic reticulum subcompartment	70	0.000466931
GO:0033290	eukaryotic 48S preinitiation complex	10	0.000528595
GO:0070993	translation preinitiation complex	10	0.000528595
GO:0016282	eukaryotic 43S preinitiation complex	10	0.000528595

GO:0042175	nuclear outer membrane-endoplasmic reticulum membrane network	70	0.000603331
GO:0005643	nuclear pore	19	0.000984502
GO:0000786	nucleosome	13	0.001190476
GO:0015630	microtubule cytoskeleton	37	0.001207996
GO:0030117	membrane coat	23	0.001586054
GO:0048475	coated membrane	23	0.001586054
GO:0044464	obsolete cell part	286	0.002400085
GO:0030684	preribosome	10	0.003301815
GO:0033176	proton-transporting V-type ATPase complex	12	0.008100814
GO:0019773	proteasome core complex, alpha-subunit complex	7	0.00821293
GO:0099512	supramolecular fiber	30	0.008297771
GO:0099513	polymeric cytoskeletal fiber	30	0.008297771
GO:0099081	supramolecular polymer	30	0.008297771
GO:0005874	microtubule	29	0.008425616
GO:0005635	nuclear envelope	20	0.008668801
GO:0015629	actin cytoskeleton	22	0.00892595
GO:0044815	DNA packaging complex	13	0.009115934
GO:0005694	chromosome	51	0.010111234
GO:0030120	vesicle coat	15	0.011874089
GO:1990904	ribonucleoprotein complex	67	0.016026713
GO:0042555	MCM complex	6	0.017925121
GO:0033180	proton-transporting V-type ATPase, V1 domain	6	0.017925121
GO:0016272	prefoldin complex	6	0.017925121
GO:0022624	proteasome accessory complex	7	0.034852701
GO:0005753	mitochondrial proton-transporting ATP synthase complex	7	0.034852701
GO:0005838	proteasome regulatory particle	7	0.034852701
GO:0030662	coated vesicle membrane	17	0.040722082
GO:1990234	transferase complex	52	0.041463839
GO:0005654	nucleoplasm	32	0.041768127
GO:0005669	transcription factor TFIID complex	5	0.042305039
GO:0000808	origin recognition complex	5	0.042305039
GO:0030286	dynein complex	5	0.042305039
GO:0098798	mitochondrial protein-containing complex	24	0.045327568
GO:0043228	non-membrane-bounded organelle	226	0.060541876
GO:0043232	intracellular non-membrane-bounded organelle	226	0.060541876
GO:0099080	supramolecular complex	34	0.061447071
GO:0033177	proton-transporting two-sector ATPase complex, proton-transporting domain	11	0.061447071
GO:0055029	nuclear DNA-directed RNA polymerase complex	14	0.061447071
GO:0016592	mediator complex	14	0.061447071
GO:0098800	inner mitochondrial membrane protein complex	14	0.061447071
GO:0000428	DNA-directed RNA polymerase complex	14	0.061447071
GO:0000276	mitochondrial proton-transporting ATP synthase complex, coupling factor F(o)	6	0.066800854

GO:0030127	COPII vesicle coat	6	0.066800854
GO:0030118	clathrin coat	7	0.085443397
GO:0030135	coated vesicle	17	0.086505632
GO:0140534	endoplasmic reticulum protein-containing complex	15	0.092930256
GO:0070469	respirasome	15	0.092930256
GO:0005869	dynactin complex	4	0.092930256
GO:0008540	proteasome regulatory particle, base subcomplex	4	0.092930256
GO:0030880	RNA polymerase complex	14	0.093855545
GO:0030176	integral component of endoplasmic reticulum membrane	10	0.096910061
GO:0016459	myosin complex	11	0.096910061
GO:0034708	methyltransferase complex	11	0.096910061
GO:0031227	intrinsic component of endoplasmic reticulum membrane	11	0.096910061
GO:0061695	transferase complex, transferring phosphorus-containing groups	19	0.104107845
GO:0005666	RNA polymerase III complex	5	0.123381321
GO:0031314	extrinsic component of mitochondrial inner membrane	5	0.123381321
GO:0030131	clathrin adaptor complex	5	0.123381321
GO:0031312	extrinsic component of organelle membrane	5	0.123381321
GO:0005885	Arp2/3 protein complex	5	0.123381321
GO:0032040	small-subunit processome	5	0.123381321
GO:0098590	plasma membrane region	5	0.123381321
GO:0048500	signal recognition particle	5	0.123381321
GO:0005742	mitochondrial outer membrane translocase complex	5	0.123381321
GO:0005905	clathrin-coated pit	5	0.123381321
GO:0005786	signal recognition particle, endoplasmic reticulum targeting	5	0.123381321
GO:0030119	AP-type membrane coat adaptor complex	6	0.141032535
GO:0031226	intrinsic component of plasma membrane	6	0.141032535
GO:0005887	integral component of plasma membrane	6	0.141032535
GO:0045263	proton-transporting ATP synthase complex, coupling factor F(o)	6	0.141032535
GO:0030133	transport vesicle	11	0.141032535
GO:0000228	nuclear chromosome	11	0.141032535
GO:0120114	Sm-like protein family complex	8	0.150096604
GO:0030659	cytoplasmic vesicle membrane	24	0.157412377
GO:0012506	vesicle membrane	24	0.157412377

TABLE S11. CELLULAR COMPONENT GO TERMS: 0 HR VS 3 HR, DOWNREGULATED GENES

ID	Name	Gene count	Benjamini
----	------	------------	-----------

GO:0005840	ribosome	158	2.56E-23
GO:0005777	peroxisome	29	5.65E-05
GO:0042579	microbody	29	5.65E-05
GO:0031903	microbody membrane	18	0.00520421
GO:0005778	peroxisomal membrane	18	0.00520421
GO:0044391	ribosomal subunit	31	0.006391892
GO:0022625	cytosolic large ribosomal subunit	8	0.012326973
GO:0043232	intracellular non-membrane-bounded organelle	184	0.030632442
GO:0043228	non-membrane-bounded organelle	184	0.030632442
GO:0022626	cytosolic ribosome	10	0.031679221
GO:0015935	small ribosomal subunit	17	0.033147512
GO:0033643	host cell part	43	0.033147512
GO:0033647	host intracellular organelle	43	0.033147512
GO:0043657	host cell	43	0.033147512
GO:0042025	host cell nucleus	43	0.033147512
GO:0033648	host intracellular membrane-bounded organelle	43	0.033147512
GO:0033646	host intracellular part	43	0.033147512
GO:0018995	host cellular component	43	0.033147512
GO:0043656	host intracellular region	43	0.033147512
GO:0015934	large ribosomal subunit	14	0.278024453
GO:0005779	integral component of peroxisomal membrane	5	0.628772174
GO:0031231	intrinsic component of peroxisomal membrane	5	0.628772174

TABLE S12. MOLECULAR FUNCTION GO TERMS: 0 HR VS 3 HR, UPREGULATED GENES

ID	Name	Gene count	Benjamini
GO:0016874	ligase activity	90	5.52E-10
GO:0140101	catalytic activity, acting on a tRNA	65	1.19E-09
GO:0016875	ligase activity, forming carbon-oxygen bonds	38	2.07E-09
GO:0004812	aminoacyl-tRNA ligase activity	38	2.07E-09
GO:0140098	catalytic activity, acting on RNA	102	1.42E-07
GO:0140640	catalytic activity, acting on a nucleic acid	148	1.10E-06
GO:0090079	translation regulator activity, nucleic acid binding	40	3.35E-06
GO:0008135	translation factor activity, RNA binding	40	3.35E-06
GO:0045182	translation regulator activity	40	7.30E-06
GO:0003723	RNA binding	190	1.59E-05
GO:0004298	threonine-type endopeptidase activity	15	4.44E-05
GO:0015252	proton channel activity	14	0.000101295
GO:0008092	cytoskeletal protein binding	59	0.000101295
GO:0046933	proton-transporting ATP synthase activity, rotational mechanism	13	0.000245491
GO:0003774	cytoskeletal motor activity	34	0.000501364
GO:0016853	isomerase activity	50	0.000679414
GO:0016741	transferase activity, transferring one-carbon groups	71	0.000703934

GO:0032553	ribonucleotide binding	467	0.001063121
GO:0005261	cation channel activity	17	0.00111645
GO:0008168	methyltransferase activity	66	0.001122512
GO:0003824	catalytic activity	1253	0.001144055
GO:0003743	translation initiation factor activity	25	0.001144055
GO:0051082	unfolded protein binding	25	0.001144055
GO:0035639	purine ribonucleoside triphosphate binding	447	0.001367313
GO:0097367	carbohydrate derivative binding	473	0.001367313
GO:0005524	ATP binding	376	0.001406484
GO:0017076	purine nucleotide binding	451	0.002178363
GO:0032555	purine ribonucleotide binding	450	0.002218922
GO:0030554	adenyl nucleotide binding	380	0.002367557
GO:0032559	adenyl ribonucleotide binding	379	0.002381846
GO:0016779	nucleotidyltransferase activity	48	0.002381846
GO:0009678	pyrophosphate hydrolysis-driven proton transmembrane transporter activity	12	0.002412528
GO:0008757	S-adenosylmethionine-dependent methyltransferase activity	32	0.002763279
GO:0016758	hexosyltransferase activity	51	0.002890681
GO:0008375	acetylglucosaminyltransferase activity	23	0.002890681
GO:0070003	threonine-type peptidase activity	15	0.003004711
GO:0015078	proton transmembrane transporter activity	37	0.004238187
GO:0046961	proton-transporting ATPase activity, rotational mechanism	9	0.004238187
GO:0042625	ATPase-coupled ion transmembrane transporter activity	9	0.004238187
GO:0044769	ATPase activity, coupled to transmembrane movement of ions, rotational mechanism	9	0.004238187
GO:0003777	microtubule motor activity	22	0.004761116
GO:0016757	glycosyltransferase activity	70	0.006174666
GO:0003779	actin binding	27	0.006174666
GO:0008194	UDP-glycosyltransferase activity	34	0.006182521
GO:0004100	chitin synthase activity	19	0.006596664
GO:1901265	nucleoside phosphate binding	515	0.006641365
GO:0000166	nucleotide binding	515	0.006641365
GO:0016866	intramolecular transferase activity	16	0.008829228
GO:0008017	microtubule binding	26	0.009449835
GO:0015631	tubulin binding	30	0.009449835
GO:0043168	anion binding	506	0.009449835
GO:0016740	transferase activity	458	0.012348526
GO:0005515	protein binding	511	0.014389852
GO:0003899	DNA-directed 5'-3' RNA polymerase activity	22	0.014389852
GO:0003746	translation elongation factor activity	11	0.014681843
GO:0036094	small molecule binding	539	0.019321239
GO:0008170	N-methyltransferase activity	17	0.019791425
GO:0140657	ATP-dependent activity	108	0.027360326

GO:0009982	pseudouridine synthase activity	10	0.030959686
GO:1901363	heterocyclic compound binding	908	0.038219017
GO:0097159	organic cyclic compound binding	908	0.038762848
GO:0005216	ion channel activity	19	0.038762848
GO:0022803	passive transmembrane transporter activity	21	0.038762848
GO:0015267	channel activity	21	0.038762848
GO:0002161	aminoacyl-tRNA editing activity	8	0.040838949
GO:0000287	magnesium ion binding	32	0.040838949
GO:0016881	acid-amino acid ligase activity	6	0.046992806
GO:0016879	ligase activity, forming carbon-nitrogen bonds	25	0.054629098
GO:0016776	phosphotransferase activity, phosphate group as acceptor	14	0.055054359
GO:0008276	protein methyltransferase activity	15	0.056897269
GO:0034062	5'-3' RNA polymerase activity	22	0.056897269
GO:0097747	RNA polymerase activity	22	0.056897269
GO:0046982	protein heterodimerization activity	20	0.05851041
GO:0017056	structural constituent of nuclear pore	11	0.08253298
GO:0016273	arginine N-methyltransferase activity	7	0.083815807
GO:0016274	protein-arginine N-methyltransferase activity	7	0.083815807
GO:0043021	ribonucleoprotein complex binding	12	0.087652144
GO:0003712	transcription coregulator activity	20	0.089807715
GO:0019205	nucleobase-containing compound kinase activity	13	0.089807715
GO:0000049	tRNA binding	13	0.089807715
GO:0016859	cis-trans isomerase activity	16	0.092702859
GO:0003755	peptidyl-prolyl cis-trans isomerase activity	16	0.092702859
GO:0008175	tRNA methyltransferase activity	9	0.128847175
GO:0046527	glucosyltransferase activity	9	0.128847175
GO:0003674	molecular function	2378	0.138831136
GO:0019829	ATPase-coupled cation transmembrane transporter activity	15	0.153582115
GO:0016810	hydrolase activity, acting on carbon-nitrogen (but not peptide) bonds	41	0.153582115
GO:0022890	inorganic cation transmembrane transporter activity	55	0.173822473
GO:0003676	nucleic acid binding	425	0.199588677
GO:0008324	cation transmembrane transporter activity	61	0.201749646
GO:0050145	nucleoside monophosphate kinase activity	7	0.211725457
GO:0004659	prenyltransferase activity	8	0.222809804
GO:0016706	2-oxoglutarate-dependent dioxygenase activity	4	0.222809804
GO:0004748	ribonucleoside-diphosphate reductase activity, thioredoxin disulfide as acceptor	4	0.222809804
GO:0031369	translation initiation factor binding	4	0.222809804
GO:0016725	oxidoreductase activity, acting on CH or CH2 groups	4	0.222809804
GO:0043023	ribosomal large subunit binding	4	0.222809804

GO:0016728	oxidoreductase activity, acting on CH or CH2 groups, disulfide as acceptor	4	0.222809804
GO:0061731	ribonucleoside-diphosphate reductase activity	4	0.222809804
GO:0016860	intramolecular oxidoreductase activity	13	0.232588171
GO:0008536	Ran GTPase binding	11	0.239138308
GO:0044877	protein-containing complex binding	24	0.256379135
GO:0016868	intramolecular transferase activity, phosphotransferases	5	0.32023136
GO:0008312	7S RNA binding	5	0.32023136
GO:0070569	uridylyltransferase activity	5	0.32023136
GO:0016423	tRNA (guanine) methyltransferase activity	5	0.32023136
GO:0015079	potassium ion transmembrane transporter activity	5	0.32023136
GO:0031072	heat shock protein binding	6	0.371639055
GO:0016668	oxidoreductase activity, acting on a sulfur group of donors, NAD(P) as acceptor	6	0.371639055
GO:0008171	O-methyltransferase activity	7	0.394038563
GO:0016861	intramolecular oxidoreductase activity, interconverting aldoses and ketoses	9	0.394670629
GO:0008173	RNA methyltransferase activity	15	0.442820683
GO:0052689	carboxylic ester hydrolase activity	14	0.470480297

TABLE S13. MOLECULAR FUNCTION GO TERMS: 0 HR VS 3 HR, DOWNREGULATED GENES

ID	Name	Gene count	Benjamini
GO:0003735	structural constituent of ribosome	146	1.11E-19
GO:0005198	structural molecule activity	152	4.52E-15
GO:0003700	DNA-binding transcription factor activity	96	1.39E-05
GO:0140110	transcription regulator activity	99	0.004065043
GO:0004672	protein kinase activity	104	0.011105988
GO:0043565	sequence-specific DNA binding	43	0.011105988
GO:0008289	lipid binding	30	0.012687508
GO:0016773	phosphotransferase activity, alcohol group as acceptor	127	0.02160891
GO:0043169	cation binding	336	0.02160891
GO:0046872	metal ion binding	332	0.027267273
GO:0003995	acyl-CoA dehydrogenase activity	7	0.06900394
GO:0000981	DNA-binding transcription factor activity, RNA polymerase II-specific	33	0.091359527
GO:0016491	oxidoreductase activity	189	0.091359527
GO:0000977	RNA polymerase II transcription regulatory region sequence-specific DNA binding	5	0.091359527
GO:0001216	DNA-binding transcription activator activity	5	0.091359527
GO:0000978	RNA polymerase II cis-regulatory region sequence-specific DNA binding	5	0.091359527

GO:0001228	DNA-binding transcription activator activity, RNA polymerase II-specific	5	0.091359527
GO:0016301	kinase activity	137	0.10482256
GO:0016829	lyase activity	48	0.10482256
GO:0005543	phospholipid binding	17	0.118393037
GO:0000987	cis-regulatory region sequence-specific DNA binding	8	0.118393037
GO:0004842	ubiquitin-protein transferase activity	20	0.12116671
GO:0019842	vitamin binding	31	0.12116671
GO:0019843	rRNA binding	14	0.12116671
GO:0035091	phosphatidylinositol binding	16	0.12116671
GO:0008081	phosphoric diester hydrolase activity	15	0.146203948
GO:0016701	oxidoreductase activity, acting on single donors with incorporation of molecular oxygen	9	0.169494967
GO:0004806	triglyceride lipase activity	4	0.169494967
GO:0033192	calmodulin-dependent protein phosphatase activity	4	0.169494967
GO:0004723	calcium-dependent protein serine/threonine phosphatase activity	4	0.169494967
GO:0019787	ubiquitin-like protein transferase activity	20	0.169494967
GO:0000976	transcription cis-regulatory region binding	8	0.169494967
GO:0001067	transcription regulatory region nucleic acid binding	8	0.169494967
GO:0016298	lipase activity	13	0.176549641
GO:0016627	oxidoreductase activity, acting on the CH-CH group of donors	25	0.222990707
GO:0004674	protein serine/threonine kinase activity	61	0.222990707
GO:1990837	sequence-specific double-stranded DNA binding	8	0.295225861
GO:0003674	molecular function	1802	0.35057499
GO:0015923	mannosidase activity	6	0.403957392
GO:0004559	alpha-mannosidase activity	6	0.403957392
GO:0015924	mannosyl-oligosaccharide mannosidase activity	5	0.423453116
GO:0004571	mannosyl-oligosaccharide 1,2-alpha-mannosidase activity	5	0.423453116
GO:0016813	hydrolase activity, acting on carbon-nitrogen (but not peptide) bonds, in linear amidines	5	0.423453116
GO:0016812	hydrolase activity, acting on carbon-nitrogen (but not peptide) bonds, in cyclic amides	3	0.423453116
GO:0008097	5S rRNA binding	3	0.423453116
GO:0005509	calcium ion binding	26	0.428418824
GO:0052692	raffinose alpha-galactosidase activity	4	0.428418824
GO:0004557	alpha-galactosidase activity	4	0.428418824
GO:0015925	galactosidase activity	4	0.428418824
GO:0070279	vitamin B6 binding	20	0.444856327
GO:0030170	pyridoxal phosphate binding	20	0.444856327
GO:0042578	phosphoric ester hydrolase activity	46	0.49841563

GO:0051540	metal cluster binding	24	0.557024283
GO:0051536	iron-sulfur cluster binding	24	0.557024283
GO:0050660	flavin adenine dinucleotide binding	29	0.557024283
GO:0016835	carbon-oxygen lyase activity	17	0.600795264
GO:0003997	acyl-CoA oxidase activity	5	0.636671232
GO:0004114	3',5'-cyclic-nucleotide phosphodiesterase activity	5	0.636671232
GO:0000104	succinate dehydrogenase activity	5	0.636671232
GO:0004112	cyclic-nucleotide phosphodiesterase activity	5	0.636671232
GO:0004499	N,N-dimethylaniline monooxygenase activity	5	0.636671232

TABLE S14. CELLULAR COMPONENT GO TERMS: 3 HR VS 6 HR, UPREGULATED GENES

ID	Name	Gene count	Benjamini
GO:0005886	plasma membrane	21	0.127935956
GO:0071944	cell periphery	24	0.168674423
GO:0016021	integral component of membrane	303	0.226295436
GO:0031224	intrinsic component of membrane	303	0.226295436
GO:0044665	MLL1/2 complex	4	0.226295436
GO:0071339	MLL1 complex	4	0.226295436
GO:0005874	microtubule	12	0.427011974
GO:0016020	membrane	335	0.427011974
GO:0099513	polymeric cytoskeletal fiber	12	0.427011974
GO:0099512	supramolecular fiber	12	0.427011974
GO:0099081	supramolecular polymer	12	0.427011974
GO:0035097	histone methyltransferase complex	4	0.659403094
GO:0000148	1,3-beta-D-glucan synthase complex	2	0.659403094

TABLE S15. CELLULAR COMPONENT GO TERMS: 3 HR VS 6 HR, DOWNREGULATED GENES

ID	Name	Gene count	Benjamini
GO:0071944	cell periphery	6	0.096924446
GO:0005618	cell wall	2	0.096924446
GO:0030312	external encapsulating structure	2	0.096924446
GO:0016021	integral component of membrane	39	0.096924446
GO:0031224	intrinsic component of membrane	39	0.096924446
GO:0005886	plasma membrane	4	0.187518478
GO:0016020	membrane	40	0.334801534

TABLE S16. MOLECULAR FUNCTION GO TERMS: 3 HR VS 6 HR, UPREGULATED GENES

ID	Name	Gene count	Benjamini
GO:0003824	catalytic activity	489	7.25E-06
GO:0016491	oxidoreductase activity	117	1.34E-05

GO:0016798	hydrolase activity, acting on glycosyl bonds	32	2.92E-05
GO:0004553	hydrolase activity, hydrolyzing O-glycosyl compounds	29	5.95E-05
GO:0016829	lyase activity	34	0.000460919
GO:0016903	oxidoreductase activity, acting on the aldehyde or oxo group of donors	13	0.004286103
GO:0003674	molecular function	860	0.007178299
GO:0008194	UDP-glycosyltransferase activity	18	0.010246953
GO:0020037	heme binding	23	0.010392654
GO:0004601	peroxidase activity	9	0.010392654
GO:0046906	tetrapyrrole binding	23	0.010905071
GO:0016787	hydrolase activity	168	0.013884419
GO:0016620	oxidoreductase activity, acting on the aldehyde or oxo group of donors, NAD or NADP as acceptor	10	0.014738921
GO:0004497	monooxygenase activity	18	0.01870216
GO:0016684	oxidoreductase activity, acting on peroxide as acceptor	9	0.01870216
GO:0019842	vitamin binding	19	0.04731196
GO:0003995	acyl-CoA dehydrogenase activity	5	0.052005858
GO:0004611	phosphoenolpyruvate carboxykinase activity	3	0.06819229
GO:0004612	phosphoenolpyruvate carboxykinase (ATP) activity	3	0.06819229
GO:0008236	serine-type peptidase activity	15	0.104264263
GO:0017171	serine hydrolase activity	15	0.104264263
GO:0051287	NAD binding	12	0.104264263
GO:0016758	hexosyltransferase activity	21	0.104264263
GO:0004100	chitin synthase activity	9	0.104264263
GO:0004252	serine-type endopeptidase activity	12	0.117221408
GO:0030170	pyridoxal phosphate binding	13	0.12693417
GO:0070279	vitamin B6 binding	13	0.12693417
GO:0008375	acetylglucosaminyltransferase activity	10	0.12693417
GO:0016616	oxidoreductase activity, acting on the CH-OH group of donors, NAD or NADP as acceptor	14	0.139192612
GO:0043167	ion binding	307	0.139192612
GO:0004096	catalase activity	3	0.150722152
GO:0016298	lipase activity	8	0.163845106
GO:0017111	nucleoside-triphosphatase activity	37	0.178631169
GO:0016830	carbon-carbon lyase activity	11	0.178631169
GO:0046912	acyltransferase, acyl groups converted into alkyl on transfer	4	0.178631169
GO:0016887	ATP hydrolysis activity	17	0.178631169
GO:0003777	microtubule motor activity	9	0.178631169
GO:0050661	NADP binding	9	0.178631169
GO:0016209	antioxidant activity	9	0.178631169
GO:0050660	flavin adenine dinucleotide binding	17	0.178631169
GO:0005085	guanyl-nucleotide exchange factor activity	15	0.178631169

GO:0005509	calcium ion binding	15	0.178631169
GO:0008184	glycogen phosphorylase activity	2	0.178631169
GO:0004451	isocitrate lyase activity	2	0.178631169
GO:1990610	acetolactate synthase regulator activity	2	0.178631169
GO:0015928	fucosidase activity	2	0.178631169
GO:0046421	methyisocitrate lyase activity	2	0.178631169
GO:0004560	alpha-L-fucosidase activity	2	0.178631169
GO:0004455	ketol-acid reductoisomerase activity	2	0.178631169
GO:0004410	homocitrate synthase activity	2	0.178631169
GO:0102499	SHG alpha-glucan phosphorylase activity	2	0.178631169
GO:0033961	cis-stilbene-oxide hydrolase activity	2	0.178631169
GO:0102250	linear malto-oligosaccharide phosphorylase activity	2	0.178631169
GO:0004351	glutamate decarboxylase activity	2	0.178631169
GO:0004645	1,4-alpha-oligoglucan phosphorylase activity	2	0.178631169
GO:0016705	oxidoreductase activity, acting on paired donors, with incorporation or reduction of molecular oxygen	16	0.178631169
GO:0016405	CoA-ligase activity	3	0.178631169
GO:0004555	alpha,alpha-trehalase activity	3	0.178631169
GO:0015927	trehalase activity	3	0.178631169
GO:0005215	transporter activity	80	0.184473759
GO:0050997	quaternary ammonium group binding	4	0.190497024
GO:0030976	thiamine pyrophosphate binding	4	0.190497024
GO:0016840	carbon-nitrogen lyase activity	4	0.190497024
GO:0004559	alpha-mannosidase activity	4	0.190497024
GO:0015923	mannosidase activity	4	0.190497024
GO:0003774	cytoskeletal motor activity	12	0.192622529
GO:0016836	hydro-lyase activity	9	0.197648084
GO:0022857	transmembrane transporter activity	77	0.200989101
GO:0016614	oxidoreductase activity, acting on CH-OH group of donors	14	0.230759464
GO:0016462	pyrophosphatase activity	37	0.230759464
GO:0036094	small molecule binding	192	0.230759464
GO:0016835	carbon-oxygen lyase activity	10	0.244876887
GO:0015095	magnesium ion transmembrane transporter activity	4	0.253783668
GO:0016878	acid-thiol ligase activity	3	0.257209064
GO:0005506	iron ion binding	15	0.275672127
GO:0016757	glycosyltransferase activity	25	0.275672127
GO:0004620	phospholipase activity	6	0.286972466
GO:0016818	hydrolase activity, acting on acid anhydrides, in phosphorus-containing anhydrides	37	0.288718889
GO:0016817	hydrolase activity, acting on acid anhydrides	37	0.296653326
GO:0030246	carbohydrate binding	8	0.296653326
GO:0016743	carboxyl- or carbamoyltransferase activity	2	0.296653326

GO:0004084	branched-chain-amino-acid transaminase activity	2	0.296653326
GO:0004743	pyruvate kinase activity	2	0.296653326
GO:0004591	oxoglutarate dehydrogenase (succinyl-transferring) activity	2	0.296653326
GO:0140678	molecular function inhibitor activity	2	0.296653326
GO:0030955	potassium ion binding	2	0.296653326
GO:0016597	amino acid binding	2	0.296653326
GO:0003843	1,3-beta-D-glucan synthase activity	2	0.296653326
GO:0042030	ATPase inhibitor activity	2	0.296653326
GO:0031420	alkali metal ion binding	2	0.296653326
GO:0016841	ammonia-lyase activity	2	0.296653326
GO:0043169	cation binding	150	0.297577372

TABLE S17. MOLECULAR FUNCTION GO TERMS: 3 HR VS 6 HR, DOWNREGULATED GENES

ID	Name	Gene count	Benjamini
GO:0022857	transmembrane transporter activity	20	0.000389509
GO:0005215	transporter activity	20	0.000389509
GO:0004553	hydrolase activity, hydrolyzing O-glycosyl compounds	7	0.005573343
GO:0016798	hydrolase activity, acting on glycosyl bonds	7	0.008468271
GO:0016810	hydrolase activity, acting on carbon-nitrogen (but not peptide) bonds	6	0.019596324
GO:0016787	hydrolase activity	25	0.030542522
GO:0015293	symporter activity	2	0.033769963
GO:0015291	secondary active transmembrane transporter activity	3	0.162310512
GO:0019135	deoxyhypusine monooxygenase activity	1	0.203546336
GO:0003674	molecular function	92	0.216674448
GO:0022804	active transmembrane transporter activity	5	0.274861937
GO:0016429	tRNA (adenine-N1-)-methyltransferase activity	1	0.279966475
GO:0016426	tRNA (adenine) methyltransferase activity	1	0.279966475
GO:0016491	oxidoreductase activity	13	0.32159545
GO:0046983	protein dimerization activity	4	0.33895375
GO:0016977	chitosanase activity	1	0.33895375
GO:0004100	chitin synthase activity	2	0.371386531

TABLE S18. CELLULAR COMPONENT GO TERMS: 0 HR VS 6 HR, UPREGULATED GENES

ID	Name	Gene count	Benjamini
GO:0032991	protein-containing complex	385	3.30E-12
GO:1905368	peptidase complex	40	7.41E-08
GO:0005737	cytoplasm	503	7.41E-08
GO:1905369	endopeptidase complex	32	8.75E-08
GO:0000502	proteasome complex	28	3.74E-07

GO:0044424	obsolete intracellular part	183	5.41E-07
GO:0043227	membrane-bounded organelle	679	6.32E-07
GO:0043231	intracellular membrane-bounded organelle	679	6.32E-07
GO:0005622	intracellular anatomical structure	959	7.06E-07
GO:0005856	cytoskeleton	66	1.13E-06
GO:0016469	proton-transporting two-sector ATPase complex	29	5.81E-06
GO:0098796	membrane protein complex	89	1.47E-05
GO:0033178	proton-transporting two-sector ATPase complex, catalytic domain	17	4.67E-05
GO:0005839	proteasome core complex	14	6.39E-05
GO:0044428	obsolete nuclear part	44	0.00016241
GO:0005730	nucleolus	45	0.00027298
GO:0012505	endomembrane system	148	0.00027298
GO:0005875	microtubule associated complex	12	0.000325212
GO:0005634	nucleus	397	0.000406924
GO:0031984	organelle subcompartment	76	0.000417253
GO:0005789	endoplasmic reticulum membrane	73	0.000418432
GO:0098827	endoplasmic reticulum subcompartment	73	0.000418432
GO:0005783	endoplasmic reticulum	89	0.000433724
GO:1902494	catalytic complex	110	0.000505003
GO:0042175	nuclear outer membrane-endoplasmic reticulum membrane network	73	0.000531532
GO:0015630	microtubule cytoskeleton	39	0.000770056
GO:0015629	actin cytoskeleton	25	0.000830704
GO:0045259	proton-transporting ATP synthase complex	16	0.00120034
GO:0031981	nuclear lumen	76	0.001582312
GO:0043226	organelle	795	0.002155129
GO:0043229	intracellular organelle	795	0.002155129
GO:0005874	microtubule	31	0.004071119
GO:0099512	supramolecular fiber	32	0.004071119
GO:0099081	supramolecular polymer	32	0.004071119
GO:0099513	polymeric cytoskeletal fiber	32	0.004071119
GO:0016459	myosin complex	14	0.004071119
GO:0031974	membrane-enclosed lumen	100	0.004071119
GO:0043233	organelle lumen	100	0.004071119
GO:0070013	intracellular organelle lumen	100	0.004071119
GO:0030117	membrane coat	23	0.004071119
GO:0048475	coated membrane	23	0.004071119
GO:0045261	proton-transporting ATP synthase complex, catalytic core F(1)	10	0.006453764
GO:0140535	intracellular protein-containing complex	78	0.009451875
GO:0005852	eukaryotic translation initiation factor 3 complex	11	0.010936679
GO:0019773	proteasome core complex, alpha-subunit complex	7	0.014172372
GO:0033176	proton-transporting V-type ATPase complex	12	0.015190883
GO:0031090	organelle membrane	182	0.018688938
GO:0099080	supramolecular complex	37	0.02557838

GO:0030120	vesicle coat	15	0.02557838
GO:0000785	chromatin	17	0.028573926
GO:0005643	nuclear pore	17	0.028573926
GO:0030662	coated vesicle membrane	18	0.028573926
GO:0031312	extrinsic component of organelle membrane	6	0.028573926
GO:0033180	proton-transporting V-type ATPase, V1 domain	6	0.028573926
GO:0016272	prefoldin complex	6	0.028573926
GO:0042555	MCM complex	6	0.028573926
GO:0031314	extrinsic component of mitochondrial inner membrane	6	0.028573926
GO:0031975	envelope	92	0.029256234
GO:0031967	organelle envelope	92	0.029256234
GO:0032993	protein-DNA complex	13	0.034851622
GO:0005743	mitochondrial inner membrane	60	0.037134433
GO:0019866	organelle inner membrane	60	0.046361972
GO:0022624	proteasome accessory complex	7	0.051604697
GO:0005753	mitochondrial proton-transporting ATP synthase complex	7	0.051604697
GO:0005838	proteasome regulatory particle	7	0.051604697
GO:0000786	nucleosome	11	0.053084524
GO:0044444	obsolete cytoplasmic part	98	0.054794075
GO:0008250	oligosaccharyltransferase complex	5	0.060269977
GO:0030286	dynein complex	5	0.060269977
GO:0044464	obsolete cell part	282	0.063671021
GO:0140534	endoplasmic reticulum protein-containing complex	16	0.063920819
GO:0030135	coated vesicle	18	0.063920819
GO:0033290	eukaryotic 48S preinitiation complex	8	0.063920819
GO:0070993	translation preinitiation complex	8	0.063920819
GO:0016282	eukaryotic 43S preinitiation complex	8	0.063920819
GO:0005575	cellular component	1663	0.064291823
GO:0005739	mitochondrion	142	0.070322257
GO:0071944	cell periphery	50	0.081518223
GO:0110165	cellular anatomical entity	1638	0.084838826
GO:0033177	proton-transporting two-sector ATPase complex, proton-transporting domain	11	0.088629007
GO:0005635	nuclear envelope	18	0.088629007
GO:0044665	MLL1/2 complex	6	0.088629007
GO:0030127	COPII vesicle coat	6	0.088629007
GO:0000276	mitochondrial proton-transporting ATP synthase complex, coupling factor F(o)	6	0.088629007
GO:0071339	MLL1 complex	6	0.088629007
GO:0030133	transport vesicle	12	0.088629007
GO:0098800	inner mitochondrial membrane protein complex	14	0.091088137
GO:0140513	nuclear protein-containing complex	97	0.111515245
GO:0030118	clathrin coat	7	0.111976518

GO:0005869	dynactin complex	4	0.116662084
GO:0008540	proteasome regulatory particle, base subcomplex	4	0.116662084
GO:0005886	plasma membrane	39	0.130114365
GO:0030176	integral component of endoplasmic reticulum membrane	10	0.139100193
GO:0005740	mitochondrial envelope	74	0.139100193
GO:0044815	DNA packaging complex	11	0.139100193
GO:0031227	intrinsic component of endoplasmic reticulum membrane	11	0.139100193
GO:0005694	chromosome	47	0.148963865
GO:0012506	vesicle membrane	25	0.16199278
GO:0030659	cytoplasmic vesicle membrane	25	0.16199278
GO:0098590	plasma membrane region	5	0.163186423
GO:0005885	Arp2/3 protein complex	5	0.163186423
GO:0030131	clathrin adaptor complex	5	0.163186423
GO:0005905	clathrin-coated pit	5	0.163186423
GO:0045263	proton-transporting ATP synthase complex, coupling factor F(o)	6	0.192713415
GO:0030119	AP-type membrane coat adaptor complex	6	0.192713415
GO:0031966	mitochondrial membrane	68	0.199621527

TABLE S19. CELLULAR COMPONENT GO TERMS: 0 HR VS 6 HR, DOWNREGULATED GENES

ID	Name	Gene count	Benjamini
GO:0005840	ribosome	168	6.54E-32
GO:0043228	non-membrane-bounded organelle	201	3.58E-06
GO:0043232	intracellular non-membrane-bounded organelle	201	3.58E-06
GO:0042579	microbody	29	1.27E-05
GO:0005777	peroxisome	29	1.27E-05
GO:0044391	ribosomal subunit	33	0.000273082
GO:0031903	microbody membrane	19	0.000338876
GO:0005778	peroxisomal membrane	19	0.000338876
GO:0022626	cytosolic ribosome	11	0.003214972
GO:0022625	cytosolic large ribosomal subunit	8	0.006293246
GO:0015935	small ribosomal subunit	18	0.006461493
GO:0033646	host intracellular part	44	0.006461493
GO:0043657	host cell	44	0.006461493
GO:0033648	host intracellular membrane-bounded organelle	44	0.006461493
GO:0033643	host cell part	44	0.006461493
GO:0043656	host intracellular region	44	0.006461493
GO:0018995	host cellular component	44	0.006461493
GO:0042025	host cell nucleus	44	0.006461493
GO:0033647	host intracellular organelle	44	0.006461493
GO:0015934	large ribosomal subunit	15	0.067897747
GO:0031251	PAN complex	3	0.287489689

GO:0031231	intrinsic component of peroxisomal membrane	5	0.510338534
GO:0005779	integral component of peroxisomal membrane	5	0.510338534

TABLE S20. MOLECULAR FUNCTION GO TERMS: 0 HR VS 6 HR, UPREGULATED GENES

ID	Name	Gene count	Benjamini
GO:0016875	ligase activity, forming carbon-oxygen bonds	37	1.50E-07
GO:0004812	aminoacyl-tRNA ligase activity	37	1.50E-07
GO:0016874	ligase activity	86	2.28E-07
GO:0008092	cytoskeletal protein binding	65	1.77E-06
GO:0003774	cytoskeletal motor activity	39	1.82E-06
GO:0140101	catalytic activity, acting on a tRNA	60	2.84E-06
GO:0004298	threonine-type endopeptidase activity	15	0.000120452
GO:0008194	UDP-glycosyltransferase activity	39	0.000238812
GO:0003779	actin binding	31	0.000270219
GO:0008375	acetylglucosaminyltransferase activity	25	0.00088073
GO:0140098	catalytic activity, acting on RNA	93	0.000960423
GO:0003777	microtubule motor activity	24	0.0014796
GO:0004100	chitin synthase activity	21	0.001484402
GO:0016758	hexosyltransferase activity	54	0.001527583
GO:0016757	glycosyltransferase activity	75	0.001989937
GO:0015252	proton channel activity	13	0.003073509
GO:0008017	microtubule binding	28	0.004818865
GO:0016853	isomerase activity	49	0.004818865
GO:0005524	ATP binding	385	0.004925198
GO:0015631	tubulin binding	32	0.005324253
GO:0046933	proton-transporting ATP synthase activity, rotational mechanism	12	0.005324253
GO:0009678	pyrophosphate hydrolysis-driven proton transmembrane transporter activity	12	0.005324253
GO:0140640	catalytic activity, acting on a nucleic acid	135	0.007113531
GO:0070003	threonine-type peptidase activity	15	0.007113531
GO:0030554	adenyl nucleotide binding	389	0.007113531
GO:0032559	adenyl ribonucleotide binding	388	0.007113531
GO:0097367	carbohydrate derivative binding	482	0.007113531
GO:0051082	unfolded protein binding	24	0.007847371
GO:0032553	ribonucleotide binding	473	0.007994224
GO:0005261	cation channel activity	16	0.008314795
GO:0035639	purine ribonucleoside triphosphate binding	454	0.008314795
GO:0005216	ion channel activity	21	0.009846691
GO:0003824	catalytic activity	1282	0.010790869
GO:0017076	purine nucleotide binding	458	0.013059445
GO:0032555	purine ribonucleotide binding	457	0.013239993
GO:0008135	translation factor activity, RNA binding	33	0.016200974
GO:0090079	translation regulator activity, nucleic acid binding	33	0.016200974

GO:1901363	heterocyclic compound binding	947	0.017388071
GO:0097159	organic cyclic compound binding	947	0.018186936
GO:0015078	proton transmembrane transporter activity	36	0.022785154
GO:0043168	anion binding	520	0.022785154
GO:0045182	translation regulator activity	33	0.022999995
GO:0016776	phosphotransferase activity, phosphate group as acceptor	15	0.031442733
GO:1901265	nucleoside phosphate binding	525	0.034127937
GO:0000166	nucleotide binding	525	0.034127937
GO:0008757	S-adenosylmethionine-dependent methyltransferase activity	30	0.034148188
GO:0036094	small molecule binding	554	0.044493707
GO:0003723	RNA binding	174	0.049503146
GO:0016741	transferase activity, transferring one-carbon groups	65	0.050608855
GO:0046527	glucosyltransferase activity	10	0.050608855
GO:0019205	nucleobase-containing compound kinase activity	14	0.051574973
GO:0002161	aminoacyl-tRNA editing activity	8	0.064176101
GO:0044769	ATPase activity, coupled to transmembrane movement of ions, rotational mechanism	8	0.064176101
GO:0046961	proton-transporting ATPase activity, rotational mechanism	8	0.064176101
GO:0042625	ATPase-coupled ion transmembrane transporter activity	8	0.064176101
GO:0015267	channel activity	21	0.073039949
GO:0022803	passive transmembrane transporter activity	21	0.073039949
GO:0008168	methyltransferase activity	60	0.073508469
GO:0016740	transferase activity	463	0.096825136
GO:0005515	protein binding	518	0.099439123
GO:0140657	ATP-dependent activity	108	0.100627658
GO:0019829	ATPase-coupled cation transmembrane transporter activity	16	0.101646336
GO:0008170	N-methyltransferase activity	16	0.101646336
GO:0003743	translation initiation factor activity	21	0.107871115
GO:0016273	arginine N-methyltransferase activity	7	0.12006167
GO:0016274	protein-arginine N-methyltransferase activity	7	0.12006167
GO:0031072	heat shock protein binding	7	0.12006167
GO:0016779	nucleotidyltransferase activity	43	0.12006167
GO:0017056	structural constituent of nuclear pore	11	0.122314949
GO:0008536	Ran GTPase binding	12	0.135405816
GO:0016866	intramolecular transferase activity	14	0.150009123
GO:0016860	intramolecular oxidoreductase activity	14	0.150009123
GO:0003674	molecular function	2463	0.186629701
GO:0009982	pseudouridine synthase activity	9	0.191972406
GO:0016879	ligase activity, forming carbon-nitrogen bonds	24	0.199500642

GO:0016861	intramolecular oxidoreductase activity, interconverting aldoses and ketoses	10	0.212394471
GO:0042626	ATPase-coupled transmembrane transporter activity	34	0.225080921
GO:0005085	guanyl-nucleotide exchange factor activity	34	0.225080921
GO:0008276	protein methyltransferase activity	14	0.241641069
GO:0035251	UDP-glucosyltransferase activity	7	0.279024331
GO:0030695	GTPase regulator activity	49	0.279024331
GO:0060589	nucleoside-triphosphatase regulator activity	49	0.279024331
GO:0008553	P-type proton-exporting transporter activity	4	0.279024331
GO:0017048	Rho GTPase binding	4	0.279024331
GO:0016725	oxidoreductase activity, acting on CH or CH2 groups	4	0.279024331
GO:0004748	ribonucleoside-diphosphate reductase activity, thioredoxin disulfide as acceptor	4	0.279024331
GO:0061731	ribonucleoside-diphosphate reductase activity	4	0.279024331
GO:0004486	methylenetetrahydrofolate dehydrogenase [NAD(P)+] activity	4	0.279024331
GO:0005048	signal sequence binding	4	0.279024331
GO:0016728	oxidoreductase activity, acting on CH or CH2 groups, disulfide as acceptor	4	0.279024331
GO:0004488	methylenetetrahydrofolate dehydrogenase (NADP+) activity	4	0.279024331
GO:0016810	hydrolase activity, acting on carbon-nitrogen (but not peptide) bonds	41	0.279024331
GO:0016746	acyltransferase activity	73	0.307475923
GO:0003746	translation elongation factor activity	9	0.319539922
GO:0003755	peptidyl-prolyl cis-trans isomerase activity	15	0.319539922
GO:0016859	cis-trans isomerase activity	15	0.319539922
GO:0003676	nucleic acid binding	436	0.324522238
GO:0043021	ribonucleoprotein complex binding	11	0.324522238
GO:0000049	tRNA binding	12	0.324522238
GO:0022890	inorganic cation transmembrane transporter activity	55	0.324522238
GO:0016407	acetyltransferase activity	31	0.355959943
GO:0015075	ion transmembrane transporter activity	85	0.369836091
GO:0008324	cation transmembrane transporter activity	61	0.371459541
GO:0016881	acid-amino acid ligase activity	5	0.371459541
GO:0070569	uridylyltransferase activity	5	0.371459541
GO:0016868	intramolecular transferase activity, phosphotransferases	5	0.371459541
GO:0004550	nucleoside diphosphate kinase activity	5	0.371459541
GO:0015079	potassium ion transmembrane transporter activity	5	0.371459541
GO:0016423	tRNA (guanine) methyltransferase activity	5	0.371459541

GO:0004343	glucosamine 6-phosphate N-acetyltransferase activity	6	0.442610059
GO:0016410	N-acyltransferase activity	30	0.442610059
GO:0008080	N-acetyltransferase activity	29	0.461533835
GO:0008171	O-methyltransferase activity	7	0.461533835
GO:0140358	P-type transmembrane transporter activity	7	0.461533835
GO:0015662	P-type ion transporter activity	7	0.461533835

TABLE S21. MOLECULAR FUNCTION GO TERMS: 0 HR VS 6 HR, DOWNREGULATED GENES

ID	Name	Gene count	Benjamini
GO:0003735	structural constituent of ribosome	156	7.35E-28
GO:0005198	structural molecule activity	162	4.34E-22
GO:0003700	DNA-binding transcription factor activity	97	5.41E-07
GO:0140110	transcription regulator activity	101	0.000140862
GO:0004672	protein kinase activity	100	0.016300726
GO:0043169	cation binding	322	0.043075959
GO:0046872	metal ion binding	319	0.043075959
GO:0019787	ubiquitin-like protein transferase activity	22	0.049317618
GO:0004842	ubiquitin-protein transferase activity	21	0.056272553
GO:0016773	phosphotransferase activity, alcohol group as acceptor	119	0.078276374
GO:0043565	sequence-specific DNA binding	38	0.114046065
GO:0000981	DNA-binding transcription factor activity, RNA polymerase II-specific	32	0.114505785
GO:0019843	rRNA binding	14	0.140164604
GO:0005543	phospholipid binding	16	0.239592478
GO:0008289	lipid binding	25	0.239592478
GO:0004806	triglyceride lipase activity	4	0.239592478
GO:0033192	calmodulin-dependent protein phosphatase activity	4	0.239592478
GO:0004723	calcium-dependent protein serine/threonine phosphatase activity	4	0.239592478
GO:0004674	protein serine/threonine kinase activity	60	0.239592478
GO:0016301	kinase activity	129	0.250379761
GO:0035091	phosphatidylinositol binding	15	0.254767476
GO:0008081	phosphoric diester hydrolase activity	14	0.315652402
GO:0005509	calcium ion binding	26	0.434469022
GO:0016298	lipase activity	12	0.434469022
GO:0004559	alpha-mannosidase activity	6	0.434469022
GO:0015923	mannosidase activity	6	0.434469022
GO:0016829	lyase activity	43	0.434469022
GO:0016903	oxidoreductase activity, acting on the aldehyde or oxo group of donors	14	0.434469022
GO:0015924	mannosyl-oligosaccharide mannosidase activity	5	0.434469022

GO:0004571	mannosyl-oligosaccharide 1,2-alpha-mannosidase activity	5	0.434469022
GO:0008097	5S rRNA binding	3	0.434469022
GO:0016812	hydrolase activity, acting on carbon-nitrogen (but not peptide) bonds, in cyclic amides	3	0.434469022
GO:0052692	raffinose alpha-galactosidase activity	4	0.434469022
GO:0000977	RNA polymerase II transcription regulatory region sequence-specific DNA binding	4	0.434469022
GO:0015925	galactosidase activity	4	0.434469022
GO:0000978	RNA polymerase II cis-regulatory region sequence-specific DNA binding	4	0.434469022
GO:0001228	DNA-binding transcription activator activity, RNA polymerase II-specific	4	0.434469022
GO:0001216	DNA-binding transcription activator activity	4	0.434469022
GO:0004557	alpha-galactosidase activity	4	0.434469022
GO:0019842	vitamin binding	27	0.522671841
GO:0140096	catalytic activity, acting on a protein	215	0.602167101
GO:0042578	phosphoric ester hydrolase activity	44	0.670036306
GO:0004114	3',5'-cyclic-nucleotide phosphodiesterase activity	5	0.670036306
GO:0003995	acyl-CoA dehydrogenase activity	5	0.670036306
GO:0003997	acyl-CoA oxidase activity	5	0.670036306
GO:0004112	cyclic-nucleotide phosphodiesterase activity	5	0.670036306